Oxidative Desulfurization of Model Diesel Fuel Catalyzed by Polyoxometalates

Reem Ghubayra

Thesis submitted in accordance with the requirements of the University of Liverpool for the degree of Doctor in Philosophy

May 2022

Abstract

The presence of sulfur impurities in transportation fuels has raised environmental concerns because, during combustion, they are converted to SO_x, and therefore not only does this lead to acid rain, but it also poisons catalytic converters used to handle exhaust emissions. Thus, liquid fuel desulfurization has received substantial interest worldwide. Much current research focuses on overcoming these problems by proposing different technologies. One of the promising techniques is oxidative desulfurization (ODS), which is a very effective method for ultra-deep desulfurization compared to the conventional hydrodesulfurization technology (HDS). ODS operates at mild reaction conditions, with high efficiency, especially for desulfurization of refractory aromatic sulfur compounds such as benzothiophenes.

Heterogeneous catalysis is a major area of interest within the field of ODS of benzothiophenes commonly found in diesel fuel. Hydrogen peroxide and oxygen are attractive oxidants for the oxidation of benzothiophenes to the corresponding sulfones due to environment-friendly chemistry, producing only water as a by-product. Polyoxometalates (POMs), especially Keggin type POMs, have attracted much attention as the ODS catalysts, being highly active both with H_2O_2 and O_2.

The main objective of this work is to investigate methods for improving oxidative desulfurization of model diesel fuel by using supported Keggin polyoxometalates as catalysts with hydrogen peroxide and oxygen (air) as the oxidants. Activated carbon (AC), which is well known for adsorption desulfurization of fuels, was used as a support for the POM catalysts (POM/AC). POM/AC catalysts have been found to be highly active for ODS under mild conditions in a biphasic system composed of a benzothiophene-containing model diesel fuel (heptane) and aqueous 30% H_2O_2. The catalytic activity of POM/AC varied due to the strong

effect of the carbon support on the integrity of the HPA structure. The results showed that phosphotungstic POM/AC, the most active ODS catalyst, exhibited 100% removal of dibenzothiophene (DBT) from model diesel fuel at 60 °C and could be recovered and reused without loss of activity.

ODS using oxygen (air) as the oxidant has attracted considerable attention, despite more forcing reaction conditions compared to H_2O_2. Aerobic oxidative desulfurization of model liquid fuel (dodecane spiked with DBT) was carried out in the presence of bulk and supported Keggin-type heteropoly acids $H_{3+n}PMo_{12-n}V_nO_{40}$ (HPA–*n*, *n* = 0–3) as heterogeneous catalysts and benzaldehyde (PhCHO) as a sacrificial reductant. In the presence of bulk $H_4PMo_{11}VO_{40}$ (HPA–1), the ODS reaction removed 100% of DBT from fuel (converted to DBT sulfone) in 2 h at 60 °C, PhCHO/DBT = 12 mol/mol and ambient air pressure. The catalyst could be reused without loss of activity.

New mechanistic insights have been gained for the ODS reaction catalyzed by POM with the use of H_2O_2 and O_2 (air) as the oxidants.

Acknowledgements

I would like to express my deepest gratitude to my advisor, Prof. I.V. Kozhevnikov, for his encouragement, support, and direction during my PhD program of study, as well as to Dr. Elena Kozhevnikova for her kind assistance with lab work and equipment. She was motivating, encouraging, and enlightening me during my PhD. Thanks are not enough to her. I am forever grateful to her.

Besides my advisor, I would like to thank my academic assessors Prof. Jose Lopez-Sanchez and Dr. Alexey Sergeev for lending their expertise to my project and for providing support and advice throughout the process. I want also to thank my other committee members as well who have read the manuscript, including Prof. Chris Hardacre and Dr. Haifei Zhang for serving as external assessors by providing comments and suggestions which has benefited my thesis.

I sincerely express my special thanks to my husband and all my family for their love, patience, support, and unwavering belief in standing by my side during my studies journey. Lastly, I would like to dedicate my thesis to my father; even he was not on my side during my studies. It is very unfortunate that he passed away, and I am sure he would have been very proud of my achievements today.

Finally, thanks should also be given to the whole Kozhevnikov's group who worked with me on many experiments together, the Department of Chemistry at the University of Liverpool for providing their support over the course of this project and my degree, and Jazan University for their support, funding, and encouragement. I have reached the goal of completing this dissertation only because of all the support and guidance I have received from all the people mentioned above.

Publications and presentations

Published papers

[1] R. Ghubayra, C. Nuttall, S. Hodgkiss, M. Craven, E.F. Kozhevnikova, I.V. Kozhevnikov, Oxidative desulfurization of model diesel fuel catalyzed by carbonsupported heteropoly acids, Appl. Catal. B 253 (2019) 309–316.

[2] R. Ghubayra, R. Yahya, E.F. Kozhevnikova, I.V. Kozhevnikov, Oxidative desulfurization over carbon-supported heteropoly acids: Effect of carbon support, Fuel 301 (2021) 121083.

[3] R. Ghubayra, R. Hindle, R. Yahya, E.F. Kozhevnikova, I.V. Kozhevnikov, Aerobic oxidative desulfurization of liquid fuel catalyzed by P-Mo-V heteropoly acids in the presence of aldehyde, Catalysts 11 (2021).

Conference presentations

[1] R. Ghubayra, E.F. Kozhevnikova, I.V. Kozhevnikov, The UK catalysis conference (UKCC 2019), Loughborough, UK 2019.

[2] R. Ghubayra, E.F. Kozhevnikova, I.V. Kozhevnikov, 14th international conference on materials chemistry (MC14 2019), University of Birmingham, UK 2019.

[3] R. Ghubayra, E.F. Kozhevnikova, I.V. Kozhevnikov, 5th edition of global conference on catalysis, Chemical engineering & technology, London, UK 2019.

[4] R. Ghubayra, E.F. Kozhevnikova, I.V. Kozhevnikov, Heterogeneous catalysts for sustainable industry, London, UK 2019.

[5] R. Ghubayra, E.F. Kozhevnikova, I.V. Kozhevnikov, Women in chemistry conference, University of Nottingham, UK 2020.

[6] R. Ghubayra, E.F. Kozhevnikova, I.V. Kozhevnikov, Faraday joint interest group

conference, Virtual conference, UK 2020.

[7] R. Ghubayra, E.F. Kozhevnikova, I.V. Kozhevnikov, International conference on environmental catalysis, Virtual conference, UK 2020.

[8] R. Ghubayra, E.F. Kozhevnikova, I.V. Kozhevnikov, Chemical engineering and catalysis conference, Virtual conference, UK 2021.

[9] R. Ghubayra, E.F. Kozhevnikova, I.V. Kozhevnikov, 15th international conference on materials chemistry (MC15 20121), Virtual conference, UK 2021.

Abbreviations

AC	Activated carbon
AODS	Aerobic oxidative desulfurization
BDS	Biodesulfurization
BT	Benzothiophene
BET	Brunauer-Emmett-Teller
BHJ	Barrett-Joyner-Halenda
DBT	Dibenzothiophene
DMDBT	4,6-Dimethyldibenzothiophene
DMF	Dimethylformamide
DMSO	Dimethyl sulfoxide
DRIFTS	Diffuse reflectance infrared Fourier transform spectroscopy
DCE	1,2-Dichloroethane
EDS	Extractive desulfurization
EPA	Environmental protection agency
FID	Flame ionisation detector
GLC	Gas liquid chromatography
GC-FID	Gas chromatography-flame ionisation detector
HDS	Hydrodesulfurization
HPA	Heteropoly acid
HPA–1	11-molybdo-1-vanadophosphoric acid
HPA–1/C	HPA–1 supported on activated carbon

HPA–1/SiO_2	HPA–1 supported on silica
HPA–2	10-molybdo-2-vanadophosphoric acid
HPA–3	9-molybdo-3-vanadophosphoric acid
ICP-OES	Inductively coupled plasma optical emission spectroscopy
IL	Ionic liquid
IR	Infrared
NMR	Nuclear magnetic resonance
NO_x	Nitric oxides
ODS	Oxidative desulfurization
OSCs	Organic sulfur compounds
PMo	Phosphomolybdic acid
PMo/AC	Phosphomolybdic acid supported on activated carbon
POM	Polyoxometalate
PTC	Phase-transfer catalyst
PW	Phosphotungstic acid
PW/AC	Phosphotungstic acid supported on activated carbon
SiW	Silicotungstic acid
SiW/AC	Silicotungstic acid supported on activated carbon
SO_x	Sulfur oxides
TGA	Thermogravimetric analysis
PXRD	Powder X-ray diffraction

Table of content

List of figures

List of tables

List of schemes

1 Introduction

1.1. Catalysis and catalysts

Catalysis is an important phenomenon, which founds applications in many chemical industries in almost all types of bulk chemical production, emission reduction, fine chemical synthesis, and production of transportation fuels. This phenomenon is not limited to the chemical industry; many biological systems employ catalysts as well. In the modern industrial economy, catalysis is of crucial importance with approximately 90% of large-scale processes using catalysts in different stages in the production of chemicals, fuels and materials. Overall, catalysis incorporates a combination of much fundamental knowledge from scientific and technical fields in inorganic and organic chemistry, surface chemistry, thermodynamics, chemical kinetics, solid-state physics, and materials science [1].

Berzelius (1779–1848) was the first who defined the concept of catalysis as "to awaken affinities, which are asleep at a particular temperature, by their mere presence and not by their own affinity". Later, a logical physicochemical concept of a catalyst was introduced by Ostwald in 1895 as a "substance that can change the reaction rate (accelerate or inhibit) without altering the reaction's energy factors". The operational catalysis term is defined, as "a catalyst is a substance that increases the rate of reaction toward equilibrium without being appreciably consumed in the process." This means that the catalyst remains chemically unchanged at the end of a reaction and can be recovered and reused [2,3].

Catalysis is a kinetic phenomenon [3], which deals with changes on the route to chemical equilibrium, so it is about reaction kinetics rather than thermodynamic equilibrium. For example, consider a non-catalyzed reaction between two molecules A and B to give a product

P. The reaction will proceed by colliding the molecules A and B with sufficient energy to overcome the activation barrier to form product P (Fig. 1.1). For the corresponding catalyzed reaction, the reaction is a cycle, which starts with the bonding of molecules A and B to the catalyst surface reacting with each other to give product P that is also bound to the catalyst surface. At the end of the cycle, the product P separates from the catalyst surface, closing the reaction cycle.

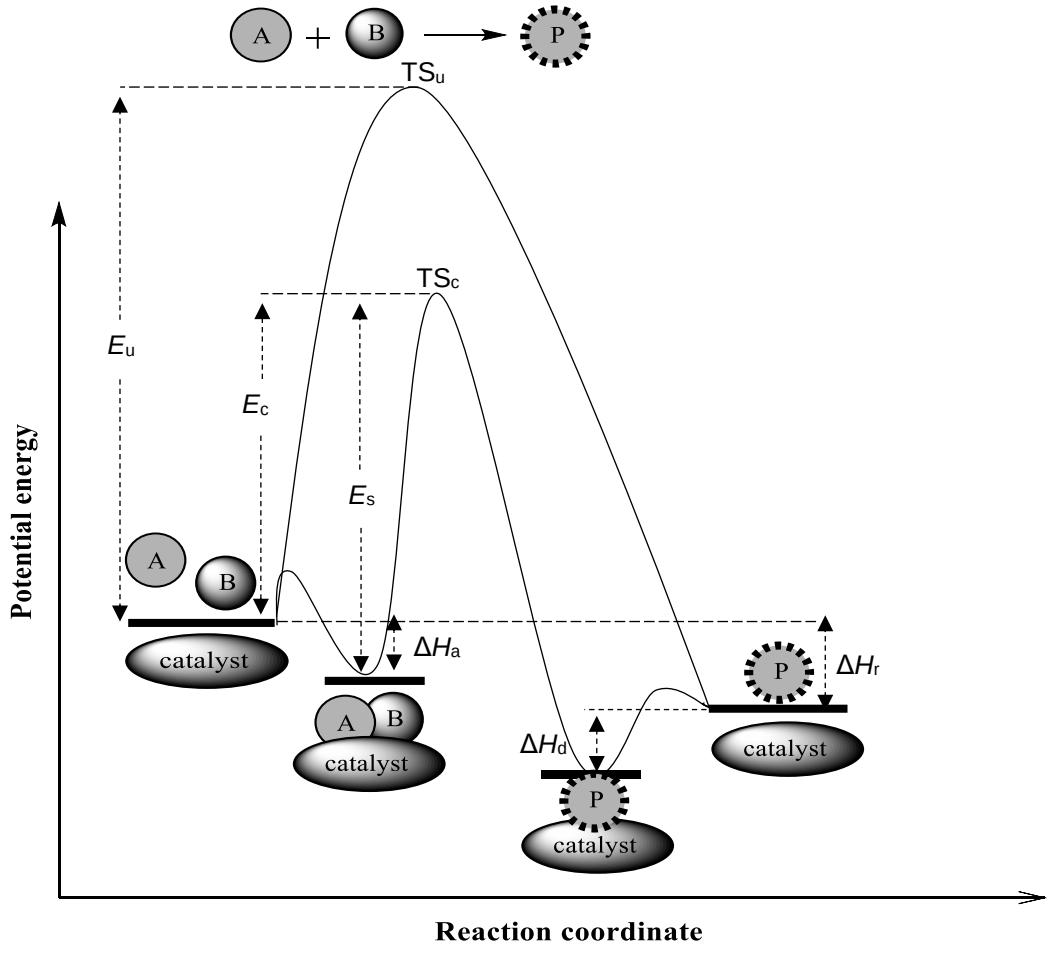

Fig. 1.1. Potential energy diagram for non-catalytic and catalytic reaction: E_u is the activation energy of uncatalyzed reaction, E_c is the activation energy of catalyzed reaction, E_s is the activation energy of surface reaction, TS_u is the transition state of non-catalytic reaction, TS_c is the transition state of catalytic reaction, ΔH_a is the enthalpy of reactant adsorption, ΔH_d is the enthalpy of product desorption, and ΔH_r is the enthalpy of reaction (adapted from [3]).

The potential energy diagram of catalyzed and uncatalyzed reaction (Fig. 1.1) shows the role of catalyst in the reaction mechanism, which offers an alternative path for the reaction that has a lower activation energy. As illustrated, the reactants A and B are binding to the catalyst surface and form an active intermediate complex (transition state). This complex reacts further along the catalytic cycle until the product is generated. Finally, at the end of the reaction, product P desorbs from the catalyst surface, and the initial state of the catalyst regenerated for the next cycle. The catalyst can be reused numerous times for the same reaction. The concept of adsorbed species on the catalyst surface is described by two mechanisms, the Langmuir-Hinshelwood and Eley-Rideal mechanisms. In the Langmuir-Hinshelwood model, both reactants A and B must be adsorbed on the catalyst surface before they can react. The Eley-Rideal model requires one reactant, for example A, to adsorb on the catalyst surface; it is then attacked by B from the fluid (gas or liquid) phase to form the product on the catalyst surface which finally desorbs [4].

Apart from accelerating the reaction, for an industrial process, the suitability of a catalyst relies primarily on the following characteristics: catalyst activity, selectivity, and stability (deactivation behavior) [5,6]. The concept of catalyst activity refers to the rate of reaction, r. The activity can be expressed per unit volume or weight of catalyst, per unit surface area, or per single catalyst active site (turnover frequency).

$$r = \frac{Converted\ amount\ of\ \ reactant}{Catalyst\ volume\ or\ mass\ \times time}\left(mol\ L^{-1}\ h^{-1}\ or\ mol\ kg^{-1}\ h^{-1}\right)$$

The rate of reaction depends on reactant concentrations and temperature. It is expressed by the fundamental rate laws, which link the rate to the rate constant k and the concentration of reactants, where α and β are the corresponding reaction orders in A and B:

$$r = k\ [A]^{\alpha}\ [B]^{\beta}$$

The rate constant *k* depends on the temperature; this dependence is expressed by the Arrhenius equation:

$$k = A\, e^{-(\mathrm{E}_a/RT)}$$

In this equation, E_a is the activation energy of the reaction, *A* is the pre-exponential factor, and *R* is the gas constant. The activation energy is an essential parameter in catalysis, which defines the energy barrier that a system needs to overcome for the reaction to occur. The E_a is ranging from a few kJ mol^{-1} to over 100 kJ mol^{-1}. If E_a is less than 20 kJ mol^{-1} the reaction may be diffusion controlled and if E_a is above 20 kJ mol^{-1} the reaction is likely to be chemically controlled.

Turnover frequency, TOF, is another expression term of activity, which is defined as the number of revolutions of catalytic cycle at the active site per unit time.

$$TOF = \frac{molecules\ of\ reactant\ converted}{(number\ of\ catalyst\ active\ sites) \times (time)}$$

Catalyst selectivity refers to the ability of the catalyst to direct the reaction to yield the desired product. Generally, the selectivity depends on the reactant conversion hence should be reported together with the conversion at which it was measured.

Lastly, the catalyst lifetime is defined as a period of time during which the catalyst maintains a sufficient level of activity and/or selectivity. It is determined by chemical, thermal, and mechanical stability of the catalyst. Numerous factors affect catalyst deactivation that need to be taken into consideration such as catalyst decomposition, coking, and poisoning.

Catalysis is classified into two groups depending on the catalytic system: heterogeneous catalysis and homogeneous catalysis. Homogeneous catalytic processes take place in a uniform liquid or gas phase in which catalysts and reactants are molecularly dispersed in the reaction

medium in the same phase. While heterogeneous catalytic processes take place in a multiphase system where catalysts are usually solids and the reactants are gases or liquids.

To conclude, the benefits of using catalysts can be abundant, especially in industry [1]. Lowering E_a for a reaction, lowers the energy requirements of the system, thus making the process more energy efficient. Catalysts improve the selectivity and accelerate chemical reactions, which gives the kinetic control to obtain the desired products. This provides environmental benefits by avoiding the use of harmful reagents, reducing reaction waste and the volume of a reaction, and removing the toxic or volatile solvents. Therefore, the development of more effective catalysts and processes is a high priority in accordance with the current environmental regulations [7,8].

1.1.1. Homogeneous catalysis vs heterogeneous catalysis

Homogeneous catalysts are most commonly mineral acids and transition metal complexes. A homogeneous catalytic reaction occurs in one phase. Both the catalyst and the reactants are reacted in one phase (usually liquid phase). Homogeneous catalysis has the advantage of high catalyst activity and selectivity, relatively mild reaction conditions and easy process control. The downsides of homogeneous catalysis are difficult product separation, catalyst recycling, and use of volatile organic solvents as a reaction medium. Biphasic catalysis can be used to solve the separation problem in homogeneous catalysis, which will be discussed later [9].

Heterogeneous catalytic reactions occur in different phases, generally using solid catalysts. Such reactions occur at active sites on the surface of a catalyst. Heterogeneously catalyzed reactions usually require more forcing reaction conditions (higher temperature and pressure), have lower selectivity and are more difficult to control due to diffusion limitations. However, heterogeneous catalysis has great advantages over homogeneous catalysis in easy product separation, easy catalyst reuse and waste minimization. As a result, heterogeneous catalysts are

widespread in the chemical and petrochemical industry. The key properties of heterogeneous and homogeneous catalysis are summarized in Table 1.1 [10]

Table 1.1. Properties of heterogeneous and homogeneous catalysis.

Property	Heterogeneous	Homogeneous
Typical composition	Solid metal Metal oxide Supported metal	Metal complexes, acids, bases, etc.
Solvent	May be required	Usually required
Thermal stability	Robust	Sensitive
Availability of active sites	Surface only	All metal centers available
Selectivity	Can be poor	Can be tuned
In situ analysis	Difficult	Can use spectroscopic techniques
Product separation	Easy	Expensive and difficult

1.1.2. Aqueous biphasic catalysis

A biphasic reaction system combines two immiscible liquid phases with the aim to facilitate product separation. Manassen theorized the application of such systems in 1973 [11]. Usually, the biphasic system involves two immiscible phases: aqueous and organic phase where the catalyst operates in one phase (usually aqueous phase) or at the interface and product concentrates in the other phase usually organic phase. As a result, an improved catalyst/product separation is achieved.

Typical mechanism for a reaction catalyzed in an aqueous biphasic system is illustrated by the catalytic cycle in Fig. 1.2. Usually, the catalyst reacts with a reagent in the aqueous phase to form a catalytically active species. The reaction occurs through interaction between catalyst and reactant at the phase boundary (interface) between the two layers. The product remains in the organic phase, and the catalytically active species are regenerated in the aqueous phase by

reacting with more reagent. Once the reaction has run to completion, the product in the organic phase can be extracted by simple phase separation techniques (e.g. decantation). At the same time, the catalyst remains in the aqueous phase, ready for reuse [11,12].

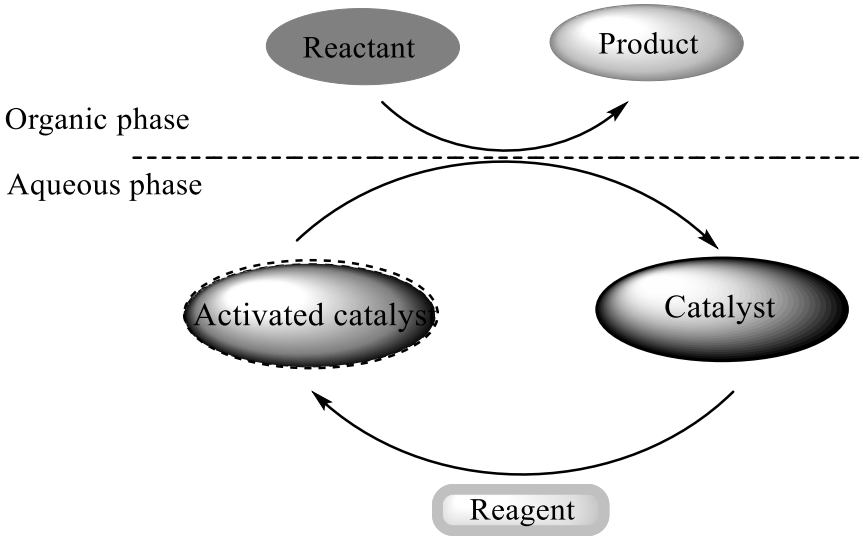

Fig. 1.2. Catalytic cycle in an aqueous biphasic system.

1.2. Desulfurization technologies

1.2.1. Environmental background

Fuel combustion in vehicles is currently one of the most critical issues for the developed countries. Diesel and gasoline are the two primary transportation fuels used today, which are produced from crude oil using fractional distillation [13]. Both of them consist of a mixture of aliphatic hydrocarbons in variable chain lengths, aromatic hydrocarbons, and traces of compounds such as nitrogen-containing and organosulfur compounds. Diesel and gasoline shared similarities in physical properties and chemical composition. The emitted gases of trace compounds in the transport fuel into the atmosphere react with atmospheric water vapour to form their corresponding acids (NO_x and SO_x as products) which causes several problems like environmental pollution and health issues.

In the past few decades, the environmental regulation has focused attention on reducing emissions of these harmful gasses from the transport sector to improve air quality and welfare [14]. By the Directive of the European Union the sulfur content in transport fuel should not exceed 10 ppm starting from 2010, while US regulations allow a maximum of 15 ppm sulfur content for diesel from 2006 and 30 ppm for gasoline from 2005. In the late 20^{th} century, the Clean Air Act introduced multiple measures to reduce air pollution in developed countries [15–17].

The main focus in this part is on describing diesel fuel chemical composition, regulations on the sulfur-containing constituents, and the current technologies employed to control sulfur content in diesel fuel.

Diesel fuel density range from 820 to 950 grams per litre while gasoline density between 710 to 740 grams per litre, which means that diesel fuel is denser than gasoline. Diesel fuel is typically a mixture of 75% aliphatic hydrocarbons (alkanes and cycloalkanes) and 25% aromatic hydrocarbons (alkylbenzenes and aryl olefins). The range of carbon and hydrogen in the average empirical formula for diesel fuel is $C_{10}H_{22}$ to $C_{15}H_{32}$ [18,19]. Diesel engines harm the environment and cause health issues due to emitting large amounts of particulate matter (PM), sulfur oxides (SO_x) and nitric oxides (NO_x) into the atmosphere. These pollutants also cause damage to the diesel engine catalytic converter, acidify the lubricating oil and reduce the fuel economy [19,20].

Organic sulfur compounds (OSCs) present in transport fuel include thiols, sulfides and thiophenes Fig. 1.3 [21]. The dominant type of sulfur compounds in diesel fuel is thiophene (T) benzothiophene (BT), and dibenzothiophene (DBT). The sulfur compounds in fuel are divided into active sulfides (easy to remove) and inactive sulfides (more difficult to remove). The active sulfides are composed of simple sulfur compounds such as hydrogen sulfide and

mercaptans. The inactive sulfides are thioethers, disulfides, benzothiophenes, and dibenzothiophenes [21]. Various desulfurization technologies have been developed to remove sulfur compounds from diesel fuel [8,22,23].

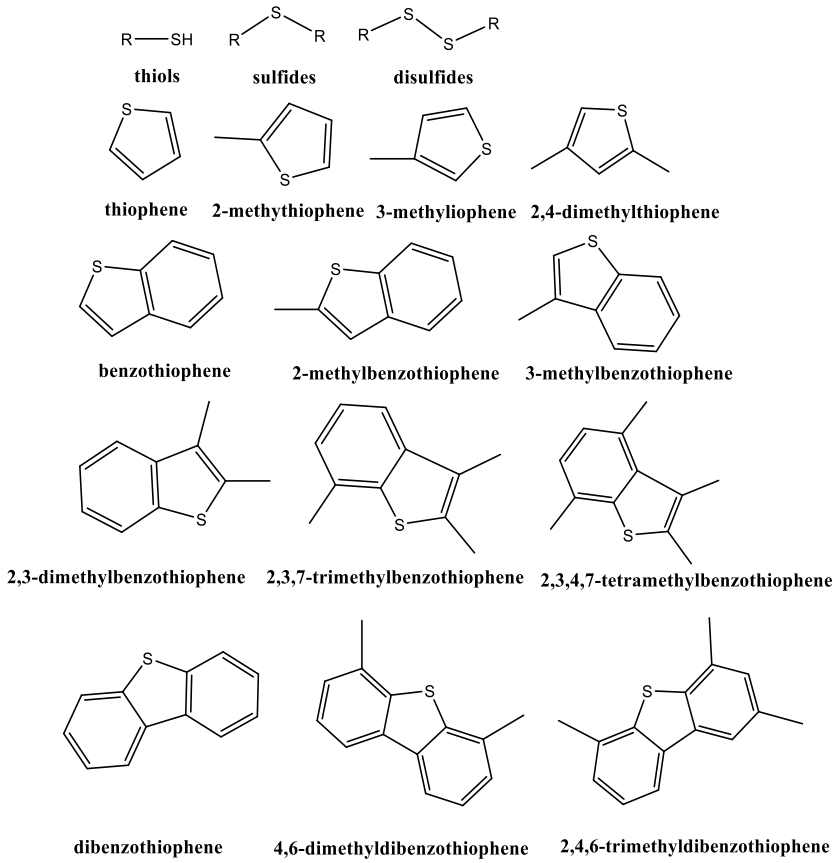

Fig. 1.3. Major types of organic sulfur compounds in diesel fuel (adapted from [21]).

1.2.2. Classification of desulfurization technologies

Desulfurization is the process of removing OSC from the refinery process. Desulfurization processes are categorized by the role of hydrogen within the system: HDS based and non-HDS based or the nature of the chemical and/or physical process used [23]. Non-HDS based processes do not need hydrogen in their operation. In contrast, HDS processes require hydrogen in their operation for decomposition and elimination sulfur from refinery streams. The process of desulfurization can be divided into different types depending on the way of the transformation of sulfur compounds (Fig. 1.4).

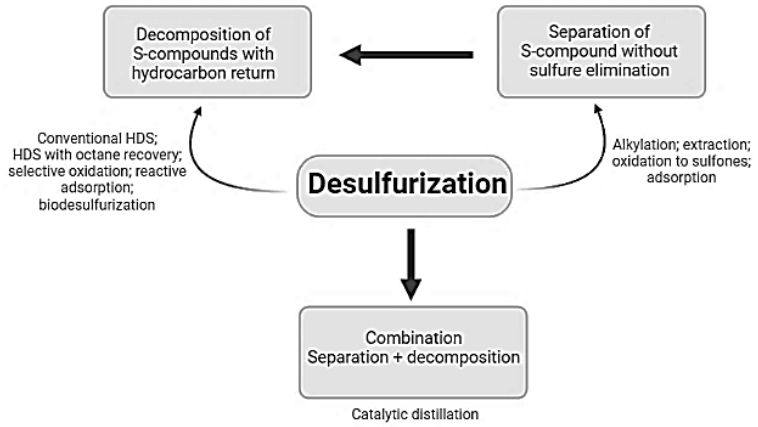

Fig. 1.4. Categorization of desulfurization technologies based on the destination of organosulfur compounds during desulfurization (adapted from [23]).

Hydrodesulfurization (HDS) is the most widely used process for the decomposition of sulfur compounds with hydrocarbon return in the refinery streams. Since HDS treatment is one of the key steps in preserving desirable fuel requirements, different combinations of refinery streams pre- or post-distillation treatments with hydrotreating may be assigned as HDS dependent processes. The technologies that catalytically transform organosulfur compounds with sulfur removal are the most evolved and commercialized. Conventional hydrotreating, hydrotreating with advanced catalysts and/or reactor design, and a combination of hydrotreating with some additional chemical processes to maintain fuel specifications are examples of catalytic conversion technologies. In contrast, non-HDS based processes represent sulfur removal processes such as alkylation, oxidation, extraction, adsorption or combination of these processes. The nature of the chemical and/or physical processes used for sulfur removal is displayed in Fig. 1.5.

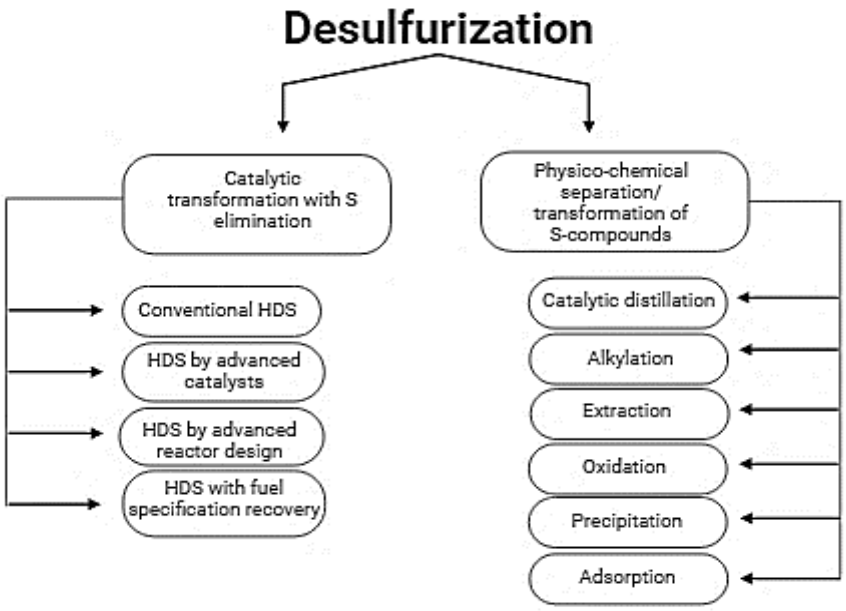

Fig. 1.5. Different types of desulfurization processes (adapted from [23]).

1.2.2.1. Hydrodesulfurization

Hydrodesulfurization (HDS) is the most widespread desulfurization method used in refinery processes since the 1950s, which is based on removing sulfur in fuels. HDS process based on catalytic treatment with hydrogen to convert the sulfur compounds to H_2S and sulfur-free organic compounds. This method operates at severe conditions at high temperature and partial pressure of hydrogen (300–400 ^oC, 30–130 atm) in presence of a catalyst such as Co-Mo or Ni-Mo [24–26].

A fixed bed reactor usually used for HDS processes. Sulfur is removed from the fuel by two processes, Claus and contact processes [27,28]. Claus process based on removing sulfur as H_2S and converted to S, while contact process convert H_2S to sulfuric acid.

HDS method is only effective for removing nonaromatic S-compounds due to their high reactivity compared to aromatic S-compounds. Fig. 1.6 shows a qualitative relationship

between the type, size, and reactivity of sulfur molecules in various distillate fuel fractions in HDS processes [29].

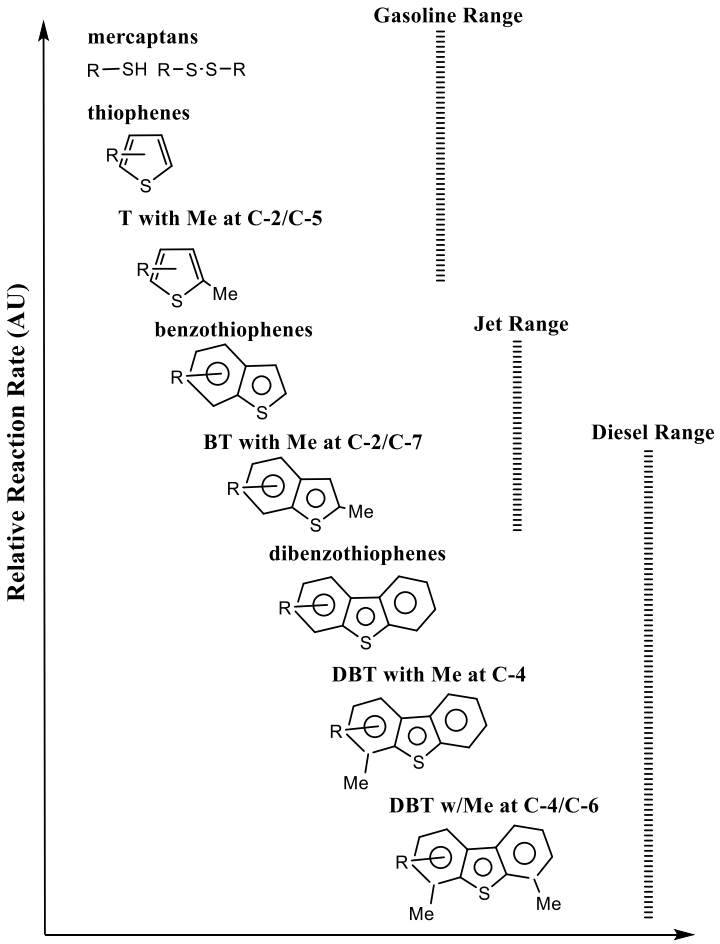

Fig. 1.6. Reactivity, ring sizes, and type of sulfur molecules in various distillate fuel fractions in HDS processes (adapted from [29]).

Aromatic S-compounds, with conjugation between the lone pairs on the S atom and the π-electrons in an aromatic ring, constitute approximately 0.2–0.3 wt.% of fuel and must be removed in order for the fuel to burn cleaner to comply with the standards imposed on fuels quality requirements [33].

Fig. 1.7 shows the desulfurization of aromatic S-compounds (dibenzothiophene, DBT) in HDS processes. Two parallel paths, direct desulfurization (DDS) and the hydrogenation (HYD) paths, are possible in the hydrodesulfurization of DBT. As shown, dibenzothiophenes are

absolutely harder to remove even after very harsh HDS treatments due to low reactivities and their stabilities at high temperature.

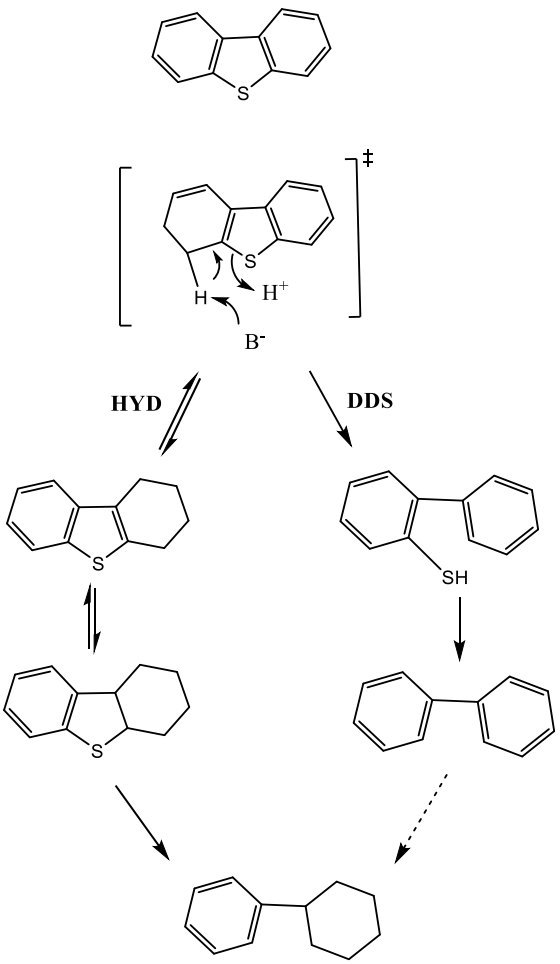

Fig. 1.7. Reaction mechanism of hydrodesulfurization of DBT (adapted from [30]).

For refinery streams, deep desulfurization is required to meet the environmental regulations. Unfortunately, deep HDS requires increasing the severity of the HDS process conditions like temperatures and pressures. In addition, it needs to improve the catalyst to fuel ratio by increasing the ratio, increasing hydrogen usage, and modification of the catalysts. Therefore, those requirements need high costs to build a reactor and pipelines, also cause poor energy efficiency due to the inability to use some of the gas and heat from the waste gas, which is an impediment for this process to use [30–33].

1.2.2.2. Non-hydrodesulfurization

Non-hydrodesulfurization (non-HDS) applies to processes such as biological desulfurization, adsorption desulfurization, extractive desulfurization, and oxidative desulfurization. These non-HDS methods are continually developed in recent desulfurization research. For example, thiophene can be extracted more effectively than removed by conventional hydrodesulfurization. Among these four processes, only oxidative desulfurization is being widely developed for commercial use.

1.2.2.2.1. Biodesulfurization (BDS)

BDS is widely used in the green processing of fossil fuels especially for the removal of sulfur compounds by using a series of enzyme-catalyzed reactions at low temperature and pressure [34–39]. BDS is a process of converting water-insoluble organic sulfur into water-soluble compounds, which are then removed by using an appropriate microbial organism or enzyme at mild conditions while the corresponding hydrocarbon compounds remain unchanged. Organosulfur compounds can be metabolised in one of three forms by several bacteria species: destructive oxidation, anaerobic biodesulfurization, and aerobic biodesulfurization. The Kodama pathway is a DBT-destructive route. This pathway involves three main steps: hydroxylation of one phenyl ring, ring cleavage and hydrolysis. However, the key issue in this pathway is the accumulation of these water-soluble end products, which significantly inhibit microbial growth and DBT oxidation.

The anaerobic BDS pathway removes sulfur from DBT by reducing DBT to biphenyl and H_2S, making this pathway selective as opposed to destructive BDS. This method, however, has its limitations due to the hydrogen requirement cost and the difficulties in maintaining anaerobic conditions.

The aerobic biodesulfurization is well known as a promising method of fuel desulfurization. This method permits the selective elimination of sulfur from organic compounds without destruction of the carbon chain. This involves a four-step enzymatic pathway: conversion of DBT to DBT-sulfoxide (DBTO) then to DBT-sulfone ($DBTO_2$) by the enzymes DszC monooxygenase and DszD, followed by conversion of $DBTO_2$ to 2-(2'-hydroxyphenyl)benzene sulfinate (HBPS) by the enzymes DszA monooxygenase and DszD, and finally conversion of HBPS to HBP and sulfite by the DszB desulfinase. Nonetheless, the challenges facing the commercial implementation of biocatalysis are cost-effectiveness, enhancing catalyst stability, maintaining biocatalyst activity over time, improving mass transport limitations, oil-water separation and product recovery, temperature, solvent tolerance, and using a broader substrate specificity to attack a greater range of heterocyclic compounds.

1.2.2.2.2. Adsorption desulfurization (ADS)

ADS is a typical process for the removal of sulfur compounds from liquid hydrocarbon fuels. Practically, any solid sorbent can adsorb selectively organosulfur compounds from refinery streams [40]. ADS has been studied over zeolites, aluminosilicate, activated carbon, alumina and zinc oxide as adsorbents for removal of sulfur compound [41–45]. The selection and preparation of adsorbents are the key factors in adsorption desulfurization. Additionally, the active adsorbent in this technique should be porous, non-reactive substance with high surface area to adsorb sulfur compounds by attaching sulfur molecules to the adsorbent and remain there as separate from the fuel. Molecular sieves, activated carbon, metal oxides, and composite metal oxide clays are currently used as desulfurization adsorbents.

Commonly, most commercially available activated carbons are widely used as adsorbents. These have strong porosity, high surface area, and are thus highly efficient in absorbing different forms of compounds [55]. Yu et al. investigated ADS using a hydrogen peroxide-activated carbon–formic acid system. The results show that more diesel sulfur content can be

extracted by that system compared to the hydrogen peroxide-formic acid system. Consequently, the oxidative removal of DBT shows a strong dependency on the content of the surface carboxylic group [42,46].

To conclude, high adsorption capacity and high selectivity for the adsorption of refractory aromatic sulfur compounds are the most common challenge that adsorption desulfurization faces, which needs further development. Due to competitive adsorption, selectivity is found to be a key problem in ADS. To show the capabilities of ADS commercially, the development of robust inexpensive adsorbent and ideal regeneration methods are required. The quest for a low-cost, effective adsorbent is ongoing, and its industrial adaptation is very limited at present [40].

1.2.2.2.3. Oxidative desulfurization (ODS)

ODS is one of the most promising technologies for deep desulfurization of diesel fuel. This process operates at low temperature (50–70 ^{o}C) and atmospheric pressure. Oxidative desulfurization consists of oxidizing heavy sulfides to the corresponding sulfoxides or sulfones by adding one or two oxygen atoms without breaking any carbon-sulfur bonds in the presence of appropriate oxidants, (Scheme 1.1). This is followed by the liquid extraction in which the oxidized compounds are extracted or adsorbed from the light oil due to their high relative polarity. This method is more effective for removing aromatic S-compounds compared to HDS [23,32,47,48].

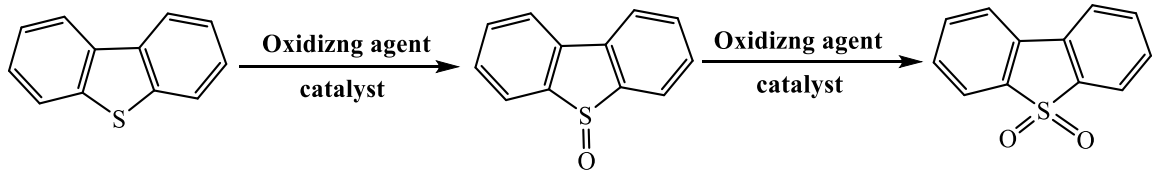

Scheme 1.1. Oxidative desulfurization of DBT (model organosulfur impurity) in n-heptane by hydrogen peroxide

Oxidized compounds can be extracted by contacting with a non-miscible solvent or by adsorption using silica gel and aluminium oxide [59,60]. Many oxidants can be utilized for ODS such as organic and inorganic peroxy acids, hydroperoxides, peroxy salts, NO_2, tert-butyl-hydroperoxide, oxygen (air), and O_3 [49,50].

The following factors must be considered when selecting an oxidant for ODS: (1) the amount of active oxygen present, (2) the capacity to apply it selectively, (3) the reaction by-product, and (4) the cost. Table 1.2 shows single oxygen atom donors of different type of oxidant [51].

Table 1.2. Properties of oxidants.

Donor	Active oxygen (wt.%)	By-product
H_2O_2	47.0	H_2O
O_3	33.3	O_2
t-BuOOH	17.8	t-BuOH
N_2O	36.4	N_2
$NaClO_2$	35.6	NaCl
NaClO	21.6	NaCl
NaBrO	13.4	NaBr
$C_5H_{11}NO_2$	13.7	$C_5H_{11}NO$
HNO_3	25.4	NO_x
$KHSO_5$	10.5	$KHSO_4$
$NaIO_4$	7.2	$NaIO_3$
PhIO	7.3	PhI

Hydrogen peroxide and oxygen (air) are the best and commonly used oxidizing agents in ODS because of their low cost, high efficiency, forming only water by-product during the reaction, and environmental friendliness [52].

During the oxidation process, it was discovered that the sulfide's electron density has a major effect on the rate of desulfurization. The rate constant of oxidation is higher when the electron

density on the sulfur atom is higher. The electron density on the sulfur atom of BT, DBT, and 4,6-DMDBT is 5.739, 5.758, and 5.760, respectively, and catalytic activity decreases in this order of substrates [53].

The oxidative desulfurization was reported in the literature as early as 1954. However, prior to the new legislation requiring the manufacture of ultra-low sulfur fuel oils, it was not given much consideration. In the last decade, many types of oxidative systems have been studied such as organic acids, HCOOH, CCl_3COOH, polyoxometalates, CF_3COOH, methyl-trioxorhenium (VII), titano silicates, and solid base in the presences of H_2O_2 oxidant. Molecular oxygen, O_2, has also been used as a favoured low-cost oxidant in combination with various initiators like aldehydes in the presence of a variety of catalysts in ODS with promising results [54].

Oxidative desulfurization can be assisted by another processes such as radiation assisted oxidation, ultrasound-assisted ODS, photooxidation, electrochemical catalytic oxidation, and plasma ODS [55–58].

1.2.2.2.4. Extractive desulfurization

Extraction methods can be used after ODS to extract the sulfoxides and sulfones produced from oil by using a non-miscible solvent. The efficiency of extraction solvent depends on polarity, which based on the selection of suitable solvents. To determine the potential for separation and recovery of the solvent for recycling and reuse, other properties such as boiling point, freezing point and surface tension need to be considered carefully [59,60]. The oxidized compounds and the solvent are extracted from the oil. To recover any traces of dissolved extraction solvent and unused oxidant, the oil is washed with water. It is then polished using other processes, such as silica gel and aluminum oxide absorption followed by a simple distillation [61]. Conventional solvents such as dimethyl sulfoxide (DMSO), dimethylformamide (DMF), and

acetonitrile are typical water-soluble polar solvents used due to their high extractability for sulfones. DMSO and DMF have a high boiling point, which is close to the boiling point of the sulfones. These solvents are not preferred because they create difficulty in separation and reuse for further extraction process [62]. Alternatively, ionic liquids (ILs) can be used, which are organic salts composed of organic cation and inorganic anions whose melting points are below 100 ^{o}C. This method can be used in two ways: as direct extraction of S-compounds (extractive desulfurization, EDS) or for extraction of oxidized S-compounds obtained from ODS [63–65]. ILs have attractive properties to be suitable extractants for sulfur compounds; these properties include non-volatility, recyclability, non-flammability, thermal/chemical stability, solubility of organic and inorganic compounds, and environmental friendliness. ILs can be tailored by appropriate cation, anion, and substituent selection, which can be performed in selective liquid-liquid separations. The challenges in the ILs method can be regeneration of IL, corrosion problems, negative effect on fuel quality, and high total costs of deep fuel desulfurization [62].

1.3. Polyoxometalates

Polyoxometalates (POMs) are the non-acidified form of heteropoly acids (HPAs). In this work, POM catalysts were introduced to the liquid-phase ODS reaction systems in their conjugate HPA forms in the presence of oxidants such as H_2O_2 and air. First, $PW_{12}O_{40}^{3-}$ (PW), $PMo_{12}O_{40}^{3-}$ (PMo), and $SiW_{12}O_{40}^{4-}$ (SiW) were used as precursors for catalytically active peroxo polyoxometalate species in aqueous biphasic oxidations with H_2O_2 for sulfur removal from the organic phase in the ODS system. Second, mixed-metal HPAs $H_{3+n}PV_nMo_{12-n}O_{40}$ (HPA–*n* ; *n* is the number of vanadium (V) ions), where $Mo^{6+}$is partially substituted by V^{5+}, are investigated as heterogeneous catalysts for the liquid-phase aerobic ODS.

1.3.1. Historical background

Berzelius reported the first heteropoly compound in 1826, by preparing ammonium 12-molybdophosphate as a yellow precipitate from the addition of ammonium molybdate to phosphoric acid. In 1848, Svanberg and Struve introduced this compound in analytical chemistry to determine phosphorus. In 1862, Marignac reported the analytical composition of the tungstosilicic acid [66,67].

During the next half-century, little progress had been made on understanding the structures of synthesized polyoxometalates. Many proposals had been viewed for the structure of heteropoly compounds. In 1933, Keggin succeeded in determining the most important structure of 12:1 type of heteropoly anions ($H_3PW_{12}O_{40}\cdot 5H_2O$) by using a powder X-ray diffraction technique and this structure is now named after him. In 1948, Anderson-Evans heteropoly anion (6:1) was reported; its structure was determined by Evans using single-crystal X-ray analysis of $Te^{6+}Mo_6O_{24}^{6-}$ salts. In 1953, Dawson also discovered an 18:2 heteropoly anion $P_2W_{18}O_{62}$ that is called Wells-Dawson's. By the early 1970s, extensive work by many groups, especially those of Souchay (France), Ripan (Romania), Spitsyn (USSR) and Baker (USA), further expanded the chemistry of polyoxometalates [68–70].

Follow-up 1980–90, the number of interested groups involved in this field was increased enormously with expanding applications of polyoxometalates. Baker and Glick reviewed the history of polyoxometalate chemistry and contributions of various groups to date. The application of modern characterization techniques provided a much better understanding of the structural principles of polyoxometalates and their properties. Even so, many fundamental questions remain unanswered like the structural principles, mechanisms of synthesis, and reactivity of polyoxometalates [71,72].

The first attempt to use polyoxometalates as catalysts was in the beginning of the 20th century. Then began a systematic investigation of polyoxometalate compounds in the early 1970s due to their enormous potential for catalytic applications and a lot of the pioneering work at that time followed in Japan (Izumi, Misono, Ono, Otake, Yoneda and co-workers) and Russia (Matveev and co-workers). As a result, polyoxometalate catalysts were successfully used in several industrial applications in the 1970–80s. Further innovative research in this field is continued to date [71,73].

1.3.2. Overview

Heteropoly acids are comprised of heteropoly anions and protons as counter cations. Heteropoly anions are polyoxometalate anions, which can be classed as a diverse class of nano-sized metal-oxide clusters having a unique structural and functional versatility. Clusters' arrangement forms a wide array of anionic structures constituting early transition-metal elements in their highest oxidation states. Chemically, anion structures in polyoxometalates are categorized as either isopoly or heteropoly anions which built up by oxygen-sharing MO_x polyhedra having the following general formula: $[M_mO_y]^{p-}$ –isopoly and $[X_xM_mO_y]^{q-}$ ($x \leq m$) – heteropoly anions, respectively. Here M represents the addendum atom (typically Mo^{VI}, W^{VI}, V^{V}, etc.) and X is the heteroatom (usually P^{5+}, Si^{4+}, As^{5+}, B^{3+}, etc.) [71].

Heteropolyanions are commonly prepared via a self-assembly process in an aqueous acidic solution to form a polyanion as represented by the following equation:

$$H_2PO_4^{2-} + 12WO_4^{2-} + 23H^+ \longrightarrow [PW_{12}O_{40}]^{3-} + 12H_2O$$

The nomenclature of POMs relies on their compositions and substituent elements, which can be categorized into an acid form and oxoanion forms. Acid form which referred to as polyacids or polyoxoacids including heteropoly acids (e.g. $H_3PW_{12}O_{40}$) and isopolyacids (e.g.

$H_2Mo_6O_{19}$), and oxoanion forms referred to as polyanions or polyoxoanions or polyoxometalates (e.g. $PW_{12}O_{40}^{3-}$). A simplified nomenclature is used in catalytic applications of polyoxometalates by omitting the charge, counterion and even the oxygen atoms, e.g. $H_3PMo_{12}O_{40}$ may be abbreviated to HPMo or PMo in a way that the heteroatom is considered as the central atom of a complex and the addenda as a ligand [71,73,74].

The relative activity of POMs depends on following properties:

Acid strength (HPA): PW > SiW ≥ PMo

Oxidation potential: PMo >> PW > SiW

Hydrolytic stability: SiW > PW > PMo

Catalysis by heteropoly compounds, heteropoly oxometalates or metal-oxygen cluster compounds, has been a significant area of research with applications in various disciplines of current technological, environmental and economic interest (e.g. catalysis, materials science, medicine and energy). Their catalytic properties have attracted much attention in the last few decades, offering significant economic and environmental benefits related to their unique physicochemical properties [74]. Several advantages associate with using heteropoly compounds as catalysts in homogeneous and heterogeneous systems starting with the most important multifunctionality and structural mobility properties. They have a very strong Brønsted acidity coupled with the ability to be highly efficient oxidants to undergo fast redox transformations under mild conditions. Their acid-base and redox properties can be manipulated by changing the chemical composition. Solid heteropoly compounds possess heteropoly anions and countercations, which can frequently preserve upon substitution or oxidation/reduction, good thermal and oxidative stabilities compared with common organometallic complexes. Heteropoly compounds are thermally stable, soluble in polar

solvents, insoluble in non-polar solvents, and exhibit very high proton mobility and pseudo-liquid behavior [71,73,74].

1.3.3. Structures of polyoxometalates

1.3.3.1. Primary, secondary and higher structures

Polyoxometalates are relatively hierarchical complex structures, and their particles can be considered a single repeating unit, which is part of a structural hierarchy. This structure hierarchy (Fig. 1.8) was proposed by Misono et al. [74], and now is widely adopted in heterogeneous catalysis by polyoxometalates to distinguish and describe the importance of structural flexibility and diversity of solid heteropoly compounds. Three structural levels have been distinguished and are defined as primary structure (polyoxoanion structure), secondary structure (crystal structure and packing), and tertiary structure (more complex HPA aggregate, i.e. particle size, porosity, surface area, distribution of protons, etc.).

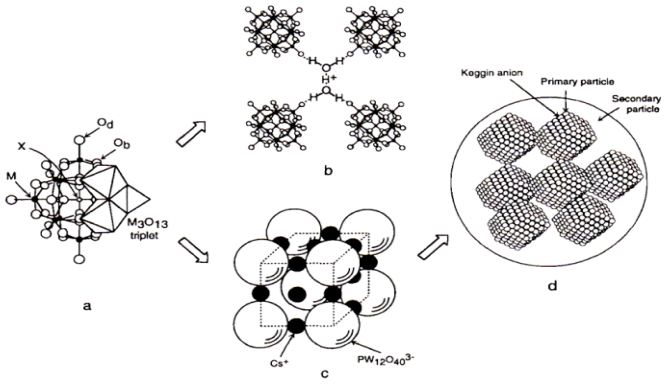

Fig. 1.8. Primary, secondary, and tertiary structures of heteropoly compounds: (a) primary structure (Keggin structure, $XM_{12}O_{40}$); (b) secondary structure ($H_3PW_{12}O_{40}.6H_2O$); (c) secondary structure ($Cs_3PW_{12}O_{40}$ unit cell); (d) tertiary structure of bulk $Cs_{2.5}H_{0.5}PW_{12}O_{40}$ [74].

Heteropoly anions are considered the primary structures, which possess many different configurations that are differing in atomic ratio of the heteroatom and metal atom present. Table 1.3 summarizes the most important structures of heteropoly anions [71].

Table 1.3. Different structures of HPAs.

X/M ratio	Chemical formula (M = Mo or W)	Structure name
1:12	$[X^{n+}M_{12}O_{40}]^{(8-n)}$	Keggin
2:18	$[X_2^{5+}M_{18}O_{62}]^{6-}$	Dawson
1:6	$[X^{n+}M_6O_{24}]^{n-}$	Anderson

In aqueous solution, heteropoly anions are present as free units of the primary structure, which are weakly solvated and may be protonated. The structural stability of these anions strongly relies on the pH; at high pH (> 2.0) these structures are degrading via hydrolysis. Protonation and hydrolysis are a major structural concern for catalysis in solution [71].

Solid heteropoly acids are ionic crystals, composed of large polyanions, countercations (H^+, Na^+, H_3O^+, $H_5O_2^+$, etc.) and hydration water. These structures are called the "secondary structure". The amount of hydration water is essential in the crystal structure of HPAs, which can be easily removed by heating without substantially changing the chemical composition of the heteropoly anions [75]. Consequently, upon hydration, the acid strength is increased. Mobility of the Keggin anions in HPA crystal, which is different from the rigid network structure of zeolites, allowed a variety of polar organic molecules and water to enter and leave HPA crystals giving structural flexibility for HPA to be used as a heterogeneous catalyst (Fig. 1.8.a). The proton structure of crystalline HPAs is essential to understanding the activity of HPAs. Two types of protons are present in crystalline HPA: hydrated protons and non-hydrated protons. Both types have different roles in catalytic features of HPA catalysts. The hydrated protons are responsible for high proton conductivity due to the high mobility of hydrated protons in the crystalline heteropoly acid. In contrast, the non-hydrated protons are much less

mobile localizing on the peripheral oxygens of the polyanion in the crystalline heteropoly acid [76].

Consequently, the state of protons and their mobility are strongly dependent on the amount of hydration water in HPA. As the amount of water decreases, the protons become restricted. Therefore, the water plays a crucial role in the formation of proton structure in the crystalline heteropoly acid and catalytic features of HPA catalysts. Controlling the water contents in HPA catalysts is the necessity for the reproducibility of catalyst preparation and their properties (particularly the acidity) which can be controlled by thermal pretreatment [77].

1.3.3.2. The Keggin structure

12:1 Keggin structure is the most common structure adopted by many polyoxometalates (Fig. 1.9). Availability and stability of Keggin POMs are the most important for catalysis [71,78].

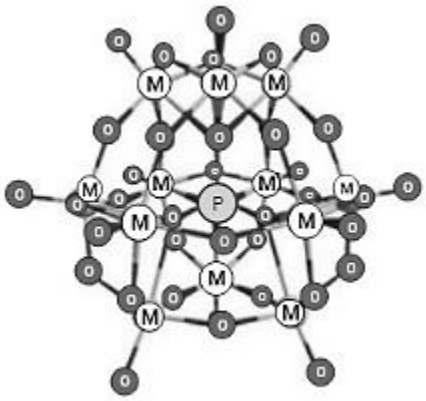

Fig. 1.9. The 12:1 Keggin structure. The heteroatom (P) located in the center of the tetrahedron, formed between itself and 4 surrounding oxygen atoms. The addenda atoms (Mo or W) are depicted M (adapted from [78]).

The Keggin heteropoly anion has a diameter of ca. 1.2 nm; it is represented by the formula $[XM_{12}O_{40}]^{x-8}$, where X is the central atom, x is its oxidation state, and M^{6+} is the metal ion (addendum atom). The structure of the Keggin anion consists of 12 edge- and corner-sharing

metal-oxygen octahedra MO_6 (typically M = Mo^{VI}, W^{VI}, etc.) which are arranged into a spherical structured framework encapsulating a central tetrahedron [XO_4] (usually X = P^{5+}, Si^{4+}, As^{5+}, B^{3+}, etc.). The metal ions can be partially substituted by many other metal ions, e.g., V^{5+}, Co^{2+}, Zn^{2+}, etc. Mo^{VI} and W^{VI} are the most frequently found addenda atoms in Keggin polyoxometalates due to their favorable ionic radius and charge combination, which improves the accessibility of the empty metal d-orbitals to the filled oxygen 2p orbitals for oxygen-metal π-bonding.

The Keggin structure comprises a total of 40 close-packed oxygen atoms [71]. The corner-sharing metal-oxygen octahedra MO_6 are arranged in four M_3O_{13} groups. The structure consist of:

- Twelve internally bridging M–O–M bonds (quasi-linear) connecting two different M_3O_{13} groups.
- Twelve edge-bridging angular M–O–M bonds shared by the octahedra within an M_3O_{13} group.
- Twelve terminal M=O bonds
- Four internal X–O–M bonds which contain the tetrahedral center.

These oxygens can be distinguished by ^{17}O NMR and fingerprint infrared spectra in the range of 600–1100 cm^{-1} [71,75].

Each of the M_3O_{13} groups can be rotated by 60° about its 3-fold axis, which leads to geometrical isomers of a total of 5: α, β, γ, δ and ε. The most common geometrical isomer is α isomer. Rotation of one, two, three, or all four M_3O_{13} groups by 60° produces the β, γ, δ and ε isomers, respectively, Fig. 1.10 [79].

The lacunary or defective derivatives of the Keggin POM anions are produced by the removal of one or more addendum atoms, which produces vacancies in the Keggin structure [80]. These vacancies have been used as a binding and/or active sites in many reactions, including oxidation reactions. Lacunary derivatives of Keggin anions could be monovacant $[XM_{11}O_{39}]^{n-}$ and trivacant $[XM_9O_{34}]^{n-}$ species which have lost one and three MO_6 octahedra, respectively [73,80]. Lacunary species can assemble into larger polyoxometalate structures directly or with the incorporation of metal ion linkers; formation of these species depends on pH of solution (will be discussed further later).

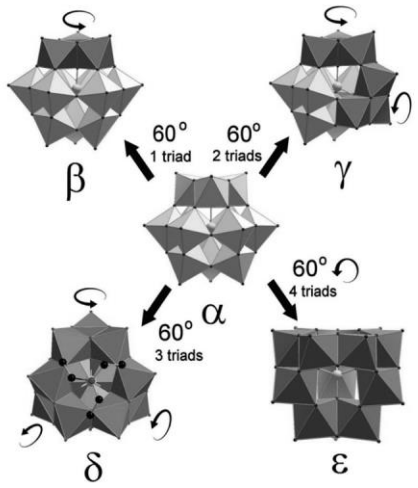

Fig. 1.10. Geometrical isomers of Keggin-type polyoxometalates [79].

1.3.4. Properties of heteropoly acids

1.3.4.1. Thermal stability of solid heteropoly acids

Some of solid heteropoly compounds have a fairly high thermal stability up to 350 ºC and can be used as catalysts in reactions at moderately high temperatures [71]. Usually, thermal stability can be measured by thermal analytical methods such as thermal gravimetric analysis (TGA), differential thermal analysis (TG-DTA), differential scanning calorimetry (DSC), and sometimes with combination with other techniques, such as X-ray diffraction, infrared spectroscopy, solid-state NMR, etc.

The thermal decomposition of POMs occurs in a complex multistage process at different temperatures that may affect the catalyst activity. Heteropoly acid hydrates based on tungsten or molybdenum (e.g. $H_3PW_{12}O_{40}\cdot xH_2O$ or $H_3PMo_{12}O_{40}\cdot xH_2O$) lose their physisorbed water at temperatures just below 100 °C. Water hydrogen bonded to acidic protons is lost between 100–280 °C, and the loss of the acidic protons and the onset of thermal decomposition of the Keggin structure occurs in the range of 370–600 °C (Scheme 1.2) [80].

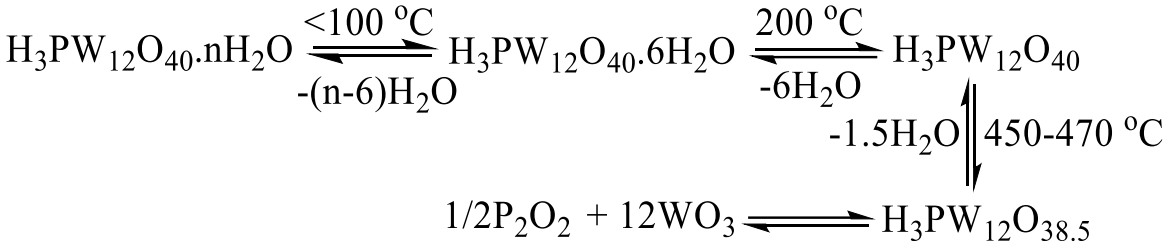

Scheme 1.2. Thermal decomposition of $H_3PW_{12}O_{40}$ hydrate.

Commonly, Keggin-type heteropoly compounds are the most stable among various polyoxometalates. According to TGA measurement, the decomposition temperature (°C) of the most typical Keggin heteropoly acids decreases in the following series [82,83]:

$$H_3PW_{12}O_{40}\ (465) > H_4SiW_{12}O_{40}\ (445) > H_3PMo_{12}O_{40}\ (375) > H_4SiMo_{12}O_{40}\ (350)$$

Obviously, $H_3PW_{12}O_{40}$ has the highest thermal stability among the Keggin HPAs.

1.3.4.2. Acid properties of heteropoly acids in solution

Keggin heteropoly acids are known as strong Brønsted acids, which are completely dissociated in aqueous solution into their constituent protons and heteropoly anions. The acid properties of Keggin heteropoly acids are well documented in terms of their dissociation constants, Hammett acidity functions, pyridine adsorption, microcalorimetry of ammonia adsorption, and temperature programmed desorption. The acid strength of heteropoly acids is much stronger than the mineral acids such as H_2SO_4, HNO_3, HCl, etc. due to the large size of the heteropoly

anions and delocalization of the negative charge. The electrostatic interaction between a proton and anion is much weaker in heteropoly acids than in mineral acids. The acid strengths of heteropoly acids follows the order [76]:

$$H_3PW_{12}O_{40} > H_4\,SiW_{12}\,O_{40} \approx H_3PMo_{12}O_{40} > H_4SiMo_{12}O_{40}$$

The acid strength and the number of acid sites of HPA can be constrained by the structure and the composition of heteropoly anions, the degree of hydration, the type of support, and the thermal pretreatment. Heteroatom and addenda affect the acid strength of heteropoly acids which is decreased when Mo^{6+} or V^{5+} replaces W^{6+} and when Si^{4+} replaces the central P^{5+}. Typically, the acid strength of HPA increases in the order of central atoms $Co^{3+} < B^{3+} < Si^{4+}$, $Ge^{4+} < P^{5+}$, and addenda atoms $V^{5+} < Mo^{6+} < W^{6+}$. Based on the electrostatic theory, the acid strength of heteropoly acids increases with a decrease in the negative charge of the heteropoly anion or an increase in the valence of the central atom [71].

1.3.4.3. Stability of heteropoly acids in solution

Keggin heteropoly acids fully dissociate in aqueous solution, making them strongly acidic. Hydrolysis affects the structure and stability of solvated POMs that mostly depend on pH of solution [71,74,80].

At low pH (≤1.5), Keggin POMs retain the Keggin structure of their heteropoly anion; while at higher pH, the POMs start to degrade loosing addenda atoms to form lacunary species. At pH 2 in aqueous solution, $PW_{12}O_{40}^{3-}$ forms the lacunary anion $PW_{11}0_{39}^{7-}$, as presented in the following equation [71]:

$$PW_{12}O_{40}^{3-} \rightleftharpoons PW_{11}O_{39}^{7-} + W\,(VI)$$

This lacunary anion is stable until pH ~ 8 and then further degrades to give the trivacant lacunary species PW_9.

Generally, the choice of the central atom and addendum atom type is critical for the stabilization of the of heteropoly compounds at a given pH. The stability of heteropoly anions towards hydrolysis in aqueous solution is dependent on the addendum atom type and decreases in the following series [84]:

$$W(VI) > Mo(VI) > V(V)$$

The central atom also affects the stability of the POM, which decreases in the following order:

$$Si^{4+} > Ti^{4+}, Zr^{4+} > Ge^{4+} > P^{5+} > As^{5+}$$

Consequently, the choice of addenda and heteroatoms affects the state of the POM at a given pH. In aqueous solution containing HPO_4^{2-} and MoO_4^{2-} in a 1:12 ratio a variety of POM species can be formed at different pH values, as demonstrated by Petterson et al. [84].

The Keggin anion $[PMo_{12}O_{40}]^{3-}$ exists at pH ≤ 1.5 in solution, but it experiences alkaline hydrolysis as the pH increases. Zhu et al. investigated the decomposition behavior of $[PW_{12}O_{40}]^{3-}$ in aqueous solution with regard to pH and identified the key species present at different pH values, as summarized in Table 1.4 [85].

Table 1.4. POM species found in $[PW_{12}O_{40}]^{3-}$ in aqueous solution at various pH [85].

pH	POM species
1.0	$[PW_{12}O_{40}]^{3-}$
2.2	$[PW_{12}O_{40}]^{3-}$, $[P_2W_{21}O_{71}]^{6-}$, $[PW_{11}O_{39}]^{7-}$
3.5	$[PW_{12}O_{40}]^{3-}$, $[P_2W_{21}O_{71}]^{6-}$, $[PW_{11}O_{39}]^{7-}$, $[P_2W_{18}O_{62}]^{6-}$, $[P_2W_{19}O_{67}]^{10-}$
5.4	$[P_2W_{21}O_{71}]^{6-}$, $[PW_{11}O_{39}]^{7-}$, $[P_2W_{18}O_{62}]^{6-}$
7.3	$[PW_9O_{34}]^{9-}$
8.3	PO_4^{3-}, WO_4^{2-}

In the light of these results, the degradation of most POM species occurs within a narrow pH range, started from the creation of the first lacunary species to complete decomposition to form monomeric anions of their constituent addenda and heteroatoms. Likewise, in liquid-phase oxidation reactions, polyoxometalates may engage in many complex equilibria to form numerous degraded POM species, and several of these can be involved in catalysis.

1.3.4.4. Redox properties of HPAs

HPAs exhibit unique redox properties and are inherently stable under oxidizing environments. Redox chemistry of these polyanions has been subject of much research and has found many applications in chemical analysis and in selective catalytic oxidation. As mentioned previously, addenda atoms in Keggin HPAs can be partially substituted by other metal ions without altering the polyanion structure. Various methods can be used to estimate the oxidizing ability of solid HPAs: rate of reduction, ESR spectra, and XPS spectra of reduced form of HPAs [71].

According to Pope, regarding their redox properties, POMs can be divided into two groups based on the number of terminal oxygen atoms (M=O) attached to each addenda atom in the polyanion: type I (momo-oxo) and type II (cis-dioxo). Type I polyanions have one terminal oxygen atom per each addenda atom; these can be represented by the Keggin and Wells-Dawson anions. While, type II polyanions have two terminal oxygen atoms in cis positions on each addenda atom; these are represented by the Dexter-Silverton anion [71]. POM structures comprised MO_6 octahedra (section 1.3.3.2). The lowest unoccupied molecular orbital in type I octahedra MO_6 is a nonbonding metal-centred orbital, contrary to type II where it is antibonding. Consequently, type I, POMs are reduced easily and reversibly to form mixed-valence species, which retain the structure of the parent oxidized anions. On the other hand, type II POMs are reduced with more difficulty and irreversibly to form complex structures. For this reason, only type I Keggin heteropoly compounds are of interest as the catalysts for oxidation reactions.

The oxidation potentials (*E*) of HPAs are strongly dependent on their addenda atoms and less on their heteroatoms; *E* decreases in the following order [71,75,78]:

V (V) > Mo (VI) >> W (VI)

Catalytic oxidations over HPAs have been widely studied in the past few decades. Especially, the redox properties of mixed-addenda HPAs such as is $H_{3+n}PMo_{12-n}V_nO_{40}$ (HPA–*n*) have attracted attention. HPA–*n* possess a high *E* and their reduced form are easily reoxidized by air in solution, which make them remarkable for catalytic oxidation. The redox mechanism is represented by equations below, where HPA–*n* is $H_{3+n}PMo_{12-n}V_nO_{40}$ [71,86]:

$$\text{HPA}-n + \text{Red} + m\text{H}^+ \longrightarrow \text{H}_m(\text{HPA}-n) + \text{Ox}$$
$$\text{H}_m(\text{HPA}-n) + (m/4)\text{O}_2 \longrightarrow \text{HPA}-n + (m/2)\text{H}_2\text{O}$$

Here Red is the reductant (substrate) and Ox its oxidized form (product). This mechanism involves stoichiometric m-electron oxidation of the substrate by catalyst to form the product and then followed by reoxidation of the reduced form of the catalyst with dioxygen.

The activity of Keggin HPAs in their reduction by hydrogen molecules has been demonstrated by using temperature-programmed reduction (TPR) which increases in the following order [71]:

$H_3PW_{12}O_{40} \approx H_3SiW_{12}O_{40} < H_3PMo_2W_{10}O_{40} < H_3PMo_6W_6O_{40} \approx H_3PMo_{12}O_{40} \leq H_4SiMo_{12}O_{40} \approx H_5PMo_{10}V_2O_{40}$

Therefore, the reduction activity is fairly in line with their oxidation potentials in solution.

1.3.4.5. Supported HPAs

Bulk Keggin HPAs have low specific surface areas (< 10 m^2/g) and high solubility in polar media [87]. This limits their use in heterogeneous catalysis. These limitations can be overcome by loading HPAs on a porous support and by using insoluble metal-exchanged HPAs.

HPA protons can be completely or partially exchanged with metal ions without affecting the primary structure [88]. HPA salts with small cations (Li^+ or Na^+) behave like the bulk acids and have high solubility in water. HPA salts with large cations (K^+, Cs^+) are insoluble in water, exhibit higher surface area (50–200 m^2/g) and higher thermal stability which are beneficial for heterogeneous catalysis [89,90].

Dispersion of HPAs on suitable solid supports with high surface areas is important for catalytic applications. Typically, HPAs are dispersed on a solid support of acidic or neutral nature such as SiO_2, active carbon, etc. [91–93]. This increases the number of active acid sites, thermal stability and, consequently, the catalytic activity is enhanced. The acidity and catalytic activity of supported HPAs depends on the type of support, the HPA loading, condition of pretreatment, etc. [94]. Basic supports like MgO and Al_2O_3 tend to decompose HPA structure due to the instability of HPAs towards bases [95]. Generally, strong interaction between heteropoly acids and support is observed at low HPA loadings, which decreases the acid strength of the HPA. Whilst at high loading, the bulk properties of HPAs are the dominant feature. Hydrogen bonding is a common type of interaction between HPAs and supports [74].

1.4. Use of polyoxometalates in catalysis

POMs/HPAs are widely used in acid catalysis and selective oxidation reactions, which are performed homogeneously in a liquid-phase system or heterogeneously in solid-liquid, solid-gas, or liquid-liquid systems [74,96,97]. In this and later chapters, only POM catalyzed oxidation reactions will be addressed.

1.4.1. Oxidation catalysis by heteropoly acids

The selective oxidation of organic compounds catalyzed in homogeneous and heterogeneous systems by heteropoly compounds has garnered much attention over the last 50 years [71,97–101]. Typically, two types of processes are feasible: (1) oxidative dehydrogenation by removing hydrogen from the target substrate, and (2) oxygenation by oxo-transfer to substrate, as summarized below [102].

$$\mathrm{Sub + OX \xrightarrow{POM\ cat} (Sub)_{Ox} + RED}$$
$$\mathrm{Sub + OD \xrightarrow{POM\ cat} SubO + D}$$

Where: Sub = substrate; OX = oxidant; RED = reduced form of oxidant; and OD = oxygen donor.

Varieties of different oxidants have been checked out for use in metal-catalyzed processes mainly those that operate as oxygen donors. Generally, the most attractive oxidants must have a high content of active oxygen, high selectivity towards the formation of active species or products, cheap to purchase, and friendly to the environment. Amongst the most desirable oxidants, O_2 and H_2O_2 suit the best these criteria. However, the oxidation chemistry of these compounds is complex in some cases and difficult to control [102]. Regarding to catalytic oxidation, polyoxometalates are viewed as robust oxidation-resistant analogues of metallo-macrocyclic compounds because POM ligand in transition metal-substituted POMs is not susceptible to oxidative degradation and thermally more stable than metallo-macrocyclic ligands [71]. Nevertheless, the solvolytic stability of POMs can be a problem in liquid-phase reactions. As discussed earlier (section 1.3.4.3), polyoxometalates in solution tend to decompose to form a variety of lacunary polyanions and mononuclear metallospecies which depend on a series of pH-dependent equilibria. For example, in oxidation reaction with H_2O_2 as an oxidant, lacunary species of POMs can interact with the oxidant to form an active catalyst

peroxo polyoxometalate (peroxo-POM) species [98,103]. While in oxidation reactions with O_2 as an oxidant, the catalytic system often operates via a redox mechanism.

1.4.1.1. Catalytic oxidation with dioxygen

Keggin-type mixed-addenda heteropoly acids $[H_{3+n}PV_nMo_{12-n}O_{40}]^{(3+n)-}$ (HPA–*n*) as catalysts for liquid-phase oxidation with O_2 were first used by Matveev et al. [104,105]. This is the most well-known and versatile system in the POM series for oxidation with O_2. There are numerous attempts to perform aerobic oxidation by other kinds of POMs [102,105,106]. Finke et al. have developed a new type POM in which a metal complex is bounded to the POM's surface, for example, $[(1,5\text{-COD})M.P_2W_{15}Nb_3O_{62}]^{8-}$, where COD is cyclooctadiene and M is Ir^I or Rh^I in the Wells-Dawson POM. These systems showed high activity in cyclohexene oxidation with O_2. Despite the fact that little catalytic chemistry for such systems has been reported so far, they may be promising for future research.

HPA–*n* polyanions are acting efficiently as a reversible redox system in conjunction with O_2 under mild conditions. The reactions catalyzed by HPA–*n* proceed by a stepwise redox mechanism, mentioned in section 1.3.4.5 [107]. The reactions catalyzed by HPA–*n* in conjunction with O_2 require a certain number of V^{5+} ions in the heteropoly anions, which is essential for the oxidation process. The reversible ion transformations are responsible for redox properties of HPA–*n*, where the reduction is accompanied by protonation to keep the charge of the polyanion. HPA–*n* in aqueous solutions are used in the certain pH range from 0.5–3.5, where they are fairly stable [75,104]. HPA–*n* combined with Pd^{II} is the most studied two-component redox system [75,104]. This system is analogous to the Wacker system $CuCl_2$+Pd^{II} that is used for the industrial oxidation of ethylene to acetaldehyde. The advantages of HPA–*n* and Pd^{II} system is that it works in absence of Cl^- ions, is more selective, and less corrosive. A variety of hydrocarbons can be homogeneously oxidized with HPA–*n* as catalyst under mild conditions [71,75]. A number of oxidations with O_2 in the presence of an aldehyde (e.g., 2-

methylpropanal) and $(NH_4)_5H_4[PMo_6V_6O_{40}]$ as a catalyst in dichloroethane solution have been studied by Ishii et al. [108]. The addition of aldehyde, acting as a sacrificial reductant, is a well-known method of promoting the liquid-phase free radical oxidation of organic compounds by O_2. The order of effectiveness of the aldehydes was shown by Mizuno et al. [109]: pivalaldehyde > isobutyraldehyde >> butyraldehyde ≥ acetaldehyde > valeraldehyde > benzaldehyde in the epoxidation of olefins by O_2 at 25 °C by $[PW_{11}O_{39}M]^{x-}$, where M = Co^{II}, $Mn^{II,}$ Fe^{III}, Cu^{II}, or Ni^{II}. In addition to that, the catalytic activity of POM is dependent on solvents; the activity of $[PW_{11}O_{39}M]$ decreases in the series of solvents: $CHCl_3$ > CH_2Cl_2 > 1,2-$C_2H_4Cl_2$ ≥ CH_3CN > C_6H_6 > DMF > DMSO. There is evidence that in the presence of aldehydes, the POM-catalyzed epoxidation of olefins with O_2 proceeds via a radical chain mechanism. Scheme 1.3 shows the mechanism of aldehyde aerobic oxidation catalyzed by POM via acyl peroxo radicals as intermediates [108,110,111].

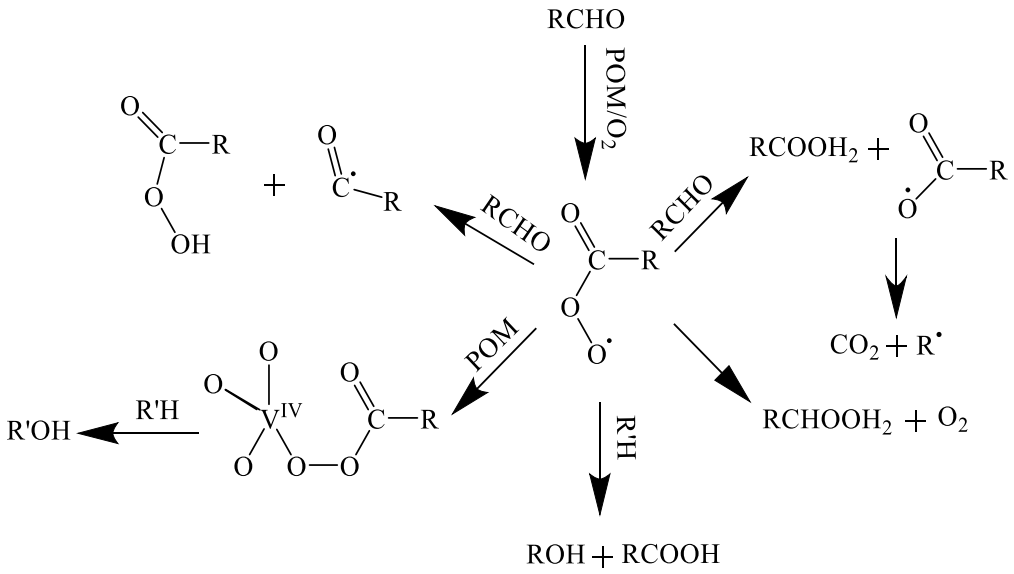

Scheme 1.3. Radical chain mechanism for aldehyde oxidation (adapted from [71]).

Biphasic system has shown an advantage in comparison to homogeneous one for the oxidation of trimethylphenol (TMP) to trimethylbenzoquinone (TMBQ) catalyzed by HPA–*n*. This system allows avoiding difficult separation problem by combining a catalytic reaction and

product separation in one unit. The oxidation TMP to TMBQ in two-phase system gives 84% TMBQ yield at 100% TMP conversion as reported by Kozhevnikov et al. [112]. The lower phase contains the catalyst (HPA–4 solution in AcOH-H_2O) and the upper phase is TMP+TMBQ solution in a hydrocarbon solvent.

The catalytic activity of heteropoly acids is enhanced by supporting them on the activated carbon. It is assumed that activated carbon increases the concentration of substrate and oxygen due to their adsorption in the vicinity of the active site. However, in the case of reactions in polar media such as oxidation of TMP to TMBQ in AcOH-H_2O, leaching of HPA–*n* form carbon support was observed [113].

1.4.1.2. Catalytic oxidation with hydrogen peroxide

Oxidation is a vital application for converting organic and inorganic materials into useful chemicals with a higher oxidation state through the loss of electrons and/or through the addition of oxygen atoms. Oxidation reactions are used for a variety of industrial applications such as manufacture of chemicals, materials, fuels, and the production of key intermediates in the synthesis of drugs [114–116].

Hydrogen peroxide is an attractive reagent for liquid-phase oxidation because it has an atom efficiency of 47% in oxidation reactions, relatively cheap, and produces water as a by-product [117,118]. It has been reported as an effective oxidizing reagent in several reactions including oxidation of alcohols, epoxidation of olefins, and oxidation of sulfides and sulfoxides [104]. Usually, in oxidation reactions, H_2O_2 needs to be activated to be able to transfer an oxygen atom to a target reactant [51,119]. Transition metal catalysts/activators are the most desired to activate H_2O_2 (Scheme 1.4). In this activation method, transition metal species react with H_2O_2 to form active peroxometalate complexes.

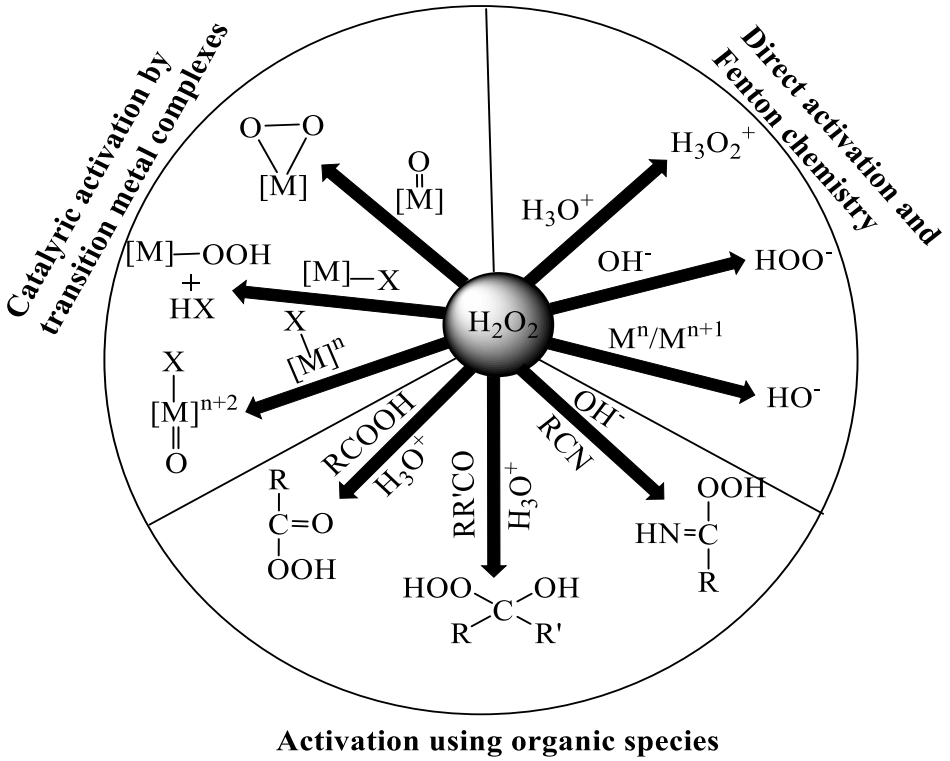

Scheme 1.4. Pathways of activation of hydrogen peroxide (adapted from [51]).

Peroxo complexes are usually generated from the reaction of d^0 transition metal oxo complexes like vanadium, tungsten, molybdenum and rhenium with hydrogen peroxide. Those peroxo complexes are the most active oxidizing agents used for organic transformations (Scheme 1.5). Furthermore, the easy and stable interconversion between oxo and peroxo species has enabled them to be an established catalytic system [51].

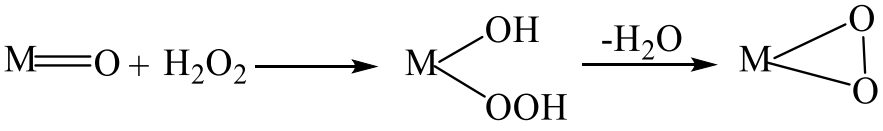

Scheme 1.5. Formation of peroxo complexes via interaction of d^0 transition metal oxo complexes with hydrogen peroxide (adapted from [51]).

It has been shown that the choice of the heteroatom (Se^{VI}, S^{VI}, As^{V}, P^{V}, Si^{IV}, etc.) can affect oxygen transfer activity of the peroxometalate species in epoxidation and sulfoxidation

reactions through the mediation of the Lewis acidity of these groups [120,121]. When using POM as the catalyst, Venturello complex can be formed by interacting POM with H_2O_2; this complex is highly effective catalyst species in epoxidation and sulfoxidation reactions [104,122–125]. Scheme 1.6 shows the operation of the Venturello complex in which heteropolyoxometalate is used as an active catalyst precursor with hydrogen peroxide.

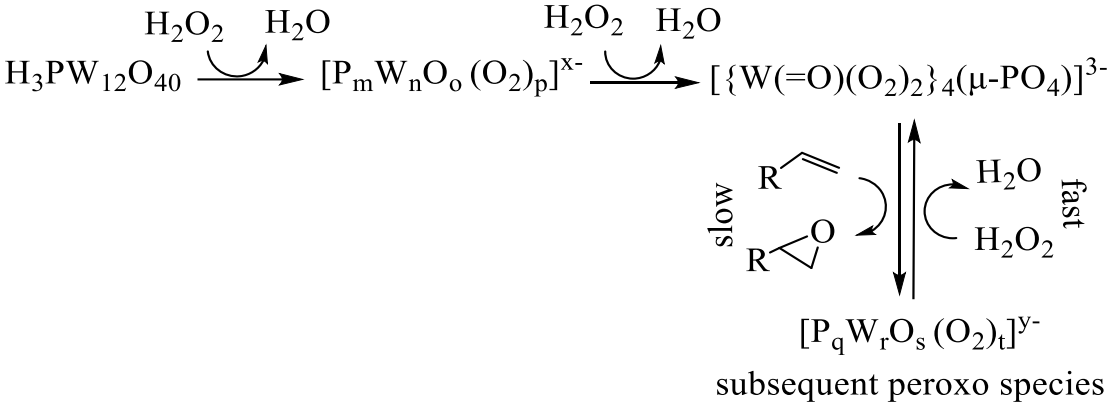

Scheme 1.6. Alkene epoxidation with H_2O_2 mediated by the Venturello peroxo complex $[\{W(=O)(O_2)_2\}_4(\mu\text{-}PO_4)]^{3-}$] (adapted from [104]).

Typically, this system contains two phases: the target olefin in the organic phase and the catalyst and H_2O_2 reagent in the aqueous phase. The key problem with this system is the phase boundary effect that may affect the reaction rate. This problem can be overcome using a phase-transfer catalyst, which facilitates the migration of a reactant in a two-phase system from one phase into the other phase where the reaction occurs [126]. Usually, addition of a solvent that behaves both water-like and organic-like can solve the issue of putting together a water soluble nucleophilic reagent and an organic water insoluble electrophilic reagent. Alternatively, a feasible and industrially efficient method has been developed which involves the use of phase-transfer agents, typically a quaternary ammonium cation, used in catalytic quantities, which transfers reactive anions from the aqueous or solid phase to the organic phase where reaction occurs. This method has proved to be environmentally sustainable and economically beneficial

for synthesizing a wide variety of organic chemicals in the fine chemicals industry. The operation system for polyoxometalate-catalyzed oxidation by phase-transfer with H_2O_2 is called the Venturello-Ishii system [127].

1.4.1.3. The Venturello-Ishii system

Much work on H_2O_2 oxidation catalyzed by heteropoly compounds has been done using Keggin-type tungsten and molybdenum polyoxometalates due to their effectiveness for the oxidation of various organic compounds by H_2O_2 such as olefin epoxidation, oxidation of thiophenes, alcohols, phenols, glycols, etc. [71,100,101,128,129]. In fact, in these reactions, the Keggin polyoxometalates are not the catalyst themselves; active peroxo-POM intermediate species are the catalysts in these reactions, which form as the POMs degrade in the presence of excess H_2O_2. These peroxo-POM species discovered independently by Venturello and Ishii, were shown to be the true catalysts. The peroxo-POM species can be obtained in two ways. Venturello et al. [104,107,123,130] have developed the epoxidation of alkenes in a DCE-H_2O biphasic system at 60–70 ^oC with 2–15% H_2O_2 oxidant. They used WO_4^{2-} and PO_4^{3-} as catalyst precursors in the presence of a quaternary ammonium cation phase-transfer catalyst (PTC) with C_6–C_{18} alkyl groups. In this system, the peroxotungstate anion $\{PO_4[WO(O_2)_2]_4\}^{3-}$, now known as the "Venturello complex" (Fig. 1.11), was isolated and characterized by X-ray analysis [103].

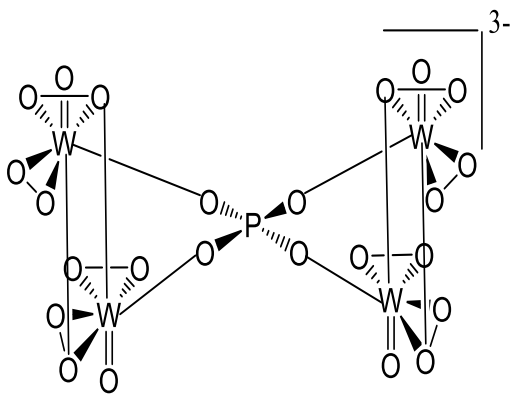

Fig. 1.11. The structure of the Venture complex $\{PO_4[WO(O_2)_2]_4\}^{3-}$ (adapted from [103]).

The peroxotungstate anion consists of the central PO_4 tetrahedron, which is connected by its oxygen atoms to two pairs of distorted pentagonal edge sharing bipyramids $W(O_2)_2O_3$. Each tungsten atom is connected to two types of peroxo groups, one non-bridging (η^2) and the other bridging (η^2, η^1), located in the pentagonal bipyramid equatorial plane [71]. This peroxo complex was postulated to be the catalytically active species in stoichiometric as well as catalytic oxidation of alkenes by H_2O_2. For instance, the epoxidation of 1-octene with 15% H_2O_2 in dichloroethane-water system at 70 °C in the presence of $\{PO_4[WO(O_2)_2]_4\}^{3-}$ affords 89% stereoselective yield of cis-epoxycyclooctane at 100% H_2O_2 conversion in 1.5 h.

Ishii et al. [122,124,131–134] have used another approach. They carried out alkene epoxidation with 35% H_2O_2 in homogeneous or biphasic systems using $H_3PW_{12}O_{40}$ as the catalyst combined with cetylpyridinium chloride (CPC) as a phase transfer agent. Ishii et al. proposed a mechanism of the H_2O_2-based epoxidation of alkenes catalyzed by $H_3PW_{12}O_{40}$ combined with phase transfer agent (Scheme 1.7).

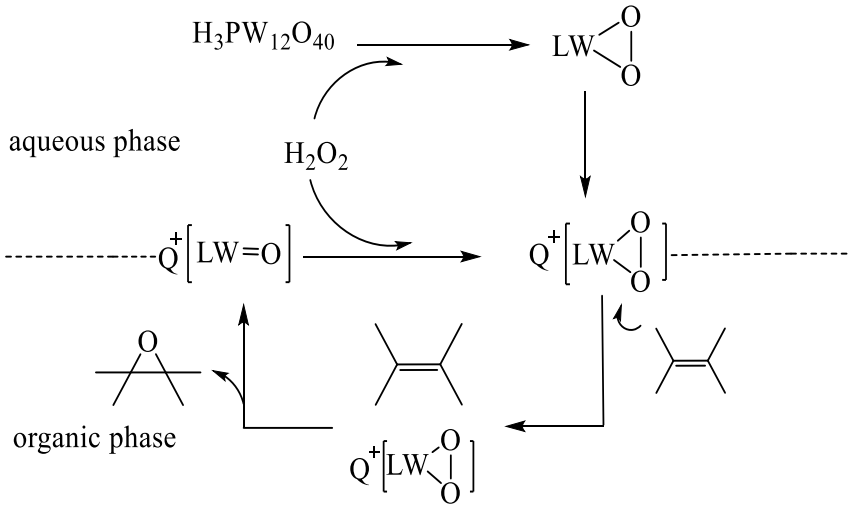

Scheme 1.7. Schematic mechanism of biphasic epoxidation of alkenes catalyzed by $H_3PW_{12}O_{40}$ combined with phase transfer agent Q+.

Later on, Brégeault et al. [135] using the Venturello conditions and Hill et al. [136] using the Ishii conditions have found that the two systems were practically identical, both forming the

same catalytically active peroxo complex $\{PO_4[WO(O_2)_2]_4\}^{3-}$, requiring a PTC to operate. The only difference between the two systems was the choice of catalyst precursors. Presently, the Venturello-Ishii system is widely used for various oxidations by H_2O_2 in the presence of a POM catalyst precursor and a phase transfer catalyst, which is usually a quaternary ammonium cation [100,122,125,137–141].

1.5. Oxidative desulfurization of model diesel fuel catalyzed by POM

Oxidative desulfurization (ODS) is a promising method to remove the refractory aromatic sulfur compounds from diesel fuel. Since 2007, there has been a rapid rise in the use of the ODS. This technology can be applied in homogeneous and heterogeneous systems under very mild conditions at near room temperature and atmospheric pressure. In ODS reaction, the divalent sulfur is oxidized to form the hexavalent sulfur of sulfones by electrophilic addition of oxygen atoms. The product sulfones can be easily removed from fuel by distillation, solvent extraction, adsorption, or decomposition [142]. Keggin heteropoly acids have been found to be most successful catalysts for this reaction due to their highly oxidizing nature [75,143–145]. Typically, the reaction is carried out in a liquid-phase system using H_2O_2 or O_2 as the oxidant. With H_2O_2, the HPA forms the peroxo species, which then oxidize the organosulfur compound to form the corresponding sulfoxide and sulfone under very mild conditions (50–70 ^oC, ambient pressure). Then the products are extracted from the fuel. The ODS with O_2 requires more forcing reaction conditions (100–150 ^oC and often elevated pressure) [146]. Its mechanism is under debate; the reaction may occur via a radical mechanism.

The important advantages of ODS are: high effectiveness of removing the refractory aromatic sulfur compounds such as dibenzothiophene and its derivatives, mild reaction conditions compared to the conventional HDS and hydrogen gas is not required for the ODS to operate [145,146].

1.5.1. Oxidation by H_2O_2

ODS of diesel fuel using H_2O_2 as the oxidant and POMs as the catalysts has attracted much interest [128,147–152]. The ODS reaction can be carried out in biphasic systems in the presence of homogeneous POM catalysts due to the high solubility of most POMs in polar solvents and insolubility in nonpolar solvents. Typically, biphasic systems are composed of an organic layer containing fuel and an aqueous layer containing H_2O_2 and POM. Generally, these systems require an efficient phase-transfer catalyst (PTC) that functions as a ligand to transfer the active peroxo species across the interface [138–141].

Hydrogen peroxide is a common oxidant used to remove the refractory sulfur compounds from the fuel in the ODS process. It has been documented that tungsten catalysts are very efficient for the oxidation of thioethers into sulfoxides and sulfoxides into sulfones by hydrogen peroxide using H_2WO_4 as a catalyst precursor and phenylphosphonic acid acts as an accelerator in a biphasic liquid–liquid system with a phase transfer catalyst (e.g., $CH_3(n\text{-}C_8H_{17})_3N^+$). The reaction occurs as illustrated in Fig. 1.12 [142].

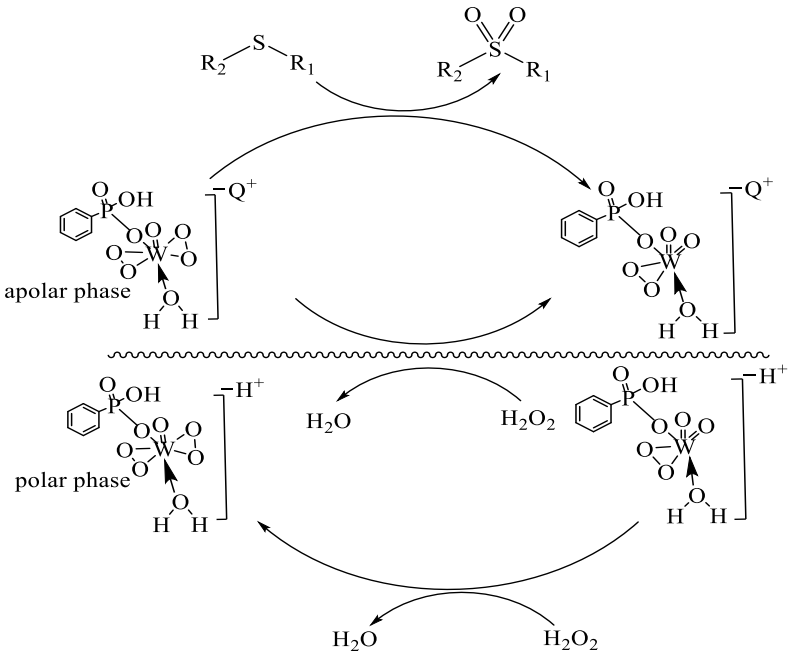

Fig. 1.12. Catalytic cycle for oxidation of sulfur compounds (adapted from [142]).

First, the catalyst precursor H_2WO_4 is rapidly peroxidised by H_2O_2 in the polar phase according to the equation $H_2WO_4 + 2\ H_2O_2 \rightarrow H_2[WO(O_2)_2(OH)_2] + H_2O$ resulting in bisperoxotungstate compound. Second, the bisperoxotungstate is transferred to the apolar phase by the phase transfer agent (Q^+) where thioethers are oxidized into sulfones and bisperoxotungstate compound can then be regenerated with H_2O_2 at the interface or moved into the polar phase to react with hydrogen peroxide. Lastly, the sulfone produced is insoluble in the apolar fuel phase and is transferred to the polar phase yielding a sulfur-free apolar phase.

The oxidation of aromatic sulfur compounds such as benzothiophene, dibenzothiophene and their derivatives has been carried out in an emulsion system (water in oil) composed of a model diesel, 30 wt.% hydrogen peroxide, and an amphiphilic POM catalyst $[C_{18}H_{37}N(CH_3)_3]_4[H_2NaPW_{10}O_{36}]$ under mild conditions [153]. This system exhibits a very high catalytic activity allowing all sulfur-containing compounds to be selectively oxidized into their corresponding sulfones at $H_2O_2/S \leqslant 3$. The reactivity of sulfur-containing compounds was found to be in the following order: benzothiophene < 5-methylbenzothiophene < dibenzothiophene < 4,6-dimethyldibenzothiophene.

The oxidation of dibenzothiophene (DBT) in model oil with H_2O_2 using surfactant-type decatungstates $Q_4W_{10}O_{32}$ {Q = $(CH_3)_3NC_{16}H_{33}$, $(CH_3)_3NC_{14}H_{29}$, $(CH_3)_3NC_{12}H_{25}$, and $(CH_3)_3NC_{10}H_{21}$)} as catalysts has been studied by Jiang et al. [140]. 99.6% DBT conversion has been reached in 1.25 h with $[(CH_3)_3NC_{16}H_{33}]_4W_{10}O_{32}$ as the catalyst. This study demonstrates that the length of carbon chains of quaternary ammonium cations plays a crucial role for the catalytic activity of decatungstate, i.e. the longer the quaternary ammonium cation carbon chain, the better the catalyst activity.

While highly active, the homogeneous POM catalysts have the drawback of their difficult separation from the treated fuel, especially in the presence of a phase transfer catalyst. A more

practical solution for this issue is to use a solid catalyst, which can improve catalyst/fuel separation in liquid-phase systems. Heterogeneous catalysis attracts considerable interest for ODS of transportation fuel.

POMs loaded onto porous supports have many applications in catalysis in liquid phase [106]. The advantage of using supported POM catalysts is in minimizing POM leaching into the product by tightly binding the POM to the support and easy catalyst separation at the end of reaction. In addition to that, supported POM catalysts possess a large surface area, which can enhance their activity as compared to the bulk POM possessing a low surface area. An example of POM catalysts loaded onto suitable supports is zinc-POM supported on activated carbon ($PW_{11}Zn$/AC). It has been shown to be an active and recyclable catalyst for the oxidation of various alcohols into the corresponding carbonyl compounds [154].

Silica-supported tungstate catalyst has been reported to selectively oxidize a variety of sulfides to sulfoxides or sulfones using 30% H_2O_2 [155]. The catalyst can be recovered and reused for at least eight reaction cycles without significant loss of reactivity. POM-based mesoporous silica nanocomposites catalyze the oxidation of various aromatic sulfur-containing compounds using hydrogen peroxide (H_2O_2/S = 4) at 70 ^oC. Most of aromatic sulfur-containing compounds are completely removed in 60 min, and the catalysts can be reused. Mesoporous silica incorporated with phosphomolybdic acid has been investigated on the oxidative desulfurization of the model fuel oil [156]. This catalyst exhibited high catalytic activity by achieving DBT and BT conversion of 100 and 99%, respectively, with hydrogen peroxide (H_2O_2/S = 5.6) at 70 °C and reaction time of 60 and 150 min, respectively. However, catalyst reuse showed a decrease in the activity, which is mainly attributed to the leaching of molybdenum. The problem with heterogeneous ODS catalysis is high consumption of hydrogen peroxide (high H_2O_2/S ratio) and catalyst leaching. These issues are addressed in our research using carbon-supported POM catalysts for the ODS of a model diesel containing benzothiophenes.

1.5.2. Oxidation by dioxygen

The use of inexpensive and abundant oxygen or air for ODS of fuel instead of hydrogen peroxide has long been desired and much research is currently carried out on catalysis for ODS with oxygen [157]. In the ODS with O_2 or air, thiophenic compounds in fuel are oxidized into the corresponding sulfones, which can be readily removed through extraction or adsorption methods. This process is known as aerobic oxidative desulfurization (AODS) [158,159]. HPAs have been reported as highly active catalysts for the aerobic ODS to remove aromatic thiophenic compounds from fuel. The remarkable features of HPAs that are beneficial for ODS catalysis include the possibility of incorporating various transition metal cations into HPA structure, tunable oxidation potential, and the possibility for the reduced forms of HPA to be reoxidised by oxygen in solution [53].

Mixed-addenda heteropoly anions have been an object of research on aerobic oxidation since the 1970s [71]. Thus, the presence of vanadium (V) ion in the HPA structure is of great interest within the field of catalytic oxidation. Vanadium ion plays a crucial role in redox properties of HPA–*n* ($H_{3+n}PV_nMo_{12-n}O_{40}$). Since reported in 1977, HPA–*n* have attracted a lot of interest. It has been reported that up to 60% of aromatic sulfur compounds is converted in 90 min using oxygen as an oxidant and $H_8[PV_5Mo_7O_{40}]$ as catalyst under mild conditions (70 °C and 1 bar O_2). Then the product (sulfuric acid) begins to inhibit the catalyst activity at higher conversions [160].

Sacrificial agents are often used as co-oxidants in the hydrocarbon auto-oxidation with oxygen. This is based on the generation of active species acting as an oxidizing agent to initiate the oxidation process such as peroxy acids, hydroperoxides, and various peroxide radicals. For the initiation of hydrocarbon auto-oxidation reactions, Rao et al. [161] used a combination of aldehyde and molecular oxygen to form acyl radicals. An acylperoxo radical is formed with further incorporation of oxygen, which abstracts a hydrogen atom from another aldehyde

molecule resulting in formation of peroxy acids and another acyl radical at the chain propagation step (Scheme 1.8). Murata et al. showed that a homogeneous catalytic system based on metal salt, aldehyde, and oxygen is active in the ODS reaction of the model diesel fuels [146]. Later, Dumont et al. studied a wide range of various homogeneous and heterogeneous catalysts, and their study indicates that it is not possible to eliminate the presence of homogeneous catalysis when using the supported oxide catalysts [162].

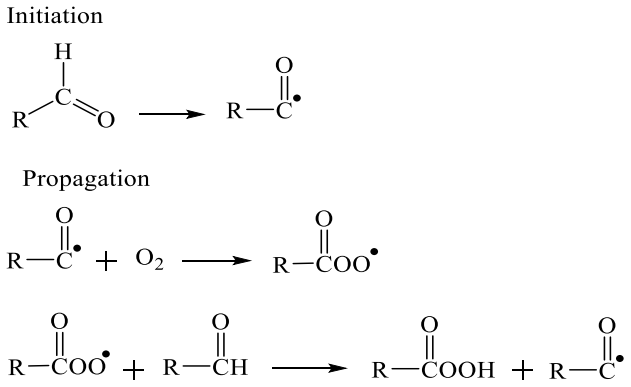

Scheme 1. 8. Mechanism of auto-oxidation of aldehyde to peracid (adapted from [161]).

Heteropoly anions in the presence of co-oxidants have been successfully used in oxidative desulfurization reactions. An emulsion system composed of polyoxometalate anion and surfactant $[C_{18}H_{37}N(CH_3)_3]_5[PV_2Mo_{10}O_{40}]$ has been used for ODS of benzothiophenes with O_2 in the presence of aldehydes under mild conditions [163]. An efficient ODS has been demonstrated by Imtiaz et al. [164] in the presence of the Keggin type heteropolyoxometalate $[C_{16}H_{33}N(CH_3)_3]_3[PW_9Mo_3O_{40}]$ with the addition of formic acid, hydrogen peroxide, and air. The conversion of DBT increased when formic acid and hydrogen peroxide were introduced to the oxidation system due to generating peroxo acid during the reaction [164]. The radical mechanism of the oxidation reaction has been proved by Gomez-Paricio et al. using electron paramagnetic resonance spectroscopy (EPR) and radical scavenging techniques. Evidence of

the formation of radicals $O_2^{\cdot}$ or $HOO^{\cdot}$ has been obtained, which initiate a radical chain auto-oxidation mechanism [165].

1.6. Objectives of study

Prior to this research, it has been demonstrated that polyoxometalates are promising catalysts for ODS reactions using hydrogen peroxide and oxygen as the oxidants. However, there is a room for improving the efficiency of POM catalysts in ODS reactions, in particular regarding their activity and recyclability. This project primarily concerns with the development of highly active heterogenized POM catalysts based on Keggin type heteropoly acids for the biphasic ODS of model diesel fuel comprising heptane and refractory benzothiophenes using hydrogen peroxide as the oxidant. We aim at improving catalysts efficiency and gaining new mechanistic insights into the ODS mechanism. Our main focus is on the investigation of carbon-supported POM catalysts. Very little has been reported so far on the use of activated carbon as the support for the ODS POM catalysts, although activated carbon is documented for adsorption desulfurization of fuels. We also aim at investigating heterogeneous catalysis by POM for the aerobic ODS in the presence of aldehydes as sacrificial reductants to compare with homogeneous POM catalysts for such reactions reported previously.

The thesis is composed of six chapters.

Chapter 1 gives an overview of catalysts that are relevant to this study, desulfurization technologies, along with an overview of the chemistry of heteropoly acids (polyoxometalates) and their catalytic properties. The up-to-date literature on the oxidative desulfurization catalyzed by POM is also reviewed.

Chapter 2 discusses the methodology used in this study. It includes the preparation methods used for the synthesis of catalysts and their modification. Also described are the techniques

used for catalysts characterization and catalyst testing procedure for liquid-phase ODS reactions.

Chapter 3 describes our investigation of heterogeneous catalysis by Keggin-type HPAs ($H_3PMo_{12}O_{40}$, $H_3PW_{12}O_{40}$ and $H_4SiW_{12}O_{40}$) supported on activated carbon Darco KB-B for the biphasic oxidative desulfurization of model diesel fuel (heptane) by aqueous 30% H_2O_2.

Chapter 4 reports the effect of activated carbon support on the activity of carbon-supported Keggin heteropoly acids $H_3PMo_{12}O_{40}$ and $H_3PW_{12}O_{40}$ in the ODS of the model diesel fuel comprising heptane and dibenzothiophene using aqueous 30% H_2O_2 as the oxidant.

Chapter 5 presents aerobic liquid-phase oxidation of dibenzothiophene using bulk and supported heteropoly acids in the presence of aldehydes as radical initiators.

Chapter 6 provides general conclusions on the results obtained in this study and outlines future work.

References

[1] J.G. De Vries, S.D. Jackson, Homogeneous and heterogeneous catalysis in industry, Catal. Sci. Technol. 2 (2012) 2009.

[2] J.C. Barona-Castaño, C.C. Carmona-Vargas, T.J. Brocksom, K.T. De Oliveira, M. Graça, P.M.S. Neves, M. Amparo, F. Faustino, Porphyrins as catalysts in scalable organic reactions, Molecules 21 (2016) 310.

[3] K. Kakaei, M.D. Esrafili, A. Ehsani, Introduction to Catalysis, Interface Sci. Technol. 27 (2019) 1–21.

[4] G. Rothenberg, Catalysis concepts and green application, Wiley-VCH, Weinheim, 2008.

[5] M. Bowker, The basis and application of heterogeneous catalysis, Oxford University Press, 1998.

[6] J.A. Dumesic, G.W. Huber, M. Boudart, Rates of catalytic reaction. In Handbook of heterogeneous catalysis, Wiley-VCH, 2008; p. 1–15.

[7] United States Environmental Protection Agency (EPA), The plain english guide to the clean air act, Washingt. D.C. 2007.

[8] Legislation.gov.uk, Clean air act 1993, https://www.legislation.gov.uk/ukpga/1993/11/introduction (accessed September 1, 2020).

[9] R.A. Henderson, The mechanisms of reactions at transition metal sites, Oxford University Press, 1995.

[10] J.M. Thomas, W.J. Thomas, Principle and practice of heterogeneous catalysis, Wiley-VCH, Weinheim, 1997.

[11] D.J. Adams, P.J. Dyson, S.J. Tavener, Chemistry in alternative reaction media, John Wiley & Sons Itd, Chichester, 2004.

[12] W.M. Nelson, Green solvents for chemistry. Perspectives and practice, Oxford University Press, New York, 2003.

[13] A. Al Ashraf, A. Al Aftab, Distillation process of crude oil, Qatar University, 2012; p. 2–3.

[14] B. Freedman, Environmental ecology: the ecological effects of pollution, disturbance, and other stresses, Elsevier, 1995.

[15] Elgowainy, J. Han, H. Cai, M. Wang, G.S. Forman, V.B. Divita, Energy efficiency and greenhouse gas emission intensity of petroleum products at U.S. Refineries, Environ. Sci. Technol. 48 (2014) 7612–7624.

[16] H.A. Waxman, G.S. Wetstone, P.S. Barnett, Cars, Fuels, and clean air: A review of title II of the clean air act amendments of 1990, Envtl. L. 21 (1991) 1947–2019.

[17] K.O. Blumberg, M.P. Walsh, Low-sulfur gasolineedan diesel: The key to lower vehicle emissions, ICCT 2003.

[18] J.G. Speight, Handbook of petroleum refining, CRC Press 2017.

[19] R. Viskup, Diesel and gasoline engines, IntechOpen 2020.

[20] Air pollution- Raw materials information system,. https://rmis.jrc.ec.europa.eu/?page=air-pollution-41a05f (accessed September 1, 2020).

[21] M. Haghighi, S. Gooneh-Farahani, Insights to the oxidative desulfurization process of fossil fuels over organic and inorganic heterogeneous catalysts: advantages and issues, Environ. Sci. Pollut. Res. 27 (2020) 39923–39945.

[22] H. Kuwahara, Desulfurization of heavy oil, Chem. Econ. Engng. Rev. 5 (1973) 35–40.

[23] I.V. Babich, J.A. Moulijn, Science and technology of novel processes for deep desulfurization of oil refinery streams: A review, Fuel 82 (2003) 607–631.

[24] I. Mochida, K. Sakanishi, X. Ma, S. Nagao, T. Isoda, 1996. Deep hydrodesulfurization

of diesel fuel: Design of reaction process and catalysts. Catal. Today, 29 (1996) 185–189.

[25] A. Röthlisberger, R. Prins, Intermediates in the hydrodesulfurization of 4,6-dimethyl-dibenzothiophene over Pd/γ-Al_2O_3, J. Catal. 235 (2005) 229–240.

[26] A.C. Byrns, W.E. Bradley, M.W. Lee, Catalytic desulfurization of gasolines by cobalt molybdate process, Ind. Eng. Chem. 35 (1943) 1160–1167.

[27] J.S. Eow, Recovery of sulfur from sour acid gas: A review of the technology, Environ. Prog. 21 (2002) 143–162.

[28] W.R. Paterson, Petroleum refining: technology and economics, New york, 1995.

[29] Song, An overview of new approaches to deep desulfurization for ultra-clean gasoline, diesel fuel, and jet fuel, Catal. Today 86 (2003) 211–263.

[30] M. Macaud, A. Milenkovic, E. Schulz, M. Lemaire, M. Vrinat, Hydrodesulfurization of alkyldibenzothiophenes: Evidence of highly unreactive aromatic sulfur compounds, J. Catal. 193 (2000) 255–263.

[31] Mochida, K.H. Choi, An overview of hydrodesulfurization and hydrodenitrogenation, J. Japan Pet. Inst. 47 (2004) 145–163.

[32] Song, X. Ma, New design approaches to ultra-clean diesel fuels by deep desulfurization and deep dearomatization, Appl. Catal. B 41 (2003) 207–238.

[33] M.J. Macías, J. Ancheyta, Simulation of an isothermal hydrodesulfurization small reactor with different catalyst particle shapes, Catal. Today 98 (2004) 243–252.

[34] N. Gupta, P.K. Roychoudhury, J.K. Deb, Biotechnology of desulfurization of diesel: prospects and challenges, Appl. Microbiol. Biotechnol. 66 (2005) 356–366.

[35] A. Abin-fuentes, Ph.D. Dissertation: Mechanistic understanding of microbial desulfurization, Massachusetts Inst. Technol 2013.

[36] N.V. Borzenkova, I.A. Veselova, T.N. Shekhovtsova, Biochemical methods of crude

hydrocarbon desulfurization, Biol. Bull. Rev. 3 (2013) 296–311.

[37] G. Mohebali, A.S. Ball, Biocatalytic desulfurization (BDS) of petrodiesel fuels, Microbiology 154 (2008) 2169–2183.

[38] K.A. Gray, G.T. Mrachkott, C.H. Squires, Biodesulfurization of fossil fuels, Curr. Opin. Microbiol. 6 (2003) 229–235.

[39] V.C Srivastava, An evaluation of desulfurization technologies for sulfur removal from liquid fuels, RSC Adv. 2 (2012) 759–783.

[40] B. Saha, S. Vedachalam, A.K. Dalai, Review on recent advances in adsorptive desulfurization, Fuel Process. Technol. 2020.

[41] H. Song, X.H. Cui, H.L. Song, H.J. Gao, F. Li, Characteristic and adsorption desulfurization performance of Ag-Ce Bimetal Ion-Exchanged Y Zeolite, Ind. Eng. Chem. Res. 53 (2014) 14552–14557.

[42] N.F. Nejad, E. Shams, M.K. Amini, J.C. Bennett, Ordered mesoporous carbon CMK-5 as a potential sorbent for fuel desulfurization: application to the removal of dibenzothiophene and comparison with CMK-3, Microporous Mesoporous Mater 168 (2013) 239–246.

[43] P. Tan, J.X. Qin, X.Q. Liu, X.Q. Yin, L. Bin Sun, Fabrication of magnetically responsive core-shell adsorbents for thiophene capture: $AgNO_3$-functionalized Fe_3O4@mesoporous SiO_2 microspheres, J. Mater. Chem. A 2 (2014) 4698–4705.

[44] Y. Yin, W.J. Jiang, X.Q. Liu, Y.H. Li, L.B. Sun, Dispersion of copper species in a confined space and their application in thiophene capture, J. Mater. Chem. 22 (2012) 18514–18521.

[45] J.X. Guo, X.L. Liu, D.M. Luo, H.Q. Yin, J.J. Li, Y.H. Chu, Influence of calcination temperatures on the desulfurization performance of Fe supported activated carbons treated by HNO_3, Ind. Eng. Chem. Res. 54 (2015) 1261–1270.

[46] G. Yu, S. Lu, H. Chen, Z. Zhu, Diesel fuel desulfurization with hydrogen peroxide promoted by formic acid and catalyzed by activated carbon, Carbon N. Y. 43 (2005) 2285–2294.

[47] J.M. Campos-Martin, M.C. Capel-Sanchez, P. Perez-Presas, J.L.G. Fierro, Oxidative processes of desulfurization of liquid fuels, J. Chem. Technol. Biotechnol. 85 (2010) 879–890.

[48] A.K. Sharipov, V.R. Nigmatullin, Finishing of diesel fuel to remove sulfure compounds after hydrotreating, Chem. Tech. Fuels Oils 41 (2005) 42–43.

[49] S. Otsuki, T. Nonaka, N. Takashima, W. Qian, A. Ishihara, T. Imai, T. Kabe, Oxidative desulfurization of light gas oil and vacuum gas oil by oxidation and solvent extraction, Energy and Fuels 14 (2000) 1232–1239.

[50] M.A. Safa, R. Al-Majren, T. Al-Shamary, J. Il Park, X. Ma, Removal of sulfone compounds formed in oxidative desulfurization of middle distillate, Fuel 194 (2017) 123–128.

[51] J.M. Brégeault, Transition-metal complexes for liquid-phase catalytic oxidation: some aspects of industrial reactions and of emerging technologies, Dalt. Trans. 2003; p. 3289–3302.

[52] J.M. Campos-Martin, G. Blanco-Brieva, J.L.G. Fierro, Hydrogen peroxide synthesis: an outlook beyond the anthraquinone process, Angew. Chemie . Int. Ed. 45 (2006) 6962–6984.

[53] J. Li, Z. Yang, S. Li, Q. Jin, J. Zhao, Review on oxidative desulfurization of fuel by supported heteropolyacid catalysts, J. Ind. Eng. Chem. 82 (2020) 1–16.

[54] Z. Jiang, H. LÜ, Y. Zhang, C. LI, Oxidative desulfurization of fuel oils, Chinese J. Catal. 32 (2011) 707–715.

[55] R.F. Zaykina, Y.A. Zaykin, G. Mirkin, N.K. Nadirov, Prospects for irradiation

processing in the petroleum industry, Radiat. Phys. Chem. 63 (2002) 617–620.

[56] Y. Shiraishi, Y. Taki, T. Hirai, I. Komasawa, Visible light-induced deep desulfurization process for light oils by photochemical electron-transfer oxidation in an organic two-phase extraction system, Ind. Eng. Chem. Res. 38 (1999) 3310–3318.

[57] H. Mei, B.W. Mei, T.F. Yen, A new method for obtaining ultra-low sulfur diesel fuel via ultrasound assisted oxidative desulfurization, Fuel 82 (2003) 405–414.

[58] W.Y. Liu, Z.L. Lei, J.K. Wang, Kinetics and mechanism of plasma oxidative desulfurization in liquid phase, Energy and Fuels 15 (2001) 38–43.

[59] F. Zannikos, E. Lois, S. Stournas, Desulfurization of petroleum fractions by oxidation and solvent extraction, Fuel Process. Technol. 42 (1995) 35–45.

[60] W. Gore, Method of desulfurization of hydrocarbons, U.S. Patent 6,274,785, 2001.

[61] M.J. Grossman, M. Siskin, D.T. Ferrughelli, M.K. Lee, J.D. Senius, Method for the removal of organic sulfur from carbonaceous materials, , U.S. Patent 5,910,440, 1999.

[62] H. Zhao, S. Xia, P. Ma, Use of ionic liquids as ‘green’ solvents for extractions, J. Chem. Technol. Biotechnol. 80 (2005) 1089–1096.

[63] Lissner, W.F. de Souza, B. Ferrera, J. Dupont, Oxidative desulfurization of fuels with task-specific ionic liquids, ChemSusChem 2 (2009) 962–964.

[64] L. He, H. Li, W. Zhu, J. Guo, X. Jiang, J. Lu, Y. Yan, Deep oxidative desulfurization of fuels using peroxophosphomolybdate catalysts in ionic liquids, Ind. Eng. Chem. Res. 47 (2008) 6890–6895.

[65] W. Zhu, H. Li, X. Jiang, Y. Yan, J. Lu, J. Xia, Oxidative desulfurization of fuels catalyzed by peroxotungsten and peroxomolybdenum complexes in ionic liquids, Energy & Fuels 21 (2007) 2514–2516.

[66] J.J. Berzelius, The preparation of phosphomolybdate ion $[PMo_{12}O_{40}]^{3-}$, Pogg. Ann. 6 (1826) 369–371.

[67] W.N. Lipscomb, Paratungstate ion, Inorg. Chem. 4 (1965) 132–134.

[68] J.F. Keggin, The structure and formula of 12-phosphotungstic acid, Proc. Roy. Soc. London. Ser. A 144 (1934) 75–100.

[69] H.T. Evans Jr, The crystal structure of ammonium and potassium molybdotellurates, J. Am. Chem. Soc. 70 (1948) 1291–1292.

[70] B. Dawson, The structure of the 9(18)-heteropoly anion in potassium 9(18)-tungstophosphate, $K_6(P_2W_{18}O_{62})14H_2O$, Acta Crystallogr. 6 (1953) 113–126.

[71] I.V. Kozhevnikov, Catalysts for fine chemical, catalysis by polyoxometalates, Wiley, 2002.

[72] L.C.W. Baker, D.C. Glick, Present general status of understanding of heteropoly electrolytes and a tracing of some major highlights in the history of their elucidation, Chem. Rev. 98 (1998) 3–49.

[73] J.B. Moffat, Metal–oxygen clusters: The surface and catalytic properties of heteropolyoxometalates, Kluwer, New York, 2002.

[74] T. Okuhara, N. Mizuno, M. Misono, Catalytic chemistry of heteropoly compounds, Academic Press 1996; p. 113–252.

[75] I.V. Kozhevnikov, Catalysis by heteropoly acids and multicomponent polyoxometalates in liquid-phase reactions, Chem. Rev. 98 (1998) 171–198.

[76] I.V. Kozhevnikov, Advances in catalysis by heteropolyacids, Russ. Chem. Rev. 56 (1987) 811–825.

[77] M. Misono, Unique acid catalysis of heteropoly compounds (heteropolyoxometalates) in the solid state, Chem. Commun 13 (2001) 1141–1152.

[78] H. Li, J. Gupta, S. Wang, N. Zhang, C. Bubeck, Photoreduction of graphene oxide with polyoxometalate clusters and its enhanced saturable absorption, J. Colloid Interface Sci. 427 (2014) 25–28.

[79] H. Sartzi, H.N. Miras, L. Vilà-Nadal, D.L. Long, L. Cronin, Trapping the δ isomer of the polyoxometalate-based keggin cluster with a tripodal ligand, Angew. Chemie Int. Ed. 54 (2015) 15488–15492.

[80] M.T. Pope, Heteropoly and isopoly oxometalates, Angew. Chem. Int. Ed. Engl. 23 (1984) 829–830.

[81] I.V. Kozhevnikov, Sustainable heterogeneous acid catalysis by heteropoly acids, Handb, Green Chem. 2010; p. 153–174.

[82] T.V. Andrushkevich, V.M. Bondareva, R.I. Maksimovskaya, G.Y. Popova, L.M. Plyasova, G.S. Litvak, A. V Ziborov, Thermolysis of heteropolyacid $H_3PMo_{12}O_{40}$ and catalytic properties of the thermal decomposition products in oxidation of acrolein to acrylic acid, Elsevier 1994; p. 837–844.

[83] J. Fraissard, L. Petrakis, Acidity and basicity of solids: theory, assessment and utility, Kluwer Academic, Dordrecht, 49 (1994) 1–513

[84] L. Pettersson, I. Andersson, L.O. Ohman, Multicomponent polyanions: speciation in the Aqueous H^+-MoO_4^{2-}-HPO_4^{2-} system as deduced from a combined Emf-^{31}P NMR Study, Inorg. Chem. 25 (1986) 4726–4733.

[85] Z. Zhu, R. Tain, C. Rhodes, A study of the decomposition behaviour of 12-tungstophosphate heteropolyacid in solution, Can. J. Chem. 81 (2003) 1044–1050.

[86] J.J. Altenau, M.T. Pope, R.A. Prados, H. So, Models for heteropoly blues, degrees of valence trapping in vanadium(IV)- and molybdenum(V)-substituted keggin anions, Inorg. Chem. 14 (1975) 417–421.

[87] J.E. Herrera, J.H. Kwak, J.Z. Hu, Y. Wang, C.H.F. Peden, Effects of novel supports on the physical and catalytic properties of tungstophosphoric acid for alcohol dehydration reactions, Top. Catal. 49 (2008) 259–267.

[88] N. Mizuno, M. Misono, Heteropolyanions in catalysis, J. Mol. Catal. 86 (1994) 319–

342.

[89] M.T. Pope, A. Müller, Polyoxometalate chemistry: an old field with new dimensions in several disciplines, Angew. Chemie Int. Ed. Engl. 30 (1991) 34–48.

[90] N. Essayem, R. Frety, G. Coudurier, J.C. Vedrine, Ammonia adsorption-desorption over the strong solid acid catalyst $H_3PW_{12}O_{40}$ and its Cs^+ and NH^{4+} salts comparison with sulfated zirconia, J. Chem. Soc. Faraday Trans. 93 (1997) 3243–3248.

[91] Y. Izumi, R. Hasebe, K. Urabe, Catalysis by heterogeneous supported heteropoly acid, J. Catal. 84 (1983) 402–409.

[92] Y. Izumi, K. Urabe, Catalysis of heteropoly acids entrapped in activated carbon, Chem. Lett. 10 (1981) 663–666.

[93] M.A. Schwegler, P. Vinke, M. van der Eijk, H. van Bekkum, Activated carbon as a support for heteropolyanion catalysts, Appl. Catal. A 80 (1992) 41–57.

[94] J.H. Clark, A.P. Kybett, D.J. Maequarrie, Supported reagents: preparation, analysis, and applications, JWS. 1992.

[95] T. Matsuda, A. Igarashi, Y. Ogino, Catalyst for synthesis of methyl tertiary butyl ether. J. Jpn. Pet. Inst. 23 (1980) 30–34.

[96] P. Zhao, M. Zhang, Y. Wu, J. Wang, Heterogeneous selective oxidation of sulfides with H_2O_2 catalyzed by ionic liquid-based polyoxometalate salts, Ind. Eng. Chem. Res. 51 (2012) 6641–6647.

[97] C. Komintarachat, W. Trakarnpruk, Oxidative desulfurization using polyoxometalates, Ind. Eng. Chem. Res. 45 (2006) 1853–1856.

[98] J.M. Brégeault, M. Vennat, L. Salles, J.Y. Piquemal, Y. Mahha, E. Briot, P.C. Bakala, A. Atlamsani, R. Thouvenot, From polyoxometalates to polyoxoperoxometalates and back again; potential applications, J. Mol. Catal. A Chem. 250 (2006) 177–189.

[99] N. Mizuno, K. Yamaguchi, Polyoxometalate catalysts: Toward the development of

green H_2O_2-based epoxidation systems, Chem. Rec. 6 (2006) 12–22.

[100] N. Mizuno, K. Yamaguchi, K. Kamata, Epoxidation of olefins with hydrogen peroxide catalyzed by polyoxometalates, Coord. Chem. Rev. 249 (2005) 1944–1956.

[101] Y. Zhou, G. Chen, Z. Long, J. Wang, Recent advances in polyoxometalate-based heterogeneous catalytic materials for liquid-phase organic transformations, RSC Adv. 4 (2014) 42092–42113.

[102] C.L. Hill, C.M. Prosser-McCartha, Homogeneous catalysis by transition metal oxygen anion clusters, Coord. Chem. Rev. 143 (1995) 407–455.

[103] C. Venturello, R. D'Aloisio, J.C.J. Bart, M. Ricci, A new peroxotungsten heteropoly anion with special oxidizing properties: synthesis and structure of tetrahexylammonium tetra(diperoxotungsto)phosphate(3-), J. Mol. Catal. 32 (1985) 107–110.

[104] J.H. Grate, D.R. Hamm, S. Mahajan, Palladium and phosphomolybdovanadate catalyzed olefin oxidation to carbonyls, Mol. Eng. 3 (1993) 205–229.

[105] K.I. Matveev, E.G. Zhizhina, N.B. Shitova, L.I. Kuznetsova, Catalysis of organic reaction by heteropoly acids, Kinet Katal. 18 (1977) 380.

[106] R. Neumann, Polyoxometalate complexes in organic oxidation chemistry, Prog. Inorg. Chem. 47 (1998) 317–370.

[107] N. Mizuno, H. Weiner, R.G. Finke, Co-oxidative epoxidation of cyclohexene with molecular oxygen, isobutraldehyde reductant, and the polyoxoanino-supported catalyst precursor $[(n\text{-}C_4H_9)_4N]_5Na_3[(1,5\text{-COD})Ir\ P_2W_{15}Nb_3O_{62}]$, J. Mol. Catal. A Chem. 114 (1996) 15–28.

[108] M. Hamamoto, K. Nakayama, Y. Nishiyama, Y. Ishii, Oxidation of organic substrates by a molecular oxygen/aldehyde/heteropolyoxometalate system, J. Org. Chem. 58 (1993) 6421–6425.

[109] N. Mizuno, T. Hirose, M. Tateishi, M. Iwamoto, A pronounced catalytic activity of

$PW_{11}CoO_{39}^{5-}$ for epoxidation of alkenes by molecular oxygen in the presence of aldehyde, Chem. Lett. 22 (1993) 1839–1842.

[110] H. Weiner, A. Trovarelli, R.G. Finke, Polyoxoanion-supported catalysis : evidence for a $P_2W_{15}Nb_3O_{62}^{9-}$ -supported iridium cyclohexene oxidation catalyst starting from [n-Bu_4N]$_5Na_3$ (1,5-COD) Ir $P_2W_{15}Nb_3O_{62}$], J. Mol. Catal. 191 (2003) 253–279.

[111] O.A. Kholdeeva, V.A. Grigoriev, G.M. Maksimov, M.A. Fedotov, A. V. Golovin, K.I. Zamaraev, Polyfunctional action of transition metal substituted heteropolytungstates in alkene epoxidation by molecular oxygen in the presence of aldehyde, J. Mol. Catal. A Chem. 114 (1996) 123–130.

[112] I.V. Kozhevnikov, $PMo_{(12-n)}V_{(n)}O_{40/(3+n)}$- heteropolyanions as catalysts for aerobic oxidation, J. Mol. Catal. A Chem. 117 (1997) 151–158.

[113] S. Fujibayashi, K. Nakayama, M. Hamamoto, S. Sakaguchi, Y. Nishiyama, Y. Ishii, An efficient aerobic oxidation of various organic compounds catalyzed by mixed addenda heteropolyoxometalates containing molybdenum and vanadium, J. Mol. Catal. A Chem. 110 (1996) 105–117.

[114] G. Centi, S. Perathoner, Selective oxidation‐ industrial, Encycl. Catal. 2002.

[115] B. Testa, S.D. Krämer, The biochemistry of drug metabolism–an Introduction, Chem. Biodivers. 6 (2009) 591–684.

[116] A. Scarso, G. Strukul, Transition-metal–catalyzed stereoselective oxidations in drug and natural product synthesis, Stereo. Synth. Drugs Nat. Prod. 2013; p. 1–28.

[117] C.W. Jones, J.H. Clark, M.J. Braithwaite, Applications of hydrogen peroxide and derivatives, R. Soc. chem, Cambridge, 1999.

[118] G. Strukul, Catalytic oxidations with hydrogen peroxide as oxidant, SSBM. 2013.

[119] W.R. Sanderson, Cleaner industrial processes using hydrogen peroxide, Pure Appl. Chem. 72 (2000) 1289–1304.

[120] K. Kamata, T. Hirano, S. Kuzuya, N. Mizuno, Hydrogen-bond-assisted epoxidation of homoallylic and allylic alcohols with hydrogen peroxide catalyzed by selenium-containing dinuclear peroxotungstate, J. Am. Chem. Soc. 131 (2009) 6997–7004.

[121] B. Zhu, Z.L. Lang, L.K. Yan, M.R.S.A. Janjua, Z.M. Su, A comparative DFT study on the mechanism of olefin epoxidation catalyzed by substituted binuclear peroxotungstates ($[SeO_4WO(O_2)_2MO(O_2)_2]^{n-}$ (M = Ti^{IV}, V^{V}, Ta^{V}, Mo^{VI}, W^{VI}, Tc^{VII}, and Re^{VII})), Int. J. Quantum Chem. 114 (2014) 458–462.

[122] C. Venturello, R. D'Aloisio, Quaternary ammonium tetrakis(diperoxotungsto)phosphates(3-) as a new class of catalysts for efficient alkene epoxidation with hydrogen peroxide, J. Org. Chem. 53 (1988) 1553–1557.

[123] C. Venturello, E. Alneri, M. Ricci, A new, effective catalytic system for epoxidation of olefins by hydrogen peroxide under phase-transfer conditions, J. Org. Chem. 48 (1983) 3831–3833.

[124] S. Sakaue, T. Tsubakino, Y. Nishiyama, Y. Ishii, Oxidation of aromatic amines with hydrogen peroxide catalyzed by cetylpyridinium heteropolyoxometalates, J. Org. Chem. 58 (1993) 3633–3638.

[125] Y. Ishii, K. Yamawaki, T. Ura, H. Yamada, T. Yoshida, M. Ogawa, Hydrogen peroxide oxidation catalyzed by heteropoly acids combined with cetylpyridinium chloride, epoxidation of olefins and allylic alcohols, ketonization of alcohols and diols, and oxidative cleavage of 1,2-diols and olefins, J. Org. Chem. 53 (1988) 3587–3593.

[126] O. Bortolini, F. Di Furia, G. Modena, R. Seraglia, Metal catalysis in oxidation by peroxides. Sulfide oxidation and olefin epoxidation by dilute hydrogen peroxide, catalyzed by molybdenum and tungsten derivatives under phase-transfer conditions, J. Org. Chem. 50 (1985) 2688–2690.

[127] S.D. Naik, L.K. Doraiswamy, Phase transfer catalysis: Chemistry and engineering,

AIChE J. 44 (1998) 612–646.

[128] Y. Zhou, Z. Guo, W. Hou, Q. Wang, J. Wang, Polyoxometalate-based phase transfer catalysis for liquid–solid organic reactions: a review, Catal. Sci. Technol. 5 (2015) 4324–4335.

[129] S.S. Wang, G.Y. Yang, Recent advances in polyoxometalate-catalyzed reactions, Chem. Rev. 115 (2015) 4893–4962.

[130] C. Venturello, M. Gambaro, A convenient catalytic method for the dihydroxylation of alkenes by hydrogen peroxide, Synth. Stuttg. 4 (1989) 295–297.

[131] G.D. Yadav, A.A. Pujari, Epoxidation of styrene to styrene oxide: synergism of heteropoly acid and phase-transfer catalyst under Ishii−Venturello mechanism, Org. Process Res. Dev. 4 (2000) 88–93.

[132] Y. Matoba, H. Inoue, J.-I. Akagi, T. Okabayashi, Y. Ishii, M. Ogawa, Epoxidation of allylic alcohols with hydrogen peroxide catalyzed by $[PMO_{12}O_{40}]^{3-}$ $[C_5H_5N^+(CH_2)_{15}CH3]_3$, Synth. Commun. 14 (1984) 865–873.

[133] S. Sakaguchi, S. Watase, Y. Katayama, Y. Sakata, Y. Nishiyama, Y. Ishii, Oxidation of allenes and alkynes with hydrogen peroxide catalyzed by cetylpyridinium peroxotungstophosphate (PCWP), J. Org. Chem. 59 (1994) 5681–5686.

[134] H. Yamamoto, M. Tsuda, S. Sakaguchi, Y. Ishii, Selective oxidation of vinyl ethers and silyl enol ethers with hydrogen peroxide catalyzed by peroxotungstophosphate, J. Org. Chem. 62 (1997) 7174–7177.

[135] L. Salles, C. Aubry, R. Thouvenot, F. Robert, C. Doremieux-Morin, G. Chottard, H. Ledon, Y. Jeannin, J.M. Bregeault, ^{31}P and ^{183}W NMR spectroscopic evidence for novel peroxo species in the "$H_3[PW_{12}O_{40}]$.cntdot.yH_2O/H_2O_2" system, synthesis and X-ray structure of tetrabutylammonium (.mu.-Hydrogen phosphato)bis(.mu.-peroxo)bis(oxoperoxotungstate) (2-): a catalyst of olefin epoxidation in a biphase

medium, Inorg. Chem. 33 (1994) 871–878.

[136] D.C. Duncan, R.C. Chambers, E. Hecht, C.L. Hill, Mechanism and dynamics in the $H_3[PW_{12}O_{40}]$-catalyzed selective epoxidation of terminal olefins by H_2O_2, formation, reactivity, and stability of $\{PO_4[WO(O_2)_2]4\}^{3-}$, J. Am. Chem. Soc. 117 (1995) 681–691.

[137] W. Zhao, B. Ma, H. Hua, Y. Zhang, Y. Ding, Environmentally friendly and highly efficient alkenes epoxidation system consisting of $[\pi\text{-}C_5H_5N(CH_2)_{11}CH3]3PW_4O_{32}/H_2O_2$/ethyl acetate/olefin, Catal. Commun 9 (2008) 2455–2459.

[138] F.M. Collins, A.R. Lucy, C. Sharp, Oxidative desulfurization of oils via hydrogen peroxide and heteropolyanion catalysis, J. Mol. Catal. A Chem. 117 (1997) 397–403.

[139] Huang, Y.J. Wang, L.M. Yang, G.S. Luo, Chemical oxidation of dibenzothiophene with a directly combined amphiphilic catalyst for deep desulfurization, Ind. Eng. Chem. Res. 45 (2006) 1880–1885.

[140] X. Jiang, H. Li, W. Zhu, L. He, H. Shu, J. Lu, Deep desulfurization of fuels catalyzed by surfactant-type decatungstates using H_2O_2 as oxidant, Fuel 88 (2009) 431–436.

[141] D. Huang, Z. Zhai, Y.C. Lu, L.M. Yang, G.S. Luo, Optimization of composition of a directly combined catalyst in dibenzothiophene oxidation for deep desulfurization, Ind. Eng. Chem. Res. 46 (2007) 1447–1451.

[142] M.C. Capel-Sanchez, P. Perez-Presas, J.M. Campos-Martin, J.L.G. Fierro, Highly efficient deep desulfurization of fuels by chemical oxidation, Catal. Today 2010.

[143] A.E.S. Choi, S. Roces, N. Dugos, M.W. Wan, Oxidation by H_2O_2 of bezothiophene and dibenzothiophene over different polyoxometalate catalysts in the frame of ultrasound and mixing assisted oxidative desulfurization, Fuel 180 (2016) 127–136.

[144] J. He, P. Wu, Y. Wu, H. Li, W. Jiang, S. Xun, M. Zhang, W. Zhu, H. Li, Taming

interfacial oxygen vacancies of amphiphilic tungsten oxide for enhanced catalysis in oxidative desulfurization, ACS Sustain. Chem. Eng. 5 (2017) 8930–8938.

[145] D.D. Whitehurst, T. Isoda, I. Mochida, Challenges in the hydrodesulfurization of polyaromatic sulfur compounds, Adv. Catal. 42 (1998) 345–471.

[146] S. Murata, K. Murata, K. Kidena, M. Nomura, A novel oxidative desulfurization system for diesel fuels with molecular oxygen in the presence of cobalt catalysts and aldehydes, Energy & Fuels 18 (2004) 116–121.

[147] M. Misono, N. Nojiri, Recent progress in catalytic technology in japan, Appl. Catal. 64 (1990) 1–30.

[148] X. Liu, Y. Ryabenkova, M. Conte, Catalytic oxygen activation versus autoxidation for industrial applications: a physicochemical approach, Phys. Chem. Chem. Phys. 17 (2015) 715–731.

[149] Papaconstantinou, Photochemistry of polyoxometallates of molybdenum and tungsten and/or vanadium, Chem. Soc. Rev. 18 (1989) 1–31.

[150] T. Yamase, Photo- and electrochromism of polyoxometalates and related materials, Chem. Rev. 98 (1998) 307–325.

[151] L.I Kuznetsova, G.M. Maksimov, V.A. Likholobov, Polyoxometalates for the study of active sites in catalytic transformations of organic substances, Kinet. Catal. 40 (1999) 622–637.

[152] M. Misono, I. Ono, G. Koyano, A. Atsushi, Heteropolyacids: versatile green catalysts in various reaction media, Pure Appl. Chem. 72 (2000) 1305–1311.

[153] Lü, J. Gao, Z. Jiang, F. Jing, Y. Yang, G. Wang, C. Li, Ultra-deep desulfurization of diesel by selective oxidation with $[C_{18}H_{37}N(CH_3)_3]_4[H_2NaPW_{10}O_{36}]$ catalyst assembled in emulsion droplets, J. Catal. 239 (2006) 369–375.

[154] E. Assady, B. Yadollahi, M. Riahi Farsani, M. Moghadam, Zinc polyoxometalate on

activated carbon: an efficient catalyst for selective oxidation of alcohols with hydrogen peroxide, Appl. Organomet. Chem. 29 (2015) 561–565.

[155] B. Karimi, M. Ghoreishi-Nezhad, J.H. Clark, Selective oxidation of sulfides to sulfoxides using 30% hydrogen peroxide catalyzed with a recoverable silica-based tungstate interphase catalyst, Org. Lett. 7 (2005) 625–628.

[156] J. Qiu, G. Wang, Y. Zhang, D. Zeng, Y. Chen, Direct synthesis of mesoporous $H_3PMo_{12}O_{40}/SiO_2$ and its catalytic performance in oxidative desulfurization of fuel oil, Fuel147 (2015) 195–202.

[157] Shafiq, S. Shafique, P. Akhter, M. Ishaq, W. Yang, M. Hussain, Recent breakthroughs in deep aerobic oxidative desulfurization of petroleum refinery products, J. Clean. Prod. 2020.

[158] Y. Lu, Y. Wang, L. Gao, J. Chen, J. Mao, Q. Xue, Y. Liu, H. Wu, G. Gao, M. He, Aerobic oxidative desulfurization: a promising approach for sulfur removal from fuels, ChemSusChem 1 (2008) 302–306.

[159] Y. Zhang, R. Wang, Recent advances on catalysts and systems for the oxidation of thiophene derivatives in fuel oil with molecular oxygen, Mini. Rev. Org. Chem. 15 (2018) 488–497.

[160] Claußnitzer, B. Bertleff, W. Korth, J. Albert, P. Wasserscheid, A. Jess, Kinetics of triphase extractive oxidative desulfurization of benzothiophene with molecular oxygen catalyzed by HPA–5, Chem. Eng. Technol. 43 (2020) 465–475.

[161] T.V. Rao, B. Sain, S. Kafola, B.R. Nautiyal, Y.K. Sharma, S.M. Nanoti, M.O. Garg, Oxidative desulfurization of HDS diesel using the aldehyde/molecular oxygen oxidation system, Energy and Fuels 21 (2007) 3420–3424.

[162] V. Dumont, L. Oliviero, F. Maugé, M. Houalla, Oxidation of dibenzothiophene by a metal-oxygen-aldehyde system, Catal. Today 130 (2008) 195–198.

[163] H. Lü, J. Gao, Z. Jiang, Y. Yang, B. Song, C. Li, Oxidative desulfurization of dibenzothiophene with molecular oxygen using emulsion catalysis, Chem. Commun. 2 (2007) 150–152.

[164] A. Imtiaz, A. Waqas, I. Muhammad, Desulfurization of liquid fuels using air-assisted performic acid oxidation and emulsion catalyst, Chin. J. Catal. 34 (2013) 1839–1847.

[165] A. Gómez-Paricio, A. Santiago-Portillo, S. Navalón, P. Concepción, M. Alvaro, H. Garcia, MIL-101 promotes the efficient aerobic oxidative desulfurization of dibenzothiophenes, Green Chem. 18 (2016) 508–515.

2 Experimental part

This chapter describes in detail all steps that were followed in the study of the oxidative desulfurization of model diesel fuel containing aromatic organosulfur compounds catalyzed by carbon-supported heteropoly acids in the presence of H_2O_2 and air as oxidant. It will begin by discussing catalyst preparations. Then move on to describe the techniques that were used to characterize the structure, stability, and properties of these catalysts. Finally, it will conclude by outlining the procedures for the reaction studies, conditions, and reusability.

2.1. Chemicals and solvents

Benzothiophene (BT, 99%), 4,6-dimethyldibenzothiophene (DMBDT, 97%) dibenzothiophene ($C_{12}H_8S$, 98%), and dibenzothiophene sulfone ($C_{12}H_8SO_2$, 97%) were purchased from Sigma/Aldrich and used without further treatment. For the preparation of carbon-supported HPA catalysts, a variety of activated carbons were purchased from Sigma-Aldrich. Heptane (Sigma-Aldrich, 99%), dodecane (Sigma-Aldrich, 99%), and toluene (BDH AnalaR, 99.5%) were used as solvents, dodecane (Aldrich, 99%) and tetradecane (Sigma-Aldrich, 99%) as internal standards for GC analysis, and toluene (Aldrich, 99%) and 1,2-dichloroethane (Fisher Scientific) and diethyl ether (Sigma-Aldrich, 99.8%) as extraction solvents. Distilled H_2O was used from the Fistreem Calypso water distiller (single distilled water with pH 5.6–6.0 and conductivity 1μS cm^{-1}). Heteropoly acids tested in this work were commercially available compounds. These compounds were obtained from Sigma-Aldrich and were used without further treatment; phosphomolybdic acid hydrate ($H_3PMo_{12}O_{40}.xH_2O$, 99.9%), phosphotungstic acid hydrate ($H_3PW_{12}O_{40}.xH_2O$, 99%), silicotungstic acid hydrate

($H_4SiW_{12}O_{40}.xH_2O$, 99.9%), disodium phosphate (99%), sodium metavanadate (99.9%), sodium molybdate dihydrate (99%), cesium carbonate (99.9%), and sodium carbonate (99.9%). Hydrogen peroxide (30 wt.% H_2O_2, Sigma-Aldrich) was used as the oxidant; its concentration in the reaction mixture was monitored before and after each reaction by titration with standardized 0.005 M $KMnO_4$. Benzaldehyde as a sacrificial reductant was purchased from Fisher Scientific. 1,4-Benzoquinone (Aldrich) and 2,6-di-tert-butyl-4-methylphenol (Lancaster Synthesis) were used as inhibitors.

2.2. Catalyst preparation

2.2.1. Carbon-supported HPA catalysts

Keggin-type HPA hydrates (HPMo, HPW, and HSiW) were used for the preparation of carbon-supported HPA catalysts, with a range of activated carbons as supports by impregnating the HPAs onto activated carbons from aqueous solution. The amount of crystallization water in HPA hydrates was determined by TGA to adjust the weight of each HPA. Anhydrous HPMo has molecular weight of 1825 g mol^{-1}, HPW 2880 g mol^{-1}, and HSiW 2878 g mol^{-1}; the HPA hydrates used for catalyst preparation had a water content of 12–20 H_2O molecules per Keggin unit (from TGA). The HPA hydrates (0.15 g per anhydrous HPA) were placed in a pre-weighed 200 ml glass beaker and dissolved in a minimum amount of distilled H_2O at ca. 40 ^oC with magnetic stirring. Activated carbons (0.85 g) were added to the beaker to afford the catalysts with an expected HPA loading of 15% wt. More water was added, if necessary, for the whole mixture to be soaked in water (total amount of water ca. 10 ml per 1 g of active carbon). The beaker was covered with a watch glass, and the mixture was stirred for 3 hours at 40 ^oC. The beaker was then placed in an oven, and the content was dried at 100 ^oC overnight to afford the catalysts as black powders. The beaker was weighed after drying to determine the catalyst weight.

2.2.2. P–Mo–V HPA catalysts

$H_{3+n}PMo_{12-n}V_nO_{40}$ (HPA–*n*) catalysts were prepared by the classical method described elsewhere [1]. The disodium phosphate and sodium metavanadate were boiled together (in stoichiometric quantities for the three HPA–*n*: $H_4PMo_{11}VO_{40}$, $H_5PMo_{10}V_2O_{40}$ and $H_6PMo_9V_3O_{40}$. The solution was then cooled and acidified with 5 M sulfuric acid. Sodium molybdate dihydrate dissolved in water was then added to the solution. More sulfuric acid was added slowly to pH ≈ 0 while the mixture was stirred vigorously and then allowed to cool to room temperature. The heteropoly acids were extracted with diethyl ether. The layer containing the heteropoly etherate was extracted and the diethyl ether was removed by passing air over it. The remaining crystals were dissolved in distilled water and allowed to crystallize in a vacuum desiccator evacuated using a membrane pump (~20 mmHg) over 96% sulfuric acid. The crystals that formed were filtered, washed with a small amount of water and allowed to air dry. The amount of water of crystallization was determined by TGA. The bulk HPA–*n* were all orange powders in appearance.

$Cs_{1.5}H_{2.5}PMo_{11}V_{40}$ (Cs-HPA–1) and $Na_2H_3PMo_{10}V_2O_{40}$ (Na-HPA–2) acidic salts were prepared by the dropwise addition of a stoichiometric quantity of aqueous Cs_2CO_3 and Na_2CO_3 to an aqueous solution of HPA–1 and HPA–2, respectively, followed by rotary evaporation and drying. HPA–1 supported on Darco KB-B activated carbon and on silica Aerosil 300 were prepared by wet impregnation from aqueous solution. The silica-supported catalyst was calcined in air in an oven at 300 °C for 2 hours to afford a fine yellow powder. The carbon-supported catalyst was air dried at 100 °C overnight to afford a fine black powder.

2.3. Catalyst characterization techniques

2.3.1. Elemental analysis

The purpose of using these analytical techniques is to quantify the elemental composition of catalysts and to determine their purity.

2.3.1.1. Inductively coupled plasma optical emission spectroscopy (ICP-OES)

ICP-OES is powerful tool used to determine the amount of most elements in a sample present in a part per billion quantity.

The ICP-OES instrumentation is relatively simple (Fig. 2.1) [2,3]. Plasma is formed in radiofrequency (RF) coil at 7000 K by igniting argon gas. Using an analytical nebulizer into a spray chamber, the sample solution is introduced as a mist directly within the plasma flame. The elements in the sample collide with plasma electrons and ions, which excite electrons to higher states within the elements. Upon relaxation, electrons emit energy photons that are quantized and characteristic of the involved element. The wavelengths of the energy emitted are recorded as emission lines by the spectrometer, and the intensities of these lines are directly proportional to the element concentration in the solution of the sample. The element concentration can then be calculated by comparing the intensity of the emission line with the standard calibrated solutions of the corresponding element [2,3].

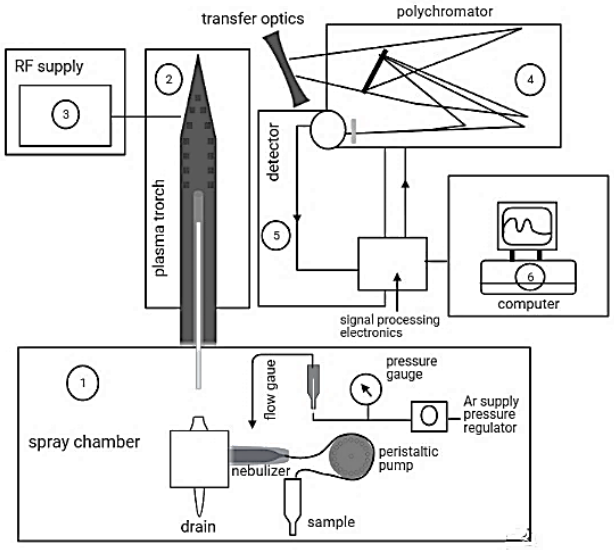

Fig. 2.1. Schematic diagram of ICP-OES instrument: sample introduction system (1), plasma torch and its gas supply (2), radio-frequency generator (3), optical spectrometer (4), detector and associated electronics (5), computerized instrument control, data collection and analysis (6) (adapted from [3]).

In this study, ICP-OES was used to determine the HPA loading in the catalysts by measuring the concentration of molybdenum, tungsten, and vanadium ions in our catalyst samples. The catalyst was weighed (20–50 mg) into a volumetric flask (50 ml). 15% KOH aqueous solution (ca. 25 ml) was added to the flask and the mixture boiled for 3 h. The mixture was left to cool overnight and made up to 50 ml with distilled water. The contents were mixed and then centrifuged for 30 min at 6000 rpm. The liquid phase in the centrifuge tube (20 ml) was then transferred to a vial for ICP analysis.

Samples were submitted to the Microanalysis Service in the University of Liverpool Chemistry Department and analyzed by George Miller on an Agilent 5110 ICP-OES spectrometer with SVDV detection equipped with the sample changer.

2.3.1.2. CHN analysis

CHN microanalysis is an effective tool for evaluating sample purity by providing precise analysis of the percentage of carbon, hydrogen and nitrogen content. The sample is burned in

excess of oxygen and the combustion products, such as carbon dioxide, water, and nitric oxide, are extracted by different traps [4].

For CHN analysis, a weighed quantity of sample (1–2 mg) is introduced into a high-temperature furnace with a continuous stream of an inert, high-purity gas such as helium passed through. A small volume of pure oxygen is added to the system to burn the sample that enhanced the exothermic combustion making the temperature reach around 1800 ° C in a few seconds. The combustion-generated gases are then swept through a series of columns. An oxidation quartz column converts carbon to CO_2, sulfur to SO_2 and hydrogen to H_2O and eliminates halogens from the gas stream. A reduction column containing metallic copper maintained at ~700°C absorbs unreacted oxygen and reduces species containing nitrogen to N_2. Then, the separation of combustion products is conducted by a chromatographic column and the gas components are determined by the thermal conductivity detector (Fig. 2.2) [5].

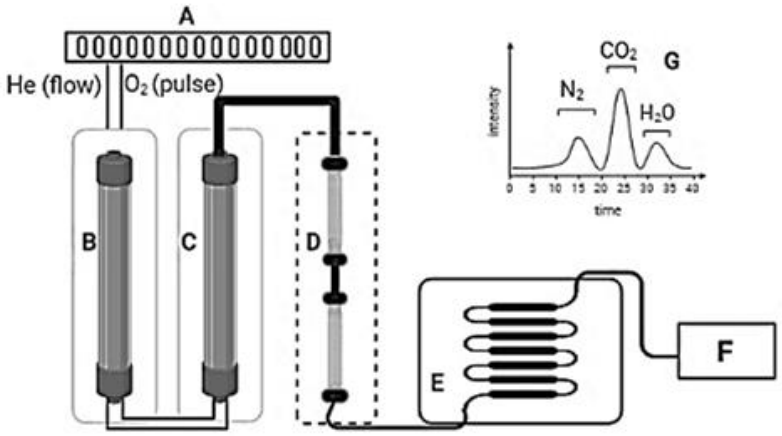

Fig. 2.2. Schematic of CHN elemental analysis instrument: autosampler (A), combustion tube (B), reduction tube (C), chemical traps (D), chromatographic column (E), detector (F), and analysis output (G) (adapted from [5]).

CHN analysis was performed on a Thermo Flash EA 1112 series analyzer by the Microanalysis Service in Chemistry Department of the University of Liverpool.

2.3.2. Thermogravimetric analysis (TGA)

Thermogravimetric analysis is used to provide information about chemisorption, dehydration, decomposition, and physical properties of materials [6,7].

The essential components of TGA instrumentation are a sample pan, a furnace, and a recorder [8]. The sample pan is placed in a furnace and attached to a precise balance that can measure the change of sample weight as a function of temperature and record it into the recording system. During the analysis, the environment inside furnace of TGA instrument is controlled through a gas inlet passing a flow of inert purge gas or air over the sample.

In this study, TGA analyses were conducted by using a Perkin Elmer TGA–7 instrument (Fig. 2.3) to analyze the thermal stability of HPA and supported HPA catalysts and to measure the amount of physisorbed water in the commercially sourced heteropoly acids for the correct amount of reactants to be used in catalyst preparation. The TGA analyses were carried out from room temperature up to 700 ^{o}C with a heating rate of 20 ^{o}C per minute under N_2 flow.

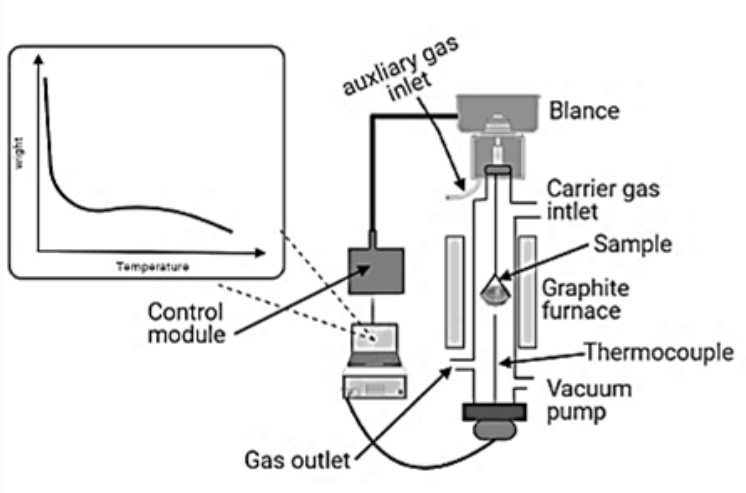

Fig. 2.3. Perkin Elmer TGA–7 instrument (adapted from [8]).

2.3.3. Fourier transform infrared spectroscopy (FTIR)

FTIR spectroscopy is an important analytical technique that provides information about the structural framework of materials. Diffuse reflectance infrared Fourier transform (DRIFT) spectroscopy was used in this study for recording FTIR spectra of catalyst samples. This technique measures the diffusely scattered light from the sample [9]. The light can be absorbed by groups on the surface or in the bulk of the powder when diffusely reflected light passes through the powder, creating a diffuse reflected spectrum. The method is especially suitable for powder catalyst samples. Highly absorbing samples can be mixed with a diffusely scattering matrix (KBr) that decreases absorption and enhances signal throughput. The set-up of the spectrometer consists of four flat mirrors (M1, M2, M5, and M6) and two ellipsoid mirrors (M3 and M4) as shown in Fig. 2.4. The light from a laser source is passed through the sample, which is diffusely reflected by mirrors M1, M2, and M3. Then, mirrors M4, M5, and M6 focus the diffusely reflected light from the sample toward the detector for analysis.

.

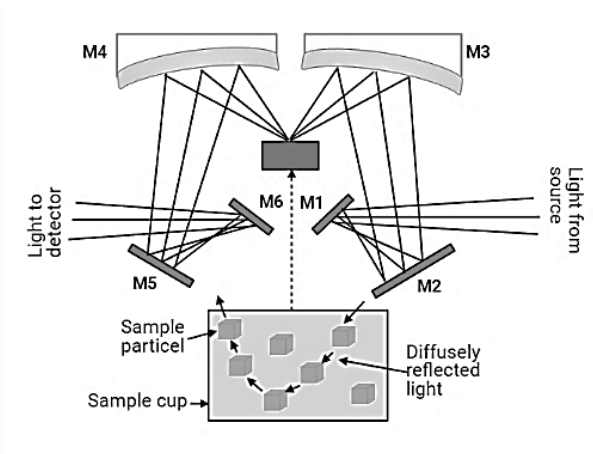

Fig. 2.4. Schematic representation of DRIFT spectroscopy (adapted from [10]).

Samples of bulk HPA and supported HPA catalysts were prepared by grinding the catalyst (8 mg) and KBr (392 mg) into a fine powder using a pestle and mortar. DRIFT spectra were recorded on a Nicolet Nexus FTIR spectrometer using powdered catalyst mixtures with KBr.

The spectra were recorded at room temperature by averaging 254 scans in the range of 4000–500 cm^{-1} with a resolution of 4 cm^{-1}. The spectra of bulk HPAs were measured against pure KBr background, the spectra of carbon-supported HPA catalysts against KBr + activated carbon background.

2.3.4. Powder X-ray diffraction (PXRD)

PXRD is a well-known nondestructive technique to study crystal structures and atomic spacing [11,12]. It provides information on structures, phases, preferred crystal orientations (texture) as well as average grain size, crystallinity, and crystal defects. X-ray diffraction peaks are generated by constructive interference of a monochromatic X-ray beam scattered at certain angles from each set of lattice planes in a sample. The distribution of atoms within the lattice determines the peak intensities. When the incident rays interact with the sample, constructive interference (and a diffracted ray) are produced when conditions satisfied Bragg's law, Eq. 1.

$$n\lambda = 2d\mathrm{Sin}\theta \quad (1)$$

In this equation, n is the reflection order, λ is the wavelength of the X-ray, d is the lattice planar spacing, and θ is the angle of diffraction.

In a crystalline sample, this rule connects the wavelength of electromagnetic radiation to the diffraction angle and lattice spacing. Then, diffracted X-rays are detected, processed, and counted through scanning the sample through different ranges of 2θ angles and all conceivable diffraction directions of the lattice due to the random orientation of the powdered material. Due to each compound has its own set of unique *d*-spacing, converting the diffraction peaks to *d*-spacing enables identification of the compound. This is typically accomplished by comparing *d*-spacing with standard reference patterns.

In this study, samples of bulk HPA and supported HPA catalysts were prepared by grinding the catalysts into a fine powder using a pestle and mortar. Then, these powder samples were placed on a sample holder by dispersing as a thin film on tape and exposed to X-radiation at room temperature. The incident X-ray beam is generated by an X-ray source, which is a copper cathode driven by high voltage, and the CuKα emission line is selected using a monochromator. Thereby, characteristic X-rays are produced when electrons attain enough energy to displace inner shell electrons of atoms. Collimated X-rays are directed onto the sample, Fig. 2.5. The Bragg's equation is satisfied by the geometry of the incident X-rays impinging on the sample, with constructive interference to occur, producing an intense peak. A detector collects and analyses the diffracted X-ray signal at an angle 2θ, converting it to a count rate that is subsequently sent to a computer monitor. The diffraction pattern is represented by the graph of peak intensity vs. detector angle 2θ.

Catalyst samples were submitted to the Crystallographic Service in the University of Liverpool Chemistry Department and analyzed on a PANalytical Xpert diffractometer with a θ–2θ system in transmission mode using a monochromatic CuKα radiation (λ = 1.542 Å) source. The patterns were recorded by averaging 120 scans over a range of 2θ = 4–100°.

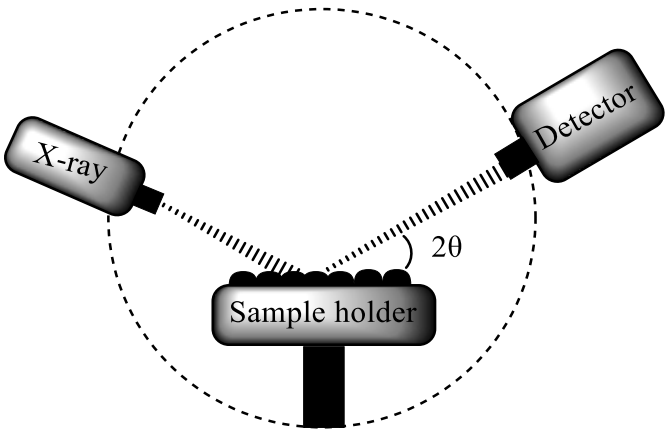

Fig. 2.5. Schematic diagram of powder X-ray diffraction diffractometer.

2.3.5. Catalyst surface area and porosity

Heterogeneous catalysts are typically porous solids with pores of different size [13]:

1- Micropores– pore size below 2 nm

2- Mesopores– pore size between 2 nm and 50 nm

3- Macropores– pore size above 50 nm

The surface area and porosity of solid catalysts are determined from nitrogen physisorption at 77 K. Experimentally, the amount of N_2 adsorbed is measured as a function of N_2 pressure. A plot of the volume of adsorbed N_2, *V*, against the relative partial pressure, P/P_o, produces an adsorption isotherm. Four types (I, II, IV, and VI) of adsorption isotherms are usually observed on solid catalysts (Fig. 2.6). Type I describes adsorption by microporous solids, type II describes adsorption by macroporous solids, type IV describes adsorption by mesoporous solids, and type VI describes absorption by uniform ultramicroporous solids. Adsorption leads to monolayer formation at a relatively low pressure. Then multilayers form at higher pressures until capillary condensation occurs [13–15].

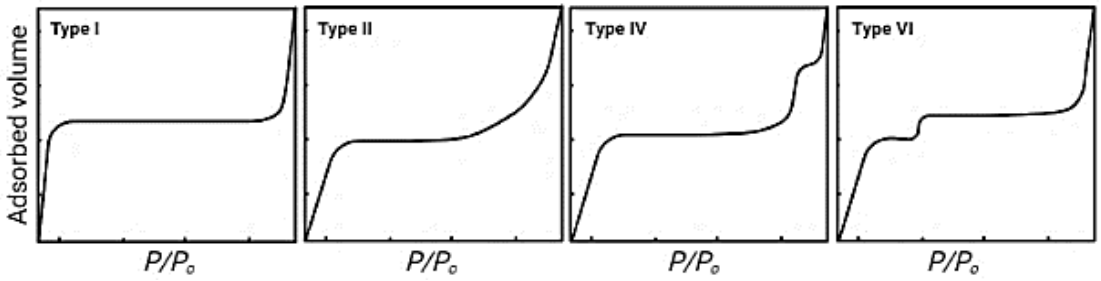

Fig. 2.6. Types of nitrogen adsorption isotherms usually observed on solid catalysts (adapted from [13]).

The process of N_2 desorption begins after saturation of the adsorbate has been reached. In the case of mesoporous solids, N_2 desorption often occurs at a lower pressure than capillary

condensation, giving a hysteresis which form is characteristic to the shape of the pores. Four types of hysteresis (H1, H2, H3, and H4) can be recognized in adsorption isotherms (Fig. 2.7), from which the shape of pores can be identified [13.14].

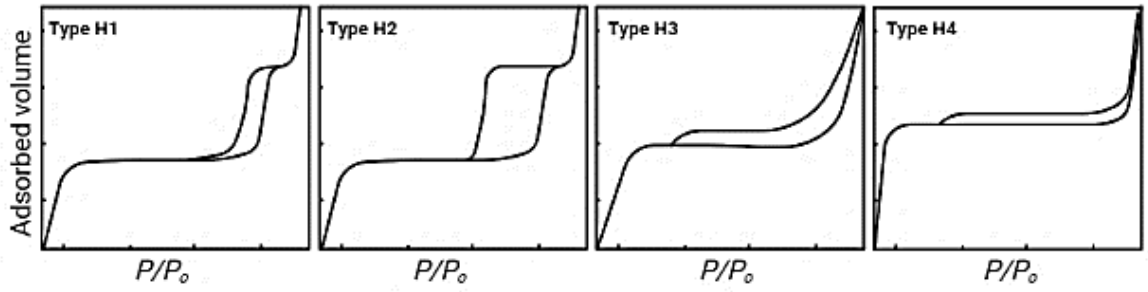

Fig. 2.7. Hysteresis types in adsorption isotherms (adapted from [13]).

Type H1 and H2 are ascribed to solids consisting of particles with cylindrical pore channels, spheroidal aggregates, or agglomerates with pores of uniform and non-uniform size and shape, for example, “ink-bottle pores”. Type H3 and H4 are attributed to solids consisting of aggregates or agglomerates forming “slit-like pores” with uniform H4 and non-uniform H3 size and shape. Active carbons and zeolites are typical examples of these types of hysteresis [13,14].

In this work, the surface area and porosity of catalysts was characterized by the BET (Brunauer–Emmett–Teller) method from nitrogen physisorption measured at 77 K on a Micromeritics ASAP 2010 instrument (Fig. 2.8). Prior to measurement, the catalysts (150–200 mg) were pretreated in a high vacuum in a tube furnace for 2–3 h at 220 ^{o}C up to 8 μmHg pressure to remove all adsorbed gasses from the pores. Then, the sample tube was cooled to room temperature and inserted into the analyzer, and immersed in liquid nitrogen. Finally, the gas pressure was allowed to stabilize before applying a series of nitrogen doses (55 total) to obtain an adsorption isotherm. The results were reported as the BET surface area (m^2g^{-1}) determined from (Eq. 2), single point total pore volume (cm^3g^{-1}) at P/P_o = 0.97–0.99 and

adsorption average pore diameter (4*V*/*A* by BET, where *V* is the pore volume and *A* is the catalyst surface area).

$$\frac{1}{V\,(P_o/P)} = \frac{1}{V_m\,C} + \frac{(C-1)}{V_m\,C} \times \frac{P}{P_o} \qquad (2)$$

In Eq. 2, *P* is the equilibrium pressure, P_o is the saturation pressure, *V* is the volume of gas absorbed at the pressure *P*, V_m is the volume of gas required to cover the surface in one monolayer, and *C* is a constant related to the heat of condensation.

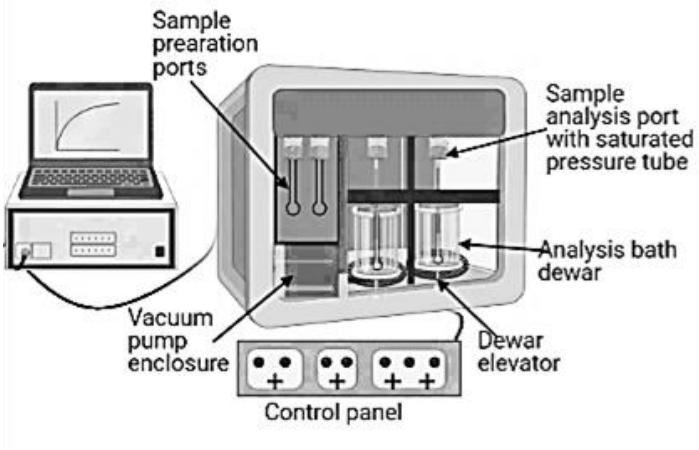

Fig. 2.8. Micrometrics ASAP 2010 instrument for adsorption measurement.

2.3.6. Measurement of surface pH of activated carbons

The surface acidity of carbon supports was determined by measuring the pH of aqueous extracts (10% of activated carbon in water) using a Fischerbrand Hydrus 300 pH meter. A sample of 0.5 g of dry activated carbon powder was mixed with 5 mL of water and stirred overnight to reach equilibrium. Following that, the sample was filtered, and the pH of the aqueous solution determined [16].

2.4. Catalyst testing in oxidative desulfurization reactions

2.4.1. Oxidative desulfurization of model diesel fuel by hydrogen peroxide

The oxidation of dibenzothiophene was carried out in 50 ml three-necked jacketed glass reactor equipped with a reflux condenser and a magnetic stirrer connected to a Grant heating circulator to control the reaction temperature (Fig. 2.9). Samples withdrawn during the reaction were spun in a centrifuge and subjected to GC analysis.

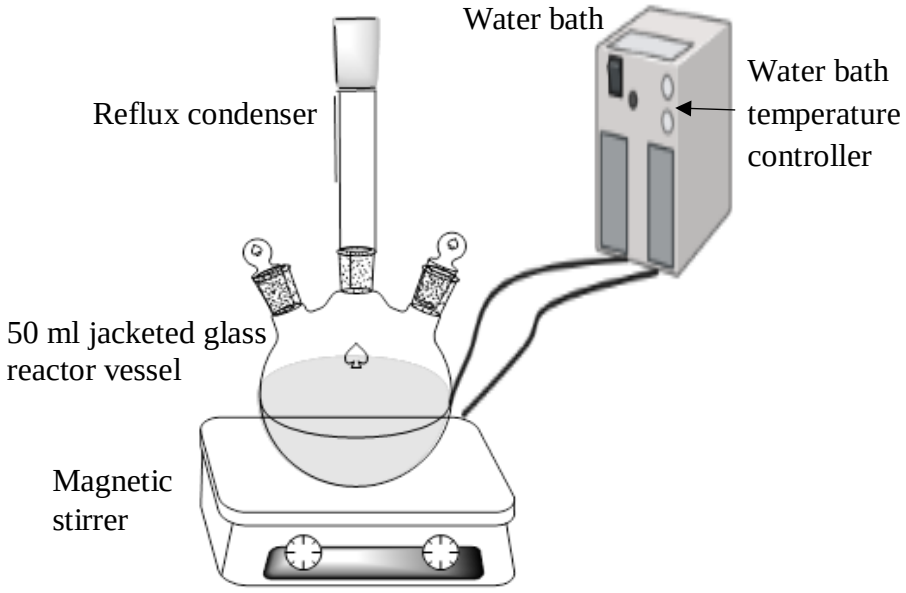

Fig. 2.9. Reactor set-up for ODS with hydrogen peroxide as oxidant.

Typically, the reaction mixture contained an supported HPA catalyst (0.0041 mmol of HPA), DBT (0.5 mmol), n-heptane (5 ml), dodecane (GC standard, 0.4 mmol) and 30% H_2O_2 (1.5 mmol). The concentration of 30% H_2O_2 stock solution was regularly checked by titration with $KMnO_4$. The mixture was stirred (1500 rpm) at 60 ^oC for 5 min, then stirring was paused. n-Heptane stock solution (5 ml, containing 0.5 mmol DBT and 0.4 mmol dodecane) was added, and stirring was recommenced immediately to start the reaction (zero time). Over a 1–2 hour period, ca. 0.1 ml aliquots of the organic phase were taken by Pasteur pipette at certain time intervals (usually 5, 10, 15, 20, 30, 45, 60, 90 and 120 min), centrifuged and analyzed by GC

using the internal standard method. The initial (zero time) quantity of DBT was measured by GC separately from an aliquot of DBT stock solution.

At the end of the reaction, distilled H_2O (5 ml) was added to the reactor vessel and stirred for 1 min at 1500 rpm. The entire mixture was transferred to a 15 ml centrifuge tube and centrifuged for 20 min at 60 rpm. Two aliquots of the aqueous phase were taken, and each added to a conical flask containing H_2SO_4 (1.0 M, 10 ml). The solution was titrated by $KMnO_4$ aqueous solution (0.005 M) to determine the conversion of H_2O_2 from which the H_2O_2 efficiency, the reaction selectivity based on H_2O_2, was calculated (Eq. 3).

$$\underset{\text{Pink sulotion}}{2KMnO_4 + 5H_2O_2 + 3H_2SO_4} \longrightarrow \underset{\text{Colourless solution}}{K_2SO_4 + 2MnSO_4 + 5O_2 + 8H_2O}$$

Titration with $KMnO_4$ produces a colourless solution when H_2O_2 is present and a pink solution when all of the H_2O_2 has reacted, which represents the end-point.

$$\text{Desulfurization } H_2O_2 \text{ selectivity} = \frac{2\times\text{Conversion of substrate (mol)}}{(\text{Intial } H_2O_2 - \text{Final } H_2O_2)(\text{mol})} \times 100 \qquad (3)$$

The adsorption of DBT on neat activated carbons and HPA/AC–*n* catalysts in the absence of H_2O_2 was tested in the same reactor at similar conditions that were used for catalytic oxidation with the same GC analysis of samples.

2.4.2. Aerobic oxidative desulfurization of model diesel fuel in the presence of benzaldehyde as a sacrificial reductant

The oxidation of dibenzothiophene was carried out in 50 ml three-necked round bottomed flask reactor placed in an oil bath. The reactor was equipped with an air flow meter, a reflux condenser, and a magnetic stirrer (Fig. 2.10). Samples withdrawn during the reaction were spun in a centrifuge and subjected for GC analysis.

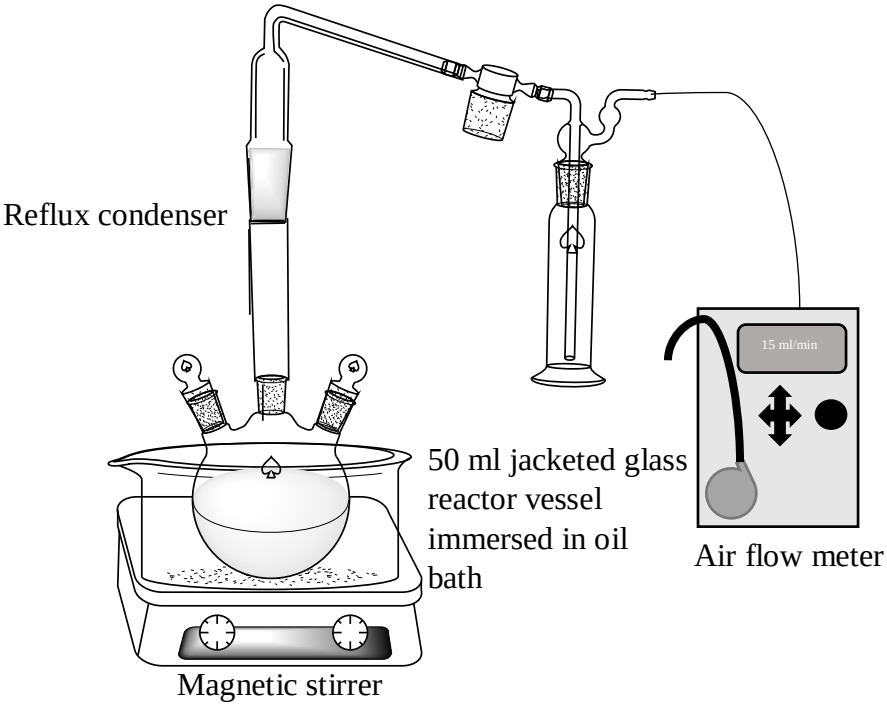

Fig. 2.10. Reactor setup for aerobic ODS.

Typically, the reaction mixture contained a HPA–*n* catalyst (0.05 mmol) and dodecane stock solution (10 ml) containing DBT (0.5 mmol) and tetradecane (GC standard, 0.4 mmol). Air was bubbled through the reaction mixture at a rate of 20 ml/min through one side neck whilst a reflux condenser was attached to the middle neck. The stirring speed was 1300 rpm. It was found through previous tests that the rate of reaction did not alter when the stirring speed was changed from 150 rpm to 1300 rpm, which indicated that the reaction was not limited by external gas-to-liquid diffusion. It was also found that the rate of reaction did not change when the air flow was increased to 30 ml/min nor when using pure oxygen instead of air. The oxidation reaction was found to occur more efficiently if the air was bubbled through the reaction mixture. When the air was blown over the top of reaction mixture, the reaction was less efficient, which indicated insufficient air delivery. However, by needing to bubble the air through the liquid phase, the apparatus had to be checked to ensure the capillary tube used to

supply the air was not blocked by sulfone product precipitate. This was achieved by placing a bubbler at the end of the reflux condenser to check the air supply visually.

The reaction was started by injecting benzaldehyde (0.4 mmol) into the reaction vessel. No reaction occurred without benzaldehyde present under the chosen conditions. The third neck was stoppered and through this neck, samples were taken at regular intervals in aliquots of approximately 0.1 ml. These samples were centrifuged for 5 min at 1300 rpm to separate the catalyst and sulfone product; the latter was not soluble in dodecane solvent. The resulting clear liquid was analysed using GC.

2.4.3. Catalyst reuse

Once the reaction was complete, an aliquot was taken to be centrifuged and analyzed by GC. The entire reaction mixture was transferred to a 15 ml centrifuge tube and centrifuged for 20 min. Toluene (5 ml) was added to the reactor vessel and stirred for 20 min (to wash any remaining catalyst, DBT and sulfone). The solvent was then removed from the centrifuge tube, and the toluene mixture in the reactor vessel transferred to the tube. The mixture was centrifuged for 30 min and the toluene removed, affording a black sludge of recovered catalyst. The catalyst was transferred back into the reactor vessel by rinsing the tube with stock solution (5 ml). The reaction was then repeated using the recovered catalyst.

2.5. Monitoring the ODS reactions

In this study, gas chromatography (GC) was used for quantitative analysis of reactants and products in the oxidation of aromatic sulfur compounds with H_2O_2 and O_2.

2.5.1. Gas Chromatography

Gas chromatography is one of the most common high-precision analytical methods for the separation and quantitative analysis of volatile compounds [10,14,17–20]. Separation of the volatilities operates on the principle of phase partition due to differing affinities of the analyzed

compounds for two phases – a mobile gas phase and a stationary solid or immobilized liquid phase. Fig. 2.11 shows a schematic gas chromatographic set-up with a flame ionization detector (FID).

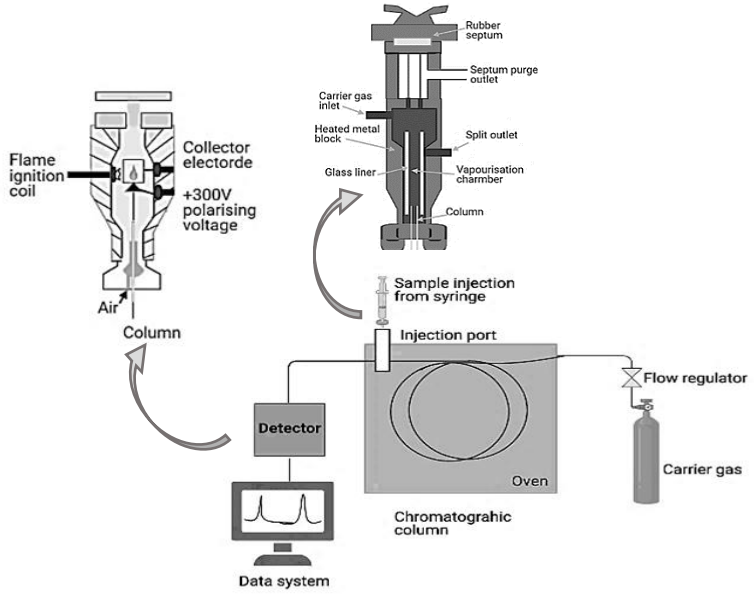

Fig. 2.11. Schematic representation of gas chromatographic analysis (adapted from [19]).

GC analysis involves vaporizing a sample and injecting onto the head of the column under a controlled temperature. The split/splitless injector, Fig. 2.11, is used to control the quantity of samples injected into the column. The sample is transported through the column by the flow of an inert gas, usually nitrogen or helium. The component that has a greater affinity for the chromatographic phase will have a longer retention time, while those with little or no affinity will pass through at shorter retention times. The separation of components is based on several properties, such as boiling point, molecular size, and polarity. Flame ionization detector (FID) (Fig. 2.11) is generally used for GC analysis of organic compounds. In FID, the column effluent is mixed with hydrogen and air and burned to produce a flame to ionize solute organic molecules with low ionization potentials. These ions are then impelled by an electrical potential towards an electrode collector under the influence of polarizing electricity between jet and

collector resulting in the current, which is converted to a voltage displayed in a chromatogram as volts vs retention time. The larger the concentration of the analyte passed through the column, the stronger the current induced and the larger the reading in a chromatogram.

In this project, a Varian CP-3380 gas chromatograph, equipped with BP1 capillary non-polar column (25 mm in length, 0.32 mm internal diameter and 0.5 μm film thickness) and FID detector was used. Nitrogen was used as the carrier at a flow rate of 2 ml/min and make-up gas at a flow rate of 30 ml/min. The injector split ratio was 1:20. Each sample was measured for a total of 12 minutes, with the column temperature programmed from 140 to 250 ºC (Fig. 2.12).

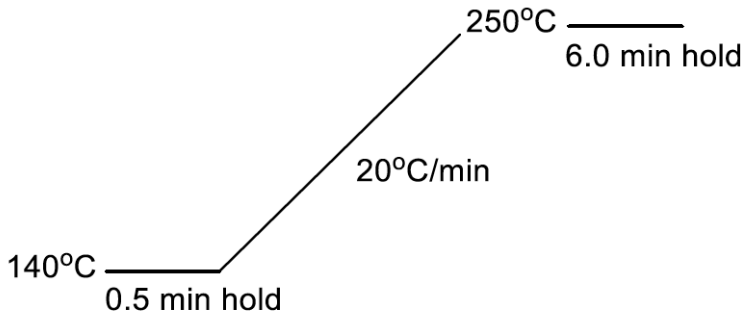

Fig. 2.12. Temperature program for GC analysis of organosulfur oxidation reaction.

2.5.2. GC calibration

In this work, GC analysis of reaction mixtures was carried out using the method of internal standard. The advantage of this method is that there is no need to control the volume of injected sample. The GC signal for each analyzed component is normalized to the signal of the internal standard used. Quantitative GC analysis was based on a calibration relationship determined for each analyzed compound using an appropriate internal standard (dodecane or tetradecane). The calibration relationships were linear plots; their gradients gave the corresponding calibration factors for the analyzed compounds.

For quantitative GC analysis, retention times and calibration factors were determined for each compound under specified conditions using commercially available reagents and analytical standards. A series of calibration samples was made by adding a fixed amount of internal standard to the feed solution of known composition. Each sample was analyzed three times. The calibration factors (*K*) of compounds were computed using Eq. 4.

$$\frac{M}{M_o} = K \times \frac{S}{S_o} \tag{4}$$

Here M/M_o is the molar ratio of the analyzed compound and internal standard, S/S_o is the ratio of area counts of the corresponding peaks, and *K* is the molar calibration factor. The retention times and the molar calibration factors for sulfur compounds are presented in Table 2.1. Fig. 2.13–2.15 show GC calibration plots and GC traces for the oxidation of sulfur compounds by H_2O_2 and air. Dibenzothiophene sulfone was observed as white precipitate formed on catalyst surface and can be detected at the end of the reaction by adding extraction solvent (toluene) to the reaction mixture, Fig. 2.16. From GC analysis, the conversion *X* of reactants was calculated using Eq. 5. The mean absolute percentage error in DBT conversion was ±5%.

$$X = \frac{(reactant\ initial - reactant\ end)mol}{(reactant\ initial)mol} \times 100 \tag{5}$$

Table 2.1. Retention times and calibration factors of reactants and products for the oxidation of sulfur compounds by H_2O_2 and air.

Compound	Retention times (min)	Calibration factor (*K*) relative to dodecane	Calibration factor (*K*) relative to tetradecane
Dodecane (standard)	3.29–3.30	1.00	-
Tetradecane (standard)	4.3	-	1.00
Heptane	2.17	Solvent	-
Toluene	2.3–2.5	Solvent	-
Dodecane	3.36	-	Solvent
Benzaldehyde	2.5	-	2.01
Benzoic acid	3.0	-	-
Benzothiophene	3.33–3.34	1.55	-
Dibenzothiophene	6.56–6.60	1.07	1.12
4,6-Dimethyldibenzothiophene	8.04–8.05	1.01	-
Dibenzothiophene sulfone	9.14–9.18	1.67	-

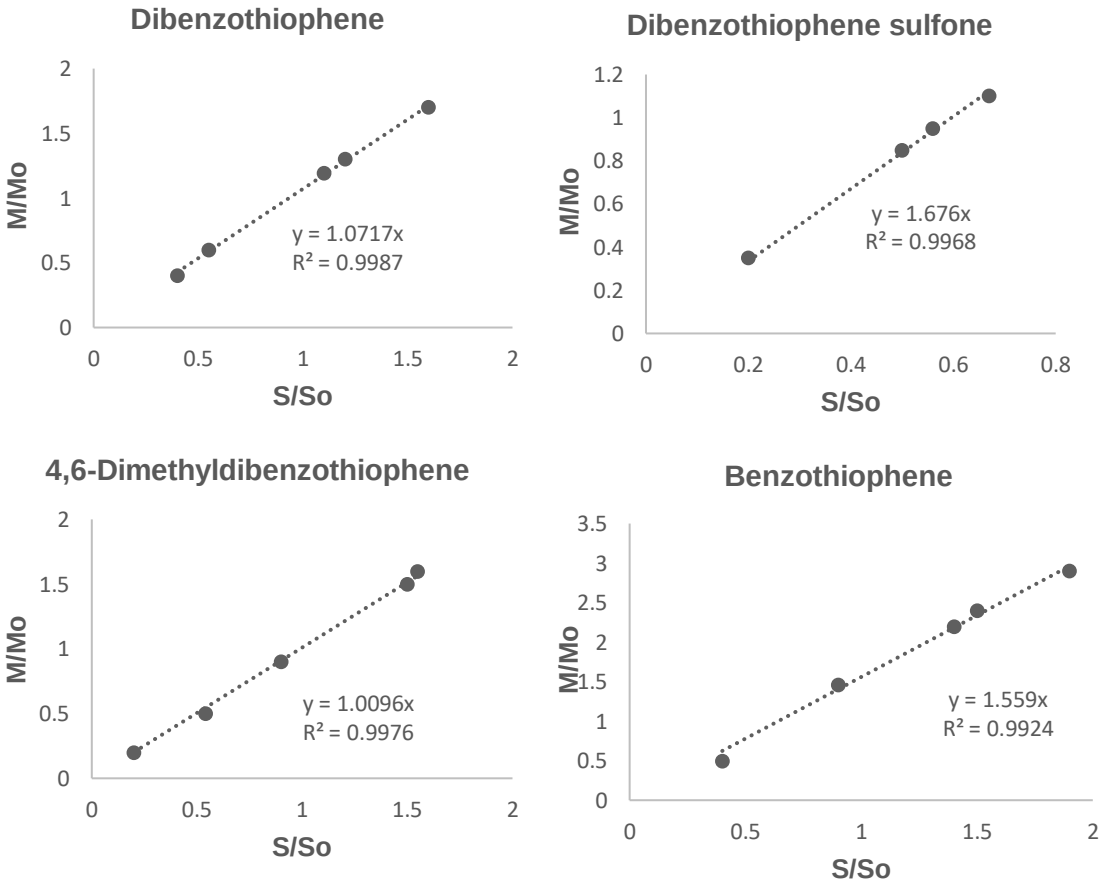

Fig. 2.13. GC calibration plots for oxidation of sulfur compounds by H_2O_2.

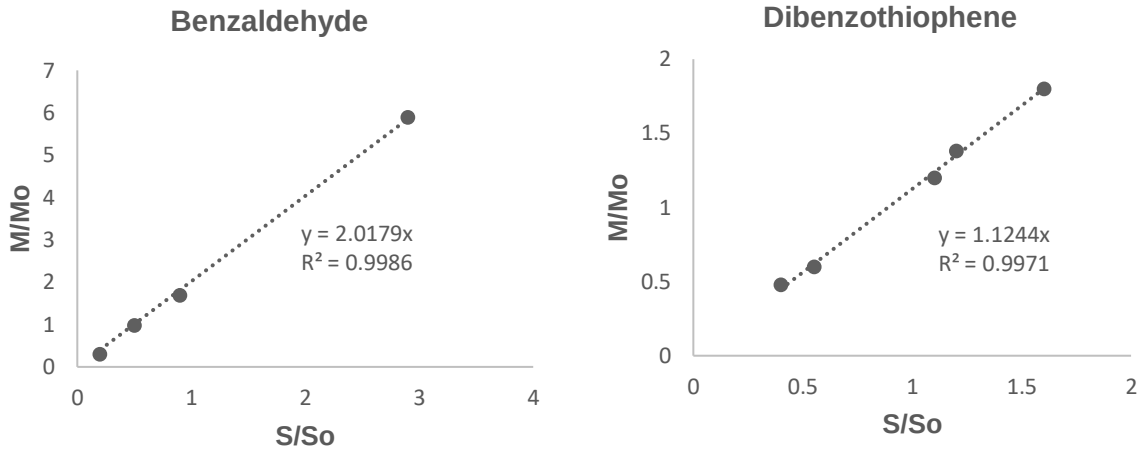

Fig. 2.14. GC calibration plots for oxidation of sulfur compounds by air.

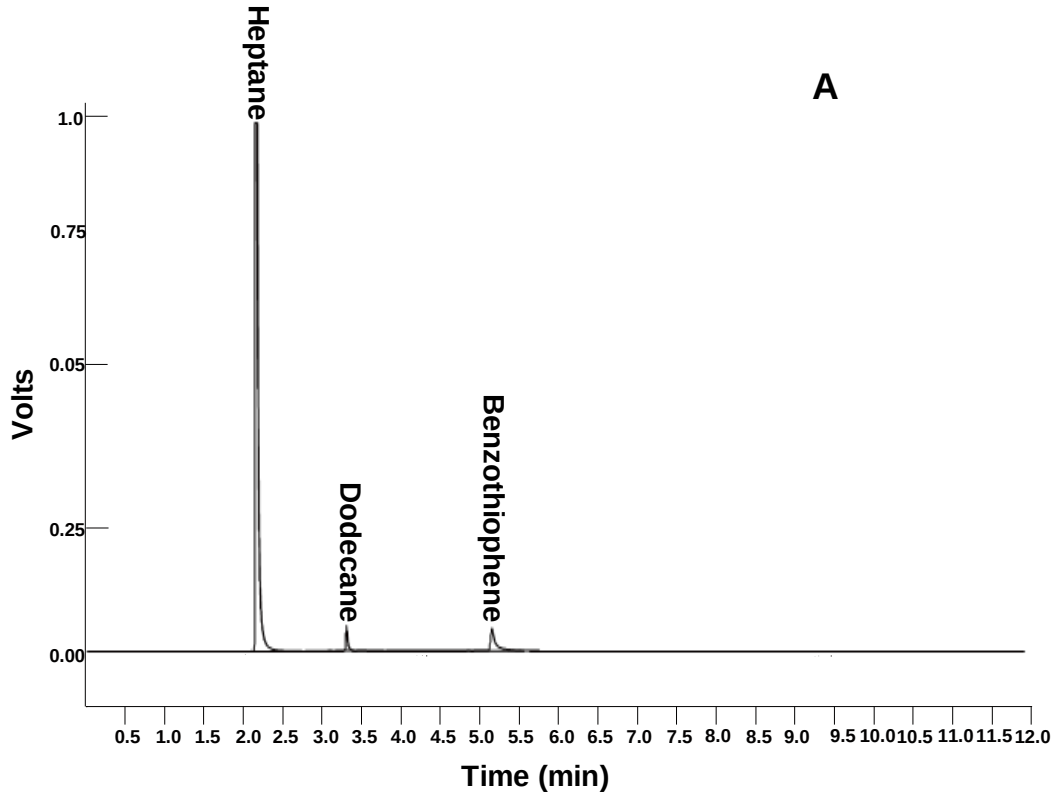

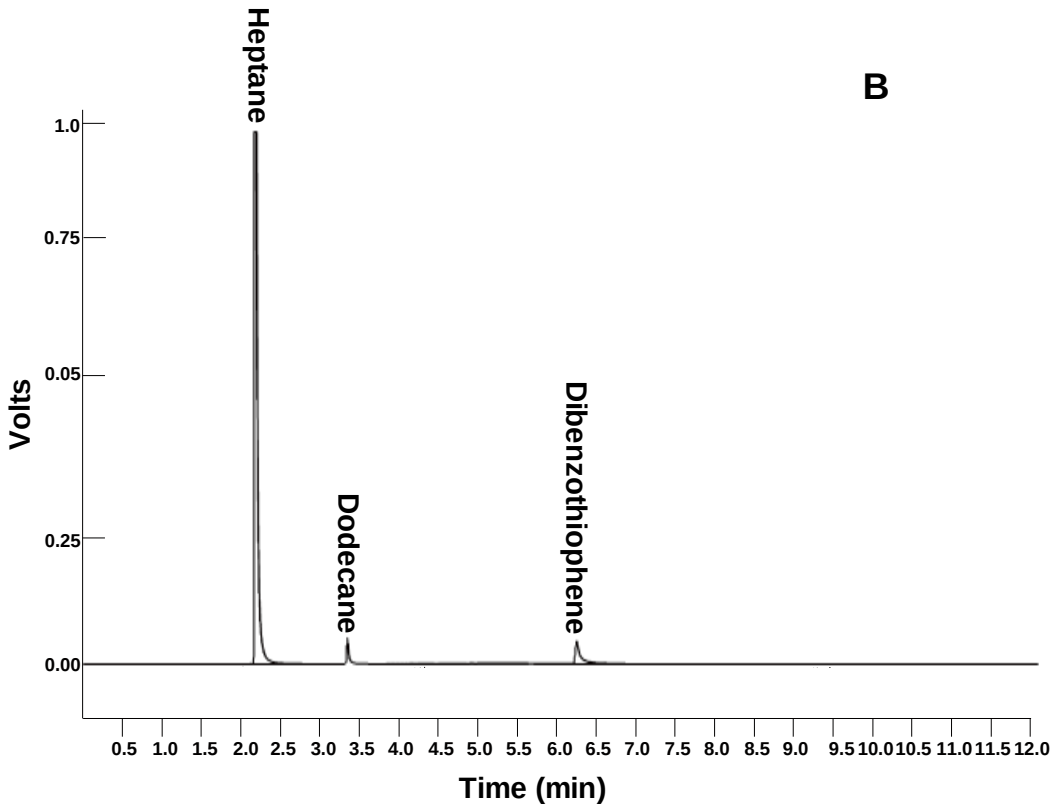
B
Heptane
Dodecane
Dibenzothiophene
Volts
1.0
0.75
0.05
0.25
0.00
0.5 1.0 1.5 2.0 2.5 3.0 3.5 4.0 4.5 5.0 5.5 6.0 6.5 7.0 7.5 8.0 8.5 9.0 9.5 10.0 10.5 11.0 11.5 12.0
Time (min)

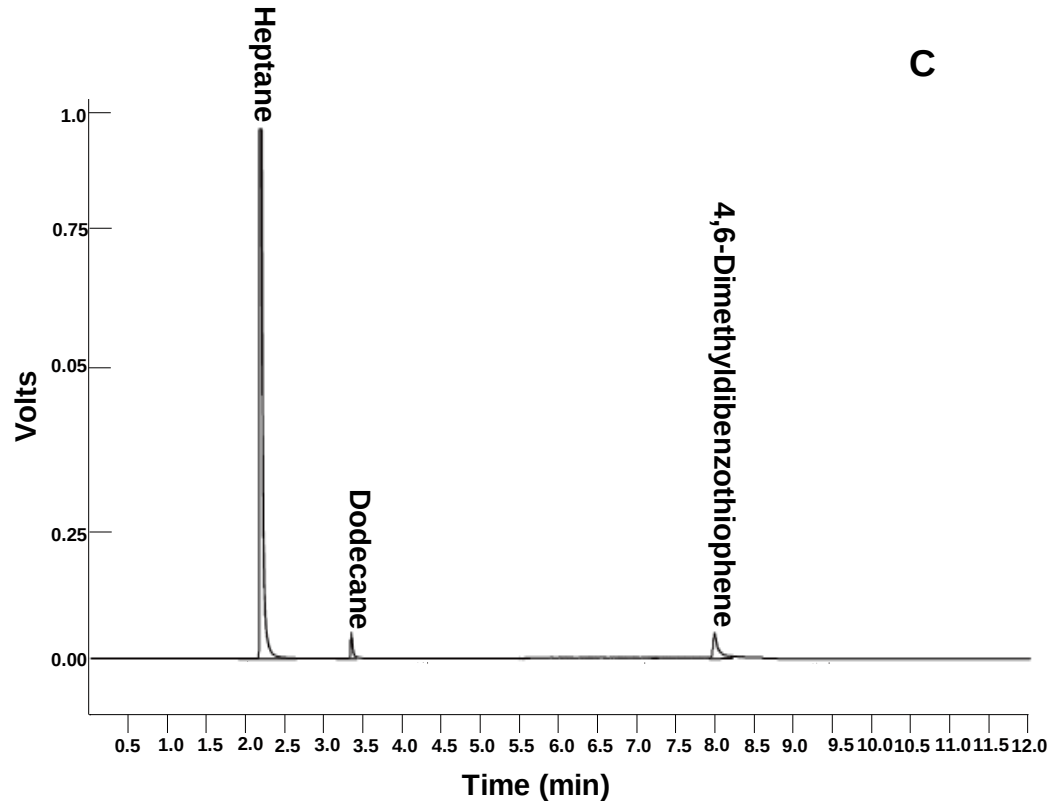
C
Heptane
Dodecane
4,6-Dimethyldibenzothiophene
Volts
1.0
0.75
0.05
0.25
0.00
0.5 1.0 1.5 2.0 2.5 3.0 3.5 4.0 4.5 5.0 5.5 6.0 6.5 7.0 7.5 8.0 8.5 9.0 9.5 10.0 10.5 11.0 11.5 12.0
Time (min)

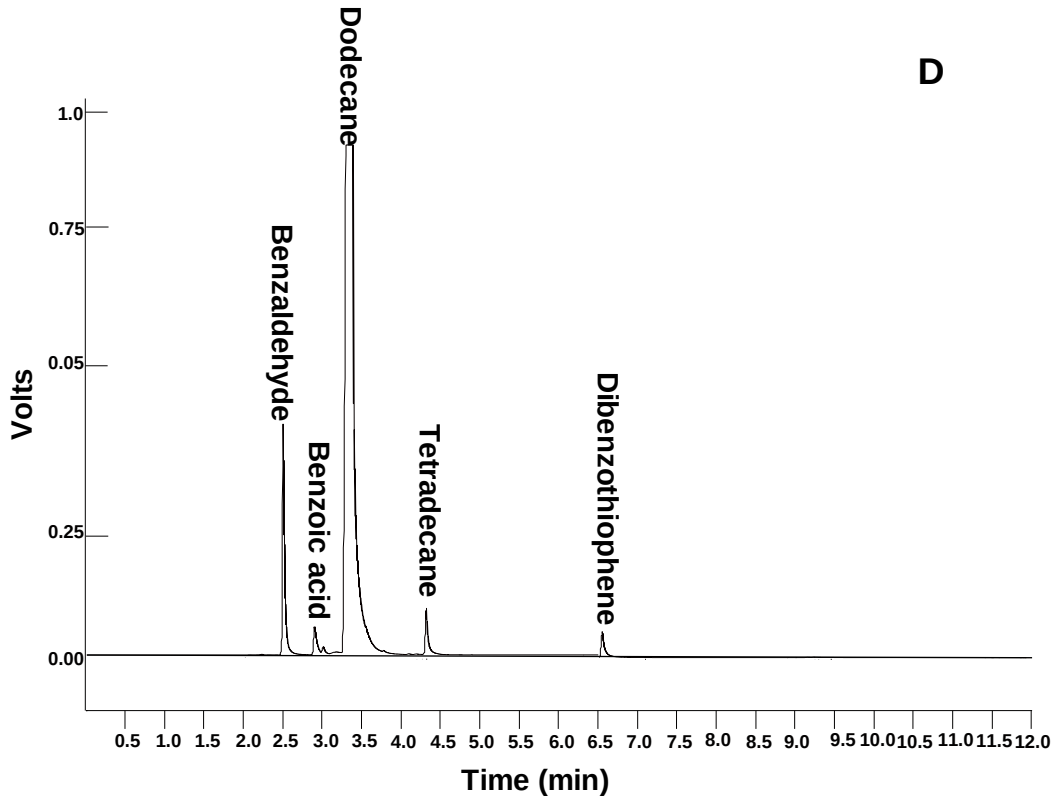

Fig. 2.15. GC traces for the oxidation of sulfur compounds (A–D).

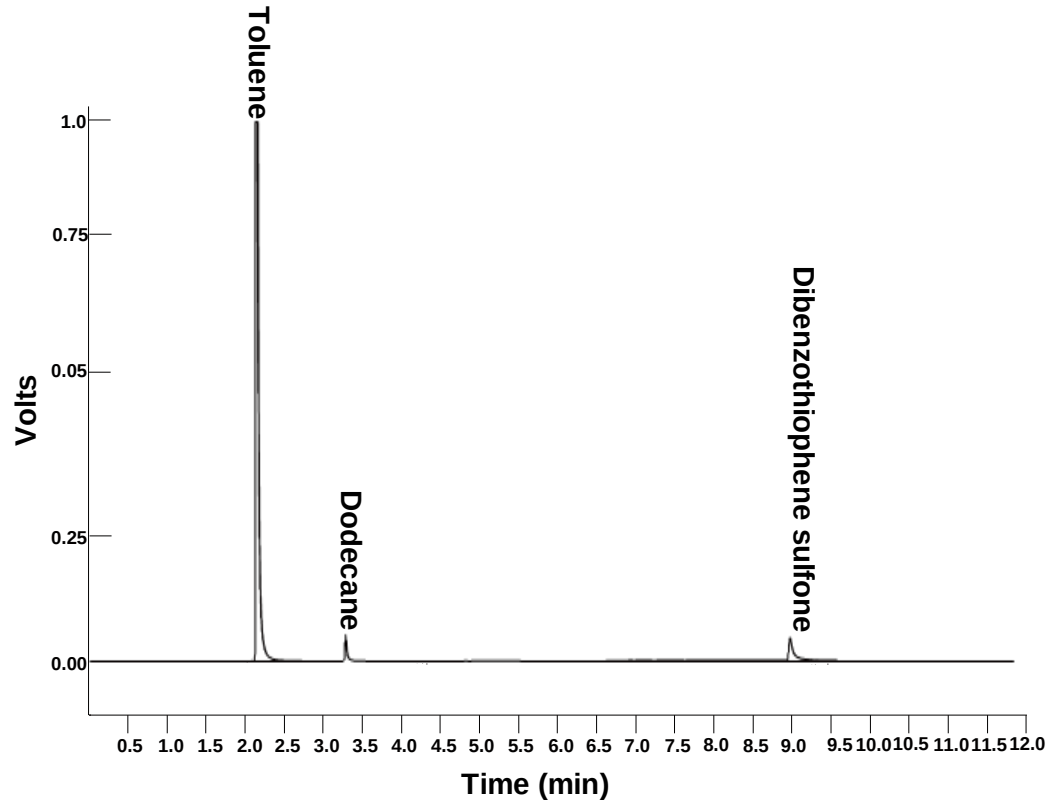

Fig. 2.16. GC trace for dibenzothiophene oxidation to dibenzothiophene sulfone (100% DBT conversion) showing the sulfone product after extraction by toluene.

Reference

[1] G.A. Tsigdinos, C.J. Hallada, Molybdovanadophosphoric acids and their salts. I. Investigation of methods of preparation and characterization, Inorg. Chem. 7 (1968) 437–441.

[2] V.A. Fassel, R.N. Kniseley, Inductively Coupled Plasma-Optical Emission Spectroscopy, Anal. Chem. 46 (1974) 1110A–1120A.

[3] Agilent, The ICP-OES principle, instrument, and analysis, https://www.agilent.com/en/support/icp-oes/icp-oes-instruments/icp-oes-faq (accessed February 1, 2021).

[4] J.R.W. Woittiez, G.V. Iyengar, K.S. subramanian, Element analysis of biological samples: Principles and practies, CRC Press 1998.

[5] M. Bird, C. Keitel, W. Meredith, Analysis of biochars for C, H, N, O and S by elemental analyzer. Biochar: A guide to analytical methods, CSIRO Publ. 39 (2017) 39–50.

[6] A.W. Coats, J.P. Redfern, Thermogravimetric analysis, Analyst 88 (1963) 906–924.

[7] S. Vyazovkin, Conversion dependence of activation energy for model DSC curves of consecutive reactions, Thermochim. Acta. 236 (1994) 1–13.

[8] R. Yahya, Ph.D. Dissertation: Polyoxometalate catalysis for oxidative desulfurization, University of Liverpool, 2015; p. 1–3.

[9] J. Mendham, R.C. Denney, J.D. Barnes, M. J.K. Thomas, Vogel's textbook of quantitative chemical analysis, Pearson Education Ltd. 2000.

[10] G. Schwedt, The essential guide to analyrical chemistry, Wiley, Chichester, 1997.

[11] B.R. Smith, Fundamentals of fourier transform infrared spectroscopy, CRC Press, 2011.

[12] W. Clegg, X-Ray Crystallography, Oxford University Press, Oxford, 2015.

[13] G. Leofanti, M. Padovan, G. Tozzola, B. Venturelli, Surface area and pore texture of

catalysts, Catal. Today 41 (1998) 207–219.

[14] M. Kruk, M. Jaroniec, Gas adsorption characterization of ordered organic-inorganic nanocomposite materials, Chem. Mater. 13 (2001) 3169–3183.

[15] R. Hetterley, Ph.D. Dissertation: Multifunctional catalysts for one-step conversion of acetone to methyl isobutyl ketone, University of Liverpool, 2008.

[16] A. Bagreev, F. Adib, T. J. Bandosz, pH of activated carbon surface as an indication of its suitability for H_2S removal from moist air streams. Carbon, 39 (2001) 1897–1905..

[17] B.P. Ismail, Basic principles of chromatography, Springer, Cham. 2017; p. 185–211.

[18] I.A. Fowlis, Gas Chromatography, john wiley & sons Ltd, Chichester, 1995.

[19] E. Ludanes, L. Reubsaet, T. Greibrokk, Chromatography: Basic principles, sample preparations, and related motheds, Wiley-VCH, 2013.

[20] L.M. Harwood, C.J. Mody, J.M. Experimental Organic Chemistry: standard and microscale, Blackwell Sci. 2001.

3 Oxidative desulfurization of model diesel fuel catalyzed by carbon-supported heteropoly acids

The sulfur content of diesel fuels used in transportation vehicles is under increasingly strict environmental regulations. It has decreased from 2000 to 10 ppm over the last 20 years and further reduction in sulfur content is desired [1,2]. Hydrodesulfurization (HDS), the most widely used technology for removing sulfur from diesel fuels, is operated at high temperature (300–400 ^{o}C) and pressure (30–130 atm) using alumina-supported Co-Mo or Ni-Mo catalysts [1,2]. The main drawbacks of HDS are severe operating conditions and low desulfurization efficiency in the case of refractory benzothiophenes. Alternative desulfurization methods have been investigated in recent years including, among others, oxidative desulfurization (ODS) [3,4], extraction [5], adsorption [6] and bio-desulfurization [7]. ODS appears to be the most promising method for deep desulfurization of diesel fuel. Typically, it involves liquid-phase biphasic oxidation of organosulfur compounds with H_2O_2 at low temperatures (50–70 ^{o}C) and atmospheric pressure to yield sulfoxides and sulfones, which can be separated from the fuel by precipitation, extraction or adsorption [3,4]. This method is highly efficient for removing refractory aromatic sulfur compounds such as thiols and benzothiophenes, which are difficult to remove by HDS [2].

Among many reported ODS catalysts, polyoxometalates (POMs), in particular Keggin-type POMs, exhibit a remarkable activity [8–13]. These compounds comprise polyanions, $XM_{12}O_{40}^{m-}$, composed of oxygen-sharing MO_6 octahedra (M = Mo^{VI}, W^{VI}, V^{V}, etc.) encapsulating a central tetrahedron XO_4^{n-} (X = P^{V}, Si^{IV}, etc.) [13]. In solution, in the presence of hydrogen peroxide, these POMs degrade to form active peroxo-polyoxometalate species (peroxo-POM) [12,14,15], e.g., the Venturello peroxo complex, $\{PO_4[WO(O_2)_2]_4\}^{3-}$ [16].

Peroxo-POMs are highly active catalysts for various biphasic oxidations with hydrogen peroxide [17–20]. In these reactions, a phase transfer agent (PTA) is required to transfer the peroxo-POM species from the aqueous phase containing H_2O_2 to the substrate-containing organic or fuel phase. Most frequently, quaternary ammonium cations are used as the PTAs in such systems, including amino-modified high molecular weight alkene oligomers [20]. Alkylaminophosphazenes have also been reported as promising phase transfer agents in POM-catalyzed biphasic oxidations with H_2O_2, including the oxidative desulfurization of benzothiophenes [12,21].

A major drawback of homogeneous POM catalysts in the PTA-assisted biphasic oxidative desulfurization is the difficulty of separating these catalysts from the fuel phase after desulfurization because the POM-PTA aggregates are highly soluble in the fuel phase. This would lead to contamination of fuel with POM. In this regard, heterogeneous ODS catalysts have the important advantage of easy catalyst separation from the fuel after reaction [22–28]. However, possible leaching of POM from the solid catalyst during the ODS reaction and post reaction catalyst treatment is a serious problem of the heterogeneous ODS systems. This may be addressed by incorporating POM within a metal-organic framework [26] or by chemical immobilization of POM onto an appropriately functionalized support [27]. A more practical solution to overcome this problem could be the use of porous supports that can strongly adsorb the active POM species.

This study aims at exploring activated carbon (AC –0) as a support for the heterogeneous ODS reaction catalyzed by POMs. Previously, it has been reported that activated carbon can strongly adsorb Keggin heteropoly acids (HPA), such as $H_3PW_{12}O_{40}$ and $H_4SiW_{12}O_{40}$, irreversibly retaining 7 –14 wt.% of HPA in polar media such as water and methanol [29–31]. As a result, the corresponding HPA/AC catalysts exhibit high stability towards HPA leaching in such media [30–32]. Strong interaction of HPA with carbon support is evidenced by a large line

broadening in ^{31}P MAS NMR spectra of $H_3PW_{12}O_{40}$ supported on activated carbon [33]. From IR and ^{31}P MAS NMR, heteropoly acids $H_3PW_{12}O_{40}$ and $H_4SiW_{12}O_{40}$ supported on a chemically (H_3PO_4) activated carbon retain the Keggin structure at an HPA loading >5 wt.% [33]. As evidenced by XRD, heteropoly acids form finely dispersed species on the carbon surface; no HPA crystal phase is developed even at a HPA loading as high as 45 wt.% [33]. Microcalorimetry of ammonia adsorption shows that the acid strength of $H_3PW_{12}O_{40}$ is greatly reduced when loading on activated carbon [34,35]. This suggests HPA bonding through protonation of the carbon framework. Scanning tunnelling microscopy and tunnelling spectroscopy studies of HPA supported on graphite have been reported [36]. Carbon-supported POMs are well-documented catalysts for liquid-phase oxidation [37–39]. Recently, a polyoxometalate $[PSPy]_3PMo_{12}O_{40}$ supported on graphite, where PSPy is N-(3-sulfonatepropyl)-pyridinium ion, has been reported as an efficient ODS catalyst [28].

This chapter describes the results of investigation of heterogeneous catalysis by Keggin-type HPAs ($H_3PMo_{12}O_{40}$, $H_3PW_{12}O_{40}$ and $H_4SiW_{12}O_{40}$) supported on Darco KB-B activated carbon (150 μm particle size from Sigma–Aldrich), hereinafter referred to as AC–0, for the biphasic oxidative desulfurization of model diesel fuel (heptane) by aqueous 30% H_2O_2. Our results for other commercial activated carbons, designated AC–1 to AC–9, are described in Chapter 4. Here, we report a highly efficient catalyst, $H_3PMo_{12}O_{40}$/AC–0, for the oxidation of benzothiophenes (benzothiophene (BT), dibenzothiophene (DBT) and 4,6-dimethyldibenzothiophene (DMDBT)) to the corresponding sulfones by H_2O_2. This catalyst shows a higher catalytic activity for the oxidation of benzothiophenes than other recently reported heterogeneous ODS catalysts in similar systems [22–27]. Strong adsorption of $H_3PMo_{12}O_{40}$ onto the carbon support stabilizes the HPA structure and prevents the HPA from leaching. In addition, our kinetic and infrared spectroscopic studies provide new insights into the mechanism of ODS reaction on carbon-supported HPAs.

Experimental details, including the chemicals used, catalyst preparation, catalyst characterization techniques and catalyst testing methodology, are described in Chapter 2.

3.1. Results and discussion

3.1.1. Catalyst characterization

The carbon-supported HPA catalysts were prepared using a simple wet impregnation procedure with HPA loading in the range of 11–13 wt.% (Table 3.1). The HPA loading did not change after stirring the catalysts (0.5 g) in water (100 mL) at 60 ^{o}C for 1 h. This confirms the strong adsorption of HPAs onto the carbon surface, in agreement with previous reports [29–31], and ensures stability of the HPA/AC–0 catalysts toward HPA leaching during the ODS process.

Table 3.1. Information about HPA/AC–0 catalysts.

Catalyst [a]	S_{BET} [b] (m^2g^{-1})	Pore volume [c] (cm^3g^{-1})	Pore diameter [d] (Å)
Activated carbon AC–0	977	0.89	35
10.9%HPMo/AC–0	1072	0.94	34
11.0%HPW/AC–0	1006	0.85	33
12.7%HSiW/AC–0	1002	0.88	34

[a] HPA loading calculated from Mo and W content determined by ICP-OES analysis. [b] BET surface area. [c] Single point pore volume. [d] Average pore diameter.

The loading of HPAs onto activated carbon had a very little effect on the microporous texture of the support, as evident from the nitrogen adsorption/desorption isotherms shown in Fig. 3.1 for activated carbon and Fig. 3.2–3.4 for HPMo/AC–0, HPW/AC–0, and HSiW/AC–0. It increased the surface area only slightly (3–10%), with the pore volume and pore diameter remaining practically unchanged (Table 3.1). This indicates that the HPA was mostly present on the outer surface rather than occupying the pores of carbon support.

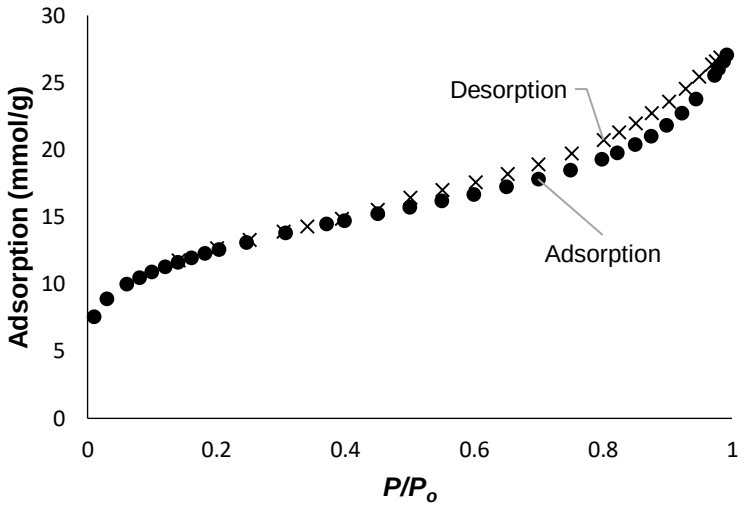

Fig. 3.1. Nitrogen adsorption/desorption isotherms for Darco KB-B activated carbon (AC–0).

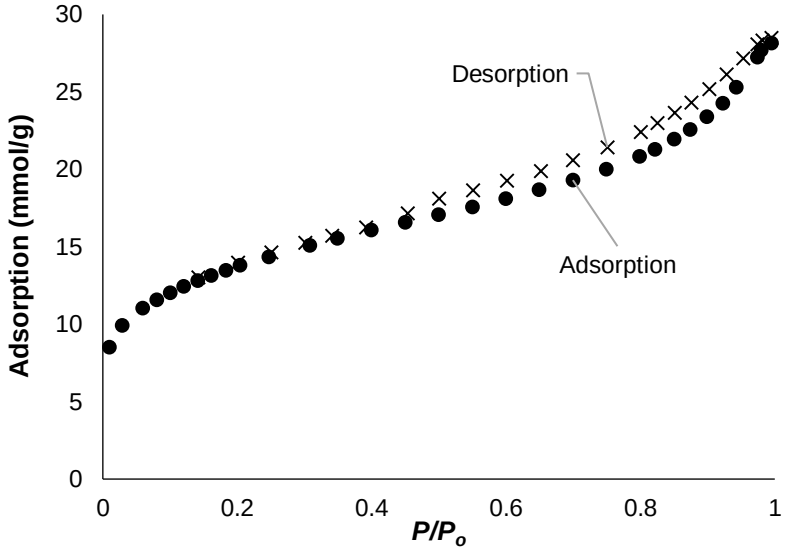

Fig. 3.2. Nitrogen adsorption/desorption isotherms for 10.9%HPMo/AC–0 catalyst.

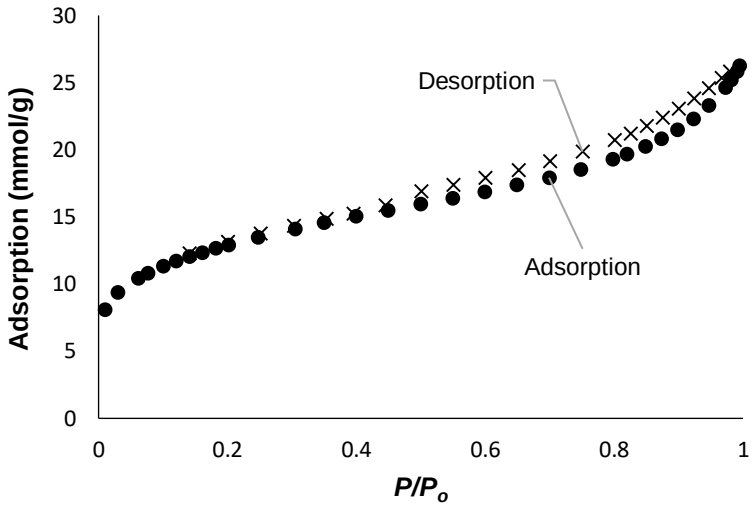

Fig. 3.3. Nitrogen adsorption/desorption isotherms for 10.9%HPW/AC–0 catalyst.

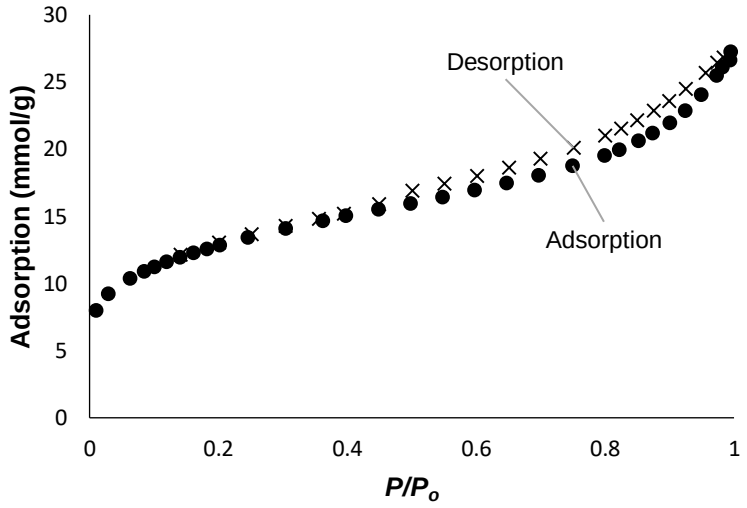

Fig. 3.4. Nitrogen adsorption and desorption isotherms for 12.7%HSiW/AC–0 catalyst

From our thermogravimetric analysis (TGA), the activated carbon and HPMo/AC–0 catalyst contained 17% and 8% of water, respectively (Fig. 3.5 and 3.6). The activated carbon had an elemental composition (%): C, 72.0; H, 3.0; N, 0.0; S, 0.0; O, 25.0 (by difference). Infrared spectrum of the activated carbon is shown in Fig. 3.7.

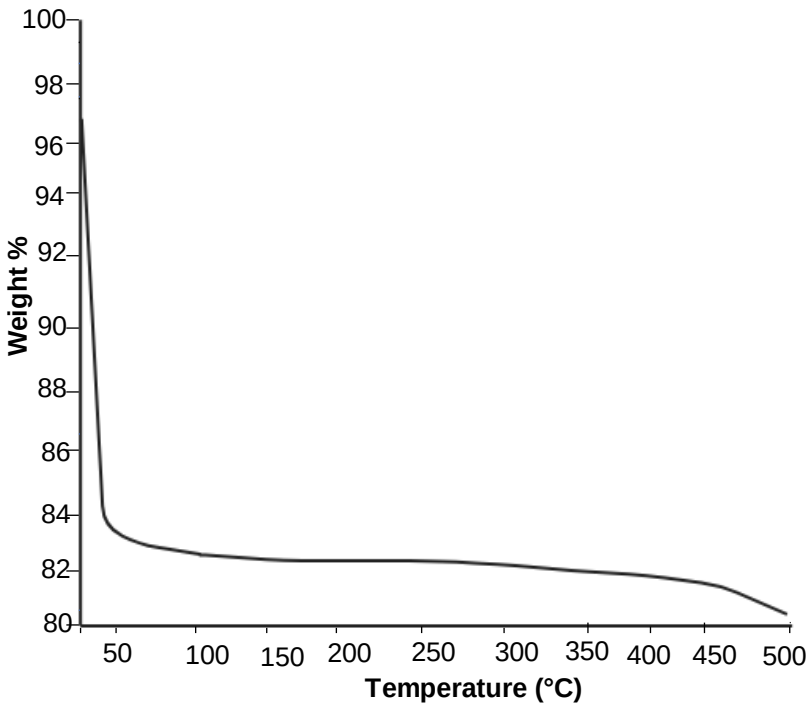

Fig. 3.5. TGA for Darco KB-B activated carbon (AC–0) in N_2 atmosphere showing 17% water content in the sample.

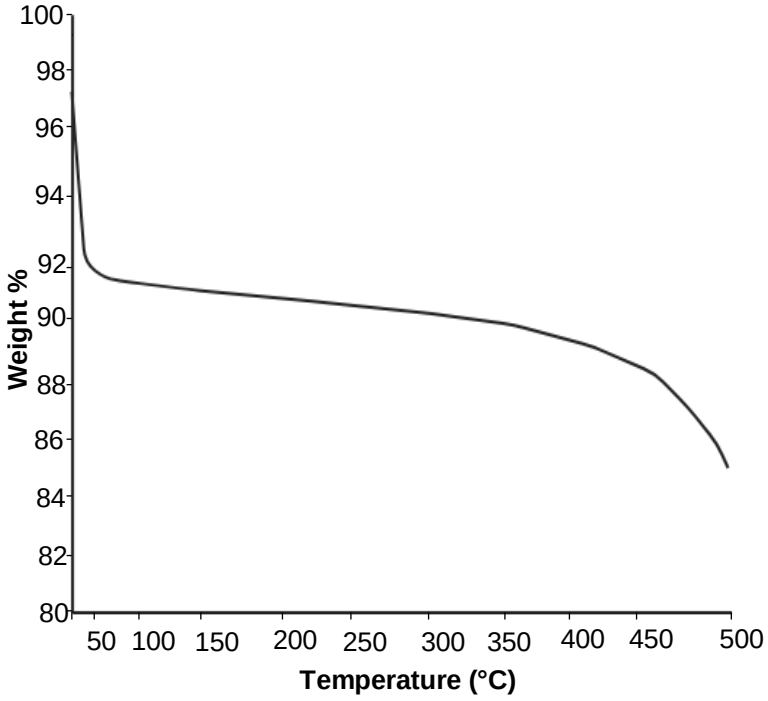

Fig. 3.6. TGA for 10.9%HPMo/AC–0 catalyst in N_2 atmosphere showing 8% water content in the catalyst sample.

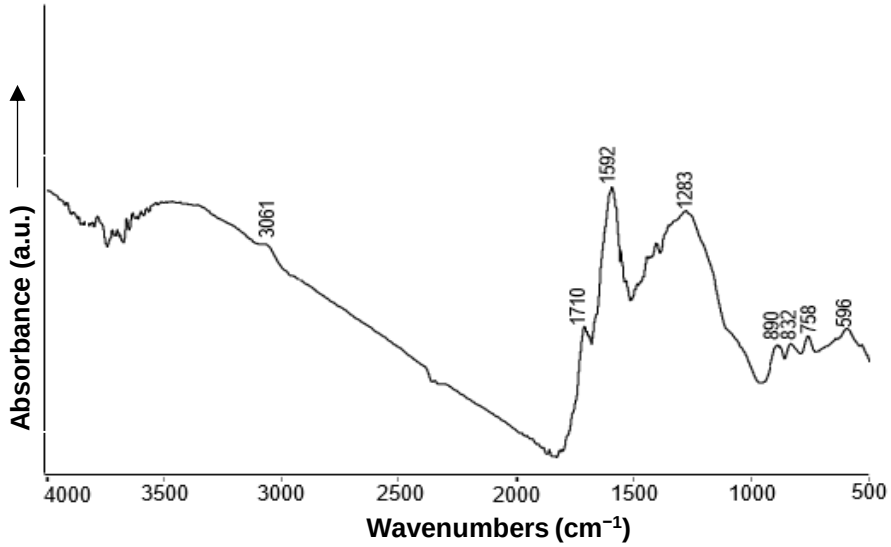

Fig. 3.7. DRIFT spectrum of Darco KB-B activated carbon, AC–0, (1% in KBr).

As evidenced by DRIFT spectroscopy, despite strong HPA-support interaction, the HPAs retained the Keggin structure upon their loading onto the carbon support. For the HPMo catalyst, this is clearly seen in Fig. 3.8, which shows the DRIFT spectra for the fresh HPMo/AC–0 catalyst (spectrum 2) and bulk crystalline HPMo (spectrum 1) as a reference; the latter shows the four characteristic bands at 1062 cm^{-1} (P–O), 960 cm^{-1} (Mo=O), 884 cm^{-1} (Mo–O–Mo corner-sharing) and 811 cm^{-1} (Mo–O–Mo edge-sharing), in agreement with the literature [40]. Close resemblance between the two spectra confirms the integrity of the Keggin structure in the carbon-supported HPMo. The same conclusion also applies to HPW/AC–0 and HSiW/AC–0 catalysts (their DRIFT spectra are presented in Fig. 3.9 and 3.10, respectively), in agreement with previous report [33].

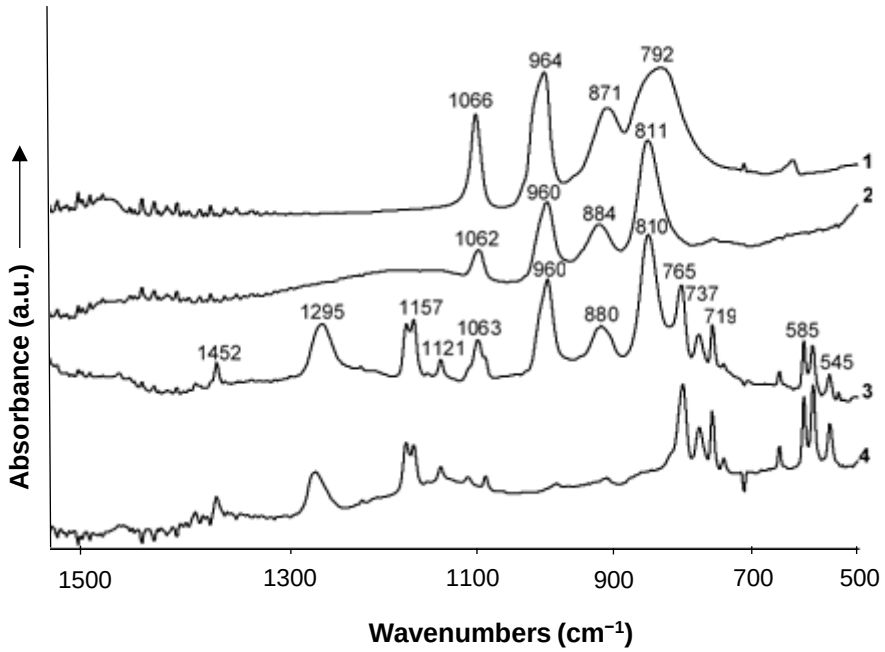

Fig. 3.8. DRIFT spectra of (1) bulk $H_3PMo_{12}O_{40}$, (2) fresh 10.9%HPMo/AC–0 catalyst, (3) spent 10.9%HPMo/AC–0 catalyst after 8 successive runs of DBT oxidation and (4) DBT sulfone adsorbed on activated carbon (powdered sample mixtures with KBr; (1) versus pure KBr background, (2)–(4) versus a mixed KBr + activated carbon background).

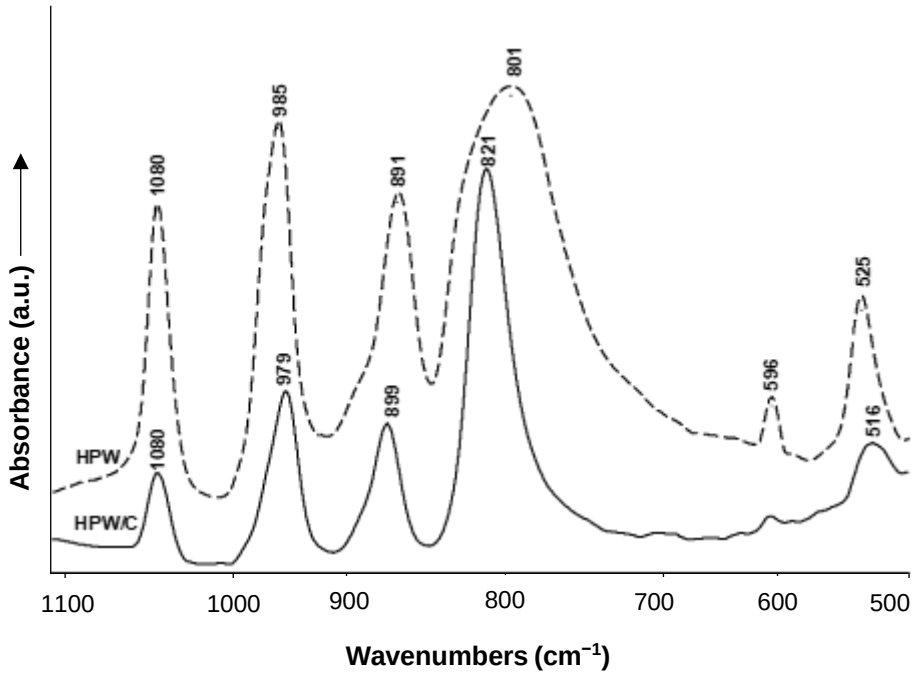

Fig. 3.9. DRIFT spectra of bulk HPW and 11.0%HPW/AC–0 (powdered sample mixtures with KBr; bulk HPW versus pure KBr background, HPW/AC–0 versus a mixed KBr + activated carbon background).

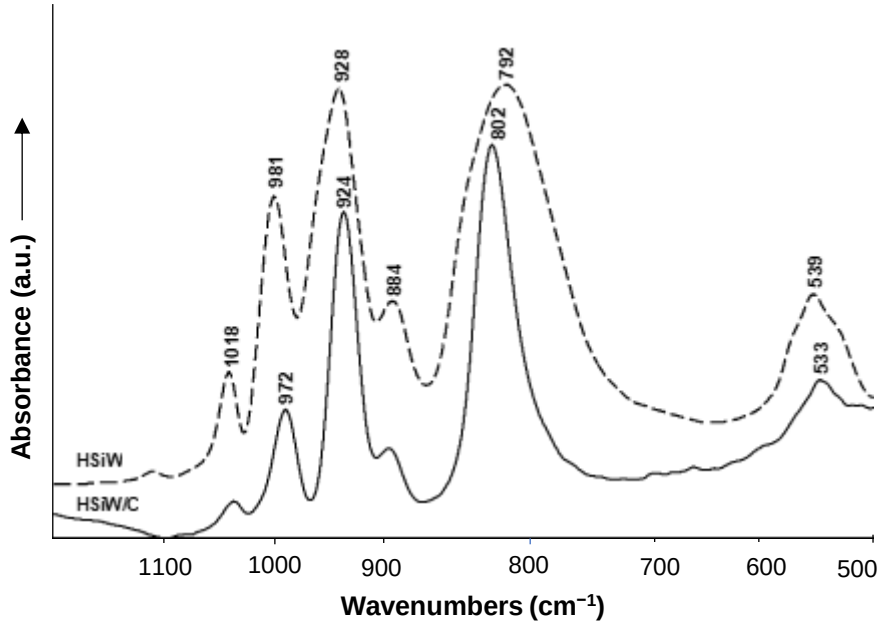

Fig. 3.10. DRIFT spectra of bulk HSiW and 12.7%HSiW/AC–0 (powdered sample mixtures with KBr; bulk HSiW versus pure KBr background, HSiW/AC–0 versus a mixed KBr + activated carbon background).

It should be noted that there is a small (10–20 cm^{-1}) blue shift of the edge-sharing M–O–M band in HPA/AC–0 catalysts in comparison to the corresponding bulk HPAs (Fig. 3.8–3.10). This may be explained by protonation of the edge-sharing bridging oxygens in supported HPAs. It is well known that protons in the HPA crystal lattice link the neighboring polyanions through the oxygen atoms of the terminal M=O groups, as evidenced by single-crystal X-ray and neutron diffraction data for HPW hexahydrate [41]. On the carbon surface, however, no HPA crystal phase has been found even at HPA loadings as high as 45 wt.% [33]; in this case, the HPA would rather exist as a molecular dispersion. In isolated HPA molecules, in contrast to the crystalline HPA, protons are likely to be localized on the edge-sharing bridging oxygens that have a larger negative charge [13].

3.2.2. Oxidation of benzothiophenes by H_2O_2 catalyzed by HPA/AC–0

The HPA/AC–0 catalysts comprising Keggin-type HPAs (HPMo, HPW and HSiW) supported onto activated carbon were used for ODS reaction in a biphasic heptane-H_2O (98:2 v/v) system,

with heptane as a model diesel fuel and benzothiophene (BT, DBT or DMDBT, ~1 wt.%) as an organosulfur compound. 30% H_2O_2 was used as an oxidant; unless otherwise stated, it was used in 50% excess to the stoichiometric amount to ensure 100% conversion of benzothiophenes. Most of the work was carried out with DBT because the oxidation of DBT is typically employed as a model reaction for testing desulfurization catalysts, hence making it easier to compare catalyst performance of different catalyst systems in the literature.

Representative results are given in Table 3.2. The catalytic activity of HPAs in the oxidation of DBT was found to decrease in the order HPMo > HPW > HSiW (entries 1–3 in Table 3.2, Fig. 3.11, see below). The same activity trend has been found previously in biphasic systems with homogeneous [12] and heterogeneous [27] POM catalysts modified with alkylaminocyclophosphazenes. Under our conditions, with H_2O_2 added in 50% excess, the oxidation of DBT gave DBT sulfone as the final product in a 100±13% yield (determined by GC analysis), with only traces of DBT sulfoxide found. Therefore, the oxidation of DBT can be represented by Scheme 3.1.

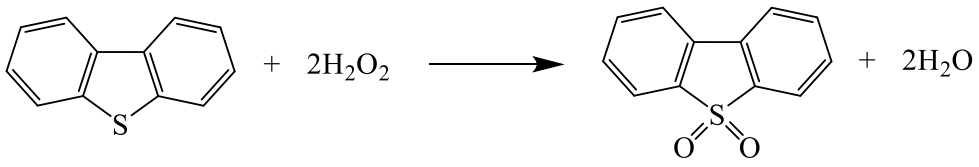

Scheme 3.1. Oxidation of DBT to sulfone by H_2O_2.

Table 3.2. Oxidation of benzothiophenes by H_2O_2 in heptane-H_2O (98:2 v/v) system using HPA/AC–0 catalysts.[a]

Entry	HPA/AC–0	Substrate	H_2O_2/S[b] (mol/mol)	Time (h)	Conversion[c] (%)
1	10.9%HPMo/AC–0	DBT	3.0	0.5	100[d]
2	11.0%HPW/AC–0	DBT	3.0	3.0	89
3	12.7%HSiW/AC–0	DBT	3.0	3.0	49
4	10.9%HPMo/AC–0	DBT	2.0	1.5	98±2[e]
7	10.9%HPMo/AC–0	BT	3.0	2.0	100[f]
8	10.9%HPMo/AC–0	DMDBT	3.0	1.0	100[d]

[a] 60 °C, HPA (0.0041 mmol), substrate (BT, DBT or DMDBT, 0.50 mmol), H_2O_2 (1.50 mmol, 0.166 mL of 30% H_2O_2 (9.05 M) unless stated otherwise), dodecane (GC standard, 0.40 mmol) and heptane (10 mL); stirring speed 1500 rpm. [b] H_2O_2/substrate molar ratio. [c] Substrate conversion to sulfone. [d] 80% H_2O_2 efficiency from post reaction titration with $KMnO_4$; the yield of DBT sulfone 100±13%. [e] Reaction at stoichiometric molar ratio H_2O_2/S = 2.0; hydrogen peroxide efficiency 98±2% (average of three runs). [f] ≥75% H_2O_2 efficiency.

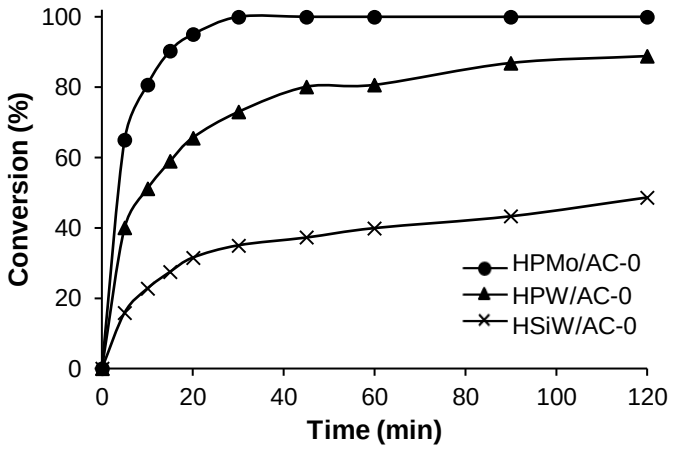

Fig. 3.11. Effect of HPA on the oxidation of DBT (0.50 mmol) by H_2O_2 (1.5 mmol) in heptane (10 mL) catalyzed by HPA/AC–0 at 60 °C (HPA, 0.0041 mmol).

Activated carbon is well known to adsorb benzothiophenes from hydrocarbon media, and this has been used for desulfurization of diesel fuel [6]. In addition, activated carbon itself has been

reported to catalyze the oxidation of DBT by H_2O_2 [43]. In this regard, we tested adsorption of DBT onto neat AC–0 and 10.9%HPMo/AC–0 in the absence of H_2O_2, other conditions being the same as in entry 1 in Table 3.2. We also tested the oxidation of DBT by H_2O_2 in the presence of neat AC–0 at the same conditions. The results are shown in Fig. 3.12. Despite a significant scatter of experimental points, it is clearly seen that the removal of DBT in all these tests was practically the same, ~25±10%. It occurred fast, reaching saturation in less than 5 min. This shows that DBT removal in these systems is largely due to DBT adsorption on AC–0, and the oxidation of DBT by H_2O_2 on the neat AC–0 does not play any significant role. It should be noted that in our initial report (R. Ghubayra et al., Appl. Catal. B 253 (2019) 309–316) the contribution of DBT oxidation on neat AC–0 at such conditions had been estimated at ~30%. The results presented in Fig. 3.12 prove this to be incorrect (for more detail see Chapter 4, sect. 4.1.2). These results provide an important mechanistic insight suggesting that the ODS reaction involves fast DBT adsorption on HPA/AC–0 catalyst followed by DBT oxidation on the catalyst surface. The mechanism of DBT oxidation is discussed in more detail in sect. 3.2.3.

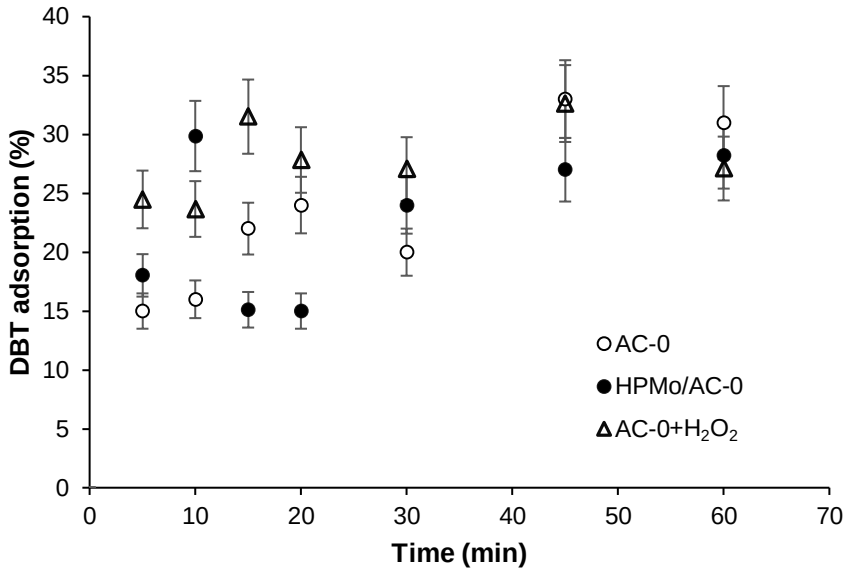

Fig. 3.12. Adsorption of DBT on AC–0 (0.062 g) (open circles) and 10.9%HPMo/AC–0 (0.685 g, 0.041 mmol HPMo) (closed circles) in the absence of H_2O_2 and adsorption of DBT on AC–0 (0.062 g) in the presence of H_2O_2 (1.5 mmol) (triangular points). Conditions: DBT (0.50 mmol), dodecane (GC standard, 0.40 mmol), heptane solvent (10 ml), 60 ^oC and 1500 rpm stirring speed.

The reactivity of benzothiophenes was found to decrease in the order DBT > DMDBT > BT (Table 3.2, entries 1, 7 and 8; Fig. 3.13). The same trend has also been observed in homogeneous and other heterogeneous ODS systems [3,4,8,9,12,28,44,45]. It can be attributed to the electron density on the S atom and steric effects of the methyl groups in DMDBT [9]. The electron density on the S atom increases in the order BT < DBT ≈ DMDBT, which can explain the lower reactivity of BT as compared to DBT and DMDBT. On the other hand, the S atom in DMDBT is sterically hindered by the two neighboring methyl groups rendering it less reactive compared to DBT [9].

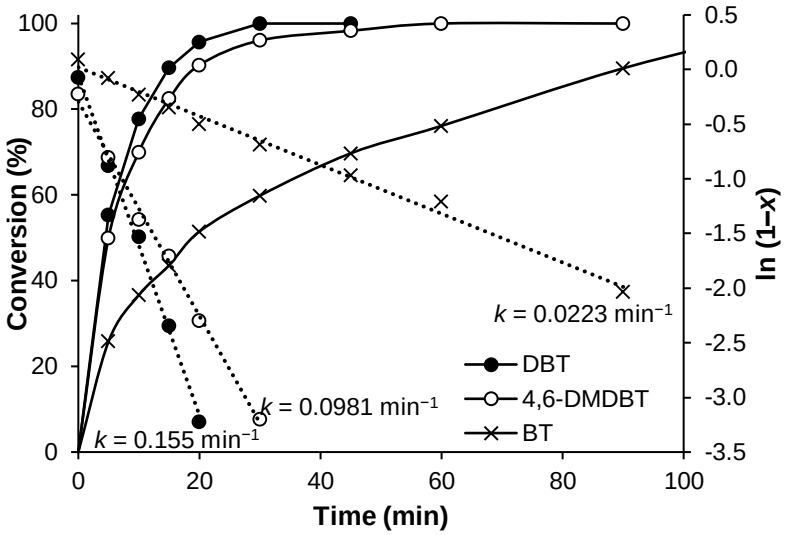

Fig. 3.13. Plot of substrate conversion (x) versus reaction time and first-order plot ln (1–x) = –kt for oxidation of BT, DBT and 4,6-DMDBT (0.50 mmol) by H_2O_2 (1.5 mmol) in heptane (10 mL) catalyzed by 10.9%HPMo/AC–0 (0.0685 g, 1.0 wt.%, 0.0041 mmol HPMo) at 60 °C.

The efficiency of ODS depended on the relative amount of H_2O_2 in the reaction mixture, increasing with an increase in the H_2O_2/DBT molar ratio. Increasing the amount of H_2O_2, however, led to a decrease of the reaction selectivity based on H_2O_2 (H_2O_2 efficiency) due to non-productive decomposition of H_2O_2 to form O_2 and H_2O. For the HPMo/AC–0 catalyst, an optimum H_2O_2/DBT molar ratio was found to be 3.0 (50% H_2O_2 excess), which gave a 100% DBT conversion at 60 °C in 0.5 h with an 80% H_2O_2 efficiency as determined by post reaction titration with $KMnO_4$ (Table 3.2). At stoichiometric ratio H_2O_2/DBT = 2.0 and otherwise the same conditions, the reaction reached a maximum 98% conversion in 1.5 h, thus providing 98% H_2O_2 efficiency (Table 3.2, entry 4). The decrease in H_2O_2 efficiency with increasing the concentration of H_2O_2 could be the result of zero order of the ODS reaction in H_2O_2 (see below) and a positive order of the non-productive H_2O_2 decomposition in H_2O_2. The H_2O_2 efficiency was also found to decrease with increasing the reaction temperature above 60 °C due to a faster decomposition of H_2O_2.

Notably, the HPMo/AC–0 catalyst was found to be more active than its recently reported homogeneous analogue with hexylaminocyclophosphazene (HexPN) as a phase transfer agent [12]. The HPMo/AC–0 catalyst gave 100% DBT conversion in 0.5 h at 60 ^{o}C (Table 3.2), whereas PMo-HexPN gave only 79% conversion under the same reaction conditions and with the same HPMo loading [12]. This may be explained by adsorption of DBT onto the surface of carbon support, which could increase the local concentration of DBT in the vicinity of active catalyst sites.

The HPMo/AC–0 catalyst showed higher activity than other heterogeneous catalysts that have been reported recently for the oxidation of DBT with hydrogen peroxide in similar systems [24–28]. Unfortunately, the data on turnover reaction rates are limited in the literature. Therefore, the results from different reports are compared on the basis of DBT conversion focusing on parameters such as H_2O_2/DBT molar ratio, reaction temperature and reaction time (Table 3.3), see below.

Ti(IV) grafted onto silica gives 99% DBT conversion to sulfone in isooctane with 10–60% H_2O_2 at 60 ^{o}C in 8 h reaction time [24]. With hybrid catalysts comprising Zr(IV) and Hf(IV) oxoclusters in poly(methylmethacrylate) matrix, 84% DBT conversion to sulfone with 94% selectivity has been obtained in octane with 30% H_2O_2 at 65 ^{o}C in 24 h [25]. A polyoxometalate-MOF composite comprising $PW_{11}Zn$ and 2-aminoterephthalic acid in octane–[BIMIM]PF_6 biphasic system at 50 ^{o}C gives 70% DBT conversion in 4 h and 100% in 6 h reaction time; however this has been obtained using a 50-fold molar excess of H_2O_2 over DBT [26]. In this system, the ionic liquid [BIMIM]PF_6 is used to extract the product sulfone from the model diesel. Keggin PMo polyoxometalate immobilized on phosphazene-modified silica PMo/BzPN-SiO_2 gives 100% DBT conversion in heptane with 30% H_2O_2 at H_2O_2/DBT = 3.0 and 60 ^{o}C, but it takes a longer reaction time of 3 h [27]. 5%$[PSPy]_3PMo_{12}O_{40}$/Graphite catalyst (1 wt.% in fuel), where PSPy is N-(3-sulfonatepropyl)-pyridinium ion, gives 100% DBT

conversion at 50 °C, H_2O_2/DBT = 3.0 and 1 h reaction time [28], which is close to the performance of our 10.9%HPMo/AC–0 catalyst (1 wt.% in fuel, H_2O_2/DBT = 3.0, 60 °C, 0.5 h). However, the 5%$[PSPy]_3PMo_{12}O_{40}$/Graphite catalyst is prepared by a tedious and lengthy hydrothermal procedure [28], whereas our catalyst is easily obtained from off-the-shelf components by a straightforward wet impregnation procedure (Chapter 2).

Table 3.3. Comparison of heterogeneous catalysts for oxidation of DBT by H_2O_2 in model diesel fuel.[a]

Catalyst	Model diesel	H_2O_2/DBT (mol/mol)	T (°C)	Time (h)	DBT conversion (%)	Reference
HPMo/AC–0	heptane	3.0	60	0.5	100	This work
Ti(IV)/SiO_2	isooctane	5.0	60	8	99	[22]
Zr(IV)/PMMA[b]	octane	3.5	65	24	84	[23]
PW_{11}Zn-MOF[c]	octane	50	50	6	100	[24]
PMo/BzPN-SiO_2[d]	heptane	3.0	60	3	100	[25]
[PSPy]PMo/C[e]	octane	3.0	50	1	100	[26]

[a] Biphasic systems comprising a model diesel phase and aqueous H_2O_2 phase. [b] Zr(IV) oxoclusters in poly(methylmethacrylate) matrix (PMMA). [c] MOF comprising PW_{11}Zn polyoxometalate and 2-aminoterephthalic acid in octane–[BIMIM]PF_6 biphasic system. [d] PMo polyoxometalate immobilized on phosphazene-functionalized silica. [e] 5%$[PSPy]_3PMo_{12}O_{40}$/Graphite (PSPy = N-(3-sulfonatepropyl)-pyridinium ion), 1% in reaction mixture.

Moreover, the HPMo/AC–0 catalyst exhibited excellent recyclability; it was reused eight times in the oxidation of DBT at 60 °C, giving 100% DBT conversion after each use (Fig. 3.14). After eight catalyst recycles, catalyst productivity amounted to 10 g DBT per 1 g catalyst and 94 g DBT per 1 g HPMo. The successful catalyst reuse indicates no leaching of HPMo from the catalyst. The lack of leaching is further supported by ICP-OES analysis, which found no

Mo in aqueous extract from the reaction mixture after reaction, thus supporting true heterogeneous catalysis in the ODS reaction.

Fig. 3.14. Catalyst reuse in oxidation of DBT (0.50 mmol, 1.3 wt.% in reaction mixture) by H_2O_2 (1.5 mmol) in heptane (10 mL) catalyzed by 10.9%HPMo/AC–0 (0.0685 g, 1.0 wt.%, 0.0041 mmol HPMo) at 60 °C, 1 h.

3.2.3. Kinetics and mechanism

Further kinetic and DRIFT spectroscopic studies provided an important insight into the mechanism of the ODS reaction catalyzed by carbon-supported HPA.

As expected, the rate of ODS reaction increased with increasing the temperature. For the oxidation of DBT with HPMo/AC–0 catalyst, the apparent activation energy was found to be 49 kJ mol^{-1} in the temperature range 40–70 °C (the Arrhenius plot is shown in Fig. 3.15). This value is high enough to indicate the absence of diffusion limitations in the reaction system, which is also supported by the independence of reaction rate from the stirring speed (Fig. 3.16).

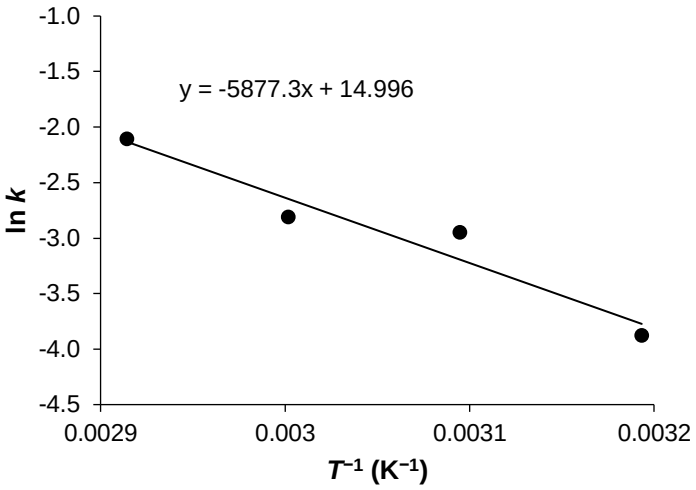

Fig. 3.15. Arrhenius plot for oxidation of DBT (0.50 mmol) by H_2O_2 (1.5 mmol) catalyzed by 10.9%HPMo/AC–0 (0.0343 g, 0.0020 mmol HPMo).

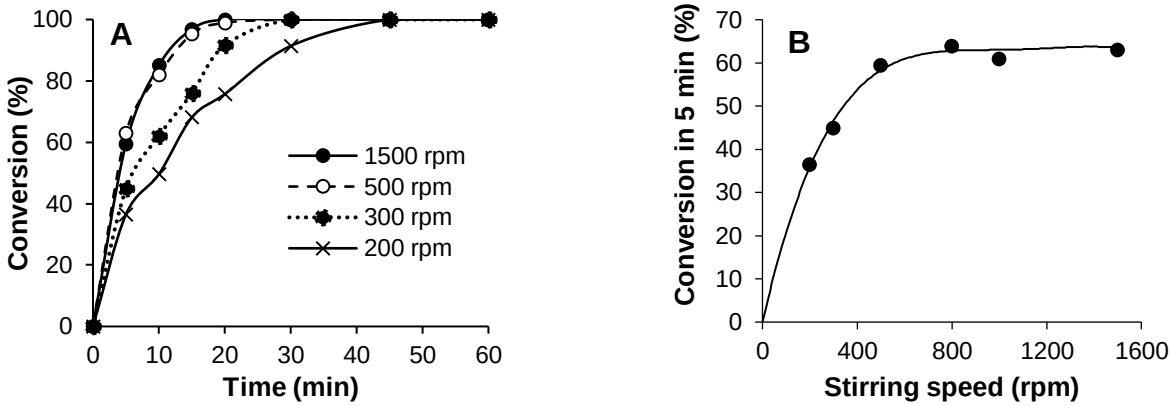

Fig. 3.16. Effect of stirring speed on DBT oxidation catalyzed by 10.9%HPMo/AC–0 at 60 °C (HPMo, 0.0041 mmol; DBT, 0.50 mmol; 30% H_2O_2, 1.5 mmol; n-heptane, 10 ml): DBT conversion vs. reaction time (A) and stirring speed (B).

The oxidation of BT, DBT and DMDBT in the presence of HPMo/AC–0 catalyst was found to be first order in benzothiophene (Fig. 3.13), with the rate constants 0.0223±0.0008, 0.155±0.004 and 0.0981±0.0031 min^{-1}, respectively, at 60 °C and other conditions specified in Fig. 3.13. The reaction was also found to be first order in the catalyst HPMo/AC–0 (Fig. 3.17).

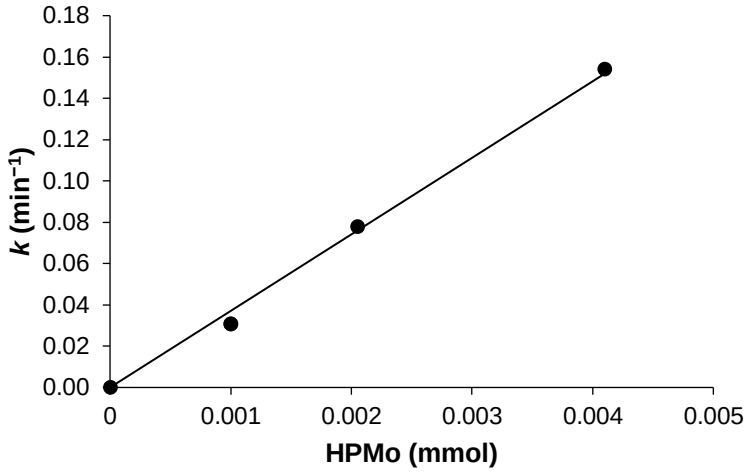

Fig. 3.17. Effect of catalyst amount on the rate of DBT (0.50 mmol) oxidation by H_2O_2 (1.5 mmol) catalyzed by 10.9%HPMo/AC–0 at 60 °C (*k* is the first-order rate constant).

Therefore, the ODS reaction in the presence of HPMo/AC–0 obeyed the rate equation (1), where k_{ODS} is the second-order rate constant. The first order in benzothiophenes has also been reported for the ODS in the presence of $[PSPy]_3PMo_{12}O_{40}$/Graphite [28].

$$-\frac{d[\mathrm{DBT}]}{dt} = k_{\mathrm{ODS}}[\mathrm{HPMo}][\mathrm{DBT}] \qquad (1)$$

It was found that a 4-fold decrease in concentration of H_2O_2 in the aqueous phase of the heptane-H_2O system did not affect the rate of DBT oxidation, which indicates zero reaction order in H_2O_2. This was monitored by changing the heptane/H_2O ratio from 98/2 to 93/7 v/v by adding 0.2–0.6 mL of H_2O to 10 mL of heptane at a constant amount of H_2O_2 (1.5 mmol) (Table 3.4).

Table 3.4. Effect of water additives on DBT oxidation catalyzed by 10.9%HPMo/AC–0.[a]

Heptane-H_2O (v/v)	H_2O added (mL)	[H_2O_2] (M)	k (min^{-1})
98/2	0.0	9.0	0.079±0.003
96/4	0.2	4.1	0.081±0.012
95/5	0.4	2.7	0.079±0.006
93/7	0.6	2.0	0.073±0.004

[a] 60 °C, HPMo (0.0041 mmol), DBT (0.50 mmol), H_2O_2 (1.5 mmol, 0.166 mL of 30% H_2O_2 (9.05 M)), heptane (10 mL).

Fig. 3.8 shows the DRIFT spectrum for the spent HPMo/AC–0 catalyst (spectrum 3) after eight successive runs presented in Fig. 3.14. Comparison with the spectrum of the fresh catalyst discussed above (spectrum 2) clearly shows that the spent catalyst retained the HPMo Keggin structure. In addition, the spent catalyst has some DBT sulfone adsorbed on its surface, as evident from comparison with the reference spectrum of the sulfone adsorbed on activated carbon (spectrum 4). This sulfone, however, did not affect catalyst activity as can be seen from the excellent catalyst reuse (Fig. 3.14).

Another important piece of evidence regarding the active state of HPA/AC–0 catalysts in the ODS system was obtained from DRIFT spectra of catalyst samples pretreated with H_2O_2 (Fig. 3.18 and Fig. 3.19). Generally, ^{31}P NMR is a very effective tool for such analysis [12,14,15]. However, carbon-supported HPAs give broad ^{31}P MAS NMR peaks [33]. In this case, DRIFTS can provide more detailed information about the integrity of HPA structure. The catalysts were treated with 30% H_2O_2 under conditions similar to those used for the ODS reaction, except in the absence of benzothiophenes. HPMo/AC–0 and HPW/AC–0 samples (0.1 g) were stirred with 30% H_2O_2 (1.5 mmol) in heptane (5 mL) at room temperature or 60 °C for 10 min, filtered off using a Buchner funnel and dried under vacuum to afford a dry, black powder. The samples were ground with KBr, and their DRIFT spectra were measured against a mixture of KBr and activated carbon as the background. As seen in Fig. 3.18, the HPMo/AC–0 catalyst treated with

H_2O_2 at room temperature as well as at 60 ^oC has exactly the same infrared spectrum as the fresh HPMo/AC–0 catalyst in the range of 700–1100 cm^{-1}, characteristic of the Keggin structure. This clearly shows that the structure remains intact after the H_2O_2 treatment. The same result was obtained for HPW/AC–0 catalyst (Fig. 3.19).

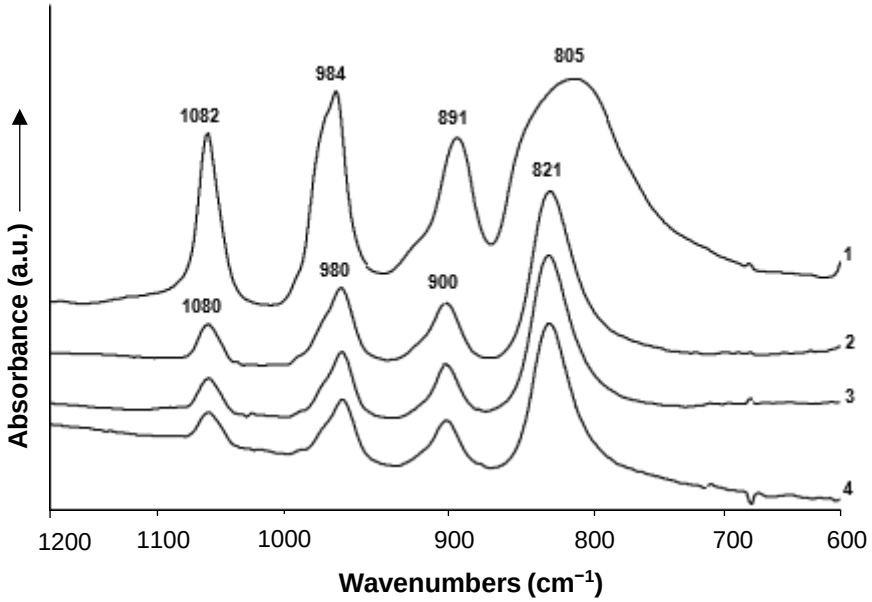

Fig. 3.18. DRIFT spectra of (1) bulk $H_3PMo_{12}O_{40}$, (2) fresh 10.9%HPMo/AC–0 catalyst, (3) 10.9%HPMo/AC–0 catalyst treated with H_2O_2 at 60 ^oC and (4) 10.9%HPMo/AC–0 catalyst treated with H_2O_2 at 20 ^oC (powdered sample mixtures with KBr; (1) versus pure KBr background, (2)–(4) versus a mixed KBr + carbon background).

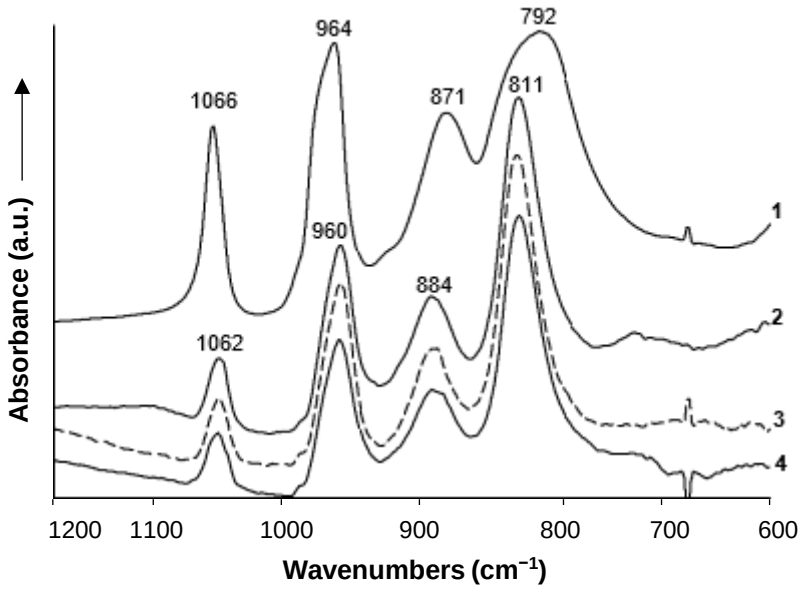

Fig. 3.19. DRIFT spectra of (1) bulk $H_3PW_{12}O_{40}$, (2) fresh 11.0%HPW/AC–0 catalyst, (3) 11.0%HPW/AC–0 catalyst treated with H_2O_2 at 60 ^oC and (4) 11.0%HPW/AC–0 catalyst treated with H_2O_2 at 20 ^oC (powdered sample mixtures with KBr; (1) versus pure KBr background, (2)–(4) versus a mixed KBr + carbon background).

Overall, our DRIFTS data provide an important insight into the mechanism of ODS reaction over carbon-supported HPA catalysts, specifically regarding the active peroxo species involved in this reaction. It is evident that there is a clear difference between homogeneous and heterogeneous ODS based on the H_2O_2/POM redox system. In homogeneous ODS and alkene epoxidation systems (including truly homogeneous as well as biphasic systems), it has been demonstrated that interaction between the Keggin POM and H_2O_2 leads to Keggin structure breakdown to form peroxo complexes (observed by ^{31}P and ^{183}W NMR), which act as the active oxidizing species in these reactions ([12,14,15] and references therein). Conversely, in the carbon-supported HPA catalysts, the Keggin structure is preserved due to strong interaction between molecularly dispersed HPA and the carbon surface. In this case, the active oxidizing species could be transient peroxo complexes formed between the intact Keggin polyanions and H_2O_2.

The vast chemistry of peroxo complexes of Mo(VI) and W(VI), including general patterns of their structure and reactivity, has been thoroughly reviewed by Dickman and Pope [46]. It is recognized that the η^2-O_2^{2-} peroxo ligand is a π-donor like the oxo ligand [46], and the terminal metal-oxo groups M=O can be converted into η^2-peroxo groups $M(O_2)^{2-}$. Thus the terminal bonds W^{VI}=O converted into η^2-peroxo groups $W^{VI}(O_2)^{2-}$ have been found in the lacunary Keggin polyanion $[(Co^{II}O_4)W_{11}O_{31}(O_2)_4]^{10-}$ [46]. It may therefore be suggested that the terminal Mo=O and W=O bonds in the Keggin HPMo and HPW can interact reversibly with H_2O_2 to form the corresponding labile η^2-peroxo complexes without breaking the Keggin structure on the carbon surface, as shown in Scheme 3.2. These complexes can then act as the active oxidizing species in ODS reaction. Strong HPA adsorption on the carbon support is thought to be the key to high stability of the Keggin unit in the presence of H_2O_2. It may not be the case with less adsorbing supports and weaker POM frameworks. Thus, the lacunary $[PW_{11}O_{39}]^{7-}$ unit within a solid hybrid catalyst has been reported to decompose upon interaction with H_2O_2 to form peroxo W^{VI} species [47].

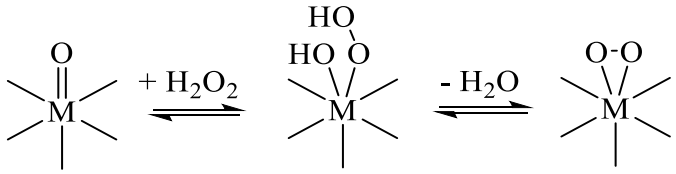

Scheme 3.2. Formation of peroxo moiety in metal-oxygen octahedron within Keggin HPA supported on activated carbon (M = Mo^{VI} or W^{VI}).

The proposed reaction scheme for the oxidation of DBT in model diesel fuel by H_2O_2 catalyzed by HPA/AC–0 is shown in Scheme 3.3. In the initial step (**1**), the HPA reacts with H_2O_2 to form the peroxo species on the carbon surface. This species then oxidizes DBT to form DBT sulfone and the initial oxo species via step (**2**), thus completing the catalytic cycle. DBT sulfoxide may be formed in step (**2**), but probably does not desorb, being readily oxidized to

DBT sulfone on the catalyst surface. In heptane-H_2O system, it was not possible to monitor the sulfoxide and sulfone during reaction because neither was soluble; however intermediate formation of DBT sulfoxide has been observed in different solvents [48]. Sulfur-free diesel fuel can be separated from the solid catalyst and precipitated sulfone by filtration. The sulfone can be separated from the catalyst by solvent extraction (e.g., with toluene), and the catalyst can be reused.

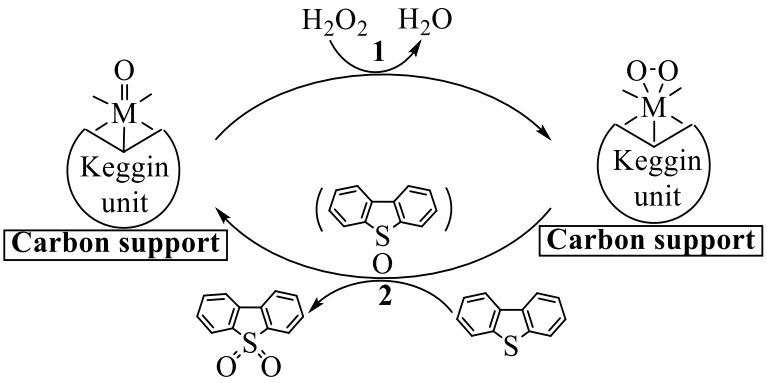

Scheme 3.3. Reaction scheme for oxidation of DBT by H_2O_2 catalyzed by HPA/AC–0 (M = Mo^{VI} or W^{VI}).

$$P(Mo{=}O)_{12} + mH_2O_2 \overset{\text{fast}}{\rightleftharpoons} \{P(Mo{=}O)_{12-m}[Mo(O_2^{2-})_m]\} + mH_2O \quad (1)$$

$$DBT + \{P(Mo{=}O)_{12-m}[Mo(O_2^{2-})_m]\} \xrightarrow{\text{slow}} Sulfoxide + \{P(Mo{=}O)_{12-m+1}[Mo(O_2^{2-})_{m-1}]\} \quad (2)$$

$$Sulfoxide + \{P(Mo{=}O)_{12-m}[Mo(O_2^{2-})_m]\} \xrightarrow{\text{fast}} Sulfone + \{P(Mo{=}O)_{12-m+1}[Mo(O_2^{2-})_{m-1}]\} \quad (3)$$

$$\{P(Mo{=}O)_{12-m+1}[Mo(O_2^{2-})_{m-1}]\} + H_2O_2 \overset{\text{fast}}{\rightleftharpoons} \{P(Mo{=}O)_{12-m}[Mo(O_2^{2-})_m]\} + H_2O \quad (4)$$

Scheme 3.4. Proposed step-by-step mechanism for DBT oxidation catalyzed by HPMo/AC–0.

Reflecting on the kinetic and DRIFTS results, the mechanism of oxidation of DBT catalyzed by HPMo/AC–0 may be represented by Scheme 3.4. In step (1), $P(Mo{=}O)_{12}$, the initial HPMo/AC–0 catalyst, reacts with hydrogen peroxide to form the peroxo species $\{P(Mo{=}O)_{12-m}[Mo(O_2^{2-})_m]\}$ as shown above in Scheme 3.2. From the DRIFTS results, the Keggin structure

remains intact in the presence of H_2O_2, which indicates that this peroxo species is labile and step (1) is probably equilibrated. This is followed by the oxidation of DBT to sulfoxide (step 2) and further to sulfone (step 3) by the peroxo species. As only traces of sulfoxide were found in the reaction products, it can be suggested that the oxidation of DBT to sulfoxide is the rate limiting step followed by fast oxidation of the sulfoxide adsorbed on the catalyst surface to sulfone. It has been reported that the sulfoxide is oxidised faster that DBT [49]. Finally, the active peroxo species is rapidly regenerated in step (4). Fast formation of the peroxo species in step (1) and its fast regeneration in step (4) will keep the concentration of the peroxo species constant as long as the amount of H_2O_2 in the reaction mixture exceeds the amount of HPMo. Consequently, as long as this stands, the ODS reaction will be first order in DBT and zero order in H_2O_2. This is indeed the case as can be seen from the data in Fig. 3.13 and Table 3.4.

The order of HPA catalytic activity in the ODS reaction, HPMo > HPW > HSiW, is directly correlated with the rate of oxygen (^{17}O) exchange of Keggin heteropoly anions in aqueous solution, which increases in the order of addenda atoms W(VI) < Mo(VI), as determined from ^{17}O NMR [50]. This is in agreement with the proposed mechanism via steps (1)–(4) because all these steps involve oxygen atom transfer to and from the addenda atoms, which can be expected to be more feasible for Mo(VI) than W(VI).

3.2. Conclusions

This work demonstrates that Keggin-type heteropoly acids supported on activated carbon are active catalysts for oxidative desulfurization (ODS) of model diesel fuel in a biphasic heptane-H_2O system using 30% H_2O_2 as an oxidant. The carbon-supported HPA catalysts are easily obtained from off-the-shelf components by a straightforward wet impregnation procedure. The catalytic activity of HPA/AC–0 decreases in the order of HPA: $H_3PMo_{12}O_{40}$ > $H_3PW_{12}O_{40}$ > $H_4SiW_{12}O_{40}$. The most active catalyst, $H_3PMo_{12}O_{40}$/AC–0, removes 100% of benzothiophenes

from model diesel fuel at 60 ^{o}C and could be recovered and reused many times without loss of activity. This catalyst outperforms other recently reported heterogeneous catalysts for ODS in similar systems. Kinetic and DRIFTS studies suggest a mechanism for heterogeneous ODS reaction on carbon-supported HPAs, which is different from that for a homogeneously-catalyzed ODS reaction. Carbon-supported HPAs, in contrast to their homogeneous counterparts, retain their Keggin structure and form labile active peroxo species without destruction of the HPA Keggin unit, which oxidize benzothiophenes to the corresponding sulfoxides and sulfones.

References

[1] V. Babich, J. A. Moulijn, Science and technology of novel processes for deep desulfurization of oil refinery streams, Fuel 82 (2003) 607–631.

[2] R. Prins, Hydrotreating, in Handbook of Heterogeneous Catalysis, ed. G. Ertl, H. Knözinger, F. Schüth, J. Weitkamp, Vol. 6, Wiley-VCH, 2008; p. 2695–2718.

[3] A.W. Bhutto, R. Abro, S. Gao, T. Abbas, X. Chen, G. Yu, Oxidative desulfurization of fuel oils using ionic liquids: A review, J. Taiwan Inst. Chem. Eng. 62 (2016) 84–97.

[4] Z. Jiang, H. Lü, Y. Zhang and C. Li, Oxidative desulfurization of fuel oils, Chin. J. Catal. 32 (2011) 707–715.

[5] U. Domańska, K. Walczak, M. Królikowski, Extraction desulfurization process of fuels with ionic liquids, J. Chem. Thermodyn 77 (2014) 40–45.

[6] J. Bu, G. Loh, C.G. Gwie, S. Dewiyanti, M. Tasrif, A. Borgna, Desulfurization of diesel fuels by selective adsorption on activated carbons: Competitive adsorption of polycyclic aromatic sulfur heterocycles and polycyclic aromatic hydrocarbons, Chem. Eng. J. 166 (2011) 207–217.

[7] D. Boniek, D. Figueiredo, A.F.B. dos Santos, M.A. de Resende Stoianoff, Biodesulfurization: A mini review about the immediate search for the future technology, Clean Technol. Environ. Policy 17 (2014) 29–37.

[8] F.M. Collins, A.R. Lucy, C. Sharp, Oxidative desulfurization of oils via hydrogen peroxide and heteropolyanion catalysis, J. Mol. Catal. A Chem. 117 (1997) 397–403.

[9] C. Komintarachat, W. Trakarnpruk, Oxidative desulfurization using polyoxometalates, Ind. Eng. Chem. Res. 45 (2006) 1853–1856.

[10] A.F. Shojaei, M.A. Rezvani, M.H. Loghmani, Comparative study on oxidation desulfurization of actual gas oil and model sulfur compounds with hydrogen peroxide promoted by formic acid: Synthesis and characterization of vanadium containing

polyoxometalate supported on anatase crushed nanoleaf, Fuel Process. Technol 118 (2014) 1–6.

[11] A.E.S. Choi, S. Roces, N. Dugos, M.W. Wan, Oxidation by H_2O_2 of bezothiophene and dibenzothiophene over different polyoxometalate catalysts in the frame of ultrasound and mixing assisted oxidative desulfurization, Fuel 180 (2016) 127–136.

[12] M. Craven, R. Yahya, E.F. Kozhevnikova, C.M. Robertson, A. Steiner, I.V. Kozhevnikov, Alkylaminophosphazenes as efficient and tuneable phase-transfer agents for polyoxometalate-catalyzed biphasic oxidation with hydrogen peroxide, ChemCatChem 8 (2016) 200–208.

[13] I.V. Kozhevnikov, Catalysts for fine chemical synthesis: Catalysis by polyoxometalates, Wiley, West Sussex, 2002.

[14] L. Salles, C. Aubry, R. Thouvenot, F. Robert, C. Doremieux-Morin, G. Chottard, H. Ledon, Y. Jeannin, J.-M. Bregeault, ^{31}P and ^{183}W NMR spectroscopic evidence for novel peroxo species in the $H_3[PW_{12}O_{40}]_yH_2O/H_2O_2$ system. Synthesis and X-ray structure of tetrabutylammonium (μ-hydrogen phosphato)bis(μ-peroxo)bis(oxoperoxotungstate)(2-): A catalyst of olefin epoxidation in a biphase medium, Inorg. Chem. 33 (1994) 871–878.

[15] D.C. Duncan, R.C. Chambers, E. Hecht, C.L. Hill, Mechanism and dynamics in the $H_3[PW_{12}O_{40}]$-catalyzed selective epoxidation of terminal olefins by H_2O_2. Formation, reactivity, and stability of $\{PO_4[WO(O_2)_2]_4\}^{3-}$, J. Am. Chem. Soc. 117 (1995) 681–691.

[16] C. Venturello, J.C.J. Bart, M. Ricci, A new peroxotungsten heteropoly anion with special oxidizing properties: Synthesis and structure of tetrahexylammonium tetra(diperoxotungsto)phosphate(3-), J. Mol. Catal. 32 (1985) 107–110.

[17] C. Venturello, M. Gambaro, A convenient catalytic method for the dihydroxylation of alkenes by hydrogen peroxide, Synthesis, 4 (1989) 295–297.

[18] C. Venturello, R. D'Aloisio, Quaternary ammonium tetrakis(diperoxotungsto)phosphates(3-) as a new class of catalysts for efficient alkene epoxidation with hydrogen peroxide, J. Org. Chem. 53 (1988) 1553–1557.

[19] Y. Ishii, K. Yamawaki, T. Ura, H. Yamada, T. Yoshida, M. Ogawa, Hydrogen peroxide oxidation catalyzed by heteropoly acids combined with cetylpyridinium chloride: Epoxidation of olefins and allylic alcohols, ketonization of alcohols and diols, and oxidative cleavage of 1,2-diols and olefins, J. Org. Chem. 53 (1988) 3587–3593.

[20] R. Yahya, M. Craven, E.F. Kozhevnikova, A. Steiner, P. Samunual, I. V. Kozhevnikov, D.E. Bergbreiter, Polyisobutylene oligomer-bound polyoxometalates as efficient and recyclable catalysts for biphasic oxidations with hydrogen peroxide, Catal. Sci. Technol. 5 (2015) 818–821.

[21] M. Craven, R. Yahya, E.F. Kozhevnikova, R. Boomishankar, C.M. Robertson, A. Steiner, I.V. Kozhevnikov, Novel polyoxometalate-phosphazene aggregates and their use as catalysts for biphasic oxidations with hydrogen peroxide, Chem. Commun. 49 (2013) 349–351.

[22] M. Zhang, W. Zhu, H. Li, M. Li, S. Yin, Y. Li, Y. Wei, H. Li, Facile fabrication of molybdenum-containing ordered mesoporous silica induced deep desulfurization in fuel, Colloids Surface A 504 (2016) 174–181.

[23] J. Zhang, A. Wang, Y. Wang, H. Wang, J. Gui, Heterogeneous oxidative desulfurization of diesel oil by hydrogen peroxide: Catalysis of an amphipathic hybrid material supported on SiO_2, Chem. Eng. J. 245 (2014) 65–70.

[24] J.M. Fraile, C. Gil, J.A. Mayoral, B. Muel, L. Roldán, E. Vispe, S. Calderón, F. Puente, Heterogeneous titanium catalysts for oxidation of dibenzothiophene in hydrocarbon solutions with hydrogen peroxide: On the road to oxidative desulfurization, Appl. Catal. B 180 (2016) 680–686.

[25] M. Vigolo, S. Borsacchi, A. Soraru, M. Geppi, B.M. Smarsly, P. Dolcet, S. Rizzato, M. Carraro, S. Gross, Engineering of oxoclusters-reinforced polymeric materials with application as heterogeneous oxydesulfurization catalysts, Appl. Catal. B 182 (2016) 636–644.

[26] D. Julião, A.C. Gomes, M. Pillinger, R. Valença, J.C. Ribeiro, B. de Castro, I.S. Gonçalves, L. Cunha Silva, S.S. Balula, Zinc-substituted polyoxotungstate@amino-MIL-101(Al) – An efficient catalyst for the sustainable desulfurization of model and real diesels, Eur. J. Inorg. Chem. 2016 (2016) 5114–5122.

[27] M. Craven, D. Xiao, C. Kunstmann-Olsen, E. F. Kozhevnikova, F. Blanc, A. Steiner, I. V. Kozhevnikov, Oxidative desulfurization of diesel fuel catalyzed by polyoxometalate immobilized on phosphazene-functionalized silica, Appl. Catal. B 231 (2018) 82–91.

[28] W. Jiang, D. Zheng, S. Xun, Y. Qin, Q. Lu, W. Zhu, H. Li, Polyoxometalate-based ionic liquid supported on graphite carbon induced solvent-free ultra-deep oxidative desulfurization of model fuels, Fuel 190 (2017) 1–9.

[29] Y. Izumi, K. Urabe, Catalysis of heteropoly acids entrapped in activated carbon, Chem. Lett. (1981) 663–666.

[30] Y. Izumi, K. Urabe, M. Onaka, Zeolite, clay and heteropoly acid in organic reactions, Kodansha/VCH, Tokyo, 1992; p. 99–161.

[31] S.M. Kulikov, M.N. Timofeeva, I.V. Kozhevnikov, V.I. Zaikovskii, L.M. Plyasova, I.A. Ovsyannikova, Adsorption of heteropoly acid $H_4SiW_{12}O_{40}$ from solutions onto porous supports, Izv. Akad. Nauk SSSR, Ser. Khim. 1989; p. 763–768.

[32] M.A. Schwegler, H. van Bekkum, N.A. de Munck, Heteropoly acids as catalysts for the production of phthalate diesters, Appl. Catal. 74 (1991) 191–204.

[33] I.V. Kozhevnikov, A. Sinnema, R.J.J. Jansen, H. van Bekkum, ^{17}O NMR determination

of proton sites in heteropoly acid $H_3PW_{12}O_{40}$. ^{31}P, ^{29}Si and ^{17}O NMR, FTIR and XRD study of $H_3PW_{12}O_{40}$ and $H_4SiW_{12}O_{40}$ supported on carbon, Catal. Lett. 27 (1994) 187–197.

[34] F. Lefebvre, P. Dupont, A. Auroux, Study of the acidity of $H_3PW_{I2}0_{40}$ supported on activated carbon by microcalorimetry and methanol dehydration reaction, React. Kinet. Catal. Lett. 55 (1995) 3–9.

[35] F.X. Liu-Cai, B. Sahut, E. Faydi, A. Auroux, G. Herve, Study of the acidity of carbon supported and unsupported heteropolyacid catalysts by ammonia sorption microcalorimetry, Appl. Catal. A 185 (1999) 75–83.

[36] M.S. Kaba, M.A. Barteau, W.Y. Lee, I.K. Song, Nanoscale characterization of acid properties of heteropolyacids byscanning tunneling microscopy and tunneling spectroscopy, Appl. Catal. A 194 -195 (2000) 129–136.

[37] R. Neumann, M. Levin, The selective aerobic oxidative dehydrogenation of alcohols and amines catalyzed by a supported molybdenum-vanadium heteropolyanion salt $Na_5PV_2Mo_{10}0_{40}$, J. Org. Chem. 56 (1991) 5707–5710.

[38] S. Fujibayashi, K. Nakayama, M. Hamamoto, S. Sakaguchi, Y. Nishiyama, Y. Ishii, An efficient aerobic oxidation of various organic compounds catalyzed by mixed addenda heteropolyoxometalates containing molybdenum and vanadium, J. Mol. Catal. A 110 (1996) 105–117.

[39] L. Xu, E. Boring, C.L. Hill, Polyoxometalate-modified fabrics: New catalytic materials for low-temperature aerobic oxidation, J. Catal. 195 (2000) 394–405.

[40] C. Rocchiccioli-Deltcheff, M. Fournier, R. Franck, R. Thouvenot, Evidence for anion-anion interactions in molybdenum(VI) and tungsten(VI) compounds related to the Keggin structure, Inorg. Chem. 22 (1983) 207–216.

[41] G. M. Brown, M.-R. Noe-Spirlet, W. R. Busing, H. A. Levy, Dodecatungstophosphoric acid hexahydrate, $(H_5O_2^+)_3(PW_{12}O_{40}^{3-})$. The true structure of Keggin's `pentahydrate' from single-crystal X-ray and neutron diffraction data, Acta Cryst. B 33 (1977) 1038–1046.

[42] I.V. Kozhevnikov, Catalysis by heteropoly acids and multicomponent polyoxometalates in liquid-phase reactions, Chem. Rev. 98 (1998) 171–198.

[43] G. Yu, S. Lu, H. Chen, Z. Zhu, Diesel fuel desulfurization with hydrogen peroxide promoted by formic acid and catalyzed by activated carbon, Carbon 43 (2005) 2285–2294.

[44] X. Jiang, H. Li, W. Zhu, L. He, H. Shu, J. Lu, Deep desulfurization of fuels catalyzed by surfactant-type decatungstates using H_2O_2 as oxidant, Fuel 88 (2009) 431–436.

[45] J. Zhang, A. Wang, X. Li, X. Ma, Oxidative desulfurization of dibenzothiophene and diesel over $[Bmim]_3PMo_{12}O_{40}$, J. Catal. 279 (2011) 269–275.

[46] M.H. Dickman, M.T. Pope, Peroxo and superoxo complexes of chromium, molybdenum, and tungsten, Chem. Rev. 94 (1994) 569–584.

[47] Z.X. Zhang, W. Zhao, B.C. Ma, Y. Ding, Catal. Commun. The epoxidation of olefins catalyzed by a new heterogeneous polyoxometalate-based catalyst with hydrogen peroxide, Chem. Commun. 12 (2010) 318–322.

[48] E. Rafiee, N. Rahpeyma, Selective oxidation of sulfurs and oxidation desulfurization of model oil by 12-tungstophosphoric acid on cobalt-ferrite nanoparticles as magnetically recoverable catalyst. Chin. J. Catal. 36 (2015) 1342–1349.

[49] B.N. Heimlich, T.J. Wallace, Kinetics and mechanism of the oxidation of dibenzothiophene in hydrocarbon solution. Oxidation by aqueous hydrogen peroxide-acetic acid mixtures, Terahedron 22 (I966) 3571–3579.

[50] M. A. Fedotov, R. I. Maksimovskaya, D. U. Begalieva, A. K. Il'yasova, ^{17}O NMR spectra and isotope exchange of oxygen in aqueous solutions of phosphorus-vanadium-tungsten heteropoly acids, Russ. Chem. Bull. 29 (1980) 1025–1028.

4 Oxidative desulfurization over carbon-supported heteropoly acids: effect of carbon support

The removal of sulfur from fuels to reduce SO_2 emission from automotive vehicles and stationary combustion sources is a high priority environmental task [1,2]. Although the sulfur content in diesel fuel has decreased dramatically over the past two decades, its further reduction is strongly desired [1,2]. In this connection, the removal of refractory aromatic organosulfur compounds such as benzothiophenes from diesel fuel is a challenging problem as these sulfur compounds are difficult to remove by the conventional hydrodesulfurization (HDS) technology. Besides, the HDS operates at rather harsh conditions (300–400 °C, 30–130 atm) in the presence of Ni–Mo and Co–Mo catalysts [1,2]. Oxidative desulfurization (ODS) is a promising alternative/complementary technology that allows deep desulfurization of diesel fuels under mild conditions [3,4]. Typically, the ODS involves liquid-phase biphasic oxidation of organosulfur compounds with hydrogen peroxide at 50–70 °C and ambient pressure to yield sulfoxies and sulfones, which are separated from fuel by extraction or adsorption [3,4]. Other oxidants, such as O_2 [5], organic peroxides [6], etc., can also be used. The primary advantage of ODS over HDS is the high efficiency in removing the refractory aromatic sulfur compounds under very mild reaction conditions.

Polyoxometalates (POMs), especially Keggin-type POMs, are exceptionally active ODS catalysts [7–12]. These POMs include heteropolyanions $XM_{12}O_{40}^{m-}$, where M is the metal ion, most frequently M = Mo^{6+} and W^{6+}, and X is the central atom, typically P^{5+}, Si^{4+}, etc. [12]. Typical Keggin POMs are commercially available as the corresponding heteropoly acids $H_mXM_{12}O_{40}$ (HPAs). Initially, POMs had been used as homogeneous catalysts in a fuel–H_2O–H_2O_2 biphasic system in combination with a phase transfer agent (e.g., quaternary ammonium

cation) transferring water-soluble POMs from aqueous to fuel phase [4,7]. There is compelling evidence that in homogeneous systems in the presence of H_2O_2, the Keggin POMs partially decompose to form peroxo-POMs, which are the catalytically active species in the ODS reaction [4,11], as well as in other oxidations by H_2O_2, e.g., alkene epoxidation [13,14]. The homogeneously catalyzed ODS, however, has a serious practical drawback, namely, the difficulty of catalyst separation from the fuel. To overcome this, in the last decade, a number of POM-based heterogeneous ODS catalysts have been reported ([15] and references therein). These include POMs supported or chemically bound onto a wide range of porous materials such as, among others, SiO_2 [16], HMS [17], SBA–15 [18], MCM–41 [19], various MOF [20], graphite [21], carbon nanotubes [22] and graphene oxide [23].

Activated carbon (AC) is well documented in adsorption desulfurization [24] and has also been reported as the POM support for ODS reaction [25–27]. It has been found that AC can strongly adsorb Keggin HPAs from polar media such as water and methanol [28–30]. As a result, the carbon-supported HPA catalysts are stable towards HPA leaching in such media [29–31]. Our group has reported Keggin HPAs supported on Darco KB-B activated carbon (fine powder of 150 μm particle size) as highly active catalysts for ODS of model diesel (heptane spiked with dibenzothiophene (DBT)) [32]. These results are described in detail in Chapter 3. The catalytic activity decreases in the order $H_3PMo_{12}O_{40}$ > $H_3PW_{12}O_{40}$ > $H_4SiW_{12}O_{40}$. The most active catalyst, 11%$H_3PMo_{12}O_{40}$/AC (~1 wt.% in diesel), exhibits 100% DBT removal from diesel at 60 ºC and H_2O_2/DBT = 3 mol/mol in 0.5 h and can be reused without loss of activity. This catalyst outperforms other reported heterogeneous ODS catalysts in similar systems. From DRIFTS, the HPAs retain their Keggin structure on the carbon surface and are suggested to form labile active peroxo species without destruction of the Keggin unit, which oxidize DBT to DBT sulfone [32].

Here, given the great diversity of activated carbons, we aim to investigate the effect of AC support on the activity of AC-supported Keggin heteropoly acids $H_3PMo_{12}O_{40}$ and $H_3PW_{12}O_{40}$ in the ODS of the model diesel fuel comprising heptane and DBT using aqueous 30% H_2O_2 as the oxidant. While certain HPA/AC ODS catalysts have been reported [25–27,32], no systematic analysis of the effect of AC on catalyst activity has been published so far to the best of our knowledge. DBT is frequently used as a sulfur-containing substrate for testing desulfurization catalysts; this allows for easy comparison of different catalyst systems reported in the literature. Ten commercial AC powder samples available from Sigma–Aldrich and Merck are tested in this study. It is demonstrated that the AC support has a strong effect on the integrity of HPA structure on the carbon surface and the activity of HPA/AC catalysts. As a result, a significant improvement of catalyst performance is achieved to exceed the activity of best reported heterogeneous ODS catalysts.

As mentioned in the experimental section (Chapter 2), a range of activated carbons includes Darco KB-B activated carbon (AC–0) studied previously [27] and nine other carbon samples (AC–1–AC–9). Their catalogue numbers and the properties, such as C, H and O elemental composition, water content, pH of aqueous extract, surface area and porosity, will be discussed later. The carbon-supported HPA catalysts (HPA/AC–*n*) were prepared as described previously by impregnating heteropoly acids HPMo and HPW onto AC supports. The oxidation of DBT by aqueous 30% H_2O_2 in the presence of HPA/AC–*n* catalysts was carried in a 50 mL jacketed glass reaction vessel equipped with a heat circulator, a magnetic stirrer and a reflux condenser as described in Chapter 2.

4.1. Results and discussion

4.1.1. Catalyst characterization

The AC samples used as the HPA support had a surface area from 480 to 2900 m^2g^{-1}, a pore volume 0.33–1.10 cm^3g^{-1} and a pore diameter 19–35 Å (Table 4.1). Water content in the samples varied from 2–17 wt.%. From combustion elemental analysis, the relatively dry AC samples (2–4 wt.% H_2O) contained ~90 wt.% C, 0.3–0.9 wt.% H and 5–13 wt.% O (oxygen content determined by difference). Wet samples AC-0 and AC-4 (17 wt.% H_2O) had a higher O and H content and a lower C content, as expected due to the presence of water.

Table 4.1. Information about activated carbon supports (AC).

AC	Cat. No.[a]	C (wt.%)	H (wt.%)	O[b] (wt.%)	H_2O[c] (wt.%)	pH[d]	S_{BET}[e] (m^2g^{-1})	Pore volume[f] (cm^3g^{-1})	Pore diameter[g] (Å)
AC–0	278106	72.0	3.0	25.0	17	4.0	977	0.89	35
AC–1	102183[h]	89.6	0.9	9.5	7	9.5	844	0.64	30
AC–2	05112	86.6	0.4	13.0	3	9.1	999	0.52	20
AC–3	05105	94.1	0.7	5.2	4	8.5	751	0.51	27
AC–4	161551	67.1	2.7	30.2	17	5.5	1408	1.10	31
AC–5	10275	94.0	0.3	5.7	2	10.1	1021	0.49	19
AC–6[i]	C9157	86.9	0.3	12.4	4	8.5	878	0.51	23
AC–7	901931	93.4	0.3	6.3	3	8.7	2901	1.05	19
AC–8	901937	87.1	0.6	12.3	8	8.3	482	0.33	27
AC–9	901933	86.7	0.4	12.9	8	8.6	791	0.75	37

[a] Sigma-Aldrich catalogue number. [b] Determined by difference. [c] From TGA weight loss at 40–200 °C. [d] pH of aqueous extracts (10% AC in water). [e] BET surface area; AC samples pre-treated at 220 °C/1 Pa. [f] Single point pore total volume. [g] Average BET pore diameter. [h] Merck catalogue number. [i] 0.4% nitrogen content.

Surface pH of AC samples, measured as the pH of aqueous extracts (10% AC in water) is an important property that can affect the state of HPA on the carbon surface, i.e. HPA structural integrity. The surface pH varied significantly, from, 4.0 to 10.1 (Table 4.1). Notably, the AC–0 carbon support studied previously [32] was the most acidic one; it had the lowest surface pH of 4.0. All other AC samples had a higher pH (>8.3), except AC–4 having pH 5.5.

DRIFT spectra for all AC samples studied are shown in Fig. 4.1 and Fig. 4.2. These spectra are similar to the spectra of different activated carbons reported in the literature [33]. The bands in the range of 3500–3800 cm^{-1} can be attributed to the OH groups in AC and adsorbed water, those at 2800–2900 cm^{-1} are attributable to the C–H stretching vibrations and the multiple bands in the range of 600–1800 cm^{-1} are characteristic of the C=O stretching vibrations and adsorption of other groups such as $–CH_3$, $–CH_2–$, C=C, C–O, etc. [33].

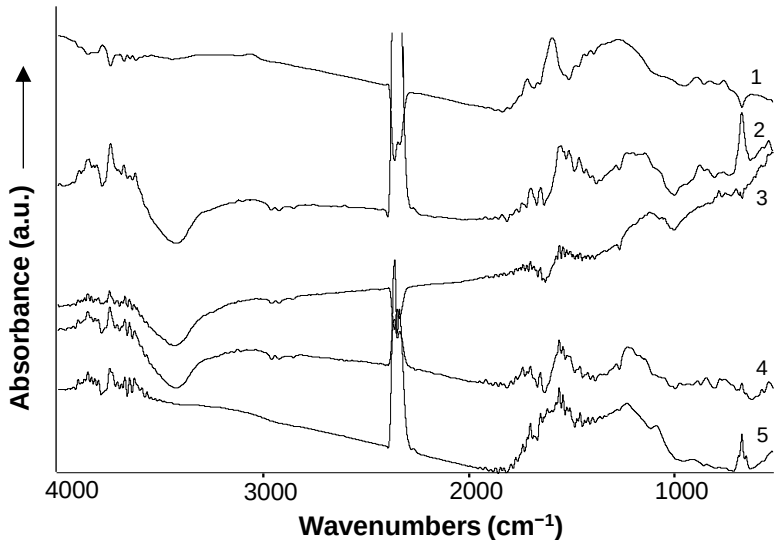

Fig. 4.1. DRIFT spectra of activated carbons (1% in KBr vs. KBr): AC–0 (1), AC–1 (2), AC–2 (3), AC–3 (4), AC–4 (5).

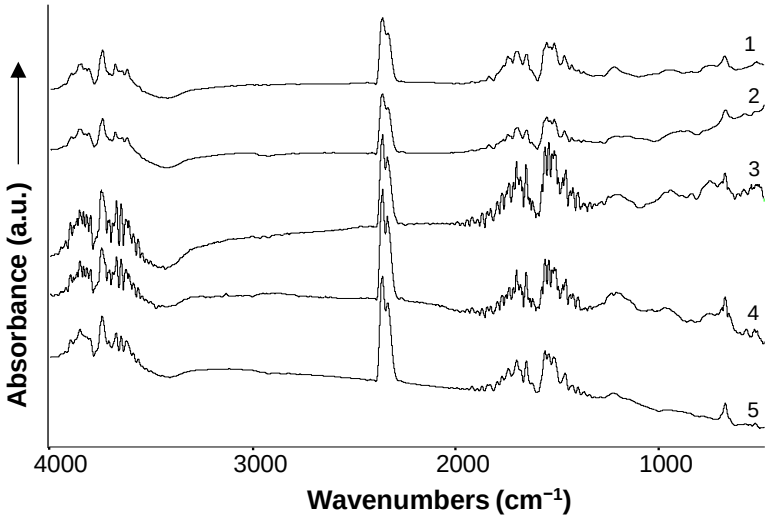

Fig. 4.2. DRIFT spectra of activated carbons (1% in KBr vs. KBr): AC–5 (1), AC–6 (2), AC–7 (3), AC–8 (4), AC–9 (5).

Information about the carbon-supported HPA catalysts studied, HPMo/AC–*n* and HPW/AC–*n*, is given in Table 4.2 including the HPA loading and catalyst texture. Comparison with the data in Table 4.1 shows that the loading of HPA caused some reduction in the surface area and pore volume, as expected, whereas the average pore diameter was practically unaffected (see below).

DRIFT spectroscopy is an indispensable technique to characterize the state of HPA on the carbon surface [32]. DRIFT spectra for more active HPMo/AC–*n* and HPW/AC–*n* catalysts (see below) are shown in Fig. 4.3 and Fig. 4.4, respectively; the spectra for less active catalysts are displayed in Fig. 4.5 and Fig. 4.6. Previous DRIFT spectroscopy study [32] has shown that both HPMo and HPW retained the Keggin structure on the surface of AC–0 support. These results were confirmed in the present work.

Table 4.2. Information about HPA/AC–*n* catalysts.

Catalyst[a]	S_{BET}[b] (m^2g^{-1})	Pore volume[c] (cm^3g^{-1})	Pore diameter[d] (Å)
11%HPMo/AC–0	1072	0.94	34
16%HPMo/AC–1	734	0.58	32
8.6%HPMo/AC–2	713	0.37	21
16%HPMo/AC–3	661	0.53	32
19%HPMo/AC–4	915	0.74	32
16%HPMo/AC–5	950	0.45	19
14%HPMo/AC–6	871	0.52	24
16%HPMo/AC–7	1358	0.67	20
13%HPMo/AC–8	609	0.56	37
14%HPMo/AC–9	944	0.96	41
11%HPW/AC–0	1006	0.85	33
17%HPW/AC–1	776	0.59	30
8.3%HPW/AC–2	785	0.41	21
14%HPW/AC–3	672	0.53	32
18%HPW/AC–4	848	0.67	32
13%HPW/AC–5	884	0.42	19
16%HPW/AC–6	770	0.45	23
17%HPW/AC–7	1471	0.73	20
17%HPW/AC–8	624	0.54	35
21%HPW/AC–9	688	0.65	38

[a] HPA loading determined from ICP-OES analysis of Mo and W content (±1%). [b] BET surface area; AC samples pre-treated at 220 ºC/1 Pa. [c] Single point pore total volume. [d] Average BET pore diameter.

For the HPMo/AC–0 catalyst, this is clearly seen in Fig. 4.3, which shows a close resemblance between the reference spectrum (1) of bulk crystalline HPMo and the spectrum (2) of HPMo/AC–0 catalyst. The reference spectrum (1) shows four characteristic infrared adsorption bands for the HPMo Keggin anion at 1065 cm^{-1} (P–O), 964 cm^{-1} (Mo=O), 871 cm^{-1} (Mo–O–Mo corner-sharing) and 792 cm^{-1} (Mo–O–Mo edge-sharing), in agreement with [34]. The same conclusion applies to HPW/AC–0 catalyst as illustrated in Fig. 4.4, which shows a close similarity between the spectra of bulk crystalline HPW reference (1) and the HPW/AC–0 catalyst (2). The reference spectrum (1) for the bulk HPW shows four characteristic bands at 1080 cm^{-1} (P–O), 984 cm^{-1} (W=O), 891 cm^{-1} (W–O–W corner-sharing) and 803 cm^{-1} (W–O–W edge-sharing), in agreement with [34]. There is a small (10–20 cm^{-1}) blue shift of the edge-

sharing M–O–M band in HPA/AC-0 catalysts in comparison to the corresponding bulk HPAs, which has been noted previously and explained by protonation of the edge-sharing oxygens in carbon-supported HPAs [32].

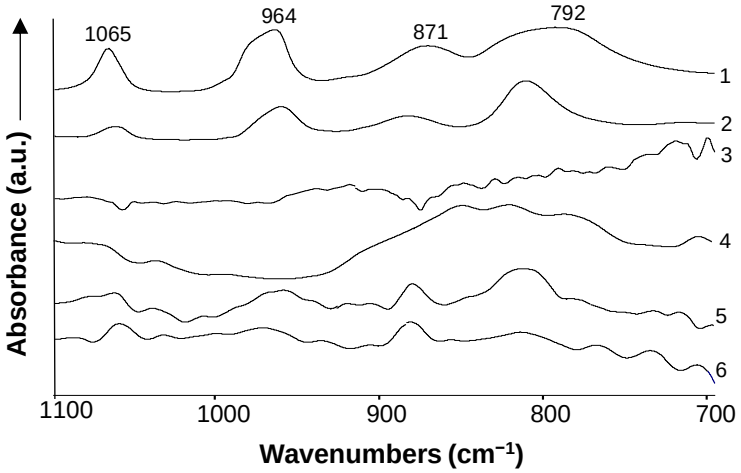

Fig. 4.3. DRIFT spectra of HPMo/AC catalysts (1% in KBr vs. KBr): bulk HPMo (1), 11%HPMo/AC–0 (2), 17%HPMo/AC–1 (3), 8.3%HPMo/AC–2 (4), 14%HPMo/AC–3 (5), 18%HPMo/AC–4 (6), 17%HPMo/AC–7 (7); spectra (3)–(7) scaled up 10-fold compared to (2).

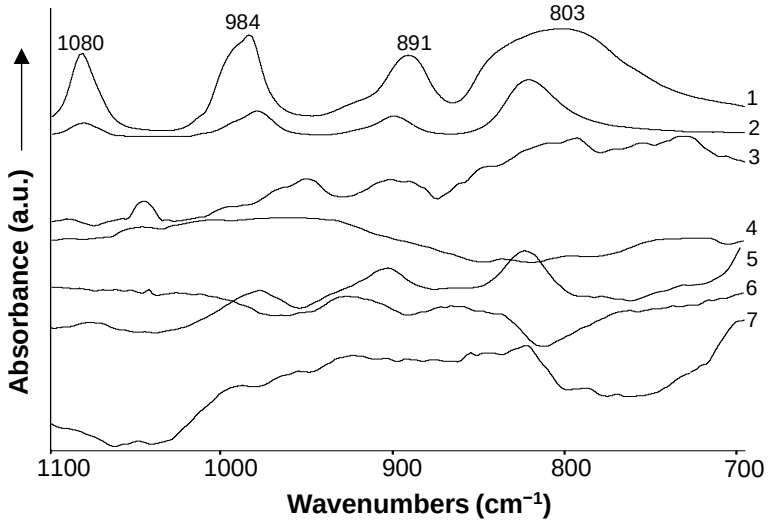

Fig. 4.4. DRIFT spectra of HPW/AC catalysts (1% in KBr vs. KBr): bulk HPW (1), 11%HPW/AC–0 (2), 17%HPW/AC–1 (3), 8.3%HPW/AC–2 (4), 14%HPW/AC–3 (5), 18%HPW/AC–4 (6), 17%HPW/AC–7 (7); spectra (3)–(7) scaled up 10-fold compared to (2).

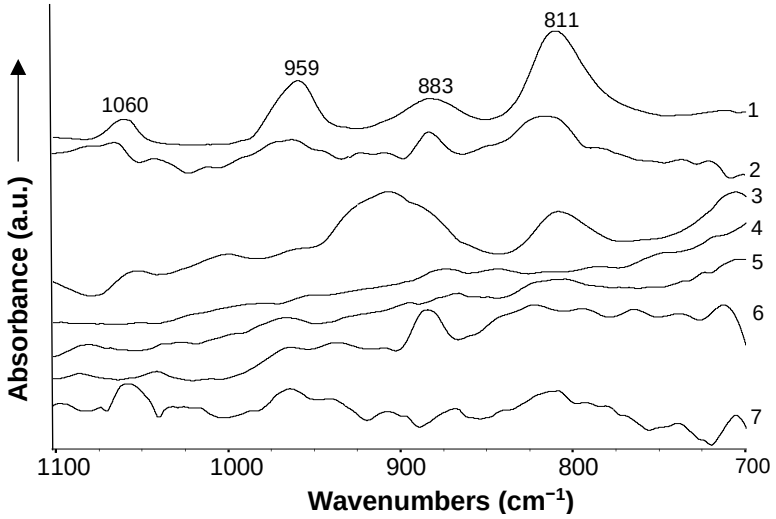

Fig. 4.5. DRIFT spectra of HPMo/AC catalysts (1% in KBr vs. KBr): 11%HPMo/AC–0 (1), 16%HPMo/AC–3 (2), 19%HPMo/AC–4 (3), 16%HPMo/AC–5 (4), 14%HPMo/AC–6 (5), 13%HPMo/AC–8, 14%HPMo/AC–9 (7); spectra (2)–(7) scaled up 10-fold compared to (1).

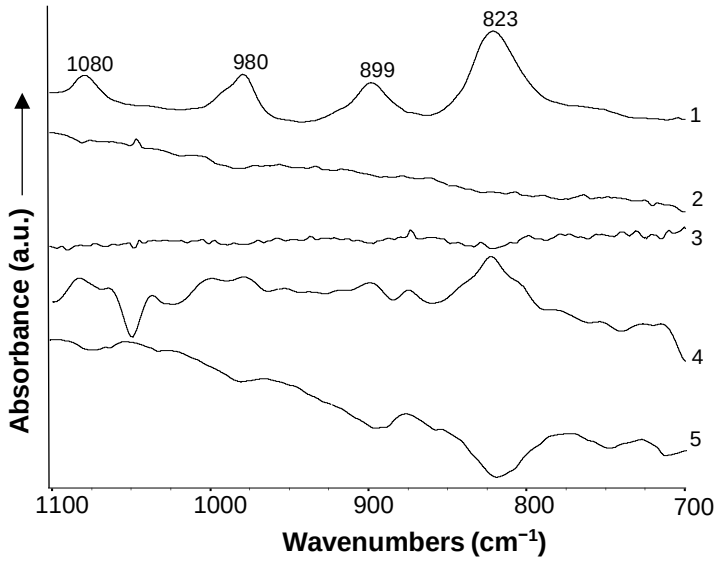

Fig. 4.6. DRIFT spectra of HPW/AC catalysts (1% in KBr vs. KBr): 11%HPW/AC–0 (1), 13%HPW/AC–5 (2), 16%HPW/AC–6 (3), 17%HPW/AC–8 (4), 21%HPW/AC–9 (5); spectra (2)–(5) scaled up 10-fold compared to (1).

The DRIFT spectra for the HPA catalysts supported on all other carbon supports AC–1 to AC–9 in the range of 700–1100 cm^{-1} characteristic of the Keggin structure were much less intense in comparison to HPA/AC–0. In Fig. 4.3–4.6, these spectra are scaled up 10-fold compared to

the spectra for HPA/AC–0 where the Keggin structure was intact. In most cases, no infrared adsorption bands characteristic of the Keggin structure can be seen, except for HPMo/AC–3, HPMo/AC–7 (Fig. 4.3, spectra 5 and 6) and HPW/AC–3 (Fig. 4.4, spectrum 5), where these bands are present, however, with a low intensity. This indicates that in these catalysts, in contrast to HPA/AC–0, the Keggin structure of HPAs was largely decomposed. The reason for this is likely to be the basicity of carbon supports AC–*n* (*n* = 1–9), as evidenced by their surface pH values (Table 4.1). In aqueous solution, the Keggin structure of HPW and HPMo is well known to be stable in acidic media at pH below 1–2; as the pH increases, it gradually decomposes to form eventually tungstate and molybdate anions [12]. Amongst the carbon supports AC–*n* (*n* = 0–9) studied here, AC–0 is the most acidic one (pH 4.0). Other supports AC–*n* (*n* = 1–9) are all basic (pH 8.3–10.1), except AC–4 (pH 5.5). Therefore, it is likely that the Keggin heteropolyanions are subjected to base-catalyzed degradation on the surface of AC–*n* (*n* = 1–9). From the DRIFTS data, this occurs even with the rather acidic AC–4 (pH 5.5). It should be noted that the difference in pH of AC–0 and AC–4 is quite significant to affect the state of heteropolyanions, as evidenced by the data shown in Table 1.4 (Chapter 1). The state of Mo^{6+} and W^{6+} in HPA/AC–*n* catalysts is as yet unknown; possibly these are monomeric and oligomeric M^{6+} oxo species on the carbon surface. Therefore, these results demonstrate that the structural integrity of HPA on the carbon surface strongly depends of the carbon support. The same can be expected for the activity of carbon-supported HPA catalysts. This is indeed the case as shown below.

4.1.2. Oxidation of DBT over HPA/AC–*n* catalysts

The oxidation of DBT in the presence of HPA/AC–*n* catalysts was carried out using the same procedure as in the previous report [32]: at 60 ^{o}C, H_2O_2/DBT = 3.0 mol/mol, 0.0056 mmol HPA, ~1 wt.% catalyst per model diesel unless stated otherwise (Chapter 3). Representative results for HPMo/AC–*n* are given in Table 4.3 and for HPW/AC–*n* in Table 4.4. These include

the DBT conversion at 20 min and 120 min reaction time unless stated otherwise, the initial turnover frequency (TOF) per mole of HPA at 5 min reaction time and the H_2O_2 efficiency (ODS selectivity based on H_2O_2). DBT sulfone was the only product observed in the ODS reaction (Scheme 4.1); it was insoluble in heptane and precipitated from the reaction mixture.

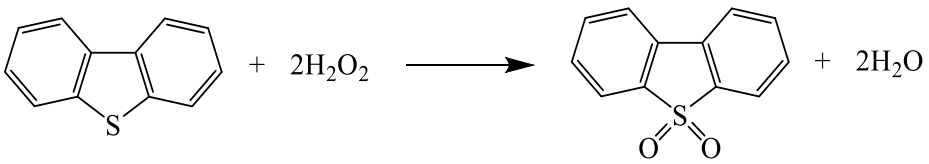

Scheme 4.1. Oxidation of DBT to DBT sulfone by H_2O_2 catalyzed by HPA/AC–*n*.

Among HPMo/AC–*n* catalysts, the HPMo/AC–0 catalyst with intact Keggin structure reported previously [32], was the most efficient one (Table 4.3, entry 1). It gave 100% DBT conversion in 30 min at 60 °C, with the highest TOF value of 9.9 min^{-1} and 80% H_2O_2 efficiency, in agreement with the previous report [32]. All other HPMo/AC–*n* catalysts, with destroyed Keggin structure, were significantly less efficient in oxidizing DBT (less than 100% DBT conversion in 120 min). Among the latter, HPMo/AC–1 and HPMo/AC–2 were better ones, giving 94–96% DBT conversion in 120 min (Table 4.3, entries 2 and 3). Within the entire series of AC–*n*, the TOF values change 5-fold, which demonstrates a strong effect of carbon support on the activity of HPMo/AC–*n* catalysts.

Table 4.3. DBT oxidation over HPMo/AC–*n*.[a]

Entry	Catalyst	Conversion(%)/Time (min)		TOF[b] (min^{-1})	H_2O_2 efficiency[c] (%)
1	11%HPMo/AC–0	96/20	100/30	9.9	80
2	16%HPMo/AC–1	86/20	94/120	9.3	68
3	8.6%HPMo/AC–2	57/20	96/120	5.6	74
4	16%HPMo/AC–3	35/20	83/120	2.4	88
5	19%HPMo/AC–4	58/20	65/120	7.7	68
6	16%HPMo/AC–5	19/20	40/120	2.0	86
7	14%HPMo/AC–6	37/20	58/120	3.8	85
8	16%HPMo/AC–7	52/20	88/120	3.9	76
9	13%HPMo/AC–8	39/20	63/120	4.4	68
10	14%HPMo/AC–9	47/20	65/120	3.8	68

[a] All catalysts tested twice, given average results; 60 °C, 0.0056 mmol HPMo, 0.05–0.12 g catalyst weight, 0.50 mmol DBT, 0.40 mmol dodecane (GC standard), 1.5 mmol H_2O_2 (30% aqueous solution), 10 ml heptane, 1500 rpm stirring speed. [b] Initial TOF per mole of HPA at 5 min reaction time. [c] From titration of unreacted H_2O_2 with $KMnO_4$ after reaction.

Contrary to the HPMo/AC–*n* catalysts, the results obtained for HPW/AC–*n* catalysts show a strong enhancing effect of carbon support on catalyst activity (Table 4.4). In this case, many of the HPW/AC–*n* catalysts with destroyed Keggin structure were found to be more efficient that the previously reported HPW/AC-0 catalyst with intact Keggin structure [32], which gives 89% DBT conversion in 120 min reaction time, with a TOF value of 7.1 min and 85% H_2O_2 efficiency (Table 4.4, entry 1), in agreement with [32]. Thus the HPW catalysts supported on AC–1, AC–4 and AC–7 were more efficient than HPW/AC–0, reaching 100% DBT conversion in 20–120 min, with greater TOF values of 12–14 min^{-1} and 85–88% H_2O_2 efficiency (entries 2, 5, 9).

Table 4.4. DBT oxidation over HPW/AC–*n*.[a]

Entry	Catalyst	Conversion (%)/Time (min)		TOF[b] (min^{-1})	H_2O_2 efficiency[c] (%)
1	11%HPW/AC–0	65/20	89/120	7.1	85
2	17%HPW/AC–1	100/20		12	85
3	8.3%HPW/AC–2	93/20	100/30	9.8	89
4	14%HPW/AC–3	65/20	99/120	7.0	87
5	18%HPW/AC–4	100/20		14	85
6	18%HPW/AC–4[d]	100/30		12	88
6	13%HPW/AC–5	13/20	38/120	1.2	68
7	16%HPW/AC–6	55/20	69/120	6.4	72
8	17%HPW/AC–7	99/20	100/30	12	88
9	17%HPW/AC–8	59/20	75/120	5.9	71
10	21% HPW/AC–9	50/20	68/120	4.6	70

[a] All catalysts tested twice, given average results; 60 °C, 0.0056 mmol HPW, 0.08–0.19 g catalyst weight, 0.50 mmol DBT, 0.40 mmol dodecane (GC standard), 1.5 mmol H_2O_2 (30% aqueous solution)), 10 ml heptane, 1500 rpm stirring speed. [b] Initial TOF per mole of HPA at 5 min reaction time. [c] From titration of unreacted H_2O_2 with $KMnO_4$ after reaction. [d] At 40 °C, data from Fig. 4.14.

Notably, these HPW catalysts were more active per mole HPA than the best molybdenum catalyst HPMo/AC–0 (Table 4.3, entry 1) and also had a higher H_2O_2 efficiency (85–88% versus 80% for HPMo/AC–0). The latter can be attributed to the low oxidation potential of HPW (0.15 V) compared to HPMo (0.65 V vs. SHE) [12].

The HPMo/AC–0 catalyst, reported previously [32], has been demonstrated to have a higher activity compared to other heterogeneous ODS catalysts reported in the literature before 2019. Recently, a new HPW/MOF catalyst, PW/UiO-66(Zr), containing 11.4% W has been reported [35], which removes 100% DBT from model diesel in 30 min at 25 °C, however at a 2-fold higher H_2O_2/DBT ratio of 6.0 mol/mol; its H_2O_2 efficiency has not been reported. Our best HPW/AC–4 catalyst with similar W content provided 100% DBT conversion at H_2O_2/DBT = 3.0 mol/mol in 20 min at 60 °C and in 30 min at 40 °C with 85–88% H_2O_2 efficiency (Table

4.4, entries 5 and 6). Given the sharp rise of ODS rate with increasing the H_2O_2/DBT ratio [32,35], the two catalysts, PW/UiO-66(Zr) and HPW/AC–4, have comparable activities. However, our catalyst has the H_2O_2 efficiency at least 2-fold higher than that of PW/UiO-66(Zr) due to the doubled H_2O_2/DBT ratio for the latter. Besides, in practical terms, our catalyst has important advantage of very easy preparation via a simple impregnation of commercially available HPW and AC–4, whereas PW/UiO-66(Zr) is obtained through a tough synthetic procedure [35]. Therefore, it can be concluded that in terms of the efficiency and practicality, the carbon-supported HPA catalysts developed in this study outperform the POM-based ODS catalysts reported to date that utilize advanced porous materials, such as MOFs, hierarchical zeotypes, etc., as POM hosts and supports [15].

Previously, it has been shown that the HPMo/AC–0 catalyst exhibits excellent recyclability [32]. In this work, the HPW/AC–4 catalyst was reused five times in the oxidation of DBT at 60 ^oC without loss of its activity (Fig. 4.7). This indicates no HPW leaching from the catalyst. The absence of leaching was also confirmed by ICP-OES analysis, which found no tungsten in aqueous extract from the reaction mixture after reaction. This indicates the true heterogeneous catalysis in ODS reaction.

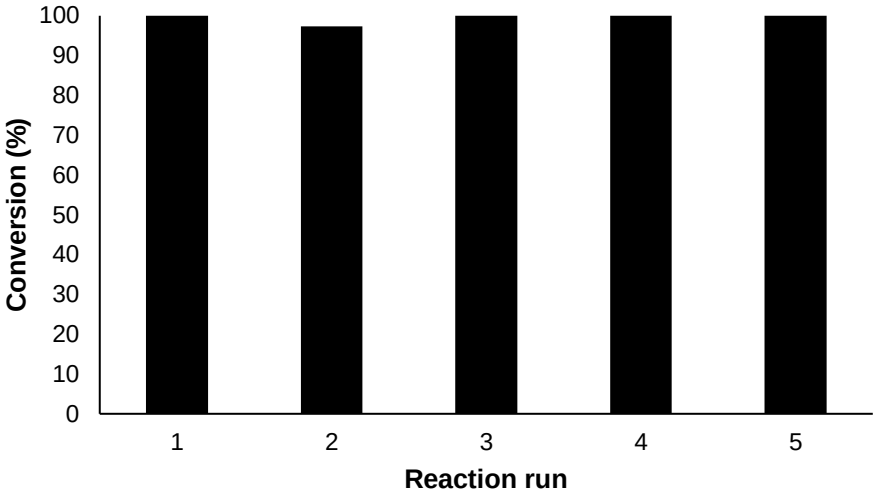

Fig. 4.7. Catalyst reuse in oxidation of DBT (0.50 mmol, 1.3 wt.% in reaction mixture) by H_2O_2 (1.5 mmol) in heptane (10 mL) catalyzed by 18%HPW/AC–4 (0.067 g, 1 wt.%, 0.0041 mmol HPW) at 60 °C, 1 h.

Since activated carbon itself can adsorb DBT from hydrocarbon media [24] as well as catalyze the oxidation of DBT by H_2O_2 [36], the relevant blank tests were carried out. The results are shown in Fig. 4.8–4.11. At the conditions similar to those used in ODS reactions, except in the absence of HPA and H_2O_2, neat AC samples adsorbed 20–40% of DBT, reaching saturation in 5–10 min. The amount of DBT adsorbed correlated with the AC surface area. Thus, AC–4 and AC–7 with the largest surface areas (1408 and 2901 m^2g^{-1}, Table 4.1) adsorbed the largest amounts of DBT (35 and 40%) (Fig. 4.9 and 4.10). Practically the same results were obtained for DBT adsorption on HPW/AC–*n* catalysts in the absence of H_2O_2 (Fig. 4.8–4.10). In the presence of H_2O_2, hardly any oxidation of DBT was observed on the neat AC samples at 60 ^oC; DBT consumption time courses were very similar with and without the presence of H_2O_2 in the system (Fig. 4.8–4.11). Similar results were obtained for HPMo/AC–0 and neat AC–0 (Chapter 3, sect. 3.2.2). Therefore, the removal of DBT in all these tests was due to DBT adsorption on activated carbon. These results clearly show that the activated carbons without HPA do not catalyze DBT oxidation by H_2O_2 in our system and HPA plays the key role in the

ODS reaction. These results also indicate that the reaction occurs through fast DBT adsorption onto the surface of HPA/AC–*n* catalysts.

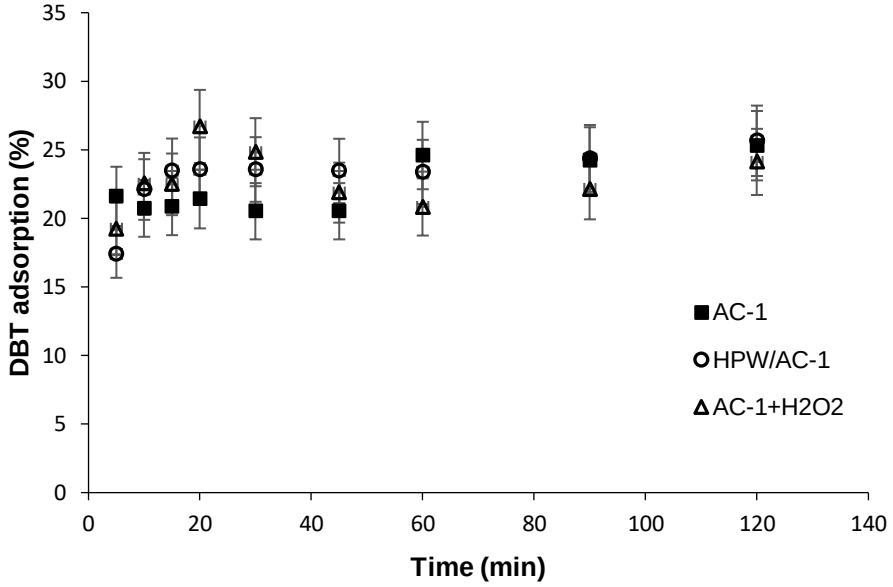

Fig. 4.8. Adsorption of DBT on AC–1 (0.0865 g) and 17%HPW/AC–1 (0.090 g) in the absence of H_2O_2 and adsorption of DBT on AC–1 (0.0865 g) in the presence of H_2O_2 (1.5 mmol). Conditions: DBT (0.50 mmol), dodecane (GC standard, 0.40 mmol), heptane solvent (10 ml), 60 ^oC and 1500 rpm stirring speed.

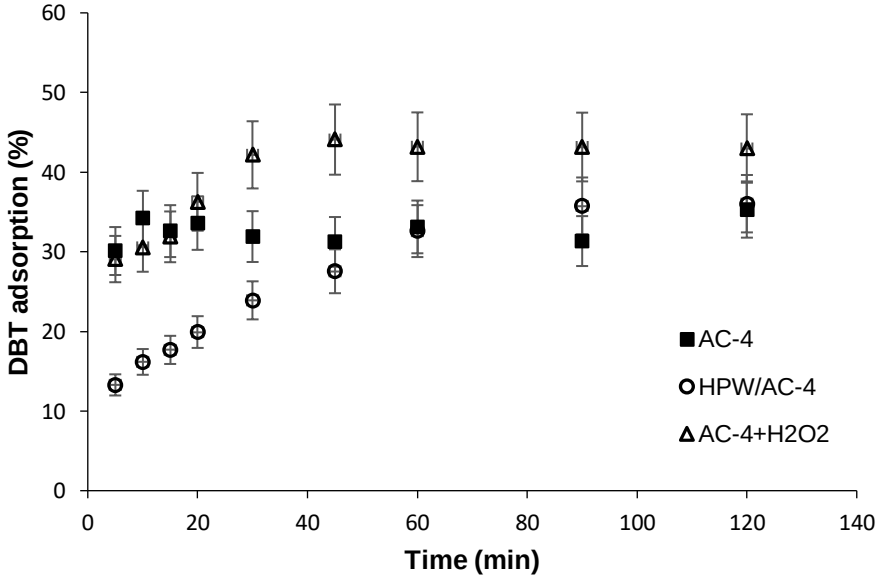

Fig. 4.9. Adsorption of DBT on AC–4 (0.0865 g) and 18%HPW/AC–4 (0.090 g) in the absence of H_2O_2 and adsorption of DBT on AC–4 (0.0865 g) in the presence of H_2O_2 (1.5 mmol).

Conditions: DBT (0.50 mmol), dodecane (GC standard, 0.40 mmol), heptane solvent (10 ml), 60 ^{o}C and 1500 rpm stirring speed.

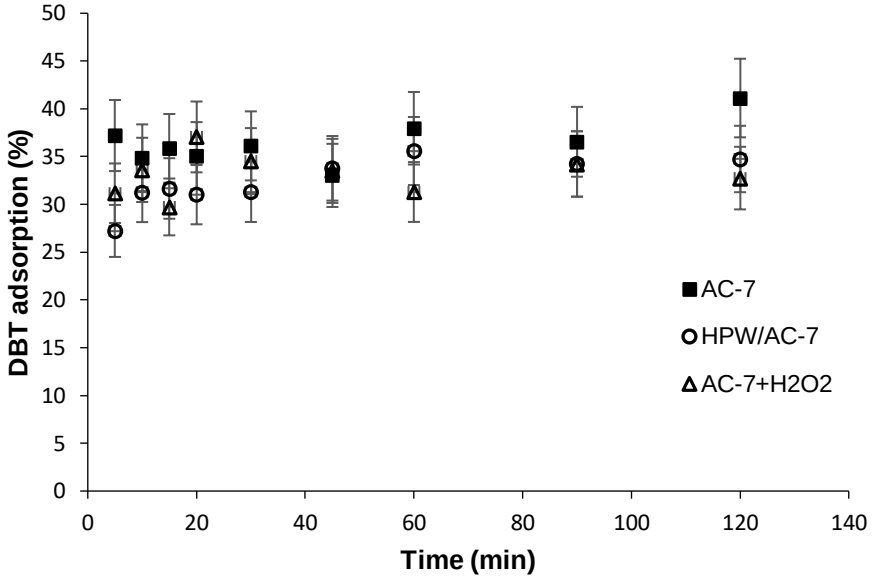

Fig. 4. 10. Adsorption of DBT on neat AC–7 (0.0865 g) and 17%HPW/AC–7 (0.090 g) in the absence of H_2O_2 and adsorption of DBT on neat AC–7 (0.090 g) in the presence of H_2O_2 (1.5 mmol). Conditions: DBT (0.50 mmol), dodecane (GC standard, 0.40 mmol), heptane solvent (10 ml), 60 ^{o}C and 1500 rpm stirring speed.

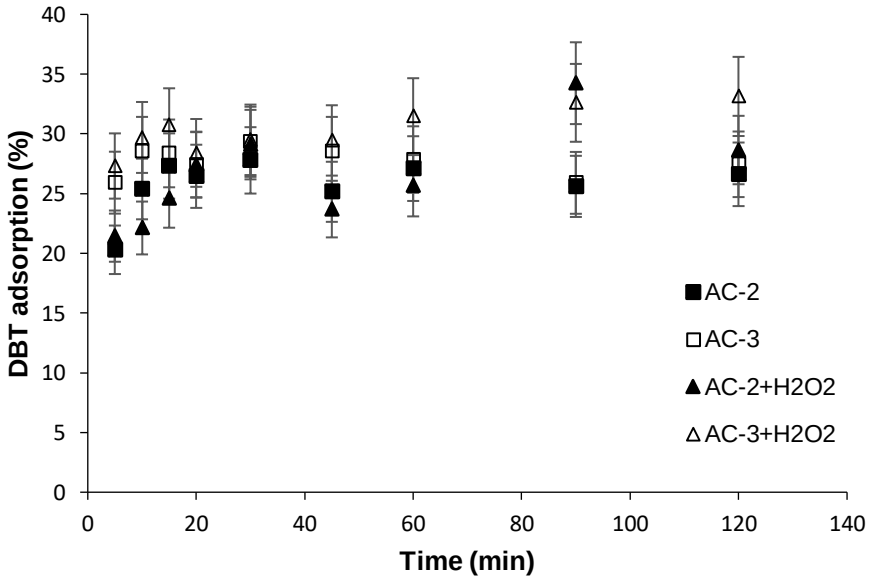

Fig. 4.11. Adsorption of DBT on neat AC–2 and AC–3 (0.0865 g) in the absence of H_2O_2 and adsorption of DBT on neat AC–2 and AC–3 (0.0865 g) in the presence of H_2O_2 (1.5 mmol).

Conditions: DBT (0.50 mmol), dodecane (GC standard, 0.40 mmol), heptane solvent (10 ml), 60 ^{o}C and 1500 rpm stirring speed.

4.1.3. Kinetics and mechanistic insight

Time courses for the most active HPMo/AC–*n* and HPW/AC–*n* catalysts at 60 ^{o}C are shown in Fig. 4.12 and Fig. 4.13, respectively, in comparison with HPA/AC–0. The ODS reactions that reached 100% DBT conversion obeyed the first-order rate law (Fig. 4.14). The first-order rate constants (min^{-1}) decrease in the following order: HPW/AC–4 (0.285) > HPW/AC–7 (0.212) > HPW/AC–1 (0.187) > HPMo/AC–0 (0.155) > HPW/AC–2 (0.127). Time courses and first-order plots for HPW/AC–4 at different reaction temperature 30–60 ^{o}C are shown in Fig. 4.15. It reached 100% DBT conversion in short time and obeyed first-order plot at least up to 90% DBT conversion. From these results, HPW/AC–4 appears to be the most active ODS catalyst among the reported analogues providing 100% DBT conversion at different reaction temperature 30–60 ^{o}C, H_2O_2/DBT = 3.0 mol/mol and 1 wt.% catalyst amount per model diesel.

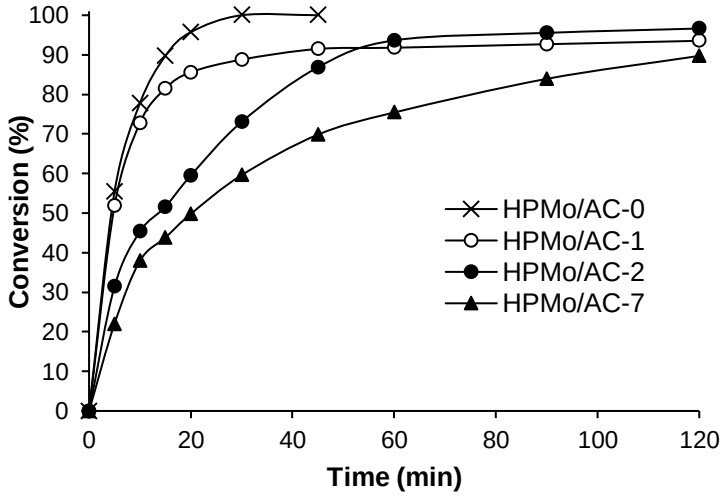

Fig. 4.12. Time course for DBT oxidation catalyzed by HPMo/AC at 60 ^{o}C, 0.0056 mmol HPMo, 0.05–0.12 g catalyst weight, 0.50 mmol DBT, 0.40 mmol dodecane (GC standard), 1.5 mmol H_2O_2 (30% aqueous solution), 10 ml heptane, 1500 rpm stirring speed.

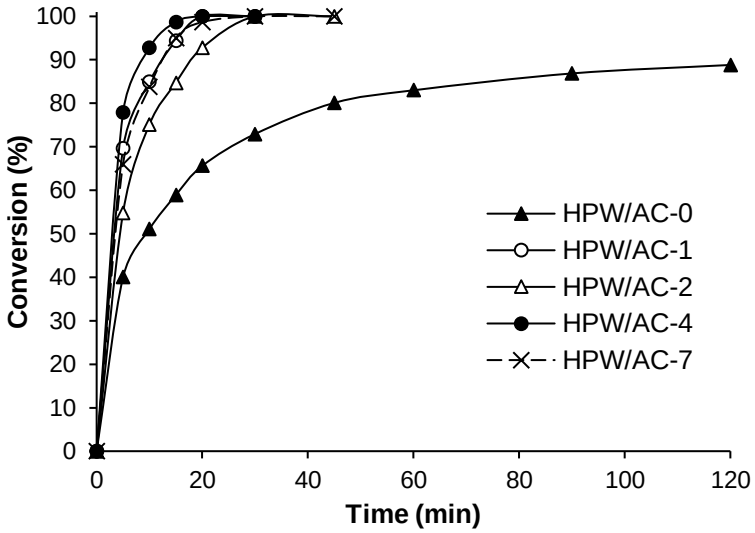

Fig. 4.13. Time course for DBT oxidation catalyzed by HPW/AC at 60 °C, 0.0056 mmol HPW, 0.08–0.19 g catalyst weight, 0.50 mmol DBT, 0.40 mmol dodecane (GC standard), 1.5 mmol H_2O_2 (30% aqueous solution)), 10 ml heptane, 1500 rpm stirring speed.

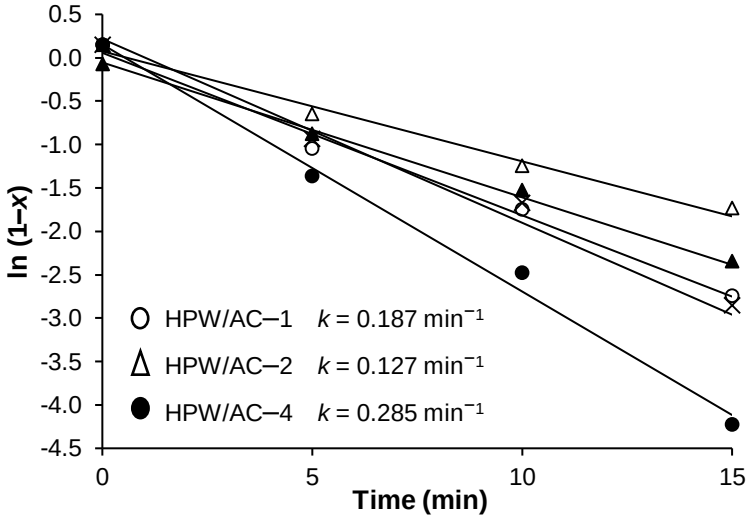

Fig. 4.14. First-order plot ln (1–*x*) = –*kt* for oxidation of DBT (0.50 mmol) by H_2O_2 (1.5 mmol) in heptane (10 mL) catalyzed by HPA/AC (0.0056 mmol HPA) at 60 °C; *x*, DBT conversion.

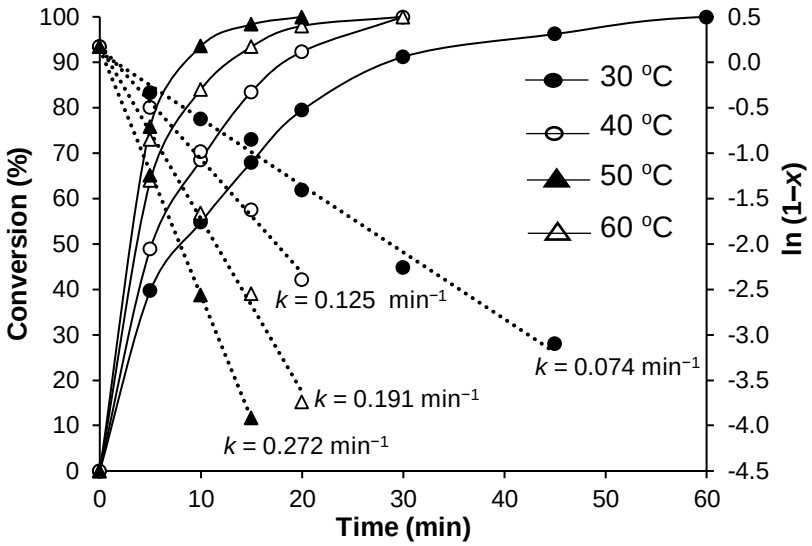

Fig. 4.15. Plot of DBT conversion (x) versus reaction time and first-order plot ln (1–x) = –kt for oxidation of DBT (0.50 mmol) by H_2O_2 (1.5 mmol) in heptane (10 mL) catalyzed by 18%HPW/AC–4 (0.067 g, 1 wt.%, 0.0041 mmol HPW) at different temperatures.

The Arrhenius plot for HPW/AC–4 in the temperature range of 30–60 °C is shown in Fig. 4.16, with an apparent activation energy E_a = 37 kJ mol^{-1}. The Arrhenius plots for HPW/AC–1 and HPW/AC–7 are shown in Fig. 4.17. From these plots, E_a values for these catalysts are 64 and 65 kJ mol^{-1}, respectively. Previously, for the oxidation of DBT with HPMo/AC–0 catalyst, the apparent activation energy of 49 kJ mol^{-1} in the temperature range 40–70 °C has been reported [32] (Chapter 3). Therefore, the most active HPW/AC–4 catalyst has the lowest activation energy among these catalysts.

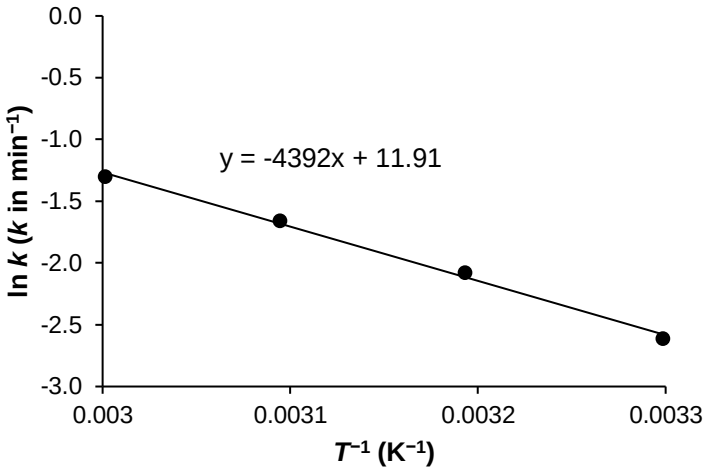

Fig. 4. 16. Arrhenius plot for oxidation of DBT (0.50 mmol) by H_2O_2 (1.5 mmol) catalyzed by 18%HPW/AC–4 (0.067 g, 0.0041 mmol HPW) in heptane (10 ml) at 30–60 °C, 1500 rpm stirring speed (*k* is the first-order rate constant); E_a = 37 kJ mol^{-1}.

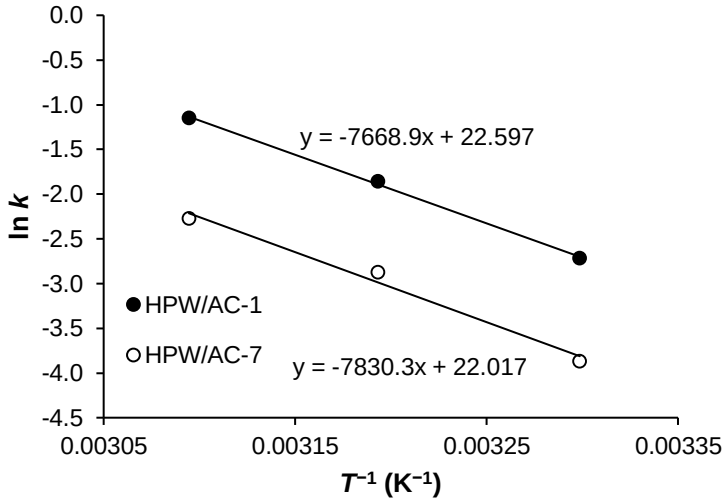

Fig. 4. 17. Arrhenius plots for oxidation of DBT (0.50 mmol) by H_2O_2 (1.5 mmol) catalyzed by 17%HPW/AC–1 and 17%HPW/AC–7 (0.0703 g, 0.0041 mmol HPW) in heptane (10 ml) at 30–50 °C, 1500 rpm stirring speed (*k* is the first-order rate constant); E_a = 64 kJ mol^{-1} for HPW/AC–1 and 65 kJ mol^{-1} for HPW/AC–7.

From DRIFT spectroscopy, HPMo and HPW retain their Keggin structure on the surface of the acidic carbon support AC–0 in the HPMo/AC–0 and HPW/AC–0 catalysts [32]. It has been suggested that the oxidation of DBT on these catalysts occurs through the formation of labile active peroxo species without destruction of the Keggin unit, which oxidize DBT to DBT

sulfone, with the HPMo peroxo species being more active than the HPW ones [32] (Chapter 3). In contrast, the HPA catalysts on more basic carbon supports AC–*n* (*n* = 1–9) studied in this work do not retain the Keggin structure; they decompose to form unidentified W^{VI} and Mo^{VI} oxo species on the carbon surface, probably monomeric and oligomeric W^{VI} and Mo^{VI} oxo species. Monomeric and oligomeric W^{VI} and Mo^{VI} oxo species can interact with H_2O_2 to form peroxo complexes of W^{VI} and Mo^{VI} containing the η^2-O_2^{2-} peroxo ligand (Scheme 4.2) [37]. Redox potentials of Mo and W determine that these peroxo complexes contain M^{VI}. Therefore, the HPA/AC–*n* catalysts are likely to operate through the peroxo complexes of W^{VI} and Mo^{VI} (Scheme 4.3) rather than through the peroxo complexes of intact Keggin units. Notably, the W^{VI} peroxo complexes are more active than the Mo^{VI} ones.

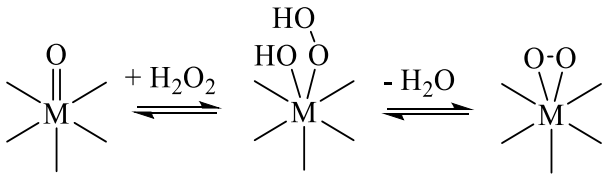

Scheme 4.2. Formation of peroxo complexes from M^{VI} oxo species on the carbon surface (M = Mo^{VI} or W^{VI}).

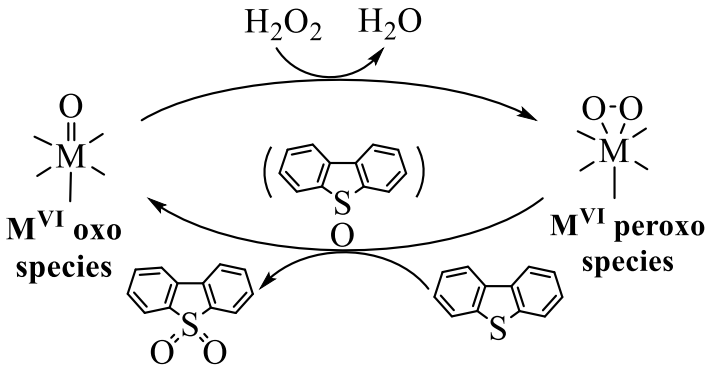

Scheme 4.3. Proposed mechanism for oxidation of DBT by H_2O_2 catalyzed by HPA/AC–*n* (M = Mo^{VI} or W^{VI}).

To date, the ODS chemistry in the POM–H_2O_2 systems, both homogeneous and heterogeneous, is well documented, with a wide variety of POM catalysts reported ([15] and references

therein). Yet the main features that determine the catalytic activity are still not clear, hence the ODS activity cannot be assumed a priori, e.g., whether molybdenum or tungsten POM catalysts are preferred. In biphasic systems, where Keggin POMs are used as homogeneous catalysts in combination with a phase transfer agent (PTA), there is overwhelming evidence that the POMs partially decompose to form peroxo-POMs, which are the catalytically active species in the ODS reaction [4,11]. In this case, the activity has been shown to depend on PTA. Thus, with quaternary ammonium cations, HPW has a higher activity than HPMo in ODS of DBT [38,39], whereas with phosphazene PTA, the opposite trend has been found: HPMo > HPW [11]. The same activity trend HPMo > HPW has also been reported for HPA immobilized on phosphazene-functionalized silica [16].

In this study, the use of more basic AC–*n* (*n* = 1–9) supports caused decomposition of Keggin HPAs, both HPMo and HPW, but with an opposite effect on catalysts activity: the activity of Mo catalysts decreased, whereas the activity of W ones in most cases increased. This may be determined by the structure and stability of the surface peroxo species of Mo^{VI} and W^{VI}. The results indicate that the AC–*n* supports with an intermediate pH range of 5.5–9.5 are favorable for more active W catalysts. The surface area of AC–*n* varied significantly, from 480 to 2900 m^2g^{-1}, however, no correlation between the activity and the surface area is observed. It should be noted that adventitious impurities in AC–*n* and those coming from activation of AC–*n* may have an effect on catalyst activity, which is difficult to assess at present. Overall, our study demonstrates significant potential of carbon materials as catalyst supports for the development of more efficient ODS catalysts based on HPAs. Further progress in catalyst development and mechanistic understanding will require continued work using AC samples with controlled texture and purity complemented by thorough characterization of active peroxo species on the carbon surface.

4.2. Conclusions

This work shows that Keggin-type heteropoly acids supported on basic activated carbons are active catalysts for the oxidative desulfurization (ODS) of model diesel fuel. Ten commercial activated carbons (all powdered samples) have been tested as the HPA support to reveal a strong effect of the carbon support on the integrity of HPA structure on the carbon surface and catalyst activity. DRIFTS studies show that the Keggin structure of HPAs decomposes on the basic carbon surface to form monomeric and/or oligomeric Mo^{VI} and W^{VI} oxo species. The most active catalysts, comprising decomposed HPW, outperform best reported heterogeneous catalysts for ODS in similar systems, exhibiting 100% DBT removal from the model diesel fuel with 85–88% H_2O_2 efficiency at 40–60 ^oC, H_2O_2/DBT = 3 mol/mol and 1 wt.% catalyst in 20–30 min reaction time and could be recovered and reused without loss of activity. Overall, this work demonstrates significant potential of carbon materials as catalyst supports for the development of more efficient ODS catalysts based on HPAs.

References

[1] I.V. Babich, J.A. Moulijn, Science and technology of novel processes for deep desulfurization of oil refinery streams, Fuel 82 (2003) 607–631.

[2] R. Prins, Hydrotreating, in Handbook of Heterogeneous Catalysis, ed. G. Ertl, H. Knözinger, F. Schüth, J. Weitkamp, Vol. 6, Wiley-VCH, 2008; p. 2695–2718.

[3] A.W. Bhutto, R. Abro, S. Gao, T. Abbas, X. Chen, G. Yu, Oxidative desulfurization of fuel oils using ionic liquids: A review, J. Taiwan Inst. Chem. Eng. 62 (2016) 84–97.

[4] Z. Jiang, H. Lü, Y. Zhang and C. Li, Oxidative desulfurization of fuel oils, Chin. J. Catal. 32 (2011) 707–715.

[5] E.A. Eseva, A.V. Akopyan, A.V. Anisimov, A.L. Maksimov, Oxidative desulfurization of hydrocarbon feedstock using oxygen as oxidizing agent (a review), Petroleum Chem. 60 (2020) 979–790.

[6] H. Wang, C. Shi, S. Chen, R. Chen, P. Sun, T. Chen, Hierarchically mesoporous titanosilicate single-crystalline nanospheres for room temperature oxidative–adsorptive desulfurization, ACS Appl. Nano Mater. 2 (2019) 6602−6610.

[7] F.M. Collins, A.R. Lucy, C. Sharp, Oxidative desulfurization of oils via hydrogen peroxide and heteropolyanion catalysis, J. Mol. Catal. A Chem. 117 (1997) 397–403.

[8] C. Komintarachat, W. Trakarnpruk, Oxidative desulfurization using polyoxometalates, Ind. Eng. Chem. Res. 45 (2006) 1853–1856.

[9] A.F. Shojaei, M.A. Rezvani, M.H. Loghmani, Comparative study on oxidation desulfurization of actual gas oil and model sulfur compounds with hydrogen peroxide promoted by formic acid: Synthesis and characterization of vanadium containing polyoxometalate supported on anatase crushed nanoleaf, Fuel Process. Technol. 118 (2014) 1–6.

[10] A.E.S. Choi, S. Roces, N. Dugos, M.W. Wan, Oxidation by H_2O_2 of bezothiophene and

dibenzothiophene over different polyoxometalate catalysts in the frame of ultrasound and mixing assisted oxidative desulfurization, Fuel 180 (2016) 127–136.

[11] M. Craven, R. Yahya, E.F. Kozhevnikova, C.M. Robertson, A. Steiner, I.V. Kozhevnikov, Alkylaminophosphazenes as efficient and tuneable phase-transfer agents for polyoxometalate-catalyzed biphasic oxidation with hydrogen peroxide, ChemCatChem 8 (2016) 200–208.

[12] I.V. Kozhevnikov, Catalysts for fine chemical synthesis: Catalysis by polyoxometalates, Wiley, West Sussex, 2002.

[13] L. Salles, C. Aubry, R. Thouvenot, F. Robert, C. Doremieux-Morin, G. Chottard, H. Ledon, Y. Jeannin, J.-M. Bregeault, ^{31}P and ^{183}W NMR spectroscopic evidence for novel peroxo species in the $H_3[PW_{12}O_{40}]_yH_2O/H_2O_2$ system. Synthesis and X-ray structure of tetrabutylammonium (μ-hydrogen phosphato)bis(μ-peroxo)bis(oxoperoxotungstate)(2-): A catalyst of olefin epoxidation in a biphase medium, Inorg. Chem. 33 (1994) 871–878.

[14] D.C. Duncan, R.C. Chambers, E. Hecht, C.L. Hill, Mechanism and dynamics in the $H_3[PW_{12}O_{40}]$-catalyzed selective epoxidation of terminal olefins by H_2O_2. Formation, reactivity, and stability of $\{PO_4[WO(O_2)_2]_4\}^{3-}$, J. Am. Chem. Soc. 117 (1995) 681–691.

[15] J. Li, Z. Yang, S. Li, Q. Jin, J. Zhao, Review on oxidative desulfurization of fuel by supported heteropolyacid catalysts, J. Ind. Eng. Chem. 82 (2020) 1–16.

[16] M. Craven, D. Xiao, C. Kunstmann-Olsen, E.F. Kozhevnikova, F. Blanc, A. Steiner, I.V. Kozhevnikov, Oxidative desulfurization of diesel fuel catalyzed by polyoxometalate immobilized on phosphazene-functionalized silica, Appl. Catal. B: Environmental 231 (2018) 82–91.

[17] M. Zhang, W. Zhu, H. Li, M. Li, S. Yin, Y. Li, Y. Wei, H. Li, Facile fabrication of molybdenum-containing ordered mesoporous silica induced deep desulfurization in

fuel, Colloids Surface A. 504 (2016) 174–181.

[18] S.O. Ribeiro, B. Duarte, B. de Castro, C.M. Granadeiro, S.S. Balula, Improving the catalytic performance of Keggin $[PW_{12}O_{40}]^{3-}$ for oxidative desulfurization: ionic liquids versus SBA-15 composite, Materials 11 (2018) 1196.

[19] G. Luo, L. Kang, M. Zhu, B. Dai, Highly active phosphotungstic acid immobilized on amino functionalized MCM-41 for the oxidesulfurization of dibenzothiophene, Fuel Proc. Technol. 118 (2014) 20–27.

[20] D. Julião, A.C. Gomes, M. Pillinger, R. Valença, J.C. Ribeiro, B. de Castro, I.S. Gonçalves, L. Cunha Silva, S.S. Balula, Zinc-substituted polyoxotungstate@amino-MIL-101(Al) – An efficient catalyst for the sustainable desulfurization of model and real diesels, Eur. J. Inorg. Chem. 2016 (2016) 5114–5122.

[21] W. Jiang, D. Zheng, S. Xun, Y. Qin, Q. Lu, W. Zhu, H. Li, Polyoxometalate-based ionic liquid supported on graphite carbon induced solvent-free ultra-deep oxidative desulfurization of model fuels, Fuel 190 (2017) 1–9.

[22] Y. Gao, R. Gao, G. Zhang, Y. Zheng, J. Zhao, Oxidative desulfurization of model fuel in the presence of molecular oxygen over polyoxometalate based catalysts supported on carbon nanotubes, Fuel 224 (2018) 261–270.

[23] A.K. Dizaji, B. Mokhtarani, H.R. Mortaheb, Deep and fast oxidative desulfurization of fuels using graphene oxide-based phosphotungstic acid catalysts, Fuel 236 (2019) 717–729.

[24] J. Bu, G. Loh, C.G. Gwie, S. Dewiyanti, M. Tasrif, A. Borgna, Desulfurization of diesel fuels by selective adsorption on activated carbons: Competitive adsorption of polycyclic aromatic sulfur heterocycles and polycyclic aromatic hydrocarbons, Chem. Eng. J. 166 (2011) 207–217.

[25] L. Liu, Y. Zhang, W. Tan, Synthesis and characterization of phosphotungstic acid/activated carbon as a novel ultrasound oxidative desulfurization catalyst, Front. Chem. Sci. Eng. 7 (2013) 422–427.

[26] L. Liu, Y. Zhang, W. Tan, Ultrasound-assisted oxidation of dibenzothiophene with phosphotungstic acid supported on activated carbon, Ultrason. Sonochem. 21 (2014) 970–974.

[27] J. Xiao, L. Wu, Y. Wu, B. Liu, L. Dai, Z. Li, Q. Xia, H. Xi, Effect of gasoline composition on oxidative desulfurization using a phosphotungstic acid/activated carbon catalyst with hydrogen peroxide, Appl. Energy 113 (2014) 78–85.

[28] Y. Izumi, K. Urabe, Catalysis of heteropoly acids entrapped in activated carbon, Chem. Lett. 1981; p. 663–666.

[29] Y. Izumi, K. Urabe, M. Onaka, Zeolite, clay and heteropoly acid in organic reactions, Kodansha/VCH, Tokyo, 1992; p. 99–161.

[30] S.M. Kulikov, M.N. Timofeeva, I.V. Kozhevnikov, V.I. Zaikovskii, L.M. Plyasova, I.A. Ovsyannikova, Adsorption of heteropoly acid $H_4SiW_{12}O_{40}$ from solutions onto porous supports, Izv. Akad. Nauk SSSR, Ser. Khim. 1989; p. 763–768.

[31] M.A. Schwegler, H. van Bekkum, N.A. de Munck, Heteropoly acids as catalysts for the production of phthalate diesters, Appl. Catal. 74 (1991) 191–204.

[32] R. Ghubayra, C. Nuttall, S. Hodgkiss, M. Craven, E. F. Kozhevnikova, I.V. Kozhevnikov, Oxidative desulfurization of model diesel fuel catalyzed by carbonsupported heteropoly acids, Appl. Catal. B 253 (2019) 309–316.

[33] S. Biniak, G. Szymanski, J. Siedlewski, A. Swiatkowski, The characterization of activated carbons with oxygen and nitrogen surface groups, Carbon 35 (1997) 1799–1810.

[34] C. Rocchiccioli-Deltcheff, M. Fournier, R. Franck, R. Thouvenot, Evidence for anion-anion interactions in molybdenum(VI) and tungsten(VI) compounds related to the Keggin structure, Inorg. Chem. 22 (1983) 207–216.

[35] G. Ye, L. Hu, Y. Gu, C. Lancelot, A. Rives, C. Lamonier, N. Nuns, M. Marinova, W. Xu, Y. Sun, Synthesis of polyoxometalate encapsulated in UiO-66(Zr) with hierarchical porosity and double active sites for oxidation desulfurization of fuel oil at room temperature, J. Mater. Chem. A 8 (2020) 19396–19404.

[36] R. Wang, G. Zhang, H. Zhao, Polyoxometalate as effective catalyst for the deep desulfurization of diesel oil. Catal Today, 149 (2010) 117–121.

[37] G. Yu, S. Lu, H. Chen, Z. Zhu, Diesel fuel desulfurization with hydrogen peroxide promoted by formic acid and catalyzed by activated carbon, Carbon 43 (2005) 2285–2294.

[38] M.H. Dickman, M.T. Pope, Peroxo and superoxo complexes of chromium, molybdenum, and tungsten, Chem. Rev. 94 (1994) 569–584.

[39] M. Te, C. Fairbridge, Z. Ring, Oxidation reactivities of dibenzothiophenes in polyoxometalate/H_2O_2 and formic acid/H_2O_2 systems, Appl. Catal. A 219 (2001) 267–280.

[40] R. Yahya, M. Craven, E.F. Kozhevnikova, A. Steiner, P. Samunual, I. V. Kozhevnikov, D.E. Bergbreiter, Polyisobutylene oligomer-bound polyoxometalates as efficient and recyclable catalysts for biphasic oxidations with hydrogen peroxide, Catal. Sci. Technol. 5 (2015) 818–821.

5 Aerobic oxidative desulfurization of liquid fuel catalyzed by P–Mo–V heteropoly acids in the presence of aldehyde

Ultra-deep desulfurization of liquid fuels is an increasingly important task to meet stringent environmental regulations worldwide [1–3]. In particular, removing refractory aromatic sulfur compounds such as benzothiophenes, which are difficult to remove using conventional hydrodesulfurization (HDS) technology, is a major challenge [1,2]. In the past two decades, oxidative desulfurization (ODS) has been under development as a promising alternative/complementary technology for removing the refractory organosulfur compounds [4,5]. Typically, ODS is carried out using hydrogen peroxide as an oxidant (H_2O_2–ODS) in the presence of a catalyst under very mild conditions (50–70 °C, ambient pressure [4,5]; cf. 300–400 °C, 30–130 atm for HDS [1,2]), with organosulfur compounds oxidized to the corresponding sulfones. The use of dioxygen, preferably air, as the oxidant for ODS has attracted considerable attention as well, despite more forcing reaction conditions of O_2–ODS compared to H_2O_2–ODS (see recent reviews [6,7] and references therein). Polyoxometalates (POMs), especially Keggin-type POMs, are exceptionally active ODS catalysts for both H_2O_2–ODS [8–15] and O_2–ODS [6,7,16–20]. POMs have also been used as the catalysts for ODS with ozone [21]. The Keggin POMs include heteropolyanions $XM_{12}O_{40}^{m-}$, where M is the metal ion, typically Mo^{6+} and W^{6+}, and X is the central atom, most frequently P^{5+} and Si^{4+} [13,22]. These POMs are produced commercially as the corresponding heteropoly acids $H_mXM_{12}O_{40}$ (HPAs).

It has been reported that addition of an aliphatic or aromatic aldehyde as a sacrificial reductant can greatly enhance the O_2–ODS of liquid fuel to remove benzothiophenes at reaction

temperatures below 100 ^{o}C and ambient pressure [23–27]. Co(II) and Mn(II) salts [23,25] and POMs [24] have been reported as highly active homogeneous catalysts for the co-oxidation of benzothiophenes and aldehydes to produce the corresponding sulfones and carboxylic acids, which can be separated from fuel by solvent extraction and adsorption with silica and alumina [23,24]. The major drawback of homogeneous ODS catalysts, however, is the difficulty of separating them from fuel; hence in practical terms, heterogeneous catalysis would generally be preferred, even at the expense of catalytic activity.

The aldehyde-assisted ODS reaction is suggested to occur through radical chain co-oxidation of aldehyde and organosulfur compound involving formation of peroxy acid intermediate and its fast reaction with the organosulfur compound to give sulfone and carboxylic acid (Eq. 1 and 2) [23,24]. Organic sulfides are commonly used as inhibitors of radical oxidation processes in liquid phase by interaction with hydroperoxides similar to reaction (Eq. 2) [28].

$$RCHO + O_2 \rightarrow RCO_3H \quad (1)$$

$$2\ RCO_3H + R'_2S \rightarrow R'_2SO_2 + 2\ RCO_2H \quad (2)$$

The use of sacrificial reductants such as aldehydes, ketones, etc. for liquid-phase selective oxidation is an established technology that has been applied industrially, for example, for olefin epoxidation [28,29]. The benefit of aldehyde-assisted ODS over direct O_2–ODS is in considerably milder reaction conditions (low temperature, ambient pressure and use of air instead of O_2), which would significantly improve process safety. The downside is the added cost of aldehyde and the necessity of removing the corresponding carboxylic acid from the treated fuel since the acidity of fuel (total acid number, TAN) is strictly regulated [30]. The aldehyde-assisted ODS makes a trade-off between aldehyde cost and ODS process safety. A wide range of aldehydes have been used effectively in this reaction [6,7,23–25]. In practice, less expensive and amply supplied acetaldehyde can be applied [23]. The removal of carboxylic

acid from the treated fuel can be achieved by extraction with aqueous Na_2CO_3 [23]. It should be noted that the use of direct O_2–ODS on real fuel (rather than a model fuel typically used in research) would inevitably cause co-oxidation of some fuel components to form organic oxygenates, including carboxylic acids, which would have to be separated like in the case of aldehyde-assisted ODS.

Here, we investigate the aldehyde-assisted aerobic ODS of model liquid fuel comprising dodecane spiked with dibenzothiophene (DBT) in the presence of benzaldehyde (PhCHO) as a model sacrificial reductant using bulk and supported Keggin-type mixed-addenda molybdovanadophosphoric heteropoly acids $H_{3+n}PMo_{12-n}V_nO_{40}$ (HPA–*n*, *n* = 0–3) as heterogeneous catalysts. PhCHO is chosen as a sacrificial reductant due to its fairly high reactivity and low volatility allowing to carry out the ODS reaction in a laboratory semi-batch reactor under air flow. HPA–*n* are well documented as catalysts for selective oxidation [13,31–33]. Especially HPA–*n* with *n* = 2–6 are widely used as the catalysts for the liquid-phase oxidation by O_2 [13,31–33]; their redox properties have been studied in detail ([13,33] and references therein). HPA–*n* possess a fairly high oxidation potential (~0.7 V vs. SHE), and their reduced forms can be re-oxidized by O_2; the latter occurs particularly easy for HPA–*n* with *n* = 2–6 probably via a multi-electron transfer mechanism [13,31–33]. It is V^{5+}/V^{4+} redox transformation within HPA–*n* that is responsible for the catalytic properties of HPA–*n* [13,33]. HPA–2 in conjunction with quaternary ammonium phase transfer agents (PTA) has been reported as an active homogeneous catalyst for the O_2–ODS of model fuel (decalin+DBT) in the presence of isobutyraldehyde [24]. No attempt of recycling this catalyst has been made, however, which would be difficult to achieve in a homogeneous POM/PTA system. Here, we aim at developing an efficient and recyclable heterogeneous catalyst based on HPA–*n* for the aerobic ODS and gaining mechanistic insights for this reaction

Bulk heteropoly acids $H_{3+n}PMo_{12-n}V_nO_{40}$ (short P–Mo–V) (HPA–*n*, *n* = 1–3) were prepared by interaction of stoichiometric amounts of Na_2MoO_4, $NaVO_3$ and Na_2HPO_4 in aqueous solution followed by crystallization as described by Tsigdinos and Hallada [34]. $Cs_{1.5}H_{2.5}PMo_{11}V_{40}$ (Cs-HPA–1) and $Na_2H_3PMo_{10}V_2O_{40}$ (Na-HPA–2) acidic salts were prepared by partial neutralization of HPA–1 with Cs_2CO_3 and HPA–2 with Na_2CO_3, respectively, in aqueous solution followed by rotary evaporation and drying. HPA–1 supported catalysts were prepared by wet impregnation. The aerobic co-oxidation of DBT and PhCHO in the presence of powdered HPA–*n* catalysts was carried in dodecane as a solvent at 40–120 ºC in a 50-ml semi-batch jacketed glass reactor equipped with a heat circulator, a magnetic stirrer, a reflux condenser and an air inlet. More details can be found in Chapter 2.

5.1. Results and discussion

5.1.1. Catalyst characterization

Heteropoly anions in all the HPA–*n* catalysts, including bulk HPA–*n*, their Cs and Na salts as well as HPA–1 supported on silica and activated carbon, had the Keggin structure, as confirmed by DRIFT spectroscopy, which is extensively used for fingerprinting purposes and structural elucidation of POMs [22]. The DRIFT spectra of the bulk catalysts are shown in Fig. 5.1; these exhibit four characteristic IR bands of P–O, M=O, M–O–M (corner-sharing) and M–O–M (edge-sharing) groups between 1100–700 cm^{-1}, for example, at 1063, 964, 866 and 786 cm^{-1}, respectively, for HPA–1, in agreement with the literature [34,35].

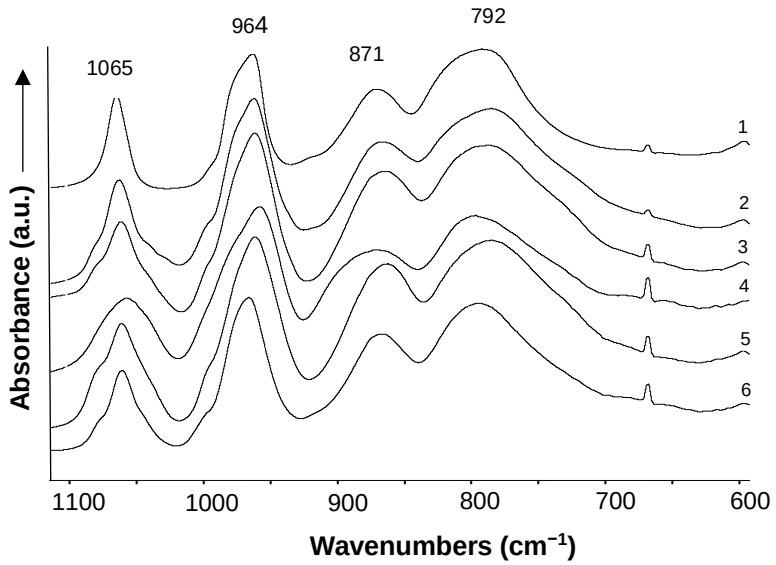

Fig. 5.1. DRIFT spectra of HPA–*n* (powdered in KBr): HPA–0 (1), HPA–1 (2), HPA–2 (3), HPA–3 (4), Na-HPA–2 (5) and Cs-HPA–1 (6).

DRIFT spectra for 15%HPA–1/C (Fig. 5.2) and 15%HPA–1/SiO_2 (Fig. 5.3) show the same bands of HPA–1; for 15%HPA–1/SiO_2, the band of P–O at 1063 cm^{-1} is obscured by the strong SiO_2 band centred at 1101 cm^{-1}.

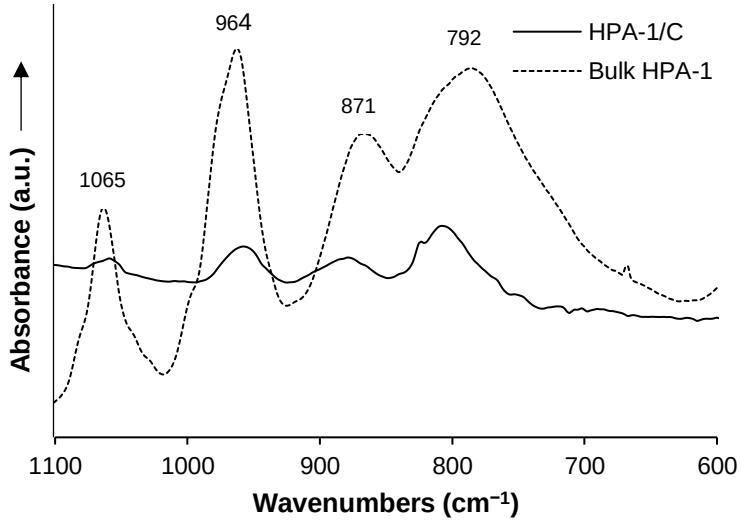

Fig. 5.2. DRIFT spectrum (in KBr) of 15%HPA–1/C and bulk HPA–1.

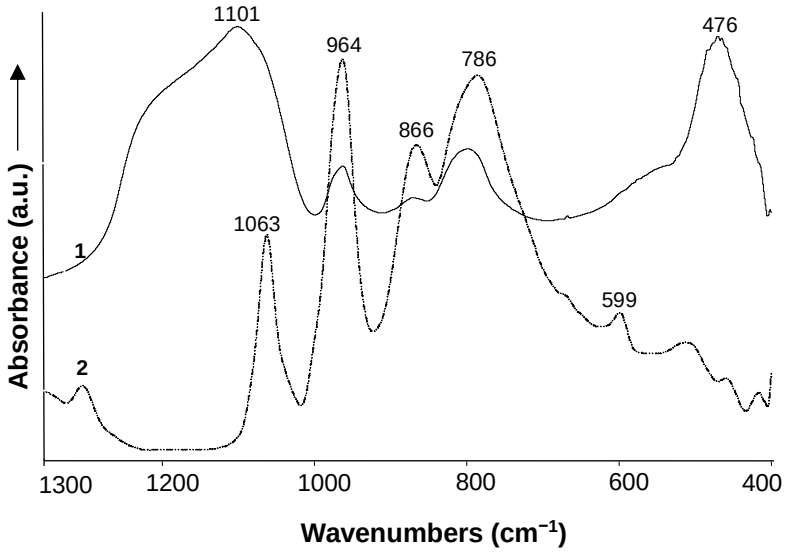

Fig. 5.3. DRIFT spectra (in KBr): (1) 15%HPA–1/SiO_2 and (2) bulk HPA–1. Bands at 476 and 1101 cm^{-1} belong to silica support. The presence of bands at 786, 866 and 964 cm^{-1} in spectrum (1) confirm that the Keggin structure of HPA–1 is intact in 15%HPA–1/SiO_2.

The XRD pattern for bulk crystalline HPA–1 (Fig. 5.4) is in agreement with the literature [36]. No HPA–1 crystal phase is observed in supported catalysts 15%HPA–1/SiO_2 and 15%HPA–1/C (Fig. 5.4), which indicates a fine dispersion of HPA–1 on the surface of supports.

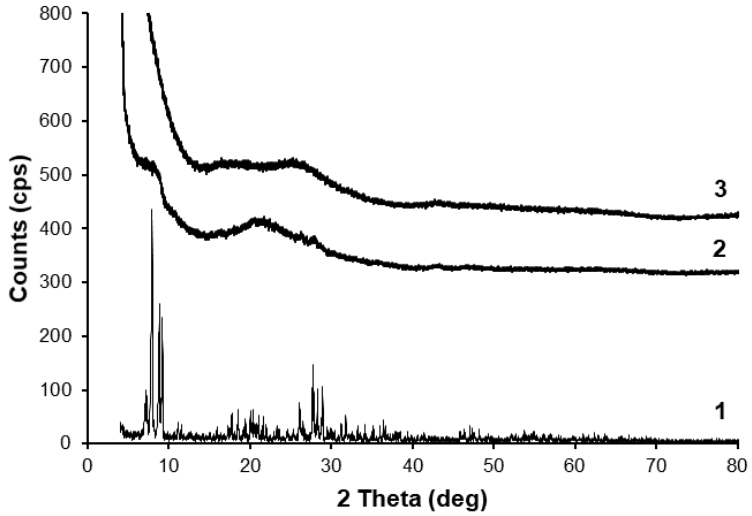

Fig. 5. 4. XRD patterns (CuKα radiation, λ = 1.542 Å) for bulk HPA–1 (1), 15%HPA–1/SiO_2 (2) and 15%HPA–1/C (3).

Table 5.1 shows information about the texture and water content for of bulk and supported HPA–*n* catalysts. Bulk HPA–*n* have small surface areas, 2–15 m^2g^{-1} (Table 5.1), which is typical of bulk heteropoly acids [13]. In 15%HPA–1/C and 15%HPA–1/SiO_2, having large total surface areas, the HPA–1 is finely dispersed on the surface of supports as confirmed by XRD as confirmed by XRD.

Table 5.1. Information about catalysts.

Catalyst	H_2O[a] (wt.%)	S_{BET}[b] (m^2g^{-1})	Pore volume[c] (cm^3g^{-1})	Pore diameter[d] (Å)
HPA–0	13.5	14.8	0.018	48
HPA–1	12.3	15.5	0.020	52
HPA–2	12.8	2.4	0.0044	72
HPA–3	12.0	2.6	0.0060	93
Cs-HPA–1	5.2	8.9	0.15	67
Na-HPA–2	13.0	1.7	0.0046	106
15%HPA–1/SiO_2		236	1.29	219
15%HPA–1/C		928	0.81	35

[a] Water of crystallization from TGA in the temperature range of 40–250 °C. [b] BET surface area; HPA samples pre-treated at 150 °C/1 Pa. [c] Single point pore total volume. [d] Average BET pore diameter.

5.1.2. Aerobic oxidation of DBT over P–Mo–V catalysts

Aerobic oxidative desulfurization (ODS) of model liquid fuel (dodecane spiked with dibenzothiophene (DBT)) was carried out in the presence of bulk and supported Keggin-type heteropoly acids $H_{3+n}PMo_{12-n}V_nO_{40}$ (HPA–*n*, *n* = 0–3) as heterogeneous catalysts and benzaldehyde as a sacrificial reductant. Fig. 5.5 shows the results of initial screening of all bulk HPA–*n* catalysts in the aerobic ODS at 60 °C and a DBT/PhCHO molar ratio of 1:12. As can be seen, the V-containing HPA–*n* (*n* = 1–3) and their Cs and Na salts exhibit significantly higher activity (89–95% DBT conversion) than the V-free HPA–0 (41% DBT conversion),

which can be explained by the lower oxidation potential of HPA–0 [14]. Reaction products were DBT sulfone and benzoic acid (from GC and FTIR analysis). The sulfone, insoluble in dodecane, precipitated out. The results indicate that the acidity of HPA–*n* does not play any significant role since the activity of the Cs and Na salts was close to that of HPA–*n* . Among the catalysts tested, HPA–1 and HPA–3 had a higher catalytic activity (95% DBT conversion). For further testing, the HPA–1 was chosen to minimize the amount of V in the catalyst. It has been reported that substitution of one V^{5+} for Mo^{6+} in $H_3PMo_{12}O_{40}$ increases the thermal stability of HPA, however, the stability decreases upon further substitution [13] making HPA–1 the most stable compound among HPA–*n* . Regarding the redox properties, HPA–1 is a one-electron oxidant due to reduction of V^{5+} to V^{4+} in the heteropoly anion with an oxidation potential ~0.7 V (vs. SHE) [13]: $[PMo_{12}V^{5+}O_{40}]^{4-} + e^- \rightarrow [PMo_{12}V^{4+}O_{40}]^{5-}$.

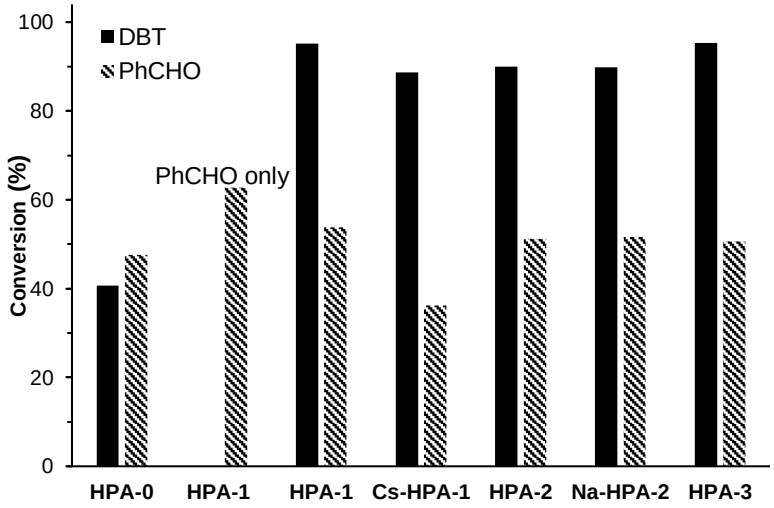

Fig. 5.5. Effect of HPA–*n* catalyst (0.10 g, 0.04–0.05 mmol) on aerobic oxidation of DBT (0.40 mmol) in the presence of PhCHO (4.9 mmol) at 60 °C, 10 ml dodecane solvent, 20 ml min^{-1} air flow, 1300 rpm stirring speed, and 2 h reaction time.

Table 5.2 shows the representative results on aerobic co-oxidation of DBT (0.50 mmol) and PhCHO (0–5.9 mmol, PhCHO/DBT = 0–12 mol/mol) in dodecane (10 ml) in the presence of bulk HPA–1 (0.10 g, 0.048 mmol) at 40–100 °C under air flow (20 ml min^{-1}, bubbling through

reaction mixture at ambient pressure) and 1300 rpm stirring speed. Every reaction run was repeated at least twice with a good reproducibility. For the reaction at 60 ^{o}C (entry 6), an average conversion of DBT of 85.8±4.0 and PhCHO of 49.5±4.3% was obtained from five repeated runs. In the absence of DBT, benzoic aldehyde was readily oxidized to benzoic acid (entry 1), whereas no DBT oxidation occurred in the absence of PhCHO (entry 2). The reaction did not depend on the rate of air flow varied from 10 to 30 ml min^{-1}. The use of pure O_2 instead of air did not affect the reaction either (cf. entries 6 and 16). This indicates sufficient oxygen supply as required for efficient radical chain propagation [28] (see below).

The efficiency of ODS reaction was greatly dependent on the PhCHO/DBT molar ratio. Thus, with increasing the PhCHO/DBT ratio from 1 to 12, the DBT conversion at 60 ^{o}C increased from 1.6 to 100% (Table 5.2, entries 3–7). A similar effect has been observed with homogeneous Co(II) catalyst [23]. Reaction temperature had also a strong effect on DBT conversion, which increased 5-fold from 18 to 100% when increasing the temperature from 40 to 100 ^{o}C (entries 10–12).

The ODS reaction was strongly inhibited by chain-breaking radical scavengers such as 1,4-benzoquinone and 2,6-di-tert-butyl-4-methylphenol [28] (cf. entry 7 and entries 8 and 9, Table 5.2). This supports the radical chain mechanism suggested in previous reports [23,24].

Table 5.2. Aerobic co-oxidation of DBT and PhCHO catalyzed by HPA–1.[a]

Entry	DBT (mmol)	PhCHO (mmol)	Temperature (°C)	Time (h)	Conversion (%)	
					DBT	PhCHO
1	0	4.9	60	2.0	-	63
2	0.50	0	60	2.0	0	0
3	0.50	1.0	60	2.0	1.6	11
4	0.50	2.0	60	2.0	23	27
5	0.50	2.9	60	2.0	31	30
6	0.50	4.9	60	2.0	86	50
7	0.50	5.9	60	2.0	100[b]	63
8[c]	0.50	5.9	60	2.0	10	42
9[d]	0.50	5.9	60	2.0	14	26
10	0.50	4.9	40	2.0	18	28
11	0.50	4.9	80	2.0	93	71
12	0.50	4.9	100	1.2	100[b]	75
13	0.50	1.8	100	2.0	55	64
14	0.50	2.8	100	2.0	100[b]	77
15	0.50	3.7	100	1.3	100[b]	69
16[e]	0.50	4.9	60	2.0	74	53

[a] 0.10 g catalyst (0.048 mmol HPA–1), 10 ml dodecane, 20 ml min^{-1} air flow rate, 1300 rpm stirring speed. [b] The amount of DBT after reaction below detection limit of FID detector. [c] 3.0 mmol of 1,4-benzoquinone added. [d] 3.0 mmol of 2,6-di-tert-butyl-4-methylphenol added. [e] Pure O_2 instead of air used (cf. entry 6).

From the results presented in Table 5.2, the aldehyde-assisted aerobic ODS with bulk HPA–1 as a heterogeneous catalyst allowed removing 100% DBT from the model fuel in 2 h reaction time either at 60 °C and PhCHO/DBT = 12 mol/mol (entry 7) or at 100 °C and PhCHO/DBT = 5.6 (entry 14). As expected, the truly homogeneous $Co(OAc)_2$ catalyst has a higher activity, removing >99% DBT in 45 min at 40 °C and PhCHO/DB = 4 mol/mol with pure O_2 as the oxidant at 1 bar pressure [23]. On the other hand, also homogeneous HPA–2/TPA catalyst in

emulsion biphasic system MeCN–decalin removes >99% DBT in 4 h at 60 ^{o}C and isobutyraldehyde/DBT = 10 with pure O_2 as the oxidant [24], hence showing a comparable activity to the bulk HPA–1 catalyst. However, the Co(II) and HPA–2/TPA catalyst was not recycled; recycling of homogeneous catalysts is a very difficult task.

In contrast to the above homogeneous catalysts, the bulk HPA–1 catalyst exhibited excellent recyclability, as illustrated in Fig. 5.6. It withstood multiple reuses without loss of its activity in five consecutive runs with 97–100% DBT conversion. No catalyst leaching was detected by ICP-OES analysis of post reaction liquid phase. This is not unexpected since HPA–1 possessing an ion crystal structure is not soluble in alkanes. From DRIFTS analysis, after five reuses, the spent HPA–1 catalyst retained the Keggin structure as evidenced by the presence of the four characteristic infrared bands in the spectrum (Fig. 5.7). Some adsorbed DBT sulfone was also present on the catalyst surface as detected by DRIFTS (Fig. 5.7).

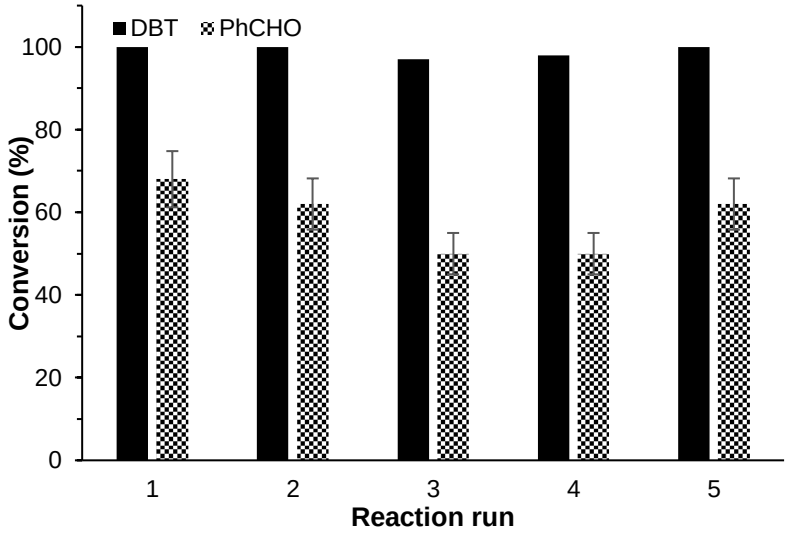

Fig. 5.6. Catalyst reuse for co-oxidation of DBT (0.50 mmol) and PhCHO (3.7 mmol) at 100°C, HPA–1 (0.10 g, 0.048 mmol), 10 ml dodecane, 1300 rpm stirring speed, 20 ml min^{-1} air flow rate, 2 h reaction time.

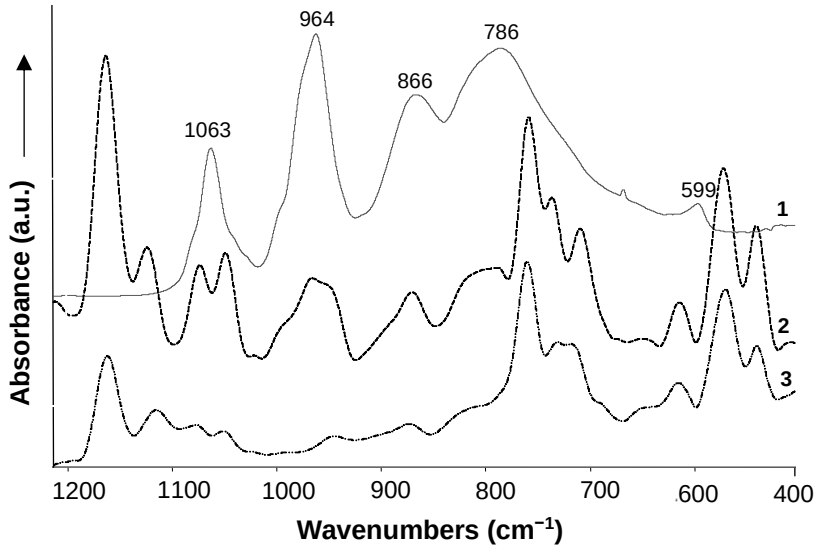

Fig. 5.7. DRIFT spectra (in KBr) of fresh and spent HPA–1 catalyst after 5 successive runs. (1) fresh HPA–1, (2) spent HPA–1 catalyst after 5 successive runs, (3) DBT sulfone.

Table 5.3 shows the results on the aldehyde-assisted ODS reaction in the presence of supported HPA–1 catalysts. Silica-supported 15%HPA–1/SiO_2 gave 61% DBT conversion at 100 °C and PhCHO/DBT = 7.4 in a 2 h reaction time; the conversion increased to 80% at 120 °C. The 15%HPA–1/C showed a low activity, giving only 11% DBT conversion in the same conditions. For comparison, bulk HPA–1 in the same conditions and with the same amount of HPA–1 (0.0082 mmol) gave 100% DBT conversion in 1 h (Table 5.3). Therefore, the supported HPA–1 catalysts were much less efficient than bulk HPA–1. This may be explained by reaction inhibition by the porous supports possessing high surface area; solid surfaces are well known for their efficient radical trapping [28].

Table 5.3. Aerobic co-oxidation of DBT and PhCHO catalyzed by supported HPA–1.[a]

Catalyst	Temperature (°C)	Conversion (%)	
		DBT	PhCHO
15%HPA–1/SiO_2	100	61	48
15%HPA–1/SiO_2	120	80	53
15%HPA–1/C	100	11	60
Bulk HPA–1[b]	100	100	69

[a] 0.10 g catalyst (0.0082 mmol HPA–1), 0.50 mmol DBT, 3.7 mmol PhCHO, 10 ml dodecane, 20 ml min^{-1} air flow rate, 1300 rpm stirring speed, 2 h reaction time. [b] Reaction with 0.0082 mmol of bulk HPA–1, 1 h reaction time.

5.1.3. Kinetics and mechanistic insight

The time course for DBT consumption showed an induction period, whereas no induction period was observed for PhCHO consumption (Fig. 5.8). Previously, an induction period has been noted for O_2 consumption in the DBT/aldehyde co-oxidation catalyzed by $Co(OAc)_2$ in agreement with the radical reaction mechanism [23].

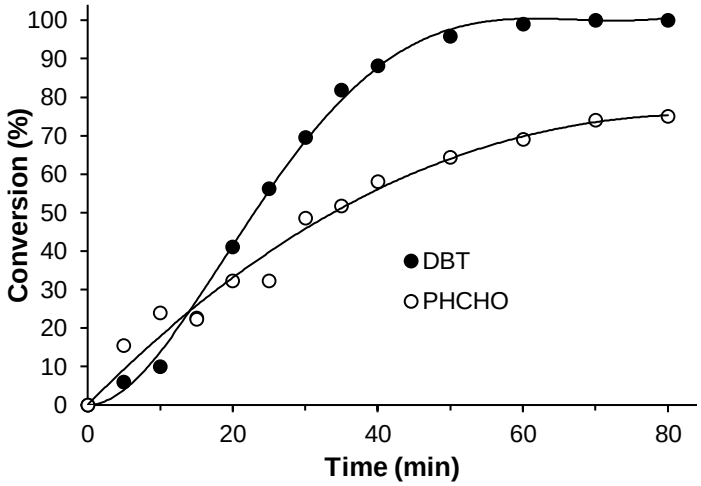

Fig. 5.8. Time course for aerobic co-oxidation of DBT (0.50 mmol) and PhCHO (4.9 mmol) catalyzed by HPA–1 (0.10 g, 0.048 mmol) at 100 °C, 10 ml dodecane, 20 ml min^{-1} air flow, 1300 rpm stirring speed).

The oxidation of PhCHO, both in the presence and in the absence of DBT, well obeyed the first-order rate law (Fig. 5.9). The oxidation of DBT also followed a first-order kinetics after the induction period (Fig. 5.10). The oxidation of PhCHO had an apparent activation energy (E_a) of 38 kJ mol^{-1} in the temperature range of 40–100 ^{o}C (Fig. 5.11). For the oxidation of DBT, the corresponding E_a value determined after the induction period was 66 kJ mol^{-1} (Fig. 5.12).

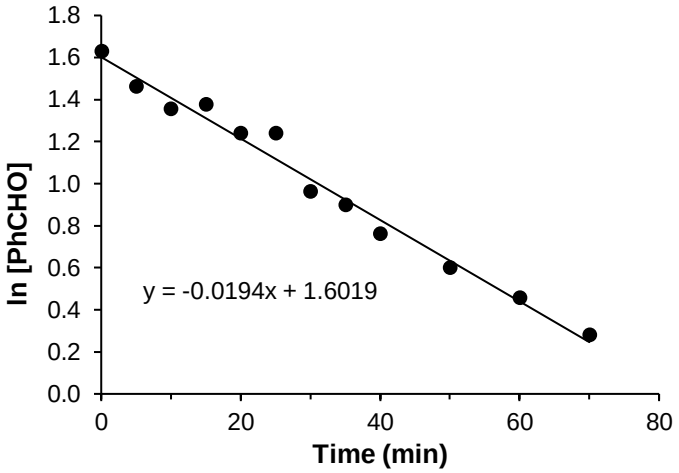

Fig. 5.9. First-order plot ln([PhCHO]/[PhCHO]$_o$) = $-k_{ald}\,t$ for aerobic oxidation of PhCHO (4.9 mmol) catalyzed by HPA–1 (0.10 g, 0.048 mmol) at 100 ^{o}C, 0.50 mmol DBT, 10 ml dodecane, 20 ml min^{-1} air flow, 1300 rpm stirring speed; k_{ald} = 0.019 min^{-1}.

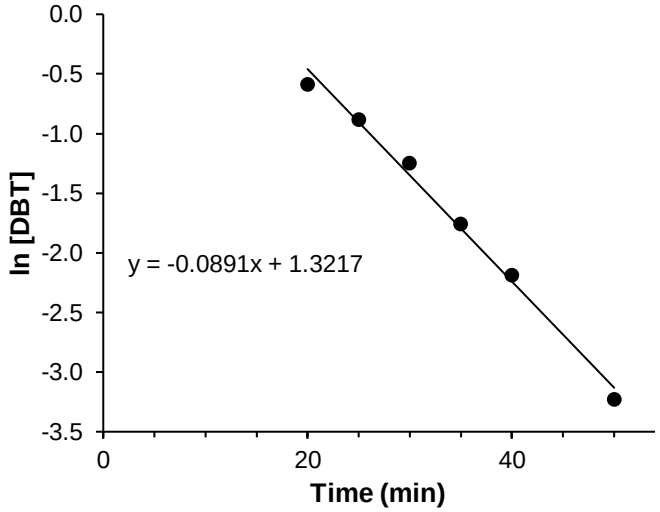

Fig. 5.10. First-order plot after induction period for aerobic oxidation of DBT (0.50 mmol) in the presence of PhCHO (4.9 mmol) catalyzed by HPA–1 (0.10 g, 0.048 mmol) at 100 ^{o}C, 10 ml dodecane, 20 ml min^{-1} air flow and 1300 rpm stirring speed; k_{DBT} = 0.089 min^{-1}.

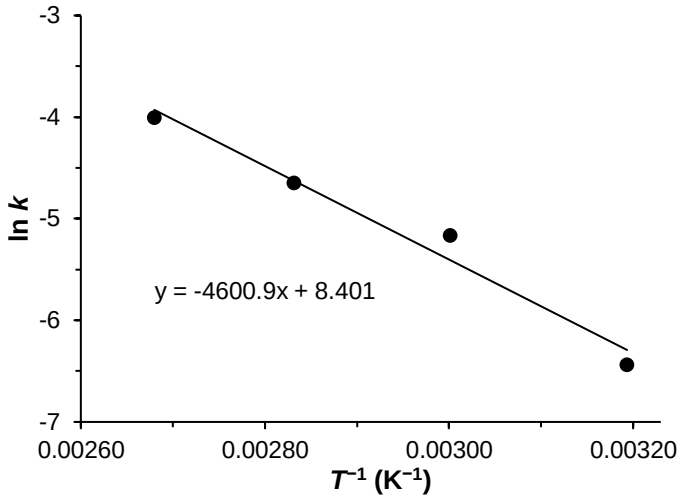

Fig. 5.11. Arrhenius plot for aerobic oxidation of PhCHO (4.9 mmol) catalyzed by HPA–1 (0.10 g, 0.048 mmol) in the presence of DBT (0.50 mmol); 10 ml dodecane, 20 ml min^{-1} air flow, 1300 rpm stirring speed; E_a = 38 kJ mol^{-1}.

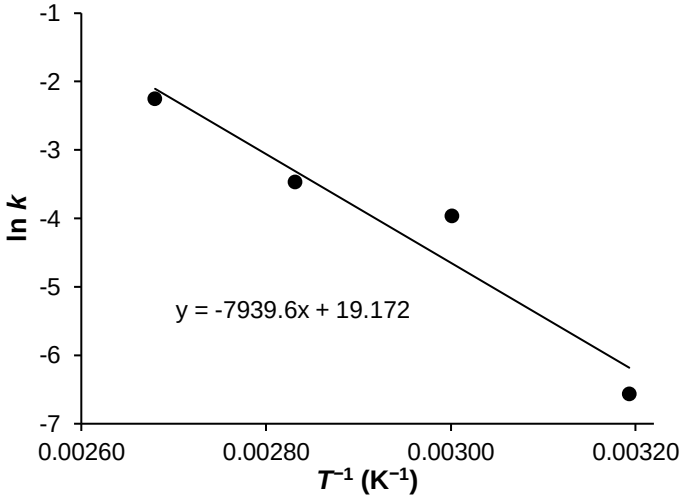

Fig. 5.12. Arrhenius plot for aerobic oxidation of DBT (0.50 mmol) catalyzed by HPA–1 (0.10 g, 0.048 mmol) in the presence of PhCHO (4.9 mmol); 10 ml dodecane, 20 ml min^{-1} air flow and 1300 rpm stirring speed; k_{DBT} is the first-order rate constant (min^{-1}) determined after induction period (see Fig. 5.8); E_a = 66 kJ mol^{-1}.

It is well established that the metal-catalyzed aerobic oxidation (autoxidation) of aldehydes occurs by the radical chain mechanism through peroxy acid intermediates to form the corresponding carboxylic acids as the final products [28]. Organosulfur compounds are well known as inhibitors of radical oxidation by intercepting organic peroxides (Eq. 2) [28].

Therefore, in the presence of DBT, the peroxy acid will predominantly react fast with DBT to form DBT sulfoxide and sulfone. From GC analysis, the products of DBT and PhCHO co-oxidation were DBT sulfone and benzoic acid. Hence the overall reaction can be represented by Scheme 5.1.

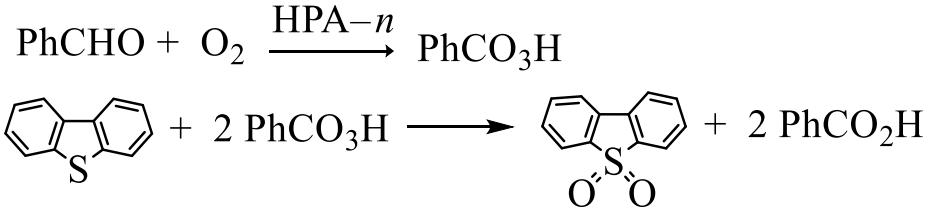

Scheme 5.1. Aerobic oxidation of DBT in the presence of PhCHO as a sacrificial reductant.

The co-oxidation of PhCHO and DBT by O_2 catalyzed by HPA–1 can be represented by an unbranched radical chain mechanism (Scheme 5.2). The initiation Step (1) is suggested to involve one-electron oxidation of PhCHO by V^{5+} on the surface of HPA–1 to produce free acyl radical PhCO· and V^{4+}. The catalyst, initially orange, turned green in the reacting mixture, which indicated its reduction. The reduction of V^{5+} to V^{4+} inside HPA–2 by aldehyde has been shown by ESR [37]. The propagation Steps (2)–(3) involve very fast reaction between PhCO· and O_2 to give the acylperoxo radical PhC(O)OO· (Step 2) followed by interaction of PhC(O)OO· with PhCHO to give the peroxy acid PhC(O)OOH and re-form the acyl radical (Step 3) [28]. The acylperoxo radical PhC(O)OO· has been registered in the autoxidation of PhCHO by ESR spin trapping [38]. The acyl radical can decompose to form alkyl radical and CO if there is an O_2 deficiency (O_2 partial pressure <10 kPa) [28], but in our system ($P_{O2} \approx 20$ kPa) this is unlikely. In the absence of DBT, benzoic acid is likely to form by Baeyer–Villiger reaction between the peroxy acid and PhCHO (Step 4) [28]. This is followed by the termination step, involving interaction of the acylperoxo radical with V^{4+} within the HPA–1 heteropoly anion, thus re-oxidizing the catalyst (Step 5). Re-oxidation of V^{4+} by O_2 is unlikely as the

oxidation of the reduced HPA–1 by O_2 is difficult in contrast to HPA–*n* with *n* = 2–6 [13,31,32]. The oxidation of PhCHO in the presence of bulk HPA–1 can be viewed as a heterogeneous–homogeneous reaction with heterogeneous initiation Step (1) and homogeneous chain-propagating Steps (2)–(3).

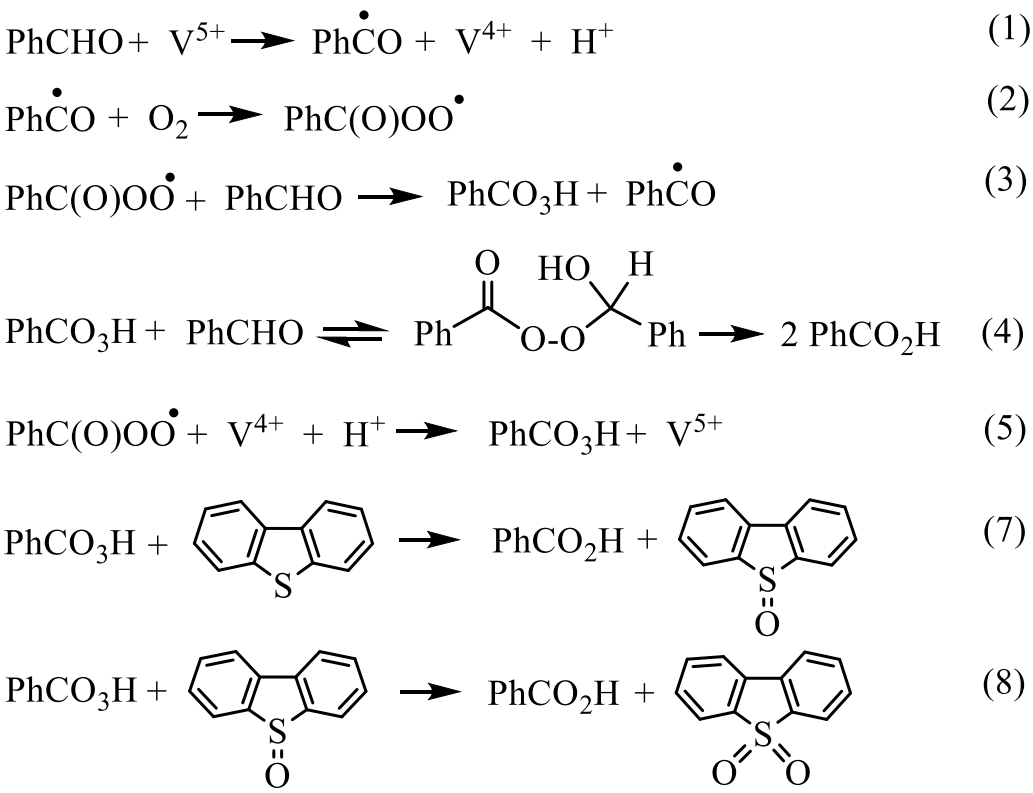

Scheme 5.2. Proposed mechanism for aerobic co-oxidation of DBT and PhCHO catalyzed by HPA–*n*.

In the presence of DBT, the peroxy acid reacts further with DBT to form DBT sulfoxide (Step 6) and sulfone (Step 7) [23]. If we assume that PhCHO is mainly consumed in Step (3), i.e., the reaction has a long chain length, and Steps (6) and (7) are faster than (4), then at PhCHO/DBT = 10 mol/mol, the rate of DBT consumption is expected to be five times faster than the rate of PhCHO consumption. This is in good agreement with the observed first-order rate constants for consumption of DBT (k_{DBT} = 0.089 min^{-1}, Figure 5.10) and PhCHO (k_{ald} = 0.019 min^{-1}, Figure 5.9)—the former is 4.7 times greater than the latter.

The proposed mechanism is supported by strong inhibition of the ODS reaction by chain-terminating inhibitors (Table 2) (for the mechanism of chain termination, see [28,39]). The induction period in DBT consumption (Figure 5) is also consistent with this mechanism since DBT oxidation follows the oxidation of PhCHO in a consecutive process. Therefore, the proposed unbranched radical chain mechanism for the aldehyde-assisted aerobic ODS reaction catalyzed by HPA–*n* is in good compliance with the experimental data. Similar radical mechanisms have been suggested for aerobic co-oxidation of alkanes [37] and alkenes [40] with aldehydes catalyzed by HPA–*n*.

5.2. Conclusions

Aerobic ODS of model liquid fuel (dodecane spiked with DBT) occurs readily at ambient air pressure in the presence of bulk heteropoly acid $H_4PMo_{11}VO_{40}$ (HPA–1) as a heterogeneous catalyst and benzaldehyde as a sacrificial reductant. It removes 100% of DBT from fuel (converted to DBT sulfone) in 2 h either at 60 °C and PhCHO/DBT = 12 mol/mol or at 100 °C and PhCHO/DBT = 5.6. The catalyst can be recycled without loss of activity. The reaction is suggested to occur through an unbranched radical chain mechanism. It can be viewed as a heterogeneous–homogeneous reaction with a heterogeneous initiation step and homogeneous chain-propagating steps.

References

[1] I.V. Babich, J.A. Moulijn, Science and technology of novel processes for deep desulfurization of oil refinery streams, Fuel 82 (2003) 607–631.

[2] R. Prins, Hydrotreating, in Handbook of Heterogeneous Catalysis, ed. G. Ertl, H. Knözinger, F. Schüth, J. Weitkamp, Vol. 6, Wiley-VCH, 2008; p. 2695–2718.

[3] B. Saha, S. Vedachalam, A.K. Dalai. Review on recent advances in adsorptive desulfurization, Fuel Process. Technol. 214 (2021) 106685.

[4] A.W. Bhutto, R. Abro, S. Gao, T. Abbas, X. Chen, G. Yu, Oxidative desulfurization of fuel oils using ionic liquids: A review, J. Taiwan Inst. Chem. Eng. 62 (2016) 84–97.

[5] Z. Jiang, H. Lü, Y. Zhang, C. Li, Oxidative desulfurization of fuel oils. Chin J Catal. 32 (2011) 707–15.

[6] E.A. Eseva, A.V. Akopyan, A.V. Anisimov, A.L. Maksimov, Oxidative desulfurization of hydrocarbon feedstock using oxygen as oxidizing agent (a review), Petroleum Chem. 60 (2020) 979–790.

[7] Y. Zhang, R. Wang, Recent advances on catalysts and systems for the oxidation of thiophene derivatives in fuel oil with molecular oxygen, Mini-Rev. Org. Chem. 15 (2018) 488–497

[8] F.M. Collins, A.R. Lucy, C. Sharp, Oxidative desulfurization of oils via hydrogen peroxide and heteropolyanion catalysis, J. Mol. Catal. A 117 (1997) 397–403.

[9] C. Komintarachat, W. Trakarnpruk, Oxidative desulfurization using polyoxometalates, Ind. Eng. Chem. Res. 45 (2006) 1853–1856.

[10] A.F. Shojaei, M.A. Rezvani, M.H. Loghmani, Comparative study on oxidation desulfurization of actual gas oil and model sulfur compounds with hydrogen peroxide promoted by formic acid: Synthesis and characterization of vanadium containing

polyoxometalate supported on anatase crushed nanoleaf, Fuel Process. Technol. 118 (2014) 1–6.

[11] A.E.S. Choi, S. Roces, N. Dugos, M.W. Wan, Oxidation by H_2O_2 of bezothiophene and dibenzothiophene over different polyoxometalate catalysts in the frame of ultrasound and mixing assisted oxidative desulfurization. Fuel 180 (2016) 127–36.

[12] M. Craven, R. Yahya, E.F. Kozhevnikova, C.M. Robertson, A. Steiner, I.V. Kozhevnikov, Alkylaminophosphazenes as efficient and tuneable phase-transfer agents for polyoxometalate-catalyzed biphasic oxidation with hydrogen peroxide, ChemCatChem 8 (2016) 200–208.

[13] I.V. Kozhevnikov, Catalysts for fine chemical synthesis: Catalysis by polyoxometalates, Wiley, West Sussex, 2002.

[14] J. Li, Z. Yang, S. Li, Q. Jin, J. Zhao, Review on oxidative desulfurization of fuel by supported heteropolyacid catalysts, J. Ind. Eng. Chem. 82 (2020) 1–16.

[15] M. Taghizadeh, E. Mehrvarz, A. Taghipour, Polyoxometalate as an effective catalyst for the oxidative desulfurization of liquid fuels: a critical review, Rev. Chem. Eng. 36 (2020) 831–858.

[16] J. Xu, Z. Zhu, T. Su, W. Liao, C. Deng, D. Hao, Y. Zhao, W. Ren, H. Lü, Green aerobic oxidative desulfurization of diesel by constructing an Fe-Anderson type polyoxometalate and benzene sulfonic acid-based deep eutectic solvent biomimetic cycle, Chin. J. Catal. 41 (2020) 868–876.

[17] N. Tang, Y. Zhang, F. Lin, H. Lu, Z. Jiang, C. Li, Oxidation of dibenzothiophene catalyzed by $[C_8H_{17}N(CH_3)_3]_3H_3V_{10}O_{28}$ using molecular oxygen as oxidant, Chem. Commun. 48 (2012) 11647–11649.

[18] J.K. Li, Y.Q. Xu, C.-W. Hu, In situ synthesis of a novel dioxidovanadium-based nickel complex as catalyst for deep oxidative desulfurization with molecular oxygen, Inorg. Chem. Commun. 60 (2015) 12–14.

[19] M. Zhang, J. Liu, H. Li, Y. Wei, Y. Fu, W. Liao, L. Zhu, G. Chen, W. Zhu, H. Li, Tuning the electrophilicity of vanadium-substituted polyoxometalate based ionic liquids for high-efficiency aerobic oxidative desulfurization, Appl. Catal. B 271 (2020) 118936.

[20] J. Claußnitzer, B. Bertleff, W. Korth, J. Albert, P. Wasserscheid, A. Jess, Kinetics of triphase extractive oxidative desulfurization of benzothiophene with molecular oxygen catalyzed by HPA–5, Chem. Eng. Technol. 43 (2020) 465–475.

[21] R. Wang, Y. Zhao, I.V. Kozhevnikov, J. Zhao, An ultrasound enhanced catalytic ozonation process for the ultra-deep desulfurization of diesel oil, New J. Chem. 44 (2020) 15467–15474.

[22] M.T. Pope, Heteropoly and isopoly oxometalates, Springer, Berlin, 1983.

[23] S. Murata, K. Murata, K. Kidena, M. Nomura, A novel oxidative desulfurization system for diesel fuels with molecular oxygen in the presence of cobalt catalysts and aldehydes, Energy Fuels 18 (2004) 116–121.

[24] H. Lu, J. Gao, Z. Jiang, Y. Yang, B. Song, C. Li, Oxidative desulfurization of dibenzothiophene with molecular oxygen using emulsion catalysis, Chem. Commun. 2007, p. 150–152.

[25] V. Dumont, L. Oliviero, F. Mauge, M. Houalla, Oxidation of dibenzothiophene by a metal–oxygen–aldehyde system, Catal. Today. 130 (2008) 195–198.

[26] T.V. Rao, P.M. Krishna, D. Paul, B.R. Nautiyal, J. Kumar, Y.K. Sharma, S.M. Nanoti, B. Sain, M.O. Garg, The oxidative desulfurization of HDS diesel: using aldehyde and

molecular oxygen in the presence of cobalt catalysts, Petrol. Sci. Technol. 29 (2011) 626–632.

[27] C. Wang, Z. Chen, W. Zhu, P. Wu, W. Jiang, M. Zhang, H. Li, W. Zhu, H. Li, One-pot extraction and oxidative desulfurization of fuels with molecular oxygen in low-cost metal-based ionic liquids, Energy Fuels 31 (2017) 1376−1382.

[28] J.H. Teles, I. Hermans, G. Franz, R.A. Sheldon, Oxidation, Ullmann's encyclopedia of industrial chemistry, Wiley–VCH, Weinheim, 2015.

[29] K. Weissermel, H.-J. Arpe, Industrial organic chemistry, 4th edn, Wiley–VCH, Weinheim, 2003.

[30] J. Li, X. Chu, S. Tian, Research on determination of total acid number of petroleum using mid-infrared attenuated total reflection spectroscopy, Energy Fuels 26 (2012) 5633−5637.

[31] I.V. Kozhevnikov, K.I. Matveev, Homogeneous catalysts based on heteropoly acids. Appl. Catal. 5 (1983) 135-150.

[32] I.V. Kozhevnikov, Catalysis by heteropoly acids and multicomponent polyoxometalates in liquid-phase reactions, Chem. Rev. 98 (1998) 171–198.

[33] I.A. Weinstock, R.E. Schreiber, R. Neumann, Dioxygen in polyoxometalate mediated reactions, Chem. Rev. 118 (2018) 2680−2717.

[34] J. Tong, W. Wang, L. Su, Q. Li, F. Liu, W. Ma, Z. Lei, L. Bo, Highly selective oxidation of cyclohexene to 2-cyclohexene-1-one over polyoxometalate/metal–organic framework hybrids with greatly improved performances, Catal. Sci. Technol. 7 (2017) 222–230.

[35] G.A. Tsigdinos, C.J. Hallada, Molybdovanadophosphoric acids and their salts. 1. Investigation of methods of preparation and characterization, Inorg. Chem. 7 (1968) 437–441.

[36] M. Kanno, T. Yasukawa, W. Ninomiya, K. Ooyachi, Y. Kamiya, Catalytic oxidation of methacrolein to methacrylic acid over silica-supported 11-molybdo-1-vanadophosphoric acid with different heteropolyacid loadings. J. Catal. 273 (2010) 1–8.

[37] A.M. Khenkin, A. Rosenberger, R. Neumann, Reaction of aldehydes with the $H_5PV_2Mo_{10}O_{40}$ polyoxometalate and co-oxidation of alkanes with molecular oxygen. J. Catal. 182 (1999) 82–91.

[38] M.M. Sankar, E. Nowicka, E. Carter, D.M. Murphy, D.M. Knight, D. Bethell, G.J. Hutchings, The benzaldehyde oxidation paradox explained by the interception of peroxy radical by benzyl alcohol. Nat. Commun. 5 (2014) 3332.

[39] K.U. Ingold, D.A. Pratt, Advances in radical-trapping antioxidant chemistry in the 21st century: A kinetics and mechanisms perspective. Chem. Rev. 114 (2014) 9022–9046.

[40] M. Hamamoto, K Nakayama, Y. Nishiyama, Y. Ishii, Oxidation of organic substrates by molecular oxygen/aldehyde/heteropolyoxometalate system. J. Org. Chem. 58 (1993) 6421–6425.

[41] R. Ghubayra, C. Nuttall, S. Hodgkiss, M. Craven, E. F. Kozhevnikova, I.V. Kozhevnikov, Oxidative desulfurization of model diesel fuel catalyzed by carbon-supported heteropoly acids, Appl. Catal. B 253 (2019) 309–316.

6 Conclusions and future outline

Diesel fuel is one of the main transportation fuels used today. It consists of aliphatic and aromatic hydrocarbons and contains traces of impurities such as organosulfur compounds. The sulfur impurity is a source of air pollution, namely acid rain caused by SO_x produced during vehicle engine combustion. It also has negative effects on catalytic converters and sensors. Because of these problems, desulfurization of transportation fuels has received much attention in recent decades. In this regard, removing refractory aromatic sulfur compounds such as benzothiophenes from diesel fuel is a major challenge. Significant efforts have been made to reduce the sulfur level of diesel fuel using different desulfurization methods such as hydrodesulfurization, biodesulfurization, adsorption, and oxidative desulfurization [1–5].

The oxidative desulfurization (ODS) is a promising and economical process to remove heavy aromatic organosulfur compounds from diesel fuels under mild conditions at low temperature and atmospheric pressure in the presence of an appropriate oxidizing agent and catalyst. The ODS process involves the oxidation and extraction steps. First, dibenzothiophene-like compounds are oxidized to sulfoxides and sulfones as illustrated in Scheme 6.1 and then the latter are removed by extraction processes [3–9].

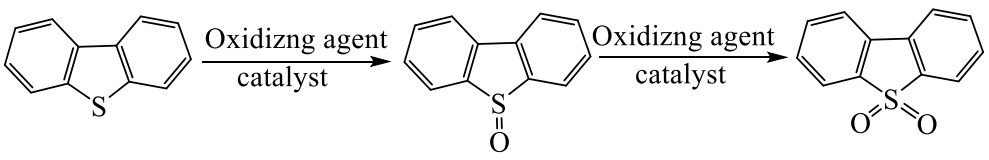

Scheme 6. 1. Catalytic oxidation of dibenzothiophene-like compounds.

Hydrogen peroxide and O_2 are the most widely used oxidizing agents in ODS processes [10–12]. The oxidizing agent activates an ODS catalyst before it reacts with the target substrate. Polyoxometalates (POM), especially those comprising Keggin-type polyanions, $XM_{12}O_{40}^{m-}$, composed of oxygen-sharing MO_6 octahedra (M = Mo^{VI}, W^{VI}, V^{V}, etc.) encapsulating a central tetrahedron XO_4^{n-} (X = P^{V}, Si^{IV}, etc.), have been widely studied as the ODS catalysts due to their remarkable desulfurization activity [13–17]. Typically, the reaction is carried out in a liquid-phase biphasic system using Keggin-type POM catalysts and an oxidant. In the H_2O_2 oxidation system, POM partially decomposes in the presence of excess hydrogen peroxide to form peroxo-POM complexes, which are known as a catalytically active species in the ODS reaction. In the air oxidation system, POM can initiate radical chain oxidation of organosulfur compounds to the corresponding sulfoxides and sulfones.

As stated in the introduction, our main objective was to investigate the process of dibenzothiophene (DBT) oxidation by hydrogen peroxide and oxygen (air) using Keggin type POMs supported on activated carbon as heterogeneous ODS catalysts and to gain new mechanistic insights into the mechanism of ODS reactions. The oxidation of DBT, which is commonly used as a model reaction for the testing of ODS catalysts, was the main subject of our research. The key advantage of heterogeneous ODS catalysts over homogeneous catalysts is in easy catalyst separation from the fuel after the reaction. However, catalyst performance may be complicated due to possible POM leaching from the support during the ODS reaction and post-reaction catalyst treatment. These aspects were also addressed in our research. As a result, we have selected highly efficient carbon-supported POM catalysts for the ODS process and optimized reaction conditions.

First, the carbon-supported POM catalysts were employed for the oxidation benzothiophenes with H_2O_2 in a biphasic system. As the catalysts were used Keggin-type heteropoly acids $H_3PMo_{12}O_{40}$, $H_3PW_{12}O_{40}$ and $H_4SiW_{12}O_{40}$ immobilised on different types of activated carbon

with the aim of improving the ease of catalyst-product separation whilst maintaining high conversion of benzothiophenes and preventing the catalyst from leaching. Analysis of the carbon-supported POM catalysts showed a strong effect of the carbon support on the integrity of POM structure and catalyst activity. It was found that in the case of moderately acidic and basic carbon supports the Keggin structure of POM was decomposed to form diverse monomeric and/or oligomeric Mo^{VI} and W^{VI} oxo species on the surface of carbon support. Whereas the more acidic activated carbon, Darco KB-B, stabilized the Keggin structure. The catalytic activities of POMs in the oxidation of DBT with H_2O_2 were found to be variable under similar reaction conditions depending on the type of carbon support used. In the case of the acidic carbon support (Darco KB-B), the catalytic activity increased in line with decreasing stability and increasing oxidative potential of POM in the order: PMo > PW > SiW. The best catalyst, PMo/C, gave 100% DBT sulfone yield with 80% H_2O_2 efficiency after 30 min in heptane/H_2O system with a molar ratio [H_2O_2]/[DBT] of 3.0. Contrary to that, when using moderately acidic and basic activated carbon supports, the catalytic activity increased in line with increasing stability and decreasing oxidative potential in the order: PW > PMo. The best catalyst, PW/AC, gave 100% DBT sulfone yield with 85% H_2O_2 efficiency after 20 min in heptane/H_2O system with the same [H_2O_2]/[DBT] molar ratio of 3.0. In both cases, the catalysts could be reused several times without observing any notable loss in activity, which confirms the high stability of catalytically active species during the reaction.

The mechanism of oxidation of DBT with H_2O_2 using carbon-supported catalysts was found to differ depending of the acid-base properties of support. The results suggest that with the catalysts comprising intact Keggin POMs on the acidic carbon surface, the ODS reaction occurs via peroxo complexes of the intact Keggin units as the active species (Scheme 6.2). In contrast, with the catalysts comprising the monomeric and oligomeric W^{VI} and Mo^{VI} oxo species on the moderately acidic or basic carbon surface, the oxidation could occur via peroxo

complexes of these species rather than through the peroxo complexes of intact Keggin units (Scheme 6.3). Overall, POM immobilization on carbon supports was successful, and carbon-supported catalysts were found to be highly efficient for oxidative desulfurization with H_2O_2.

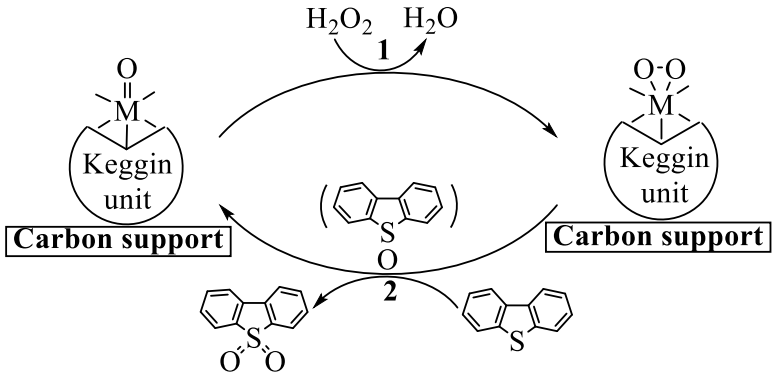

Scheme 6. 2. Reaction scheme for oxidation of DBT by H_2O_2 catalyzed by POM/AC–0 comprising intact Keggin POM on carbon surface (M = Mo^{VI} or W^{VI}).

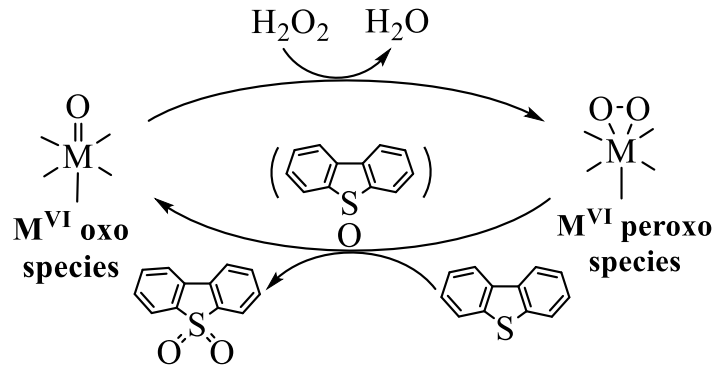

Scheme 6. 3. Proposed mechanism for oxidation of DBT by H_2O_2 catalyzed by POM/AC–*n* comprising monomeric and oligomeric W^{VI} and Mo^{VI} oxo species on carbon surface.

Further, we used air as the oxidant instead of H_2O_2 in the aerobic oxidative desulfurization process. In this part, we investigated the aldehyde-assisted aerobic ODS of model liquid fuel comprising dodecane and dibenzothiophene in the presence of benzaldehyde (PhCHO) as a model sacrificial reductant using bulk and supported Keggin-type mixed-addenda molybdovanadophosphoric heteropoly acids $H_{3+n}PMo_{12-n}V_nO_{40}$ (HPA–*n*, *n* = 0–3) as heterogeneous catalysts. It was demonstrated that the monovanadium HPA–1 was the most

efficient catalyst for removing DBT from the fuel. With this catalyst, 100% removal of DBT from the model fuel was achieved at mild conditions (60 ^{o}C, ambient pressure, 20 ml/min air flow and 2 h reaction time). The catalyst could be reused many times without any loss in activity. In the presence of benzaldehyde as the sacrificial reductant and HPA–1 as the catalyst, a radical chain reaction mechanism including co-oxidation of DBT and benzaldehyde with air was proposed (Scheme 6.4).

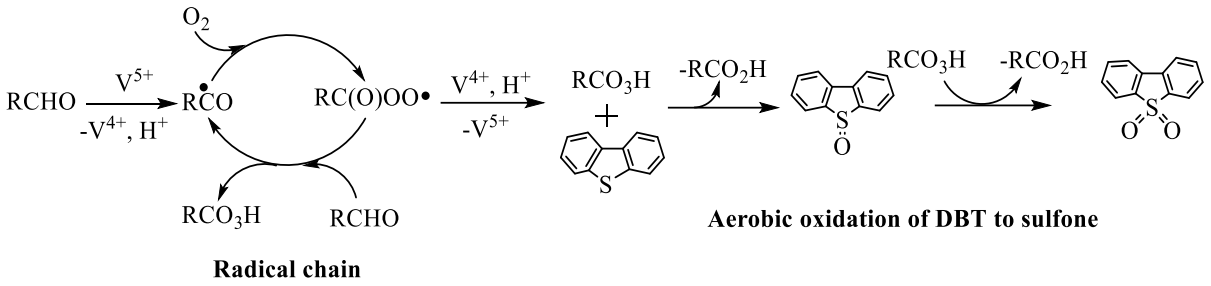

Scheme 6. 4. Proposed radical chain mechanism for aerobic oxidation of DBT catalyzed by HPA–*n* in the presence of PhCHO as a sacrificial reductant.

Future research may focus on further expanding the range of carbon materials used as supports for POM. It is interesting to look at the carbon materials with controlled texture such as carbon nanotubes. Also interesting are carbon materials modified with heteroatoms. In this regard, nitrogen-modified porous carbon materials are of particular interest since the nitrogen surface sites (e.g., surface amino groups) can strongly adsorb polyoxometalates, thus improving catalyst stability.

Further in-depth kinetic and mechanistic studies of POM-catalyzed ODS reactions complemented by thorough characterization of active Mo and W peroxo species on the carbon surface could provide new insights into the mechanism of these reactions to facilitate catalyst and process development. Particularly interesting is using multinuclear NMR (especially ^{31}P, ^{95}Mo, ^{183}W, and ^{17}O) to identify the local structure of HPA surface species, X-ray photoelectron

spectroscopy (XPS) to determine the oxidation state of Mo and W in HPA catalysts and Raman spectroscopy to characterize the chemical structure of supported HPA catalysts.

Another promising area of future research concerns with potential applications of the products of ODS of refractory aromatic sulfur compounds, i.e., aromatic sulfones. Sulfones are the core scaffolds in many sulfur containing medicines (e.g. sulfonamides) and numerous drug candidates that are under development for the treatment of a large number of human diseases worldwide (for a comprehensive review see [18]).

References

[1] J.H. Gary, J.H Handwerk, M.J Kaiser, D. Geddes, Petroleum refining: technology and economics. CRC press. London, 5th edn, 2007.

[2] H. Kuwahara, Desulfurization of heavy oil, Chem. Econ. Engng. Rev. 5 (1973) 35–40.

[3] C. Song, An overview of new approaches to deep desulfurization for ultra-clean gasoline, diesel fuel and jet fuel. Catal. Today, 86 (2003) 211–263.

[4] I.V. Babich, J.A. Moulijn, Science and technology of novel processes for deep desulfurization of oil refinery streams, Fuel 82 (2003) 607–631.

[5] R. Prins, Hydrotreating, in Handbook of Heterogeneous Catalysis, ed. G. Ertl, H. Knözinger, F. Schüth, J. Weitkamp, Vol. 6, Wiley-VCH, 2008; p. 2695–2718.

[6] A.W. Bhutto, R. Abro, S. Gao, T. Abbas, X. Chen, G. Yu, Oxidative desulfurization of fuel oils using ionic liquids: A review, J. Taiwan Inst. Chem. Eng. 62 (2016) 84–97.

[7] Z. Jiang, H. Lü, Y. Zhang and C. Li, Oxidative desulfurization of fuel oils, Chin. J. Catal. 32 (2011) 707–715.

[8] Song, X. Ma, New design approaches to ultra-clean diesel fuels by deep desulfurization and deep dearomatization, Appl. Catal. B 41 (2003) 207–238.

[9] J.M. Campos-Martin, M.C. Capel-Sanchez, P. Perez-Presas, J.L.G. Fierro, Oxidative processes of desulfurization of liquid fuels, J. Chem. Technol. Biotechnol. 85 (2010) 879–890.

[10] E.A. Eseva, A.V. Akopyan, A.V. Anisimov, A.L. Maksimov, Oxidative desulfurization of hydrocarbon feedstock using oxygen as oxidizing agent (a review), Petroleum Chem. 60 (2020) 979–790.

[11] Y. Zhang, R. Wang, Recent advances on catalysts and systems for the oxidation of thiophene derivatives in fuel oil with molecular oxygen, Mini-Rev. Org. Chem. 15 (2018) 488–497.

[12] R. Noyori, M. Aoki, K. Sato, Green oxidation with aqueous hydrogen peroxide, ChemCommun 16 (2003) 1977–1986.

[13] F.M. Collins, A.R. Lucy, C. Sharp, Oxidative desulfurization of oils via hydrogen peroxide and heteropolyanion catalysis, J. Mol. Catal. A Chem. 117 (1997) 397–403.

[14] C. Komintarachat, W. Trakarnpruk, Oxidative desulfurization using polyoxometalates, Ind. Eng. Chem. Res. 45 (2006) 1853–1856.

[15] M. Taghizadeh, E. Mehrvarz, A. Taghipour, Polyoxometalate as an effective catalyst for the oxidative desulfurization of liquid fuels: a critical review, Rev. Chem. Eng. 36 (2020) 831–858.

[16] M. Craven, R. Yahya, E.F. Kozhevnikova, C.M. Robertson, A. Steiner, I.V. Kozhevnikov, Alkylaminophosphazenes as efficient and tuneable phase-transfer agents for polyoxometalate-catalyzed biphasic oxidation with hydrogen peroxide, ChemCatChem 8 (2016) 200–208.

[17] J. Xu, Z. Zhu, T. Su, W. Liao, C. Deng, D. Hao, Y. Zhao, W. Ren, H. Lü, Green aerobic oxidative desulfurization of diesel by constructing an Fe-Anderson type polyoxometalate and benzene sulfonic acid-based deep eutectic solvent biomimetic cycle, Chin. J. Catal. 41 (2020) 868–876.

[18] M. Feng, B. Tang, S. H. Liang, X. Jiang, Sulfur containing scaffolds in drugs: synthesis and application in medicinal chemistry, Curr. Top. Med. Chem. 16 (**2016)** 1200–1216.